OSCILLATORY ARCHITECTURE of MEMORY CIRCUITS

Nikolaos Karalis

Thesis submitted to the
Faculty of Medicine
Ludwig-Maximillians-University Munich
in partial fulfillment of the requirements
for the degree of *Doctor rerum naturalium*

February 2019

Aus dem Biozentrum der LMU - Department Biologie II –
Lehrstuhl für Cognition and Neural Plasticity –
Medizinische Fakultät und Fakultät der Biologie
der Ludwig-Maximillians-Universität München

Vorstand: Prof. Dr. Herwig Stibor

Oscillatory architecture of memory circuits

Dissertation
zum Erwerb des Doktorgrades der Naturwissenschaften
an der Medizinischen Fakultät der
Ludwig-Maximilians-Universität zu München

vorgelegt von
Nikolaos Karalis

aus
Athen

Jahr
2019

Mit Genehmigung der Medizinischen Fakultät
der Ludwig-Maximilians-Universität München

Betreuer:	Prof. Dr. Anton Sirota
Zweitgutachter:	Prof. Dr. Bernd Sutor
Dekan:	Prof. Dr. med. dent. Reinhard Hickel
Tag der mündlichen Prüfung:	25.02.2019

To my parents,
with love and gratitude.

τυγχάνει μέγιστον ἀγαθὸν ὂν ἀνθρώπῳ τοῦτο,
ἑκάστης ἡμέρας περὶ ἀρετῆς τοὺς λόγους ποιεῖσθαι
ὁ δὲ ἀνεξέταστος βίος οὐ βιωτὸς ἀνθρώπῳ
Plato, Apology of Socrates, 38a 1-6

ABSTRACT

The coordinated activity between remote brain regions underlies cognition and memory function. Although neuronal oscillations have been proposed as a mechanistic substrate for the coordination of information trans- fer and memory consolidation during sleep, little is known about the mechanisms that support the widespread synchronization of brain regions and the relationship of neuronal dynamics with other bodily rhythms, such as breathing.

During exploratory behavior, the hippocampus and the prefrontal cortex are organized by theta oscillations, known to support memory encoding and retrieval, while during sleep the same structures are dominated by slow oscillations that are believed to underlie the consolidation of recent experiences. The expression of conditioned fear and extinction memories relies on the coordinated activity between the mPFC and the basolateral amygdala (BLA), a neuronal structure encoding associative fear memories. However, to date, the mechanisms allowing this long-range network synchronization of neuronal activity between the mPFC and BLA during fear behavior remain virtually unknown.

Using a combination of extracellular recordings and open- and closed-loop optogenetic manipulations, we investigated the oscillatory and coding mechanisms mediating the organization and coupling of the limbic circuit in the awake and asleep brain, as well as during memory encoding and retrieval. We found that freezing, a behavioral expression of fear, is tightly associated with an internally generated brain state that manifests in sustained 4Hz oscillatory dynamics in prefrontal-amygdala circuits. 4Hz oscillations accurately predict the onset and termination of the freezing state. These oscillations synchronize prefrontal-amygdala circuits and entrain neuronal activity to dynamically regulate the development of neuronal ensembles. This enables the precise timing of information transfer between the two structures and the expression of fear responses. Optogenetic induction of prefrontal 4Hz oscillations promotes freezing behavior and the formation of long-lasting fear memory, while closed-loop phase specific manipulations bidirectionally modulate fear expression.

Our results unravel a physiological signature of fear memory and identify a novel internally generated brain state, characterized by 4Hz oscillations. This oscillation enables the temporal coordination and information transfer in the prefrontal-amygdala circuit via a phase-specific coding mechanism, facilitating the encoding and expression of fear memory.

In the search for the origin of this oscillation, we focused our attention on breathing, the most fundamental and ubiquitous rhythmic activity in life. Using large-scale extracellular recordings from a number of structures, including the medial prefrontal cortex, hippocampus, thalamus, amygdala and nucleus accumbens in mice we identified and characterized the entrainment by breathing of a host of network dynamics across the limbic circuit. We established that fear-related 4Hz oscillations are a state-specific manifestation of this cortical entrainment by the respiratory rhythm. We characterized the translaminar and transregional profile of this entrainment and demonstrated a causal role of breathing in synchronizing neuronal activity and network dynamics between these structures in a variety of behavioral scenarios in the awake and sleep state. We further revealed a dual mechanism of respiratory entrainment, in the form of an intracerebral corollary discharge that acts jointly with an olfactory reafference to coordinate limbic network dynamics, such as hippocampal ripples and cortical UP and DOWN states, involved in memory consolidation.

Respiration provides a perennial stream of rhythmic input to the brain. In addition to its role as the *condicio sine qua non* for life, here we provide evidence that breathing rhythm acts as a global pacemaker for the brain, providing a reference signal that enables the integration of exteroceptive and interoceptive inputs with the internally generated dynamics of the hippocampus and the neocortex. Our results highlight breathing, a perennial rhythmic input to the brain, as an oscillatory scaffold for the functional coordination of the limbic circuit, enabling the segregation and integration of information flow across neuronal networks.

Keywords: *in vivo* electrophysiology, sleep, memory consolidation, optogenetics, hippocampus, prefrontal cortex, amygdala, slow oscillations, sharp-wave ripples, local field potentials, fear, oscillations, 4Hz, respiration

ZUSAMMENFASSUNG

Das präzise Timing von Aktionspotentialen durch Koordination und Synchronisation neuronaler Ensembles ist ein effizienter und flexibler Kodierungsmechanismus, der im Gehirn für sensorische und kognitive Verarbeitung weit verbreitet ist.

Jahrzehntelange Forschung hat neuronale Oszillationen als mechanistisches Substrat für die Bildung von funktionalen Zellverbänden und der Koordination des Informationstransfers zwischen entfernten Hirnregionen identifiziert.

Während explorativen Verhaltens werden Hippokampus und präfrontaler Kortex durch Theta-Oszillationen organisiert, die eine Rolle bei der Enkodierung und dem Abruf von Erinnerungen spielen, während dieselben Strukturen im Schlaf von langsamen Oszillationen dominiert werden, die der Konsolidierung neuerer Erfahrungen zugrunde liegen.

Es wird angenommen, dass der mediale präfrontale Kortex (mPFC) Angstverhalten mittels Projektion zur Amygdala reguliert, einer Struktur die assoziative Angsterinnerungen enkodiert.

Neuere konvergierende Resultate legen nahe, dass der Abruf konditionierter Angst- und Extinktionserinnerungen auf der koordinierten Aktivität zwischen mPFC und basolateraler Amygdala (BLA), zweier bidirektional dicht miteinander verbunder Strukturen, beruht. Bis heute sind jedoch die Mechanismen, die diese weitreichende Netzwerksynchronisation zwischen mPFC und BLA während des Angstverhaltens erlauben, praktisch unbekannt.

In der vorliegenden Arbeit haben wir mit einer Kombination aus extrazellulären elektrophysiologischen Ableitungen und open- sowie closed-loop optogenetischen Manipulationen untersucht welche oszillatorischen und temporalen Kodierungsmechanismen der mPFC-BLA Kopplung während des Angstverhaltens unterliegen.

Wir fanden heraus, dass das Freezing, ein Verhaltensausdruck von Angst, eng mit einem intern erzeugten Gehirnzustand verbunden ist, der sich in einer anhaltenden Oszillationsdynamik von 4Hz in präfrontal-amygdaloiden Schaltkreisen manifestiert. 4-Hz-Oszillationen sind ein zuverlässiger Prädiktor für Beginn und Beendigung des Freezingzustands. Diese Oszillationen synchronisieren präfrontal-amygdaloide Schaltkreise und neuronale Aktivität, um die Entwicklung von neuronalen Ensembles dynamisch zu regulieren. Dies ermöglicht das präzise Timing des Informationstransfers zwischen beiden Strukturen und das Auftreten von Angstreaktionen. Die optogenetische Induktion präfrontaler 4Hz-Oszillationen fördert Freezingverhalten und die Bildung eines stabilen Angstgedächtnisses, während phasenspezifische Manipulationen bidirektional die Angstausprägung modulieren.

Unsere Ergebnisse entschlüsseln eine physiologische Signatur des Angstgedächtnisses und identifizieren einen neuartigen, intern erzeugten Gehirnzustand, der durch 4Hz-Oszillationen gekennzeichnet ist. Diese Oszillation ermöglicht die zeitliche Koordination und Informationsübertragung in präfrontal - amygdaloiden Schaltkreisen durch einen phasenspezifischen Kodierungsmechanismus, der die Enkodierung und den Abruf von Angsterinnerungen erleichtert.

Obwohl die meisten bekannten neuronalen Oszillationen von intrazerebralen Schrittmachern und Schaltkreisen erzeugt werden, haben wir uns hier auf die Atmung, die grundlegendste und allgegenwärtigste rhythmische Aktivität des Lebens, als möglichen Ursprung dieser 4Hz-Oszillation konzentriert. Unter Verwendung extrazellulärer elektrophysiologischer Ableitungen mittels hochauflösender Siliziumsonden in Mäusen identifizieren und charakterisieren wir die rhythmische Beeinflussung einer Vielzahl von Netzwerkdynamiken der limbischen Schaltkreise einschließlich präfrontalem Kortex, Hippocampus, Amygdala und Nucleus accumbens und damit Strukturen, die entscheidend an Lernen, Gedächtniskonsolidierung und Gedächtnisabruf beteiligt sind. Es zeigt sich dass angstbezogene 4Hz-Oszillationen eine Gehirnzustand-spezifische Manifestation des Entrainment kortikaler Aktivität durch den Atemrhythmus ist.

Wir charakterisieren das translaminare und transregionale Profil dieses Entrainments und zeigen eine kausale Rolle der Atmung bei der Synchronisation neuronaler Aktivität und Netzwerkdynamiken zwischen diesen Strukturen in einer Vielzahl von Verhaltenszuständen im Wach- und Schlafzustand.

Die Atmung liefert einen durchgehenden Strom rhythmischen Inputs an das Gehirn. Neben seiner Rolle als *condicio sine qua non* für Leben liefern wir hier Hinweise darauf, dass der Atemrhythmus als globaler Schrittmacher für das Gehirn fungiert und ein Referenzsignal liefert, das

die Integration von exterozeptiven und interozeptiven Inputs mit der intern generierten Dynamik von Hippocampus und Neocortex ermöglicht.

Unsere Ergebnisse heben die Atmung als einen neuen oszillatorischen Mechanismus hervor, der interregionale Synchronisation limbischer Gedächtnisschaltkreise vermittelt und zur Bildung, Konsolidierung und Expression neuronaler Ensembles beiträgt.

PUBLICATIONS

This thesis contains work reported in the following publications:

- Karalis, N. and Sirota, A. (2018). "Breathing coordinates limbic network dynamics underlying memory consolidation." In: *bioRxiv*.

The author of this thesis (Nikolaos Karalis) identified the described phenomenon, performed all recordings and experiments, designed the experiments and data analysis, performed all the data analyses and interpreted the data included in this thesis work.

- Karalis, N., Dejean, C., Chaudun, F., Khoder, S., R Rozeske, R., Wurtz, H., Bagur, S., Benchenane, K., Sirota, A., Courtin, J., and Herry, C. (2016). "4-Hz oscillations synchronize prefrontal-amygdala circuits during fear behavior." In: *Nature Neuroscience* 19.4, pp. 605–612.

The author of this thesis (Nikolaos Karalis) identified the described phenomenon, performed parts of the electrophysiological recordings used in the study, designed the experiments and data analysis, performed all the data analyses and interpreted the data included in this thesis work.

Other publications containing work undertaken during the doctoral period but not reported here:

- Rozeske, R. R., Jercog, D., Karalis, N., Chaudun, F., Khoder, S., Girard, D., Winke, N., and Herry, C. (2018). "Prefrontal-Periaqueductal Gray-Projecting Neurons Mediate Context Fear Discrimination." In: *Neuron* 97.4, pp. 898–910.
- Dejean, C., Courtin, J., Karalis, N., Chaudun, F., Wurtz, H., Bienvenu, T. C., and Herry, C. (2016). "Prefrontal neuronal assemblies temporally control fear behaviour." In: *Nature* 535.7612, pp. 420–424.
- Courtin, J., Chaudun, F., Rozeske, R. R., Karalis, N., Gonzalez-Campo, C., Wurtz, H., Abdi, A., Baufreton, J., Bienvenu, T. C. M., and Herry, C. (2014b). "Prefrontal parvalbumin interneurons shape neuronal activity to drive fear expression." In: *Nature* 505.7481, pp. 92–96.
- Courtin, J., Karalis, N., Gonzalez-Campo, C., Wurtz, H., and Herry, C. (2014a). "Persistence of amygdala gamma oscillations during extinction learning predicts spontaneous fear recovery." In: *Neurobiology of Learning and Memory* 113, pp. 82–89.

CONTRIBUTIONS

The specific contributions for each figure included in this thesis are summarized in the tables below.

	Data acquisition	Data analysis	Figure preparation	Publication
Figure 3.1	NK, JC	NK	NK	Karalis et al. 2016
Figure 3.2	NK, JC	NK	NK	Karalis et al. 2016
Figure 3.3	NK, JC, FC	NK	NK	Karalis et al. 2016
Figure 3.4	NK, JC	NK	NK	Karalis et al. 2016
Figure 3.5	RR	NK	NK	Karalis et al. 2016
Figure 3.6	FC	NK	NK	Karalis et al. 2016
Figure 3.7	NK, JC	NK	NK	Karalis et al. 2016
Figure 3.8	NK, JC	NK	NK	Karalis et al. 2016
Figure 3.9	NK, JC	NK	NK	Karalis et al. 2016
Figure 3.10	NK, JC	NK	NK	Karalis et al. 2016
Figure 3.11	NK, JC	NK	NK	Karalis et al. 2016
Figure 3.12	NK, JC	NK	NK	Karalis et al. 2016
Figure 3.13	NK, JC	NK	NK	Karalis et al. 2016
Figure 3.14	JC, FC	NK	NK	Karalis et al. 2016
Figure 3.15	JC, FC	NK	NK	Karalis et al. 2016
Figure 3.16			NK	Karalis et al. 2016

NK: Nikolaos Karalis
JC: Julien Courtin
FC: Fabrice Chaudun
RR: Robert Rozeske

	Data acquisition	Data analysis	Figure preparation	Publication
Figure 4.1	NK	NK	NK	Karalis & Sirota, 2018
Figure 4.2	NK	NK	NK	Karalis & Sirota, 2018
Figure 4.3	NK	NK	NK	Karalis & Sirota, 2018
Figure 4.4	NK	NK	NK	Karalis & Sirota, 2018
Figure 4.5	NK	NK	NK	Karalis & Sirota, 2018
Figure 4.6	NK	NK	NK	Karalis & Sirota, 2018
Figure 4.7	NK	NK	NK	Karalis & Sirota, 2018
Figure 4.8	NK	NK	NK	Karalis & Sirota, 2018
Figure 4.9	NK	NK	NK	Karalis & Sirota, 2018
Figure 4.10	NK	NK	NK	Karalis & Sirota, 2018
Figure 4.11	NK	NK	NK	Karalis & Sirota, 2018
Figure 4.12	NK	NK	NK	Karalis & Sirota, 2018
Figure 4.13	NK	NK	NK	Karalis & Sirota, 2018
Figure 4.14	NK	NK	NK	Karalis & Sirota, 2018
Figure 4.15	NK	NK	NK	Karalis & Sirota, 2018
Figure 4.16	NK	NK	NK	Karalis & Sirota, 2018
Figure 4.17	NK	NK	NK	Karalis & Sirota, 2018
Figure 4.18	NK	NK	NK	Karalis & Sirota, 2018
Figure 4.19	NK	NK	NK	Karalis & Sirota, 2018
Figure 4.20	NK	NK	NK	Karalis & Sirota, 2018
Figure 4.21	NK	NK	NK	Karalis & Sirota, 2018
Figure 4.22	NK	NK	NK	Karalis & Sirota, 2018
Figure 4.23	NK	NK	NK	Karalis & Sirota, 2018
Figure 4.24	NK	NK	NK	Karalis & Sirota, 2018
Figure 4.25	NK	NK	NK	Karalis & Sirota, 2018
Figure 4.26	NK	NK	NK	Karalis & Sirota, 2018
Figure 4.27	NK	NK	NK	Karalis & Sirota, 2018
Figure 4.28	NK	NK	NK	Karalis & Sirota, 2018
Figure 4.29	NK	NK	NK	
Figure 4.30	NK	NK	NK	
Figure 4.31	NK	NK	NK	
Figure 4.32	NK	NK	NK	
Figure 4.33	NK	NK	NK	
Figure 4.34	NK	NK	NK	Karalis & Sirota, 2018
Figure 4.35	NK	NK	NK	Karalis & Sirota, 2018
Figure 4.36	NK	NK	NK	Karalis & Sirota, 2018
Figure 4.37	NK	NK	NK	
Figure 4.38	NK	NK	NK	
Figure 4.39	NK	NK	NK	Karalis & Sirota, 2018
Figure 4.40	NK	NK	NK	Karalis & Sirota, 2018
Figure 4.41	NK	NK	NK	Karalis & Sirota, 2018
Figure 4.42	NK	NK	NK	Karalis & Sirota, 2018
Figure 4.43			NK	Karalis & Sirota, 2018

NK: Nikolaos Karalis

Habe nun ach! Philosophie,
Juristerei und Medizin,
und leider auch Theologie! durchaus studiert mit heissem Bemühn.
Da steh ich nun, ich armer Tor! und bin so klug als wie zuvor!

Johann Wolfgang von Goethe - Faust (1808)

ACKNOWLEDGMENTS

I would first like to express my deep gratitude to my advisor Anton Sirota for his unflagging support over the past few years. His creativity, scientific curiosity, and intelligence have served as an inspiration and guide in our effort to understand the workings of the brain. Through our long discussions, he helped me develop as a scholar and has critically influenced my scientific thought and future directions.

I am also truly grateful to my M.Sc. thesis supervisor Cyril Herry for his dedication to my training and for exposing me for the first time to the magic world of systems and circuit neuroscience. His mentorship during my first steps in neuroscience proved catalytic for my future path.

I am grateful to Daniel Voisin and the Neurasmus organizers who opened the door of neuroscience for me by giving me the opportunity to join the program, as well as my past supervisors Ana-Luisa Piña, Marietta Zille, Irene Karanasiou and Dimitris Matthaiou for their advice and mentorship over the years. I would also like to express my indebtedness to my uncle Michalis Antonopoulos for his intellectual encouragement during my formative years, that paved my way to a life in science.

This trip would not have been as enjoyable without the company of creative and dedicated colleagues and friends. I would like to highlight the contribution of my good friends Gerrit Schwesig, Julien Courtin and Robert Rozeske, who over the years provided a wonderful intellectual environment and contributed to my scientific maturation through our extensive discussions. They were always there to troubleshoot experiments, dive in the literature, share our enthusiasm and lend a helping hand when needed. Our joint efforts have proven already fruitful and I look forward to our future collaborations. I would also like to thank Evgeny Resnik for battling with bureaucracy to ensure all of us can perform our research uninterrupted. He is a great colleague and he was always helpful with advise and tips on both technical, scientific and personal topics. I would also like to thank Jialiang Lu for the help and fun times while working together, as well as Rizwan Ahmed for the technical help. Finally, I would like to thank all my co-authors and all members of Sirota and Herry laboratories.

Over the years, I received the help of countless people in various settings and roles. Importantly, I am grateful to the mechanical and electronics workshop of the Centre for Integrative Neuroscience (CIN), as well as the personnel of the animal facilities at CIN and Biozentrum LMU, for their help and support. This work depended critically on the work of many others who contributed to the development of open-source hardware and software and graciously shared the fruits of their labor. I would thus like to express my respect and appreciation to Goncalo Lopes for developing Bonsai as well as to Josh Siegle, Jakob Voigts and all contributors to the OpenEphys project. Finally, I need to mention all the anonymous and eponymous contributors to online communities, fora and code repositories that helped generate a comprehensive knowledge-base that has accelerated my work.

Finally, I am grateful to Vasiliki Mourgela, for her love, patience and support. Most importantly, I am thankful to my parents Gerasimos and Fotini, and my brother Vasilis, for their unconditional love and unwavering support throughout the years and their constant guidance and encouragement to pursue my dreams.

CONTENTS

LIST OF FIGURES

ACRONYMS

AAV	Adeno-associated virus
ACC	Anterior cingulate cortex
ACh	Acetylcholine
ANN	Artificial neural network
ANOVA	Analysis of Variance
AP	Anterior-posterior
AUC	Area under the curve
BLA	Basolateral amygdala
BOLD	Blood-oxygen-level dependent
BötC	Bötzinger complex
CA	Cornu ammonis
CEA	Central amygdala
ChR2	Channelrhodopsin-2
CNS	Central nervous system
cre	Causes recombination
CS	Conditioned stimulus
CSD	Current-source density
DG	Dentate Gyrus
DS	Dentate spikes
DV	Dorso-ventral
EC	Entorhinal cortex
ECG	Electrocardiogram
EEG	Electroencephalogram
EMG	Electromyogram
FFT	Fast Fourier transform
GABA	γ-Aminobutyric acid
GFP	Green fluorescent protein
ICA	Independent component analysis
IL	Infralimbic cortex
IN	Interneuron
ISI	Inter-spike interval
ITI	Inter-trial interval
LEC	Lateral entorhinal cortex
LED	Light emitting diode
LFP	Local field potential
MD	Mediodorsal nucleus of the thalamus
MEC	Medial entorhinal cortex
mPFC	Medial prefrontal cortex
MRL	Mean resultant length
MSDBB	Medial septum - diagonal band of Broca
MTL	Medial temporal lobe
MUA	Multi-unit activity
NAc	Nucleus accumbens
NREM	Non-REM sleep
OB	Olfactory bulb
OSN	Olfactory sensory neurons
PAG	Periaqueductal gray area
PCA	Principal components analysis
PL	Prelimbic cortex
PN	Projection neuron
preBötC	PreBötzinger complex
PSD	Power spectral density
PTSD	Post-traumatic stress disorder
PV	Parvalbumin
REM	Rapid eye movement sleep
RMS	Root-mean-squared
ROC	Receiver operating characteristics
ROI	Region of interest
RSA	Respiratory sinus arrhythmia
SEM	Standard error of the mean
SN	Substantia nigra
SNR	Signal-to-noise ratio
SO	Slow oscillation
SVM	Support vector machine
SWR	Sharp-wave ripple
SWS	Slow-wave sleep
TTL	Transistor-transistor logic
US	Unconditioned stimulus

1

INTRODUCTION

Throughout the 19th and 20th century, a large part of the psychology and medical research focused on the study of human and animal behavior. This led to the qualitative and quantitative description of the behavioral repertoire and the traits of each species which in turn enabled the scientific discourse to proceed to the question of the source and nature of the behavioral control and the neural underpinnings of behavior (Gerard, 1955). This causal level of description has facilitated the development of animal models of human behavior and disease, that are amenable to intervention and which enables the development of therapeutic strategies for a host of somatic and mental disorders (Akil et al., 2010; Tye and Deisseroth, 2012). Importantly though, it holds the promise of allowing us to understand and improve the human condition.

A fundamental question in modern neuroscience is how neuronal circuits mediate behavior. To answer this question, we need to understand the mechanisms that underlie the coordination of neuronal activity within and across remote brain regions. Over the past century, since the first electrical recordings of brain activity, it has become evident that neuronal activity exhibits oscillatory dynamics. These patterns of activity are associated with the behavior and internal state of the organism and are believed to be important for the coordination of activity across distributed neuronal networks. Oscillatory synchronization between remote regions is believed to play a fundamental role in memory formation and retrieval, while slow and fast oscillatory dynamics during sleep are believed to underlie memory consolidation across regions.

Although brain oscillations are prominent in humans and can be recorded non-invasively, the biophysical properties of the primate brain and its enclosure in the skull present critical limitations to the study of brain oscillations. In contrast, the mouse brain exhibits a lissencephalic macrostructure and the microcircuit organization is similar to that of other mammals and humans, while there is an exhaustive literature on the mouse physiology and neuroanatomy. Further, the rich behavioral and cognitive repertoire of these animals, paired with the unprecedented genetic toolbox available for that species, establish *Mus musculus* as an ideal model organism for the detailed study of neural circuits (Luo et al., 2008).

The past decades and the advent of the 21st century saw a dramatic change in our abilities to study and intervene in the workings of the brain (Fenno et al., 2011). The successes in genetic research led to an explosion of research in the field of neuronal circuits. The new tools and techniques have provided us with an unprecedented ability to observe and manipulate the functioning nervous system of awake, freely-behaving animals (Deisseroth, 2014).

When taken together, the robust behavioral work and theoretical questions of the past centuries and the modern powerful approaches of circuit neuroscience provide a fertile ground for the

answering of tantalizing questions about the nature of the brain function. However, we still know surprisingly little about the origin, nature, and role of most observed oscillatory patterns.

To try to understand these aspects of neuronal organization and to bridge the gap between different levels of studying and understanding the brain, we utilize state-of-the-art tools and techniques of modern neuroscience to record and manipulate brain activity in freely-behaving rodents. We aim to explore the oscillatory landscape of cortical and subcortical brain regions in the mouse brain and to identify and characterize the oscillatory patterns of activity and their biophysical properties throughout behavior. Further, we aim to understand the origin and functional role of these oscillations in organizing neuronal activity across brain regions during behavior. Finally, we attempt to characterize the relationship of brain oscillations with other bodily rhythms and understand how the body and brain act in concert to optimize function and generate behavior.

By understanding the small and large-scale dynamics of brain activity, we open a window that allows us to peer into the functioning of neuronal networks, which in turn will help us understand and decode the information processing that takes place in the brain during behavior.

1.1 RELEVANCE AND SIGNIFICANCE OF THIS WORK

The different aspects of the work described herein, although not directly translatable to clinical applications, are nevertheless pertinent to a series of different questions about the function and malfunction of the brain. Taking advantage of the conserved defensive behaviors across species, fear conditioning enables the study of maladaptive defensive behavioral patterns and is utilized widely as an animal model for post-traumatic stress disorder (PTSD) and anxiety disorders. The mechanistic understanding and the unraveling of the neuronal circuits that support such disorders will potentially enable the development of strategies that ameliorate the harmful effects of traumatic experiences on the human psyche.

The present work is predominantly focused on two pathways, the one between the prefrontal cortex and the amygdala and the one between the hippocampus and the prefrontal cortex. The prefrontal cortex-amygdala pathway is known to be involved in the retrieval and expression of fear memories as well as the extinction of fear memories (Herry and Johansen, 2014). The understanding of the interaction between these structures is crucial for the understanding and resolution of the causes of PTSD (Liberzon and Abelson, 2016). The pathway between the hippocampus and the prefrontal cortex is known to be involved in both working memory and the consolidation of long-term memories (Euston et al., 2012; Maren et al., 2013), while it has become evident that the dysfunction of this pathway is causally involved in the onset and symptoms of depression, schizophrenia, and PTSD (Godsil et al., 2013; Jin and Maren, 2015).

Over the course of this work, we identified the breathing rhythm, the one perpetual vital rhythmic activity, as a potent driver of neuronal activity across all the above brain regions involved in memory and cognition. Respiration is enabling the coupling between remote brain regions and supports the information transfer between them, potentially supporting memory functions. This major finding will hopefully shift the attention of experimental work to the connection between

the body and the brain, and how the interplay of interoception and exteroception is giving rise to the embodied cognition (Thompson and Varela, 2001). As exemplified by the following experiments, respiratory changes are a hallmark of anxiety state, while in humans, cognitive control of breathing is a commonly employed technique for relaxation and the attainment of a mindful state.

A major part of the experiments in this work consists of recordings and manipulations of the brain activity in the quiet and sleeping rodent. The goal here is to study the oscillatory mechanisms that enable information transfer within and across brain structures (Buzsáki and Draguhn, 2004). These mechanisms are believed to underlie memory consolidation (Dudai et al., 2015), the phenomenon of strengthening and stabilization of memories that is linked to sleep (Diekelmann and Born, 2010; Stickgold, 2005). Importantly, disturbed sleep is a key symptom of many psychiatric diseases and an associated aspect of these diseases is memory loss (Wulff et al., 2010). Understanding the mechanisms and pathways that support memory consolidation will not only potentially enable the restoration of memory in patients but importantly will hopefully allow the editing and erasing of trauma-related memories (Agren et al., 2012). Finally, understanding the neural basis of memory encoding, consolidation, and retrieval can inform and guide the development of effective educational processes that are all the more relevant in the age of information (McGaugh, 2000).

1.2 MEMORY

The understanding of the neural correlates of learning and memory constitutes one of the major objectives of modern neuroscience. Memory refers to the property of a physical system to incorporate information from the past that influence future behavior. In biological systems equipped with a nervous system, it is defined as the ability of an organism to encode, store and retrieve information with the ultimate goal of using it in the future to provide a survival advantage (James, 1884). This property underlies adaptive behavior and is fundamental to the survival of the organism. It is known that memories of experiences are encoded in representations that consist of physical and chemical changes in neurons and their interconnections. Although memory appears to be a universal property of animals with a nervous system, it does not comprise a single system but rather multiple memory systems exist in the brain. These systems are composed of multiple brain regions, consisting of distinct but interconnected neuronal networks, involved in the encoding and retrieval of distinct forms of memories (Squire, 2004). The neurobiological implementation can be classified based on the type of information involved and its behavioral relevance. Memory systems can be classified based on multiple properties, such as anatomical level, timescale, content, and function.

Episodic memory can be defined as the memory containing information about a specific event, tied to the spatial, temporal and other situational contexts in which the event occurred (Tulving, 2002). An episodic memory must contain information about the event and its context integrated into a single representation that allows the memory to be utilized in the future to support adaptive behavior.

The hippocampus, a homologous structure existing in multiple species, together with the entorhinal cortex as well as the perirhinal and other parahippocampal cortices, forms the medial temporal lobe (MTL) and has been identified as a structure critically involved in episodic memory. Hippocampal damage results in profound anterograde and retrograde amnesia, hindering the ability to form lasting episodic and semantic memories (Scoville and Milner, 1957). Episodic memory depends on an intact hippocampus and medial temporal lobe (Cohen and Squire, 1980; Nyberg et al., 1996; Squire, 2004), while non-declarative memory is independent of MTL function (Squire and Zola, 1996; Spiers et al., 2001; Squire, 2004; Vargha-Khadem et al., 1997). The study of the hippocampal formation in relation to the episodic memory (Scoville and Milner, 1957) has revealed the central role of this system in the memory of spatial location (Penfield and Rasmussen, 1950; Olton and Samuelson, 1976; Morris et al., 1982) and particularly in the formation of an allocentric cognitive spatial map (O'Keefe and Dostrovsky, 1971; O'Keefe and Conway, 1978). Since the pioneering work of John O'Keefe and the discovery of place cells in the rodent hippocampus (O'Keefe and Dostrovsky, 1971) the existence of cognitive representations of the environment (Tolman, 1948) is well accepted. Place cells are sparsely representing space and their ensembles activity is encoding the instantaneous position of the animal (Wilson and McNaughton, 1993). In the hippocampus, the dentate gyrus (DG) subregion is unique to mammals (Treves et al., 2008) and its anatomy makes it ideal for pattern separation (Yassa and Stark, 2011), since it contains an order of magnitude more cells than its main input, the entorhinal cortex, while the intrinsic connectivity is dominated by local interneurons. This enables the sparsification of the input, both in terms of the number of active cells but also at the level of the neuronal activity (Leutgeb and Leutgeb, 2007).

Throughout life, animals have a variety of experiences that form distinct episodic memories. Some events are more relevant to the behavioral needs and informative for future behavior, whereas others are inconsequential. The retention of all the collected information for extended periods would be difficult, inefficient and redundant. The majority of the events are gradually forgotten, while some experiences can and do persist in memory for many months or years (Russell and Nathan, 1946). Forgetting can be either the result of the decay of the memory trace or of the overwriting of the trace by a new memory, a phenomenon termed retroactive interference. Interestingly, the susceptibility of memory to disruption is inversely proportional to its age (Ribot, 1882; Russell and Nathan, 1946). This hypothesis has been confirmed by a century of accumulating evidence showing that the most recent memories are most sensitive to hippocampal damage and other perturbations such as electroconvulsive stimulation and protein synthesis inhibitors (Squire, 1975; McGaugh, 2000; McGaugh, 2015). The extent of retrograde amnesia is proportional to the hippocampal damage incurred, ranging from a few months to decades.

The phenomenon of temporally graded retrograde amnesia has given rise to a two-stage model for long-term memory (Marr, 1971; Buzsaki, 1989). According to this model, memories are initially stored during awake behavior in the hippocampus, while during the subsequent sleep the memory traces are progressively transferred to the sites of their permanent storage that reside in

the neocortex (Stickgold, 2005). In artificial neural networks (ANNs), such as Boltzmann machines and deep belief networks, it has been shown that the alternation between online (wake) and offline (sleep) states enhances memory encoding and maintenance (Hinton et al., 2006; Hinton et al., 1995). During the sleep state, the ANN is not receiving external inputs and its output is re-entering the input layer of the network via feedback connections. This process alters the weights of the feedforward connections. During awake the reverse process takes place and the external inputs modify the feedback connections. This model has striking similarities to the suppression of sensory inputs to the neocortex during sleep. Moreover, the training process of such network necessitates multiple iterations of the sleep-wake loop, similarly to sleep-dependent memory consolidation. This reversal of the information flow serves the comparison of the recent information with the pre-existing representations (Ackley et al., 1985). This enables the stabilization of the novel representation (Hopfield et al., 1983) and the avoidance of catastrophic interference (McClelland et al., 1995), a phenomenon that can devastate the performance of ANNs employing distributed representation, as is the case for the mammalian neocortex. It has been proposed that animal sleep serves a similar function (Crick and Mitchison, 1983; Sejnowski, 1995) and computational models supporting this role have been elaborated (Treves and Rolls, 1994; Lörincz and Buzsaki, 2000).

While all episodic-like memories are initially labile, a subset of memories undergoes a process of consolidation enabling its retention for longer time. Memory consolidation refers to the process by which labile newly formed memory traces are progressively strengthened, stabilized and integrated with the pre-existing memories (McGaugh, 1999; Lechner et al., 1999). The selection of memories that will be consolidated is believed to be mediated by dopaminergic activity during learning in the VTA and the locus coeruleus (Takeuchi et al., 2016; Sara, 2015). Memory consolidation comprises a wide set of processes acting at different levels. Synaptic consolidation depends on protein synthesis and acts at the cellular level, whereas systems consolidation involves the interaction and information transfer across remote brain structures. This reorganization of the new information is preferentially taking place during sleep and over the years there have been accumulating evidence suggesting a role of sleep in the process of systems consolidation and the retention of previously learned information.

The two types of consolidation, synaptic and systems consolidation, are not mutually exclusive but rather occur independently, at a different level of organization and importantly at a different timescale while serving different purpose (Dudai, 2004, 2012; McGaugh, 2000). Synaptic consolidation takes place shortly after memory encoding, enabling the short-term retention of the acquired information. Essentially this process stabilizes the synaptic connectivity changes and tags the memories that might later undergo systems consolidation. Protein synthesis is necessary for late-phase synaptic plasticity and synaptic consolidation. Importantly, without the process of systems consolidation, these memories would not be retained for long, although the exact duration of their retention remains unclear and is highly dependent on the nature of the particular memory.

Systems consolidation is a longer process that can last hours to weeks during which memories are believed to be gradually reorganized within and across neural circuits (Squire and Cohen, 1979). While encoding and short-term expression of memories rely on the hippocampus, accumulating evidence suggests that with the passage of time, the neocortex becomes involved in the retrieval of remote memories, which become partly independent from the hippocampus (Frankland and Bontempi, 2005; Wiltgen et al., 2004). In parallel, the remote memories become dependent on the prefrontal and anterior cingulate cortices (Frankland et al., 2004; Maviel et al., 2004; Wang et al., 2009; Wang and Morris, 2010), which also support remote spatial (Teixeira et al., 2006) and object memories (Weible et al., 2012). Further, secondary sensory cortices support the memory storage and long-term memory retrieval of sensory stimuli in a modality-specific way (Sacco and Sacchetti, 2010; Weinberger, 2004). Interestingly, the site of long-term storage in the neocortex is tagged during learning (Lesburguères et al., 2011; Kitamura et al., 2017). This type of systems consolidation appears to be a general principle of memory consolidation across species, since it seems to be true also for invertebrates (Frankland and Bontempi, 2005).

The formation of additional representations within the cortices and the hippocampal formation has been referred to as the 'multiple-trace' hypothesis (Atkinson and Shiffrin, 1968; Nadel and Moscovitch, 1997; Winocur et al., 2010). According to this model, the hippocampus maintains an index for the neocortical memory traces and supports the complete and efficient retrieval of remote memories (Teyler and DiScenna, 1986). Further, it has been proposed that the consolidation of episodic memories and their redistribution in neocortical sites underlies the abstraction of episodic memories and their transformation to semantic memories (McClelland et al., 1995; Buzsaki and Moser, 2013). However, the relationship between episodic and semantic memories remains unclear. A related concept is the generalization of episodic memories into "schemas" (Bartlett, 1932; Tse et al., 2007), a process believed to take place in cortical networks and that is related to the long-attributed role of mPFC in generalizing related experiences and extracting the general concept (Preston and Eichenbaum, 2013).

1.3 NEURONAL ASSEMBLIES

Experience is known to induce long-lasting changes in the brain, a phenomenon termed plasticity (Krech et al., 1964). During behavior, information about the external and internal sensory world is collected and imprinted in the brain. This is achieved by chemical and structural modifications onto a subset of cells that form the "engram" of the memory onto the neuronal network. Presumably, the reactivation of the same subset of cells is enough to trigger the recollection of the memory. A critical milestone towards understanding the neural mechanisms underlying memory is the elucidation of how populations of individual neurons form network representations of events and how these representations are transformed with time across distinct brain structures and form memory traces.

Encoding of information in a neuronal network is believed to occur either via a rate code, according to which the instantaneous firing rate carries the information to the downstream targets, or via a temporal code, in which case the exact timing and sequence of spiking inputs to a neuron is the unit of information (Decharms and Zador, 2000; Theunissen and Miller, 1995). Similarly, at

the output level, different neuronal types and in different behavioral or neuromodulatory states can exhibit distinct types of firing, ranging between sparse firing of single action potentials to complex bursts of many spikes in a few milliseconds (Ranck, 1973) which are believed to support spike transmission and plasticity induction (Lisman, 1997; Xu et al., 2012).

These coding schemes correspond to the ability of neurons to act as either coincidence detectors or as temporal integrators. Effectively, the mode of operation for different cells determines the coding scheme and plasticity mechanisms employed (Abeles, 1982; König et al., 1996). The different types of neural coding are not mutually exclusive and can be employed in parallel or at different times and in different structures.

In the case of coincidence detection, the cells necessitate coincident inputs from distinct sources, arriving potentially on different dendritic compartments, in order to be sufficiently depolarized. Synchronized inputs support the propagation of activity and the induction of plasticity (Buzsaki and Chrobak, 1995; MacLeod et al., 1998; Nicolelis et al., 1995; Salinas and Sejnowski, 2001; Singer, 1999; Varela et al., 2001; Buzsaki and Draguhn, 2004; Womelsdorf et al., 2007). In the case of temporal integration, persistent inputs to a cell over time culminate in its depolarization. The integration window corresponds to the EPSP width, which is in the order of 10-30ms (Magee, 2000; Spruston and Johnston, 1992; Destexhe et al., 1999b). In addition to the intrinsic properties of the cell, different interneurons have unique properties in terms of the targeted neuronal compartment and temporal specificity of their action, which increases the possible modes of input processing performed in the single neuron level (Milstein et al., 2015).

In the past decades, it has become evident that the representation of information is reflected in the functional organization of neurons into coordinated sequential cell assemblies (Hebb, 1949), that represent anatomically distributed and interconnected neuronal populations that are repeatedly co-activated in the timescale of 10-30ms (Harris et al., 2003). Cell assemblies are primarily formed based on the structural connectivity between cells (Ko et al., 2013, 2011) and internally generated internal dynamics. In addition to these factors, inputs to the network, such as low-order sensory inputs or higher-order pre-processed information from another structure, activate an assembly and trigger its association with other assemblies and valence information. Each neuron can participate in multiple assemblies, which enables the association and interrelation of information (McNaughton and Morris, 1987). The repeated coincident activation of a subset of neurons is sufficient to recruit them to a neuronal ensemble that can be spontaneously reactivated, triggered by the activity of even one of its members (Carrillo-Reid et al., 2016). These properties of neuronal ensembles result in the formation of network attractors which enable the implementation of pattern completion (Hopfield, 1982).

One of the fundamental questions is how specific memories are allocated to a particular subset of cells and what are the determinants of participation in an ensemble. Evidence from a range of structures, including the lateral amygdala (Han et al., 2009; Zhou et al., 2009; Yiu et al., 2014; Gouty-Colomer et al., 2015), insular cortex (Zhou et al., 2009) and dentate gyrus (Park et al., 2016), suggests that temporally specific intrinsic excitability (Yiu et al., 2014), mediated by the expression of the transcription factor CREB (Zhou et al., 2009). Interestingly, artificial place-conditioned

depolarization of single DG cells is enough to inherit them with place-cell properties (Diamantaki et al., 2016). Depolarized cells are preferentially recruited in neuronal ensembles (Han et al., 2007; Zhou et al., 2009; Choi et al., 2011; Garner et al., 2012; Yiu et al., 2014; Stefanelli et al., 2016; Diamantaki et al., 2016), while vice-versa associative learning and ensemble participation is associated with induced depolarization (Moyer et al., 1996; Thompson et al., 1996).

1.4 FEAR MEMORY

Fear can be elicited either by innately fearful stimuli, such as the odor or sight of a predator, or can be a learned association between a neutral stimulus and an aversive event. Over the past decades, classical auditory and contextual fear conditioning has emerged as a powerful behavioral model to study the neuronal basis of learning and memory as well as the neural circuits underlying the learning, expression and regulation of fear responses (Davis, 1992; LeDoux, 2000). In this behavioral model, fear memory is formed after the repeated association of a previously innocuous auditory stimulus (the conditioned stimulus; CS) with a coincident mild aversive stimulus (unconditioned stimulus; US). After fear conditioning, re-exposure to the CS elicits a wide range of conditioned fear-related behavioral and physiological responses. In addition to the explicitly associated CS, the animals exhibit fear responses selectively to the context where the US was experienced, but not when exposed to a novel context (Blanchard and Blanchard, 1972; Bolles et al., 1980).

Fear conditioning is a valuable tool in the study of memory since it can be acquired rapidly (single-trial learning) and gives rise to a long-lasting and even life-long memory (Gale et al., 2004). Interestingly, fear conditioning has been successfully employed in a variety of vertebrate and invertebrate animal models as well as single-cell organisms, enabling comparative approaches for the study of universal learning principles and their neural implementation (Watson and Rayner, 1920; Rescorla, 1968; Dudai et al., 1976). Fear conditioning as a form of associative learning can be understood as the learning of hierarchical relationships between events that enables the rich neural representation of the environment (Rescorla, 1988). This learning is facilitated by the informational value of the CS regarding the US occurrence (Rescorla and Wagner, 1972). Contextual conditioning has provided a very valuable tool for the study of memory consolidation (Squire and Alvarez, 1995; Squire, 2004) and the time-limited role of the hippocampus in memory retrieval (Kim and Fanselow, 1992). In contextual fear conditioning, the animals associate a particular physical environment with the unconditional stimulus (US). In contrast to auditory fear conditioning, the conditioned stimulus(CS) is not explicit and synchronously presented with the US (Fanselow, 1990). Instead, the CS consists of the implicit features of the environment where the US is experienced (Blanchard and Blanchard, 1969; Bolles and Collier, 1976). Thus, it necessitates the processing of multimodal sensory information consisting of persistent environmental features.

In order to survive threatening situations, animals have developed innate defensive coping strategies. The fear-related behavioral repertoire of different animals in response is wide (Bouton and Bolles, 1980), while fear expression typically involves elements from three levels of responses, behavioral, autonomic and endocrine (Davis, 1992).

Fear memory retrieval elicits various stereotypic conditioned fear responses, including an immobilization reaction termed freezing (Blanchard and Blanchard, 1969). Freezing is typically defined as a postural immobilization of the animal, characterized by the absence of any movement except for respiration. However, the animal is an awake, highly vigilant state, associated with increased muscle tone and deep breathing and can be considered as a preparatory state, with the animal being capable to switch rapidly to a "fight or flight" escape behavior. This state is in stark contrast to the relaxed immobilized posture and reduced vigilance exhibited during sleep or quiet wakefulness. A characteristic of the fear-related vigilance is the potentiation of acoustic startle responses, a reflexive muscle contraction that is part of the defense mechanism (Davis, 1989; Koch, 1999). During fear state, in addition to the freezing behavior, animals exhibit reduced propensity to explore and locomote (Hebb, 1946; Blanchard et al., 1990), interact with conspecifics (File, 1980) or to seek food or reward (Leaf and Muller, 1965) and engage in other conditioned responses (Estes and Skinner, 1941; Fanselow et al., 1988; Kim et al., 1996).

1.5 FEAR CIRCUITS

Decades of research have revealed a widely distributed network of brain structures differentially involved in the acquisition and expression of fear and extinction memories. These regions include the extended amygdaloid complex, the ventral hypothalamus, the medial prefrontal cortex and the hippocampus.

Although the hippocampus is involved in neither the acquisition nor the expression of auditory conditioned fear memory, it has been repeatedly shown that an intact hippocampus is necessary for the processing of contextual stimuli (Bast et al., 2003; Stiedl et al., 2000) and the acquisition (Anagnostaras et al., 2001; Phillips and LeDoux, 1992) and expression (Kim and Fanselow, 1992) of contextual fear memory (Curzon et al., 2009), in rodents and humans alike (Alvarez et al., 2008; Marschner et al., 2008). In contrast to the differential role of the hippocampus, both contextual and cued fear memory depend on the amygdala (Phillips and LeDoux, 1992; Gale et al., 2004; Poulos et al., 2016).

Amygdala is an almond-shaped structure of the medial temporal lobe (Burdach, 1822; Meynert, 1868), part of the olfactory system and remarkably phylogenetically conserved across evolution and believed to originate at least from the ancestral tetrapods (Pabba, 2013). Amygdala stimulation elicits feelings of fear or anxiety in humans, accompanied by autonomic responses (Chapman et al., 1954). In the past century, mounting evidence established the role of the amygdaloid complex in fear learning and expression (LeDoux, 2000; Tovote et al., 2015).

The amygdaloid complex consists of more than ten nuclei, forming 3 main subdivisions: basolateral (BLA), cortical, and centromedial amygdala (CEA) (Aggleton, 2000; Sah et al., 2003). BLA and CEA are two structures that have been predominantly involved in fear learning and expression. BLA is reciprocally connected with the hippocampus and rhinal cortices (McDonald, 1998) as well as the medial prefrontal cortex (mPFC) (Cassell and Wright, 1986). In terms of connectivity with the prefrontal cortex, LA is reciprocally connected with the infralimbic cortex

(IL) while the BA targets the anterior cingulate cortex (ACC), the prelimbic cortex (PL) and the infralimbic cortex (McDonald, 1991; Hoover and Vertes, 2007).

During fear conditioning, sensory inputs from every modality, such as auditory (LeDoux et al., 1990), visual (Shi and Davis, 2001) and olfactory (Luskin and Price, 1983a), are relayed via both a direct thalamic (internal capsule axons) and via an indirect cortical pathway (external capsule axons) to the BLA and the CEA (Maren and Quirk, 2004). Recently a feedback projection from LA to the auditory cortex was identified, that undergoes synaptic remodeling after fear learning (Yang et al., 2016). This opens the possibility of the existence of other yet unknown feedback projections to other cortices.

Inputs from multiple sensory and limbic brain structures such as the BLA, hippocampus and entorhinal cortex are converging to the medial prefrontal cortex (mPFC), where they are integrated. mPFC has been involved in almost every task and behavior examined, which is to be expected given the wide afferent and efferent connectivity of this structure. mPFC has been implicated in the regulation of many brain functions related to working memory, attention, emotional behavior (Fuster, 2015) and adaptive executive control (Euston et al., 2012), while dysfunction of the prefrontal circuits has been involved in psychiatric disorders such as post-traumatic stress disorder (PTSD) and anxiety disorders (Shin, 2006; Pitman et al., 2012). mPFC is believed to support executive control (Miller, 2000) and behavioral inhibition (Narayanan and Laubach, 2006), while prefrontal damage diminishes the ability to suppress impulsive responses (Kim and Lee, 2011). mPFC is involved in attention (Dias et al., 1996; Kim et al., 2016), working memory (Floresco et al., 1997; Spellman et al., 2015), goal representation, action and conflict monitoring (Mansouri et al., 2009), cognitive flexibility and strategy shifting (Milner, 1963; Durstewitz et al., 2010; Peyrache et al., 2009). Along the same lines, stress is known to modify the architecture and function of the mPFC and is resulting in cognitive deficiencies (Arnsten, 2015), while mindfulness meditation induces functional changes to the mPFC (Tang et al., 2015).

Based on the classic characterization, the rodent mPFC comprises four subregions: the frontal cortex area 2 (Fr2), the anterior cingulate cortex (ACC, area 24b), the prelimbic region (PL, area 32) and the infralimbic region (IL, area 25) and it is distinguished by the lateral prefrontal cortex and the orbitofrontal cortex. The distinction between the prefrontal subregions is based on cytoarchitectonic differences as well as patterns of anatomical projections (Vertes, 2006). The Fr2 has vastly different connectivity compared to other mPFC areas and is a premotor region. The PL is characterized by a disorganized layer 5, in contrast to the well-defined layer 5 of the ACC. The IL can be separated from the PL based on the prominent and wide layer 2 and the lack of borders between different layers (Eden and Uylings, 1985). Interestingly, the PL is characterized by a very low number of PV-expressing interneurons (almost completely absent in the superficial layers) as well as very sparse amygdalar input and a prominent shift of the location of BLA-projecting neurons to deeper layers an d a prominent input from the midline thalamus (Matyas et al., 2014).

The two defining characteristics of the medial prefrontal cortex (mPFC) are the reciprocal connections to the mediodorsal thalamus (MD) and its agranular nature (Uylings and Eden, 1990). Recent findings elaborate on the known patterns and suggest a topography of inputs from lateral

MD towards the medial MD and midline thalamus to the dorsal and ventral mPFC subregions of the mPFC respectively (Matyas et al., 2014). The thalamus is reciprocally connected to the cerebral cortex. It innervates massively the neocortex, including the mPFC, conveying sensory as well as non-sensory information (Jones, 1985). These pathways have been termed specific and non-specific respectively (Groenewegen and Berendse, 1994) and are known to underlie distinct cortical responses, namely the "augmenting" and the "recruiting" response, with unique electrophysiological profile (Morison and Dempsey, 1943; Jasper, 1949). In return, it receives massive projections from deep cortical neurons.

The various subregions of the mPFC are involved in different functions of the complex repertoire of mPFC (Uylings et al., 2003) and they have been implicated in various aspects of fear behavior (Waterhouse, 1957). PL is involved in fear expression, projecting to BLA PNs that in turn project to CEA (Pape and Pare, 2010). Specifically, BA neurons that are active during fear expression project specifically to the PL (Senn et al., 2014) and PL neurons are activated during fear expression (Herry and Mons, 2004; Sotres-Bayon et al., 2012; Burgos-Robles et al., 2009), while the expression of fear memory depends critically on the PL activity (Vidal-Gonzalez et al., 2006; Corcoran and Quirk, 2007; Laurent and Westbrook, 2009; Sierra-Mercado et al., 2010). Sustained firing of PL neurons during CS presentation correlates with fear expression but not fear extinction (Milad and Quirk, 2002; Burgos-Robles et al., 2009; Sierra-Mercado et al., 2010), while chemical lesion of medial frontal cortex reduces autonomic (Buchanan and Powell, 1982) and behavioral fear responses (Frysztak and Neafsey, 1991). Surprisingly, mPFC cells with similar anatomical and electrophysiological properties exhibit distinct activity during behavior, better characterized by the projection pattern of the cells (Ye et al., 2016). Prefrontal PV-expressing interneurons are necessary for the expression of fear behavior (Carlén et al., 2012), receive BLA input (Gabbott et al., 2006) and PV-mediated disinhibition of prefrontal PNs projecting to BLA is necessary and sufficient to drive fear expression (Courtin et al., 2014b). Further, it has been suggested that PL contributes to the renewal of conditioned fear responses after extinction (Knapska and Maren, 2009; Knapska et al., 2012). A subset of ACC neurons reduce their firing during freezing and increase their firing upon freezing offset in trace fear (Steenland et al., 2012). In parallel, mPFC and ACC are involved in the fear learning and the formation of aversive memories (Smith et al., 1992; Bissière et al., 2008), while long-term depression (LTD) of this structure facilitates extinction learning (Klavir et al., 2012). This might be partly associated with the involvement of the ACC in pain experience (Johansen et al., 2001) and perception (Wiech et al., 2006), related to the fact that electrical or chemical stimulation of the ACC elicits vocalizations (Jürgens, 2009), cardiovascular responses (Buchanan et al., 1985), autonomic (Damasio et al., 1990) and fear behavior (Johansen and Fields, 2004; Tang et al., 2005). Interestingly, certain autonomic responses are mediated by prefrontal but not amygdala circuits (Tranel and Damasio, 1989).

1.6 OSCILLATORY PATTERNS OF ACTIVITY

The activity in the brain is to a large extend rhythmic. This fact was appreciated already from the first intra- and extra-cranial recordings obtained from humans and other animals (Caton, 1875; Berger, 1929; Adrian, 1942, 1944). The mammalian cerebral cortex generates a host of distinct

oscillations in different frequencies which can be recorded using electrodes placed on the surface of the brain (electrocorticography - ECoG), the scalp (electroencephalography - EEG) (Berger, 1929) or in the extracellular space (extracellular electrophysiology) (Adrian and Zotterman, 1926a).

EEG records the extracellular ionic current dipoles produced by the post-synaptic potentials in the superficial layers of the cortex. When recording from the surface of the skull, cortical currents have to go through multiple conductive and resistive layers (cerebrospinal fluid, meninges, skull, and scalp) (Srinivasan et al., 1996), and are thus undergoing filtering and diffusion. Consequently, the signals recorded from the surface are distorted and spatially smoothed. At a given point on the scalp, the signal is a mixture of signals generated in multiple underlying brain sources and varying distances (5-9 cm in humans) (Nunez and Srinivasan, 2006) and volume conducted (Makeig et al., 1996). The EEG signal thus represents the synchronous average activity of thousands of cells in the vicinity of the electrode. A popular alternative to the EEG is magnetoencephalography (MEG), which takes advantage of the fact that the skull and scalp are transparent to magnetic fields. This allows the recording of cortical activity without the dumping effect of skull and scalp on the propagation of electrical activity which enables a finer spatial resolution (Buzsáki et al., 2012a).

Local field potential (LFP) is the spontaneous, induced, or evoked electrical activity recorded using an electrode placed inside the brain and specifically in the extracellular space of a particular brain structure. Although the nature and biophysics of this signal are the same as the EEG, the main difference is the spatial scale of integration and spatial smoothing between the two. Since the LFP signal is not filtered by the skull and meninges, it reflects a less distributed activity and that is the reason for the adjective "local" (Lindén et al., 2011). ECoG stands between EEG and LFP in terms of the spatial extent of the underlying sources.

Extracellular potentials are generated from electrical currents flowing across the cellular membrane from or into the extracellular medium (Buzsáki et al., 2012a). Any excitable element of the neural circuitry contributes to the generation of the extracellular field. Any cell membrane that allows current flow contributes with different polarity to the observed LFP. Current flow towards the inside of the cell is termed sink, while current flow towards the outside is termed source. A source-sink pair comprises a dipole and constitutes the core of the generated extracellular potential. The mainstream interpretation of neuronal LFP relies on the simplified abstraction of neuronal cells, which lies far from the complex 3D morphology of neurons (Gulyás et al., 2016). In this view, a neuron can be approximated by an electrical circuit, which follows Kirchhoff's free-charge conservation law. Accordingly, the total membrane current of a cell is always zero. This fact necessitates that there is no charge accumulation in the circuit. A given excitatory input (sink) to a dendrite results in excitatory post-synaptic current (EPSC) in the form of an influx of Na^+ into the dendrite and the generation of the corresponding excitatory post-synaptic potential (EPSP). However, to maintain the zero membrane current, an instantaneous low-amplitude passive return current of opposite polarity is distributed along the cell and is entering the cell from the extracellular space by means of ions passively diffusing across the cell membrane towards the extracellular space (Gulyás et al., 2016; Buzsáki et al., 2012a). In general, the fields generated

by synaptic and return currents cancel each other out. However, recent observations raise the possibility of the additional existence of electric monopoles due to charge inertia (Hunt et al., 2011; Riera et al., 2012; Destexhe and Bedard, 2012). In addition to the excitatory and inhibitory post-synaptic potentials, that constitute the dominant sources of oscillatory extracellular fields, spike afterpotentials such as Ca^{2+}-mediated potassium currents (Nadasdy et al., 1999) and intrinsic currents (Jutras et al., 2009; Buzsaki, 2002).

The observed field is resulting according to the principle of electric superposition, i.e. the linear and algebraic summation of the transmembrane currents generated from various excitable elements (Eccles, 1951). The final waveshape of the extracellularly reflected field depends on both the spatial and temporal characteristics of the contributing signals. Importantly, the density and alignment, as well as the synchronization of each underlying signal source, will dictate the final result (Buzsáki et al., 2012a). Depending on the neuronal architecture and anatomical organization of the particular region, the formed dipoles can be aligned or randomly distributed. When the dendritic trees of multiple cells are parallel to each other, such as in a cortical column, the currents are summed forming an open-field configuration (Lorente de No, 1947) and the generated potentials are amplified. In contrast, in subcortical nuclear structures, the disordered arrangement of neuronal subtypes and neuronal sub-compartments results in the cancelation of currents and small-amplitude field potentials.

Due to the dipolar field nature of the signal that gives rise to the LFP, the power drops as a function of the square of the distance from the electrode ($1/r^2$), an effect attributed to the properties of electrical dipoles as well as the capacitive and resistive elements in the tissue that dictate the extracellular conductivity (Pettersen and Einevoll, 2008; Nunez, 1998; Bédard et al., 2006b). Consequently, LFPs reflect the activity of local populations of neurons (a few thousand cells) and the signal can change over a few hundred microns (Holsheimer and Feenstra, 1977; Katzner et al., 2009). Action potentials typically form concatenated dipoles (quadrupoles) and this signal attenuates as a function of $1/r^3$ (Milstein and Koch, 2008). As a result, neural spikes are recorded only within few tens of microns from the cell body (Gold, 2006). The wave-shape changes as a function of the position and distance of the cell body to the electrode site and thus enables the identification of the spiking activity from multiple nearby neurons. Using multiple closely spaced electrodes (such as tetrodes and polytrodes) allows the successful blind-source separation from multiple cells (Neto et al., 2016).

However, LFPs can also reflect passively volume-conducted signals from far regions that are not related to the local population (Sasaki, 1975; Kajikawa and Schroeder, 2011). Volume-conduction of signals can be modeled with the quasi-static approximation of Maxwell equations (Plonsey and Heppner, 1967), ignoring inductive, magnetic, and propagative effects which is true for frequencies considered in the LFP (<500Hz) (Robinson, 1968). However, in practice, the inhomogeneity and anisotropicity (Nicholson, 1965) of the brain tissue can complicate the interpretation of such models. Neurons are commonly considered as electrotonically compact cylinders with no capacitive effect and embedded in an Ohmic medium (perfectly resistive and non-capacitive) (Lorente de No, 1947; Freeman and Nicholson, 1975). However, the extracellular

space is not a homogeneous fluid, but rather neuropil consists of a compact mixture of fluids inside narrow spaces (200Å) and membranes (Spocter et al., 2012; Peters and Sethares, 1991) and appears to have non-ohmic properties (Gomes et al., 2016), a fact that contributes in a non-trivial manner to the generation of field potentials. Direct measurements of the impedance spectrum of the brain reveal that gray matter is largely isotropic with resistance in the order of 3Ω (Ranck, 1963; Mitzdorf, 1985; Logothetis et al., 2007), between and across columns in the cortex, whereas white matter is characterized by anisotropic resistance, with the direction of the fibers having lower resistance (Nicholson, 1965; Logothetis et al., 2007). Finally, there have been reports of behavior and activity-dependent dynamic and layer-specific changes in the resistivity of the brain (López-Aguado et al., 2001) that can further complicate the interpretation of the recorded signals.

When recording the extracellular field, we are capturing the composite image of the local activity in the vicinity of the electrode. However, to understand the profile of inputs that the local network receives, we need to characterize the pattern of transmembrane current flow and identify the location of the current sources that contribute to the LFP. To do this we need to record or estimate the flow of current across somatodendritic axis (Buzsáki et al., 2012a). To achieve this, we need to record the local field simultaneously from multiple points across this axis and calculate the current-source density (CSD). CSD is the net membrane current in a local volume and is estimated by solving the electrostatic forward problem using the second-order spatial derivative of the extracellularly recorded local field potential, under the assumption of a homogeneous and isotropic medium (Nicholson and Freeman, 1975; Freeman and Nicholson, 1975; Mitzdorf, 1985). Net outward membrane current results in a current source, while net inward current results in current sink. Identifying pairs of current sinks and sources, taken together with the prior knowledge of the anatomy of a brain region, allows the identification of neuronal dipoles that reflect the soma and dendrites of a subset of cells that receive the corresponding synaptic input. Due to the nature of the spatial differentiation, CSD allows us to overcome the effect of volume conduction and work on locally generated signals since the volume conducted signals appear identical in the nearby channels and are canceled by the differentiation.

LFP signals follow two basic laws that dictate many of the observed properties. First, the LFP exhibits a pink (or 1/f) noise structure, meaning that the frequency spectrum is linear in logarithmic scale (Buzsáki, 2006; Buzsaki and Mizuseki, 2014). This phenomenon has at least two different sources. The properties of the extracellular medium that dictate ionic diffusion (Bédard et al., 2006b,a; Gomes et al., 2016) and the morphology of the local neurons (Pettersen and Einevoll, 2008) underlie the frequency-specific filtering of LFPs. First, the capacitive elements of the medium (i.e. neural tissue), contribute to a low-pass filtering property (Nunez, 1998; Bédard et al., 2006b,a). Additionally, the faster oscillations (short periods), only allow time for a small subset of neurons to fire in a given cycle. Slower oscillations, however, enable many more cells to get involved and the temporal overlap of the corresponding synaptic currents, resulting in stronger mean fields. These differences in the number and spatial distribution of cells engaged in different oscillations, a result of the axonal conductance speed and the synaptic delays, bestow the neuronal circuits with an intrinsic low-pass filtering. As a result, slower oscillations travel further

and exhibit wider spatial correlation compared to faster oscillations and spiking activity (Destexhe et al., 1999a). The second basic property of EEG signals is self-similarity of the spectra across scales (from few hundred micrometers and a few thousand cells in LFP to tens of centimeters and millions of cells in EEG).

1.7 ROLE AND FUNCTION OF NETWORK OSCILLATIONS

Network oscillations and self-organizing dynamics are a prominent feature of neuronal circuits. Their ubiquity has provided room for hypotheses about their potential role in as a mechanistic substrate for the encoding and retrieval of memories as well as the communication and information transfer between structures. However, to this day, there is only scarce evidence about this role. The major limitation that is slowing down the progress on this front is the intricate and inextricable relationship of network oscillations with the activity of the neurons that participate in these phenomena.

In order to understand the role of oscillations in shaping neuronal activity, we have to clarify the mechanisms that generate and maintain them. From the standpoint of one individual neuron, its participation in the oscillation is dictated by two parameters: (a) its connectivity pattern with excitatory, inhibitory and neuromodulatory cells within and across brain regions and (b) its intrinsic resonance properties, inherited to the cell by the molecular machinery and intracellular cascades. Importantly, the connectivity patterns are not static but are rather dynamically changing as a function of behavior and plasticity.

In concert, these parameters modulate the participation of a subset of cells in a given oscillation. The subset of cells active during the depolarizing cycles of an oscillation is believed to form a dynamically changing "neuronal ensemble" (Gray et al., 1989; Singer and Gray, 1995; Buzsáki and Draguhn, 2004; Womelsdorf et al., 2007; Ikegaya et al., 2004; Engel et al., 2001; Harris et al., 2003; Singer, 1993). This coordinated activity of neurons belonging to the same ensemble provides temporal windows for plasticity induction. In this view, neurons are not actively selected to participate in an oscillation but rather the cells that fulfill the criteria for participation in a given cycle are participating and given the opportunity to join the active ensemble. Along these lines, oscillations provide the rhythmically recurring opportunities for ensemble formation or disassembly. The known mechanisms for synaptic plasticity induction require the synchronized activity of pre- and post-synaptic cells with millisecond precision. Suitably, the depolarizing phase of a gamma cycle is lasting 5-15ms. The coordinated depolarization of a cell ensemble during this short time is ideal for the induction of spike timing dependent plasticity (STDP). Interestingly, typically neural oscillations are asymmetric (Cole and Voytek, 2017) and exhibit features of non-harmonic oscillators (Sirota and Buzsaki, 2005). The shape and asymmetry of the waveform reflect the contributing elements as well as the processing and potential role of the underlying activity (Buzsáki et al., 2003). However, the read-out of such information is not straightforward, although occasionally higher-order information can be decoded from such features (Agarwal et al., 2014; Taxidis et al., 2015).

In contrast to fast oscillations that are locally generated and arise from the concerted interaction of excitatory and inhibitory cells, slower oscillations tend to be generated by external pacemakers, cells that are intrinsically rhythmic and provide strong input and neuromodulation to the local network. Due to the nature of their generation, slower oscillations typically entrain large populations of neurons and consequently modulate the power and occurrence of faster local oscillations. This supports their role in facilitating the long-range interaction between remote brain regions. This is achieved by means of the coherent fluctuations in cellular excitability of neuronal populations across distant brain regions. It is important to note that without such modulation of the faster oscillations by the slower oscillations, it would be difficult to implement plasticity mechanisms across regions, due to the limited conduction velocities and synaptic delays. Additionally, the rhythmic occurrence of fast oscillations with the frequency imposed by the slower oscillations is repetitively reactivating the neuronal ensembles in time-scales conducive to long-term potentiation. This combination of STDP in faster timescale and LTP in slower timescale is believed to underlie encoding of memories (Bliss and Lømo, 1973; Bliss and Gardner-Medwin, 1973; Levy and Steward, 1983; Markram et al., 1997)

By far the most popular role attributed to oscillations is that of a scaffold for the information transmission between remote brain regions (Fries, 2015; Engel et al., 2001). According to these theories, the phase synchronization between brain regions is underlying the flow of information between these structures, presumably by coordinating faster dynamics and organizing the synchronous activation of neuronal ensembles in both structures (Varela et al., 2001). The phase offset between the oscillations in the two regions provides a hint for and a potential mechanism for the directionality, which can be dynamically controlled and reversed (Sirota and Buzsaki, 2005; Buzsáki and Draguhn, 2004).

A further important aspect of neuronal oscillations is exemplified in the entorhinal-hippocampal circuit, where the phase of the CA1 theta oscillation modulates distinct gamma oscillations related to either entorhinal or CA3 (Montgomery and Buzsaki, 2007). This is providing an elegant mechanism for the temporal segregation of information transfer and processing in different phases of the same oscillation. Importantly, the rhythmic alternation between the two different input streams is potentially not coincidental and might relate to the computational properties of the circuit in the context of memory encoding and retrieval (Hasselmo et al., 2002; Hasselmo, 2005; Colgin and Moser, 2010).

The best-known oscillation of the human brain is the alpha rhythm (8-12Hz), which can be recorded from the EEG electrodes over the posterior parts of the skull during wakeful relaxation with closed eyes (Berger, 1929; Adrian, 1944; Andersen and Andersson, 1968). The oscillation originates predominantly from the visual cortex in the parieto–occipital lobe and is predictive of behavior (Thut et al., 2006). It is generated and propagates in the cortex and eventually reaches the thalamus, while eye-opening eliminates this rhythm. It is believed to be related to local inhibition, since it is accompanied by reduced high-frequency EEG oscillations (Andersen and Andersson, 1968; Scheeringa et al., 2011) and blood-oxygenation-level-dependent (BOLD) signal (Goldman et al., 2002; Scheeringa et al., 2011). Alpha rhythm and its modulation have been

involved in multiple cognitive and mental functions (Niedermeyer, 1997; Steriade, 2000) such as attention (Klimesch, 2012), information routing (Zumer et al., 2014), meditation (Cahn and Polich, 2006) and predictive processing (Sherman et al., 2016). Alpha oscillations are generated and spread within the cerebral cortex before reaching the thalamus (Lopes da Silva et al., 1973, 1980)

An oscillation with similar frequency (9-11Hz) can be observed in the resting state above the rolandic regions (motor cortex) and is termed sensorimotor mu rhythm (Kuhlman, 1978). Limp movement or tactile stimulation abolishes this oscillation above the corresponding cortex (Jones et al., 2010), while desynchronization also occurs by observing the relevant action (Gastaut and Bert, 1954; Arroyo et al., 1993). A related, but distinct oscillation is the sensorimotor cortex beta. In humans, these oscillations (15-30Hz) are correlated with spinal motoneuron activity during maintained voluntary contractions (Conway et al., 1995).

Although different structures are characterized by distinct oscillatory patterns with their own behavioral correlates, some common patterns can be observed (Headley and Pare, 2017). In mammals, awake or active states are characterized by low-voltage, high-frequency EEG activity across the cortex, termed "activated" or "desynchronized" state (Steriade, 2000; Destexhe et al., 1999b), whereas, during sleep, slower activity and bimodal fluctuations of the membrane potential of neurons and the occasional burst firing (Ranck, 1973) population activity patterns dominate brain activity (Hobson and Pace-Schott, 2002). The oscillatory component of these states reflects the neuronal network dynamics that emerge from the local and global activity. These dynamics are dictated by both the structural and functional connectivity, as well as by the state-dependent neuromodulatory tone, set by subcortical centers (Steriade and McCarley, 1990; Hasselmo, 2006).

The transition from quiet to active wakefulness is associated with changes at multiple levels (Vinck et al., 2015; McGinley et al., 2015). During wakefulness, acetylcholine and monoamines are released in the hippocampus and the cortex (Hasselmo, 1999). This release results in depolarization of the thalamocortical cells, enabling the transmission of sensory inputs to the cortex (Constantinople and Bruno, 2011; Poulet et al., 2012; Pinto et al., 2013; Chen et al., 2015; Vinck et al., 2015). This neuromodulatory tone enhances the responsiveness of principal cells to synaptic inputs, by attenuating their after-hyperpolarization, which enables the generation of fast oscillatory patterns. Interestingly, acetylcholine suppresses preferentially feedback connections, such as from CA3 to the entorhinal cortex and from higher order to primary sensory cortices, as well as recurrent connections in CA3, via muscarinic receptor activation, while feedforward connectivity is enhanced via nicotinic receptor activation (Hasselmo, 2006). It thus acts as a gateway controlling the direction of intraregional information transmission.

Although the aroused state is termed desynchronized, transient inter-regional synchronization enables the communication between distinct brain regions. Importantly, the directionality and temporal order of the neuromodulatory and cortical activation is not established, since sensory stimulation is enough to elicit the transition to active wakefulness. However, it is accepted that arousal is modulating circuit dynamics and result in increased signal-to-noise ratio of sensory

responses and reduced noise correlations, thus accounting for some effects of attention to sensory processing (Vinck et al., 2015).

Whereas during active behavior cells are depolarized and neuronal activity is diverse, during quiet awakening and SWS, hippocampal and cortical acetylcholine levels are drastically reduced. This change releases glutamatergic synapses from the cholinergic suppression and membrane potentials are characterized by slow, high-amplitude fluctuations, synchronously present in nearby cells (Poulet and Petersen, 2008; Gentet et al., 2010; Zhao et al., 2016). The sensory-dependent desynchronization is dependent on thalamic inputs (Poulet et al., 2012). These oscillations can be also observed in the extracellularly recorded LFP and during awake, quiet immobility, similar high-amplitude slow oscillations have been observed in multiple cortical areas (Crochet and Petersen, 2006; Okun et al., 2010; Niell and Stryker, 2010; Reimer et al., 2014; Zhou et al., 2014; Zagha et al., 2013; Einstein et al., 2017; Zhao et al., 2016; Schneider et al., 2014; Parker et al., 2014; Bennett et al., 2013; Polack et al., 2013; Fernandez et al., 2016).

1.7.1 *Theta oscillations*

During active exploratory behavior, in addition to the properties of the aroused states described above, the animals are locomoting as well as actively examining the sensory landscape via active sniffing and whisking, visual exploration and touch. In the rodent, these behaviors are associated with the occurrence of prominent rhythmic theta oscillations (4-12Hz), initially termed rhythmic slow activity (RSA), in the hippocampus (Jung and Kornmüller, 1938; Green and Arduini, 1954; Vanderwolf, 1969; Winson, 1974; Mitchell and Ranck, 1980; Alonso and García-Austt, 1987a,b). Theta oscillations have been described in both rabbits (Jung and Kornmüller, 1938), rats (Buzsaki et al., 1983) and mice (Buzsáki et al., 2003), as well as humans (Lega et al., 2012; Burgess and Gruzelier, 1997; Ekstrom et al., 2005; Moroni et al., 2007; Cantero et al., 2003; Rutishauser et al., 2010) and non-human primates (Stewart and Fox, 1991), and most recently bats (Ulanovsky and Moss, 2007). They are associated with voluntary, preparatory, orienting or exploratory behaviors (Grastyán et al., 1959; Vanderwolf, 1969), such as attentive head-scans (Monaco et al., 2014) and working memory (Raghavachari et al., 2001; Lisman, 2010), memory formation (Siegel et al., 2012; Rutishauser et al., 2010; Fuentemilla et al., 2014) as well as paradoxical (REM) sleep (Jouvet, 1969; Cantero et al., 2003).

Hippocampal theta oscillations are believed to support synaptic plasticity and memory encoding. Abolishing theta generators impairs learning (Winson, 1978; Givens and Olton, 1990), while theta occurrence and power during learning predict memory acquisition and ability to recall (Berry and Thompson, 1978; Seager et al., 2002; Nokia et al., 2008; Griffin et al., 2004). In addition to the occurrence and power of the oscillation, multiple studies have investigated the importance of theta phase for learning and plasticity induction. Stimulation at the peak of theta induces LTP, whereas stimulation at the trough of the oscillation induces LTD and synaptic depotentiation in different subregions of the hippocampus, both *in vitro* and *in vivo* (Pavlides et al., 1988; Huerta and Lisman, 1995; Hölscher et al., 1997; Hyman et al., 2003; Orr et al., 2001; Kwag and Paulsen, 2009). Recent results from the optogenetic inhibition of CA1 in specific phases of theta oscillation

suggest a distinct role of different theta phases in encoding and decoding processes (Siegle and Wilson, 2014).

Beyond the hippocampal formation, theta oscillations and the corresponding modulation of local cells have been identified throughout the limbic circuit, including the medial prefrontal cortex (Siapas et al., 2005; Sirota et al., 2008), anterior cingulate (Leung and Borst, 1987; Womelsdorf et al., 2010; Colom et al., 1988), amygdala (Paré and Gaudreau, 1996; Collins et al., 1999; Paré and Collins, 2000), thalamus (Tsanov et al., 2011a,b; Vertes et al., 2001), mammillary bodies (Kocsis and Vertes, 1994), and the subiculum (Bullock et al., 1990; Anderson and O'Mara, 2003; Jackson et al., 2011; Jackson et al., 2014), perirhinal cortex (Muir and Bilkey, 1998; Collins et al., 1999; Bilkey and Heinemann, 1999; Muir and Bilkey, 2003), inferior colliculus (Pedemonte et al., 1996), superior colliculus (Natsume et al., 1999) dorsal raphe (Kocsis and Vertes, 1992) and Gudden's tegmental nuclei (Bassant and Poindessous-Jazat, 2001; Kocsis et al., 2001).

During spatial and working memory tasks, theta frequency oscillations can be observed in the rodent mPFC (Jones and Wilson, 2005b,a; Hyman et al., 2005; Siapas et al., 2005; Sirota et al., 2008; Fujisawa and Buzsaki, 2011). These LFP oscillations are phase and amplitude synchronized with hippocampal theta oscillations, while a large proportion (~40%) of prefrontal neurons are phase locked to the past of the hippocampal theta oscillation, indicative of a directionality in the interaction between the two structures (Hyman et al., 2005; Siapas et al., 2005; Sirota et al., 2008). It has been suggested that this interaction is via the ventral hippocampus (O'Neill et al., 2013) that is the origin of the majority of hippocampal projections to the mPFC (Dégenètais et al., 2003; Hoover and Vertes, 2007; Jay and Witter, 1991).

This interaction is stronger during behaviorally relevant instances and is associated with working memory (Jones and Wilson, 2005b; Fujisawa and Buzsaki, 2011) as well as rule-learning (Benchenane et al., 2010). In support of this idea, the mPFC-HPC theta synchronization correlates with behavioral performance (Jones and Wilson, 2005b; Hyman et al., 2010; Sigurdsson et al., 2010), while disconnection of the two structures impairs spatial learning (Floresco et al., 1997; Wang and Cai, 2006; Izaki et al., 2008). Recently, optogenetic inhibition of the vHPC-mPFC afferents in a spatial working memory task identified a role of this pathway in the encoding but not retrieval of the spatial cues (Spellman et al., 2015). Interestingly, inhibition of these projections perturbs gamma but not theta coherence between the two structures, suggesting that prefrontal theta field oscillations are the result of distinct mechanism (Spellman et al., 2015). Further, theta synchrony and phase-locking impairment have been associated with circuit dysfunction and psychiatric disorders (Sigurdsson et al., 2010).

During fear behavior, theta synchronization between the mPFC and the BLA has been suggested to underlie the retrieval of the CS-US association (Likhtik and Gordon, 2014; Seidenbecher et al., 2003; Pape et al., 2005; Popa et al., 2010). Decrease in this synchronization correlates with extinction learning (Lesting et al., 2011) and synchronization correlates with resistance to extinction (Livneh and Paz, 2012), but no clear picture has emerged so far (Lesting et al., 2013). Fear eliciting conditioned stimuli induce the resetting of stimulus-induced short-lived prefrontal theta oscillations and synchronize prefrontal populations, an effect mediated by PV-expressing

interneurons (Courtin et al., 2014b). During REM sleep, such synchronization is considered relevant to fear memory consolidation (Popa et al., 2010). Anxiety has been associated with theta synchronization between vHPC and mPFC (Adhikari et al., 2011, 2010) and optogenetic inhibition of ventral hippocampal terminals in the mPFC reduces both theta synchronization and anxiety behavior (Padilla-Coreano et al., 2016).

1.7.2 *Gamma oscillations*

During awake behavior, the mammalian EEG is characterized by low-amplitude, fast rhythmic activity (40-100Hz) termed gamma oscillations. Gamma oscillations have been observed in rodents, human (Halgren et al., 1977; Llinas and Ribary, 1993; Uchida et al., 2001; Canolty et al., 2006) and non-human primates (Kreiter and Singer, 1996; Womelsdorf et al., 2006) and have been described throughout the limbic brain, including most cortices (Gray et al., 1989; Murthy and Fetz, 1992; Singer and Gray, 1995; Fries et al., 2001; Sirota et al., 2008; Boeijinga and Lopes da Silva, 1988; Engel et al., 1991), the hippocampus (Stumpf, 1965; Buzsaki et al., 1983; Bragin et al., 1995), entorhinal cortex (Chrobak and Buzsaki, 1998), striatum (Berke et al., 2004; Tort et al., 2008), olfactory bulb (Adrian, 1942; Freeman, 1975), thalamus (Pinault and Deschenes, 1992) and the amygdala (Halgren et al., 1977; Popescu et al., 2009; Courtin et al., 2014a; Stujenske et al., 2014).

Cortical neurons are typically modulated by the phase of local gamma oscillations (Gray et al., 1989; Murthy and Fetz, 1992; Steriade and Amzica, 1996; Csicsvari et al., 2003). Gamma oscillations, similarly to other oscillations, arise from the interaction of distinct cell types with either intrinsic active pacemaking properties (Gray and McCormick, 1996) or passive resonating properties (Llinas, 1988; Alonso and Llinás, 1989; Llinas et al., 1991; Nuñez et al., 1992), organized in phase-coupled oscillators (Somers and Kopell, 1993, 1995). Under particular conditions, purely interneuronal networks are able to generate gamma frequency oscillations (Wang and Morris, 2010; Buzsáki et al., 2012b)

The modulation of excitatory cells occurs by gamma rhythmic inhibition provided by local interneurons that are modulated and are critical for the generation of gamma (Buzsaki et al., 1983; Whittington et al., 1995; Traub et al., 1996). This rhythmic firing of the interneurons imposes an oscillatory synaptic input onto excitatory cells, which results in the rhythmic modulation of their membrane potential, near but below the spike threshold (Buzsaki and Chrobak, 1995). This modulation is believed to support the synchronization between groups of cells firing within few milliseconds in the same phase of gamma (Singer and Gray, 1995; Traub et al., 1998; Engel et al., 2001).

The coupling between theta and gamma oscillations is modulated by behavior and cognitive load (Tort et al., 2009). Interestingly, the amplitude of gamma oscillations both in the hippocampus (Bragin et al., 1995; Chrobak and Buzsaki, 1998; Buzsaki, 2002; Tort et al., 2009) and the neocortex (Canolty et al., 2006; Sirota et al., 2008; Fuentemilla et al., 2014) is larger at the peak of theta oscillation, whereas the excitatory cells firing preferentially at the trough. However, perisomatic-targeting interneurons fire mostly at the peak, in line with their contribution to the generation of gamma oscillations (Hajos, 2004; Lasztóczi and Klausberger, 2014). This fact is at odds with

the phase modulation by gamma, suggesting a dual mechanism of phase segregation and the importance of the dynamic interplay between slow and fast oscillatory components (Lisman and Jensen, 2013; Canolty and Knight, 2010).

1.8 SLEEP

The brain state alternates between arousal (preparatory) and non-arousal (consummatory) or sleep. The two different states are both behaviorally and electrophysiologically distinct. Sleep is the only physiological condition associated with lack of consciousness and humans spend a third of their life in this unconscious state. Sleep and its relationship to consciousness has been the focus of investigations for thousands of years, dating back to Hippocrates, Galen and Aristotle. Sleep is a ubiquitous phenomenon across the Animalia kingdom. Every animal with a nervous system exhibits a sleep phenotype, defined as periodic episodes of reversible behavioral quiescence and reduced responsiveness. Sleep is not only physiologically present but is also necessary for the survival of an organism. Prolonged periods of sleep deprivation are fatal (Shaw et al., 2002) while mild sleep deprivation is negatively affecting the abilities and cognitive functions (Van Dongen et al., 2003; Havekes et al., 2013) and has negative impact on the health of the individual (Brown et al., 2012). Sleep has been described and studied primarily in mammalian species (Capellini et al., 2008), however, sleep has been observed in all other vertebrate classes as well as in worms (Iwanir et al., 2013) and insects (Bushey et al., 2011).

During sleep, the heart-rate, breathing, muscle tone and body temperature are markedly different from during awake behavior. Usually sleep is preceded by preparatory behavior such as grooming and nest-building (Hediger, 1969; Meddis, 1975; Eban-Rothschild et al., 2016). In addition to the behavioral and physiological features associated with sleep, the electrophysiological signatures of the sleeping brain are important elements for the definition of sleep (Bremer, 1935). Interestingly, sleep is not a homogeneous process. Throughout sleep, there are continuous alternations between distinct brain states that are reflected in the activity of neurons and the oscillatory components of the LFP recorded in different brain regions. The mammalian brain is characterized by two distinct states during sleep, the slow-wave sleep (SWS) and the rapid eye movement (REM) sleep (Aserinsky and Kleitman, 1953). Deep sleep is usually referred to as SWS sleep because the neocortical EEG is characterized by prominent slow oscillations (SO), i.e. high-amplitude, low-frequency (0.5-4Hz) oscillations and occasional spindle events (Steriade and McCarley, 2013). Another distinction is between non-REM (NREM) and REM sleep, which serves to distinguish REM periods that occur sporadically between deep sleep episodes. REM sleep occurs sporadically between deep sleep episodes and is characterized by rapid movement of the eyes (Márquez-Ruiz and Escudero, 2008), low muscle tone and an awake-like, desynchronized state of the cortex (Llinas and Ribary, 1993), associated with theta oscillations in the hippocampus. Typically, the sleep progresses from wakefulness to light and deep sleep. In humans, the first half of the night is occupied by mainly SWS, while in the later part REM sleep predominates (Wurts and Edgar, 2000). During the first months of life, newborn humans exhibit prolonged REM period and fragmented sleep. Gradually, sleep becomes entrained by the circadian clock and REM sleep duration decreases.

The transition between awakening and sleep and vice versa, as well as between SWS and REM sleep, is regulated by sleep regulatory centers in the brainstem and basal forebrain (BF) (Economo, 1930; McGinty and Sterman, 1968; Saper et al., 2005). This sharp state transition depends on mutual inhibition between the arousal- and sleep-promoting centers in the brain. In addition to the transition between awake and sleep state, it is clear that the different sleep stages are characterized by distinct neuromodulatory tone (Jouvet, 1962; Hobson et al., 1975; Weber and Dan, 2016). The activity of the pontomedullary network during sleep controls the transition to and from REM sleep (Siegel et al., 1979; Kanamori et al., 1980; Weber et al., 2015), while the interaction of aminergic and cholinergic neurons of the mesopontine junction has given rise to the reciprocal interaction model (McCarley and Hobson, 1975), that results in the alternation of REM and NREM sleep (Pace-Schott and Hobson, 2002; Lu et al., 2006).

1.9 SLOW WAVE SLEEP

In humans, NREM sleep comprises three stages, N1, N2, and N3. A qualitative description would be light (N1), intermediate (N2) and deep (N3) sleep. N1 stage follows awake state and is typically very short in duration. Stage N2 constitutes about half of the sleep duration, whereas N3 is characterized by high-amplitude delta waves and constitutes ~10% of sleep, predominantly the first one-third of the total sleep period. In rodents, partly due to the fragmented pattern of sleep episodes (Richardson et al., 1985; Veasey et al., 2000), the distinction between light and deep sleep is not as pronounced as in humans (Van Twyver, 1969; Genzel et al., 2014), although distinct sub-states have been identified (Jarosiewicz and Skaggs, 2004). In mammals, NREM sleep is homeostatically regulated, with animals spending more time in NREM at sleep onset and proportionally less time in NREM as the sleep pressure is reduced as sleep progresses (Lancel et al., 1992; Borbély and Achermann, 1999; Tononi and Cirelli, 2014; Vyazovskiy et al., 2009).

NREM sleep is associated with reduced muscle tone, cardiovascular tone, respiratory rate (Krieger, 2005) and body temperature (Obál et al., 1985). During NREM sleep, the neuromodulatory tone changes dramatically in comparison to both awake and REM states (Hobson et al., 1975) and acetylcholine levels are decimated (Hasselmo, 1999), a phenomenon that reduces the effective connectivity between brain regions (Gerstein and Perkel, 1969; Tononi and Sporns, 2003; Esser et al., 2009) and results in functional deafferentation of the neocortex from thalamic inputs which diminishes the cortical responsivity to sensory stimulation. It is believed that these properties underlie the role of NREM in memory consolidation (Hasselmo and McGaughy, 2004). Interestingly, protein synthesis occurs more during SWS than in REM sleep or wakefulness (Ramm and Smith, 1990). During slow wave sleep (SWS), the neocortex and the thalamus are characterized by a slow oscillation (0.1-1Hz) of the field potential, spatially coherent across the cerebral cortex (Blake, H.; Gerard, 1937; Amzica and Steriade, 1995; Cossart et al., 2003). Slow oscillations have been described in multiple mammalian species (Oakson and Steriade, 1982, 1983; Lyamin et al., 2008) including humans (Henry and Scoville, 1952; Achermann and Borbély, 1997), as well as birds (Rattenborg et al., 1999; Voirin et al., 2016) and reptiles (Shein-Idelson et al., 2016) and are believed to be involved in memory consolidation (Dudai et al., 2015). Even slower (<0.1Hz; infra-slow) patterns of neuronal activity have been described during sleep, associated

with modulation of the heart rate, muscle tone (Terzano et al., 1988) and other physiological processes (Hughes et al., 2011; Hiltunen et al., 2014).

The slow oscillation (SO) reflects the spontaneous and recurrent synchronous alternation of neocortical neurons and glial cells (Amzica and Steriade, 1998; Amzica and Steriade, 2000) between depolarized (UP) states, accompanied by increased firing of the cells, and quiescent hyperpolarized (DOWN) states. The SO is characterized by spontaneous abrupt transitions of the membrane potential and the periodic alternation of the cerebral network between active and quiescent states. Because of these transitions, during SO the population of neocortical neurons exhibits a bimodal distribution of membrane potentials (Isomura et al., 2006). During DOWN states synaptic activity is diminished, cortical neurons are hyperpolarized and are not firing action potentials. In contrast, during UP states the firing rates of cortical cells is comparable to that of awake activity (Steriade et al., 1993a; Steriade et al., 1993d; Sanchez-Vives and McCormick, 2000; Steriade, 2006; Crunelli and Hughes, 2010; Chauvette et al., 2010; Timofeev et al., 2001). The UP state is reflected extracellularly as negative field potential when recorded near the neuronal cell bodies in the deep cortical layers. This is due to the summation of population-level EPSPs (field EPSP; fEPSP). When recording at the surface of the cortex, the negative potentials are reverted due to the long vertical apical dendrites terminating in superficial cortical layers (Contreras and Steriade, 1995). Consequently, UP states are recorded as positive waves in the surface EEG (Steriade and Amzica, 1998a). In contrast, the DOWN state is a depth (infragranular layers) positive and surface negative. During the UP state, cortical cells fire in high rate and the mixture of excitatory and inhibitory inputs enables the generation of gamma oscillations. Neurons receive a barrage of excitatory and inhibitory post-synaptic potentials (EPSPs and IPSPs respectively) (Haider, 2006), lowering their input resistance and consequently increasing the membrane conductance (Destexhe et al., 1999b). These characteristics convey distinct computational properties to the UP states (Destexhe et al., 2003; Destexhe and Contreras, 2006). It has been suggested that UP states represent fragments of awake activity during sleep (Destexhe et al., 2007), due to the similarity of EEG and intracellular dynamics during these states with the ones during activated awake states (Steriade et al., 2001). The prolonged depolarization during UP states leads to tbe progressive decrease of extracellular Ca^{2+} concentration (Massimini and Amzica, 2001) resulting in the increase of the input resistance, which reduces the synaptic efficacy and results in the disfacilitation of cortical neurons (Contreras and Steriade, 1996), guiding the network to a DOWN state. This is complemented by the reduced firing of thalamocortical (Glenn and Steriade, 1982) and neuromodulatory neurons (Steriade et al., 1982, 1990). Further, the constraints posed by the Na^{+}/ K^{+} -ATPase pump and the Ca^{2+} -dependent K+ currents (IK(Ca)) (Timofeev et al., 2001) are largely responsible for the recurring hyperpolarizing events. Further, 5-HT release from dorsal raphe during SWS results in the hyperpolarization of thalamocortical cells (Sakai and Crochet, 2001; Monckton and McCormick, 2002). During the DOWN state, miniature EPSPs depolarize gradually the principal cells and trigger the transition to the UP state (Bazhenov et al., 2002; Cowan and Wilson, 1994; Wilson and Groves, 1981).

The transition between the two states is termed K-complex (Loomis et al., 1938) and constitutes the largest event in healthy human EEG. Typically, it is defined as a sequence of UP-DOWN-UP states and is associated with the occurrence of thalamocortical spindles. They occur during the slow oscillations (Amzica and Steriade, 1997; Steriade and Amzica, 1998b), predominantly in stage II light sleep, as well as in response to unexpected external sensory stimulation (Blake, H.; Gerard, 1937; Loomis et al., 1938; Davis et al., 1939; Halasz et al., 1985; Roth et al., 1956) and are generated in widespread cortical areas (Cash et al., 2009). Such quick alternation of depolarization and hyperpolarization, as seen during K-complexes, has been shown to be effective in inducing plasticity in cortical slices (Chauvette et al., 2012). The first stages of sleep are characterized by less regular KCs and the SO appears less organized and synchronized. The occurrence of a DOWN state with duration 200-500ms is characterized by the presence of power in the δ range (1-4Hz) and is thus termed delta wave (Gloor et al., 1977; Ball et al., 1977; Petsche et al., 1984). Delta waves are generated from the interaction between thalamic and neocortical nuclei and tend to be more localized than global SO. Delta waves are generated partly locally in the cortex since they can be observed following thalamectomy (Steriade et al., 1993c) but can also occur in thalamocortical cells of decorticated animals (Dossi et al., 1992).

During awake states, the activity of midbrain reticular neurons and mesopontine cholinergic nuclei provides a constant depolarization to thalamocortical cells. Upon sleep, however, the activity of these cells is drastically reduced (Steriade et al., 1982). This results in a hyperpolarization of thalamocortical cells, creating the conditions for the initiation and propagation of the SO. In support of this, stimulation of the midbrain, the pedunculopontine tegmentum (PPT) or the nucleus basalis (NB) cholinergic neurons generates awake-like EEG dynamics (Fourment et al., 1983; Steriade et al., 1993b). Similarly, stimulation of thalamus induces cortical desynchronization, while thalamic inactivation insulates the cortex from sensory induced desynchronization (Poulet et al., 2012). SO can be recorded after thalamic lesions (Steriade et al., 1993c) as well as from isolated cortical structures *in vivo* (Timofeev et al., 2000b) and *in vitro* (Sanchez-Vives and McCormick, 2000) but not from the thalamus after decortication (Timofeev and Steriade, 1996), which support the cortical origin of SO. Transitions from DOWN to UP states are accompanied by firing of locus coeruleus (LC) neurons and the release of norepinephrine (NE) to their cortical and subcortical targets (Eschenko et al., 2012), promoting the induction of synaptic plasticity within the active subsets of neurons (Sara, 2015).

Although SO are globally observed throughout the cerebral cortex, they are not occurring simultaneously but are propagating by spreading to nearby cortical columns. SO are initiated in the deep infragranular layers of the cortex and they propagate both vertically to the superficial layers (Sanchez-Vives and McCormick, 2000; Sakata and Harris, 2009; Chauvette et al., 2010; Beltramo et al., 2013) and laterally to other cortical areas (Sanchez-Vives and McCormick, 2000; Stroh et al., 2013; Cossart et al., 2003). In humans, SO are most prominent in medial regions of the PFC (Brazier, 1949; Massimini, 2004; Dang-Vu et al., 2008; Murphy et al., 2009) and they propagate throughout the cortex in the form of a traveling wave, typically in a frontal to posterior direction (Brazier, 1949; Massimini, 2004), a phenomenon observed in multiple mammalian

species (Volgushev, 2006; Mohajerani et al., 2010; Leemburg et al., 2010) as well as in birds (Beckers and Rattenborg, 2015; Beckers et al., 2014). Interestingly, after sleep deprivation the increase in SO activity is greater in prefrontal areas (Finelli et al., 2001) while after learning the increase is more localized to the cortex most involved during behavior (Huber et al., 2004). SO can also occur in confined local brain regions (Mohajerani et al., 2010; Vyazovskiy et al., 2011), however, they propagate across cortical regions (Mohajerani et al., 2013) and over transcallosal interhemispheric connections and are synchronized between the two hemispheres (Mohajerani et al., 2010).

Slow oscillations are also observed in the striatum (Wilson and Groves, 1981; Stern et al., 1998) and the nucleus accumbens (Wilson, 1993; O'Donnell and Grace, 1995) which is however only weakly related to the cortical SO (Wilson and Groves, 1981). Further, SOs are described in the hippocampus (Sirota et al., 2003; Isomura et al., 2006; Wolansky et al., 2006; Hahn et al., 2006) and the amygdala (Gaudreau and Pare, 1996; Pare et al., 2002; Windels et al., 2010). Interestingly, similar frequency oscillations can be observed even in the trapezius and upper extremity muscles (Westgaard et al., 2002) which have been associated with the cortical SO. The hippocampal slow oscillation reflects the state transitions of the entorhinal cortex (Isomura et al., 2006; Hahn et al., 2007). During UP states, CA1 depolarization is mainly due to the L3 entorhinal input and the trisynaptic pathway, while during DOWN states the main input is from CA3 (Isomura et al., 2006).

Sleep spindles are transient waxing and waning oscillatory bouts (7- 15Hz) that appear to accompany and are nested within SO (Morison and Dempsey, 1943). They constitute a hallmark of light slow-wave sleep (Uchida et al., 1994; Lancel et al., 1992). Spindles are recurrent with a periodicity of 0.2-0.5Hz (Steriade and Deschenes, 1984), lasting from 500ms to 3s, during which the thalamus sends strong excitatory volleys to the neocortex. They exhibit global coherence across thalamic and neocortical areas (Verzeano and Negishi, 1960; Contreras and Steriade, 1996) while recently reverberation of stereotypic spatiotemporal patterns of spindle activity was identified during human sleep (Muller et al., 2016). Spindles are generated in the thalamocortical system (Andersen and Andersson, 1968; Contreras and Steriade, 1996) and initiated in the TRN (Steriade, 1997), while they can be generated within the thalamus in the absence of both cortex and brainstem (Morison and Bassett, 1945). During sleep, it is believed that the synchronous firing of cortico-thalamic cells during the UP states drives TRN inhibitory cells, that induce rhythmic IPSPs onto thalamocortical cells. The rhythmic post-inhibitory rebound of these cells generates rhythmic EPSPs in downstream cortical neurons, generating spindle oscillations that shape in turn the SO (Steriade and Pare, 2009). The reciprocal nature of the mechanism underlying the genesis of the spindle oscillations results in augmentation of the thalamocortical responses throughout the cycles of the oscillation which has been implicated in plasticity in the thalamocortical and intracortical network.

1.9.1 *Sharp-wave ripples*

During slow wave sleep (SWS) and particularly light sleep, quiet wakefulness, and other non-exploratory wake states, the hippocampus is characterized by large irregular activity, accompanied

by massive population bursts that give rise to sharp waves-ripple complexes (SWRs) (Buzsaki, 2015).

The CA3 region of the hippocampus is characterized anatomically by extensive recurrent connectivity. During SWS, the strongly reduced levels of acetylcholine in the hippocampus enhance recurrent connectivity (Gais and Born, 2004; Power, 2004; Marrosu et al., 1995). This afferent disinhibition and increased recurrency give rise to self-organized synchronous bursts of activity during slow-wave sleep. The synchronous bursting of thousands of CA3 cells, potentially due to mossy fiber input (Rex et al., 2009), and the consequent action potentials traveling down the CA3 axons innervating the CA1 region (Schaffer collaterals), leads to a strong depolarization of the CA1 stratum radiatum, the dendritic layer of CA1 region that receives the CA3 input. This depolarization of the apical dendrites is reflected in the extracellularly recorded LFP as large-amplitude negative polarity deflections, most prominent in the stratum radiatum, termed "sharp-waves" (SPWs) (Buzsáki and Buzsaki, 1986). SPWs are mostly synchronous along the dorsoventral axis of the hippocampus and propagate to the downstream structures.

These potentials are in turn usually associated with population bursts of pyramidal cells and increased firing of interneurons, which are engaged in an oscillatory interplay, reflected in fast-field oscillations (100-250Hz), confined to the pyramidal layer of the CA1 region (Vanderwolf, 1969; O'Keefe, 1976; Buzsaki et al., 1983). Together, they are termed sharp-wave ripple complexes. During the time window of an SPWR (50-200ms), tens of thousands of neurons are synchronously activated across the hippocampal formation, establishing these events as the most synchronous activity pattern in the brain. Each pyramidal cell is depolarized and increases its firing rate (Ylinen et al., 1995), however, doesn't fire in each cycle of the ripple. The shape and oscillatory nature of the ripple component in the CA1 is a result of the rhythmic alternation between distal excitation and proximal inhibition. The synchronous excitatory input from CA3 results in mini population spikes of the pyramidal cell population in the troughs of the ripple oscillation (Ylinen et al., 1995). These local excitatory bursts of CA1 pyramidal cells recruit massive perisomatic inhibition (Traub and Bibbig, 2000; Stark et al., 2014) from the local interneuron population and predominantly the PV expressing basket, bistratified and chandelier interneurons. This results in synchronous IPSPs on the pyramidal cells and the corresponding transient inhibition and following disinhibition (Brunel and Wang, 2003; Ylinen et al., 1995). PV-expressing axo-axonic cells fire in the first half of the ripple and are silent in the second half (Klausberger et al., 2003).

During SWR, the CA3 cell firing induces the ensemble firing in the downstream CA1 cells (Csicsvari et al., 2000) and transient assemblies within CA1 partly inherit their activation patterns from CA3 activity (Both et al., 2008; Matsumoto et al., 2013). In each ripple, 10–20% of all neurons of the hippocampal formation discharge synchronously (Jutras et al., 2009; Csicsvari et al., 1999; Csicsvari et al., 2000; O'Neill et al., 2008) and in a slower timescale the occurrence of SWS during SWS is predictive of increased in the hippocampal firing (Miyawaki and Diba, 2016). CA3 burst firing is transient and eventually, SWRs are terminated and followed by a GABA mediated hyperpolarization (English et al., 2014) but the exact mechanisms leading to the termination are not yet understood. SWRs occur predominantly during slow wave sleep,

awake immobility, drinking, grooming and eating (Vanderwolf, 1969; Buzsáki and Buzsaki, 1986; O'Keefe, 1976) and they have been observed in all mammalian species studied, including humans (Freemon and Walter, 1970; Bragin et al., 1999; Axmacher et al., 2008) and non-human primates (Freemon et al., 1969; Leonard et al., 2015; Leonard and Hoffman, 2016; Kaplan et al., 2016).

SWR triggered BOLD fMRI has revealed a widespread activation of multiple brain regions, while subcortical sites were predominantly inhibited (Logothetis et al., 2012; Ramirez-Villegas et al., 2015). SWRs have been associated with slower ripples in output structures of the hippocampal formation such as the subiculum, presubiculum and parasubiculum as well as deep layers of entorhinal cortex (Jutras et al., 2009; Mizuseki et al., 2009). Further, SWRs drive neuronal activity in the perirhinal cortex (Collins et al., 1999), as well as the mPFC (Siapas and Wilson, 1998). Interestingly, SWRs trigger transitions to UP states in cells of the core of nucleus accumbens (Goto and O'Donnell, 2001). In dorsal raphe, both serotoninergic and glutamatergic cells are silent before ripples and optogenetic activation of this structure suppresses ripple occurrence (Wang et al., 2015).

1.10 SLEEP AND MEMORY CONSOLIDATION

It is now understood that sleep is important for the long-term retention of memories and the optimization of recall. The role of sleep in the post-encoding consolidation of memories has been well established in many species (Jenkins and Dallenbach, 1924; Derégnaucourt et al., 2005; Rasch and Born, 2013; McGaugh, 2000). There has been a wealth of data supporting the notion that SWS is important for memory consolidation (Rasch and Born, 2013). However, this effect pertains to declarative and episodic memories and specifically memories that rely heavily on the hippocampus (Squire and Zola, 1996). Typically, procedural-sequential tasks do not fall in this category, however, explicit learning components of these tasks appear to promote hippocampal involvement (Schendan et al., 2003; Robertson et al., 2004) and the interaction between the consolidation of different components of a task has been reported (Brown and Robertson, 2007). A major role of the consolidation process is the integration of new information into the pre-existing conceptual and knowledge framework (Dudai et al., 2015; Tse et al., 2007). For rodents, typical examples of hippocampus-dependent tasks include contextual fear conditioning, passive and active place avoidance, object-in-place recognition and temporal order tasks. Humans that sleep after learning a list of syllables, exhibit improved memory retrieval (Jenkins and Dallenbach, 1924). In fear conditioning, the short-term contextual component of the aversive memory, that is hippocampus-dependent, is vulnerable to sleep deprivation. To the contrary, the memory of the association between an auditory conditioned stimulus and the aversive foot-shock remains intact (Graves, 2003). Both the duration of SWS (Diekelmann et al., 2012; Fogel and Smith, 2006), as well as the amplitude and coherence of the slow oscillation, increase following a declarative memory task (Molle et al., 2004)and have been associated with memory improvement overnight (Wilhelm et al., 2011; Moroni et al., 2014). Additionally, heavy cognitive load and synaptic potentiation during awake behavior upregulates the duration and SO power of SWS (Tononi and Cirelli, 2014) in a behavior and relevant cortex specific manner (Huber et al., 2004). Interestingly, entraining and enhancing slow oscillations during sleep improves memory consolidation of

hippocampus-dependent declarative memories in both humans and rodents (Marshall et al., 2006, 2004; Ngo et al., 2013; Ngo et al., 2015; Binder et al., 2014; Bellesi et al., 2014).

1.10.1 *Replay*

Neural activity patterns in the hippocampus and the cortex that occur during awake behavior are spontaneously reactivated during subsequent sleep, a phenomenon termed replay (Pavlides and Winson, 1989; Wilson and McNaughton, 1994). In the case of the hippocampus, replay typically refers to sequences of activity and the correlation structure of place cells during awake experience that are observed during subsequent sleep. It is believed that replay is a reflection of the reactivation of memory traces and is important for memory consolidation.

Replay occurs predominantly during SWRs in both SWS (Wilson and McNaughton, 1994; Skaggs and McNaughton, 1996; Nadasdy et al., 1999; Lee and Wilson, 2002; O'Neill et al., 2008) and quiet awake state (Foster and Wilson, 2006; Diba and Buzsáki, 2007; Jackson et al., 2006). Further, replay has been described for SWRs occurring during brief pauses of the exploratory behavior in the awake animal (O'Neill et al., 2006; Carr et al., 2011; Karlsson and Frank, 2009). In the awake SWRs, cells within their place field fire more robustly than the ones outside (O'Neill et al., 2006, 2008; Cheng and Frank, 2008), while the firing of cell pairs with overlapping place field is more synchronized during replay (O'Neill et al., 2008), preserving distance (Wilson and McNaughton, 1994) and temporal order (Skaggs and McNaughton, 1996) and replayed sequences extend to multiple long trajectories (Davidson et al., 2009) as well as temporally remote experiences (Karlsson and Frank, 2009). During SWRs, the neuronal sequences are temporally compressed by about 20 times, independently of the animal speed during experience (Nadasdy et al., 1999; Lee and Wilson, 2002; Davidson et al., 2009) and sequential activation of ensembles is reflected in the extracellular field potential (Taxidis et al., 2015). Replay is observed concurrently in the hippocampus and the cortex as frames of stepwise increase in neuronal population activity sparsely distributed during SWS that replay the awake activity (Lee and Wilson, 2002; Ji and Wilson, 2006). The replay sequences are coordinated between the two structures to match the same awake experience. Interestingly, the cortical frames precede and predict the hippocampal ones, hinting towards a feed-forward interaction from the cortex to the hippocampus (Ji and Wilson, 2006; Rothschild et al., 2016a). According to the two-stage model of memory formation (Buzsaki, 1989), during awake behavior, information is stored in the hippocampus, that is dominated by theta oscillations, in a transient labile form. In this model, SWRs support the incidental learning of single events by repeatedly reactivating temporally distinct representations, in a compressed time-scale. This enables the interaction and merging of these representations in one coherent representation (Buzsaki, 1984).

Although replay has been predominantly described in the rodent hippocampus (Pavlides and Winson, 1989; Wilson and McNaughton, 1994), replay events have been reported in multiple neocortical structures, including the visual (Ji and Wilson, 2006), auditory (Rothschild et al., 2016a), motor (Ramanathan et al., 2015) and prefrontal cortex (Euston et al., 2007; Peyrache et al., 2009; Benchenane et al., 2010; Jadhav et al., 2016), the thalamus (Peyrache et al., 2015) and the striatum (Pennartz, 2004; Lansink et al., 2012) in rodents, birds (Dave and Margoliash,

2000), monkeys (Hoffman and McNaughton, 2002) and humans (Maquet et al., 2000; Peigneux et al., 2004; Staresina et al., 2013; Tambini et al., 2010; Deuker et al., 2013). Neocortical replay is temporally associated with the occurrence of hippocampal SWRs (Jadhav et al., 2016; Wierzynski et al., 2009; Rothschild et al., 2016b) and the cortical UP states (MacLean et al., 2005; Luczak et al., 2013; Johnson et al., 2010), but reactivation of non-random patterns seems to be a general motif of cortical activity (Ikegaya et al., 2004; Hoffman and McNaughton, 2002; Prut et al., 1998; Luczak et al., 2007; Luczak et al., 2009; Mokeichev et al., 2007).

External stimulation during sleep using olfactory (Rasch et al., 2007; Barnes and Wilson, 2014) or auditory (Hars et al., 1985; Rudoy et al., 2009; Bendor and Wilson, 2012; Cousins et al., 2014; Rothschild et al., 2016a; Fuentemilla et al., 2013) cues, associated with the task, triggers reactivation of memories and the replay of hippocampal (Bendor and Wilson, 2012) and cortical (Rothschild et al., 2016b) patterns of activity and has been shown to improve consolidation of the related memories (Guerrien et al., 1989; Rasch et al., 2007; Rudoy et al., 2009; Bendor and Wilson, 2012; Cousins et al., 2014). Similarly, dreaming of a task is associated with the consolidation of that particular memory (Wamsley et al., 2010). The exact mechanisms supporting the reactivation remain however unknown (Valero et al., 2017).

Electrical stimulation of the ventral hippocampal commissure (VHC) backfires CA3 cells and results in a population spike and subsequent inhibition. This effect has been utilized as a tool for the closed-loop termination of SWRs. Using this method, it was shown that SWR disruption during the post-training sleep results in impaired learning and performance over days in a hippocampus-dependent spatial memory task (Girardeau et al., 2009a; Ego-Stengel and Wilson, 2009; Jadhav et al., 2012). Interestingly, SWR termination results in a homeostatic increase in the rate of SWR events after learning (Girardeau et al., 2014). It is important to note that the SWR disruption by means of commissural stimulation is perturbing both the intra-hippocampal and the extra-hippocampal consolidation. To this day, there has been no causal proof of neither the necessity nor the existence of information transfer from the hippocampus to the neocortex during SWRs. The presentation of a sensory stimulus following SWRs, which induces transient sensory evoked theta frequency oscillation, perturbs learning of trace eyeblink conditioning in rabbits, a hippocampus-dependent associative task (Nokia et al., 2012). This is hypothesized to happen by the perturbation of hippocampo-cortical synchronization which goes beyond the SWR duration. In contrast, training stimulus presentation just after SWRs accelerates learning in the same task (Nokia et al., 2010). Similarly, SWRs can be associated with rewarding stimulation, resulting in the intrinsic up-regulation of SWRs (Ishikawa et al., 2014).

According to the two-stage model for long-term memory (Marr, 1971; Buzsaki, 1989), episodic memories are initially acquired in the hippocampal network and specifically in the CA3 and CA1. During sleep, hippocampal sequences of activity are replayed in a temporally compressed manner, which leads to the strengthening of the representation within the CA3 and CA1 as well as across the neocortical targets of HPC pyramidal cells (Buzsaki, 1996; Buzsáki and Buzsaki, 1998). Evidence for the interaction between hippocampus and neocortex during sleep are provided by the investigation of the temporal relationship of the oscillatory events in the different structures.

SWRs are correlated with the neocortical SO and are occurring predominantly around K-complexes and specifically at the transition between DOWN and UP states (Sirota et al., 2003; Battaglia et al., 2004; Mölle et al., 2006; Isomura et al., 2006; Nir et al., 2011). SWRs tend to be associated with the occurrence of spindles in the cortex (Siapas and Wilson, 1998; Sirota et al., 2003; Mölle et al., 2009) and are phase locked to the troughs of spindle oscillations. However, the cortical responses to the hippocampal SWRs are gated by the existence of spindles and the corresponding recruitment of local inhibition (Peyrache et al., 2011). Hippocampal activity precedes prefrontal activity by ~100ms (Wierzynski et al., 2009; Peyrache et al., 2011). In contrast, sensory and motor cortices tend to precede hippocampal activation (Sirota et al., 2003; Ji and Wilson, 2006). Similarly, the vast majority of anterior cingulate (ACC) neurons was found to be activated before SWRs, while only a subset of neurons, receiving direct input from CA1, were activated following SWR events (Wang and Ikemoto, 2016). Neocortical bursts during spindles bias the occurrence of CA3 population spikes and the resulting CA1 ripples that occur (Sirota et al., 2003; Isomura et al., 2006). These results are characteristic of the intricate bidirectional interaction between hippocampus and neocortex during sleep (Sirota et al., 2003; Sirota and Buzsaki, 2005).

The biasing of SWRs to the depolarized phase of SO (Sirota et al., 2003; Battaglia et al., 2004; Mölle et al., 2006; Isomura et al., 2006; Nir et al., 2011; Wang and Ikemoto, 2016) suggests that the cortical activity propagates to the neocortex. This can happen either via the entorhinal cortex that is gating the inputs to the hippocampus or via recently identified direct projections from the ACC to the dorsal hippocampus (Rajasethupathy et al., 2015). Interestingly, SWRs during awake quiet immobility and so in the absence of SO are not preceded by cortical activity (Wang and Samworth, 2016). Instead, they transiently synchronize their activity with slow gamma oscillations in the hippocampus (Remondes and Wilson, 2015), known to modulate hippocampal replay (Carr et al., 2012). During SWRs PFC subpopulations are reactivated in synchrony with hippocampal reactivations carrying similar environmental representation, while prefrontal cells carrying unrelated representations are inhibited (Jadhav et al., 2016). This directionality during awake SWRs and the content bias is consistent with the identification of the functional importance of ventral CA1 inputs to PFC for the encoding of information and the formation of spatial representations in a working memory task (Spellman et al., 2015).

2

METHODS

2.1 ANIMALS

Naive male C57BL6/J mice (3 months old, Janvier or Charles River Laboratories) and PV-IRES-Cre mice (3 months old, Jackson Laboratory, B6;129P2-Pvalbtm1(cre)Arbr/J) were individually housed for at least a week before all experiments, under a 12 or 14h light-dark cycle, ambient temperature 22°C and provided with food and water *ad libitum*. A running wheel was provided and mice were allowed to use it freely throughout the day. Animals were individually habituated to the investigator by daily handling for at least 3 days. All experiments were performed during the light phase. All procedures were performed in accordance with standard ethical guidelines (European Communities Directive 86/60-EEC) and were approved by the responsible committees. All efforts were made to minimize the number of animals used and the incurred discomfort.

2.2 BEHAVIOR

2.2.1 *Auditory Fear conditioning*

Auditory fear conditioning consisted of three different sessions taking place in two different contexts (context A and B). On day 1, mice were subjected to a habituation session in context A, during which the CS^+ and CS^- (7.5kHz, 80dB or white-noise, 80dB) were presented 4 times each. Each CS presentation consists of 27 pips (50ms duration, 2ms rise and fall) with 1.1s inter-pip interval. The frequencies used for CS^+ and CS^- were counterbalanced across animals. Discriminative fear conditioning was performed 4 hours later, by pairing CS^+ with a US (1s foot-shock, 0.6mA, 5 CS^+-US pairings, inter-trial intervals 20-180s). The offset of the CS^+ was immediately followed by the onset of the US. The CS^- was never associated with the US and served as internal control. The retrieval session took place the next day in a distinct context B. During retrieval, mice were presented with 4 CS^- and 4 CS^+ presentations. For long-term memory retention, a second retrieval session took place 30 days after fear conditioning. For auditory fear extinction, mice were exposed to 4 CS^- and 12 CS^+ repeatedly for 3 consecutive days. For experiments involving pharmacological manipulation, a second retrieval session took place 12 days after fear conditioning.

2.2.2 *Innate Fear*

For experiments involving innate fear responses, mice were exposed for 10 min to a neutral context while a small filter paper, scented with the odorant 2-methyl-2-thiazoline (2MT) (M83406-25G; Sigma Aldrich), was placed in the environment. 2MT is a synthetic odorant, chemically related to the fox anogenital gland secretion 2,4,5-trimethyl-3-thiazoline (TMT) (Kobayakawa et al., 2007), that induces robust innate fear responses, in contrast to TMT (Isosaka et al., 2015).

2.2.3 *Other environments*

Electrophysiological recordings of the mice took place before and after each behavioral session in the home-cage. Home-cage consisted of clear Plexiglas filled with woodchip bedding and a metal grid ceiling which was removed for the purposes of the recordings. Food pellets were distributed in the home-cage and water was placed inside a plastic cup. Nesting material was available in the home-cage and utilized by the mice (typically building a nest in a corner). For recordings of the awake brain activity of the mice as well as for calcium imaging and novelty induced changes in hippocampal and prefrontal activity, an open arena (60cm diameter Plexiglas cylinder) and a linear track Plexiglas box (1m x 10cm x 60cm) were used. Additionally, to induce exploratory and sniffing behavior, a cheeseboard maze was used, consisting of a 60cm diameter Plexiglas cylinder with wooden laminated floor perforated with 10mm diameter holes. For recordings of mice running freely on a wheel, a horizontal wheel (Flying Saucer) was permanently placed inside the homecage. The mice typically exhibited long running episodes on the wheel, with interspersed sleep episodes.

2.2.4 *Head-fixed recordings*

For high-density silicon probe recordings, we exploited the advantages of head-fixed mouse preparation. Mice were implanted with a lightweight laser-cut stainless steel head-plate (Neurotar) above the cerebellum. After recovery from surgery, mice were habituated daily for 3-4 days to head-fixation prior to experimentation. A modified Mobile HomeCage (Neurotar) device was used, enabling mice to locomote within a customized free-floating carbon fiber enclosure (180mm diameter and 40mm wall height). Animal behavior was monitored using two modified 30fps, 1080p infrared cameras (ELP, Ailipu Technology Co), equipped with modified macro zoom lenses.

2.3 BEHAVIORAL QUANTIFICATION

For the purposes of behavioral state detection, the movement of the animal was tracked using a 3-axis accelerometer (ADXL335, Analog Devices) incorporated in the headstage, which constitutes the ground truth for the head motion. Accelerometer data were sampled at 30kHz and the sensitivity of the accelerometer is 340mV/g (g is the standard acceleration due to gravity; $\sim 9.8 m/s^2$)). Since the accelerometer measures simultaneously the dynamic acceleration due to head movement and the static acceleration due to gravity, the first temporal derivative of the acceleration was calculated (jerk; units: g/s). This measure eliminates the effect of gravity and the dynamic acceleration dominates. The effect of gravity on the different axes is amplified during head rotations. The jerk of each axis was analyzed separately for the quantification of head-motions, however for the behavioral state detection the magnitude of the jerk was quantified as $J = \sum_{k=1}^{3} \left| \frac{\partial \overrightarrow{a_k}}{\partial t} \right|$ where $\overrightarrow{a_k}$ is the acceleration for each axis. Additionally, the activity of the mice was tracked using an overhead camera (Logitech C920 HD Pro). The camera data were transferred to a computer dedicated to the behavior tracking and were acquired and processed in real-time using a custom-designed pipeline based on the Bonsai software (Lopes et al., 2015). Video data were synchronized with the electrophysiological data using network events. The magnitude of the jerk vector was calculated and smoothed in time using a narrow Gaussian

window (2s, 100ms s.d.). Complete immobility is easily distinguishable using this measure, due to the low amplitude and small variance. A threshold was set manually such that even small muscle twitches during sleep are captured. Using the density of head micro-motions and muscle twitches, we were able to classify behavioral segments as active awakening, quiescence or sleep. For head-fixed recordings, we relied solely on high-resolution video of the mouse snout. Video was preprocessed to extract the frame-to-frame difference and calculate a compound measure that we found provided an excellent proxy for the behavioral state.

2.3.1 *Freezing detection*

For the tone-fear conditioning experiments, freezing was detected using an automated infrared beam detection system (Coulborn Instruments) located on the bottom of the experimental chambers. The animals were considered to be freezing if no movement was detected for 2 s during the fear retrieval sessions. For a subset of the analyses, in order to differentiate freezing from immobility state, EMG recordings were employed. Video-based automated assessment of freezing has been shown to correlate very well with different measures of fear response (Anagnostaras, 2000) and, in our hands, it correlated robustly with the ground-truth values obtained using the accelerometer. For further studies of the respiratory entrainment of prefrontal circuits, we developed a video-tracking method to detect freezing episodes. For this, exclusive or (XOR) logical operation was performed on each pair of consecutive thresholded frames and the sum of the pixels from the resulting frame was used as a proxy for the movement of the mouse. This measure was found to provide a very good index of the movement or freezing behavior of the mouse. For the electrophysiological recordings involving headstages with accelerometers, the accelerometer data were used to provide the most sensitive measure of motion.

2.4 SURGERIES

Anesthesia was induced with 4% Isoflurane and surgical plane of anesthesia was maintained using 1% Isoflurane in O_2. Body temperature was maintained at 37 °C with a custom heating pad. Mice were secured in a stereotaxic frame (Kopf Instruments) using non-rupture ear-bars. D-panthenol (Bepanthen eye ointment, Bayer AG) was applied to the eyes to protect them from drying during anesthesia. Analgesia was provided by means of subcutaneous administration of meloxicam (5mg/kg) pre-operatively and local subcutaneous administration of a mixture of lidocaine (5mg/kg) and bupivacaine (5mg/kg) 5 minutes before incision. Saline (subcutaneously, 0.10 mL NaCl 0.9%) was administered pre- and post-operatively to prevent dehydration. The scalp was incised mid-sagitally. The periosteum was removed and the skull was thoroughly cleaned and disinfected using iodine and 2% H_2O_2. The skull was aligned in horizontal stereotaxic position (Paxinos et al., 2004) (same bregma and lambda dorsoventral position and same dorsoventral position for the following two reference point: AP: -2mm, ML: ± 2mm). For free behavior recordings, electrode bundles, multi-wire electrode arrays or silicon probes were implanted chronically in the medial prefrontal cortex (stereotaxic coordinates: 1.7-2mm anterior to the bregma (AP), 0.3mm lateral to the midline (ML) and 0.8 to 1.4mm ventral to the cortical surface (DV)) and dorsal hippocampus (AP: -2.3mm, ML: 1.5mm, DV: 0.8 – 1.5mm) (Paxinos et al., 2004).

For BLA recordings the coordinates used were AP: -1.7mm, ML: 3mm, 4mm DV) and for NAc AP: 1.2mm, ML: 1mm, DV: 4mm, while for vlPAG AP:-4.3mm, ML:0.55mm, DV:2.20mm. These coordinates are calculated based on Paxinos et al., 2004. For head-fixed recordings, a craniotomy above the target brain region was performed, dura matter was left intact and craniotomies were sealed with Kwik-Cast (WPI, Germany) after surgery and after each recording session. For electromyographic (EMG) and electrocardiographic (ECG) recordings, two 125µm Teflon-coated silver electrodes (AG-5T, Science Products GmBH) were sutured into the right and left nuchal muscles or dorsal intercostal muscles, using bio-absorbable sutures (Surgicryl Monofilament USP 5/0). Wires were guided subcutaneously and connected to a connector attached to the skull. For the recording of the neural activity of the olfactory epithelium, which was used as a proxy of respiration (Ottoson, 1960; Ottoson, 1955), a small hole was drilled above the anterior portion of the nasal bone (AP: +3mm from the nasal fissure, ML: +0.5mm from midline) until the olfactory epithelium was revealed. A 75µm Teflon-coated silver electrode (AG-3T, Science Products GmBH) or thermistor (McAfee et al., 2016) was inserted into the soft epithelial tissue. Approximately 500µm of insulation was removed from the tip of this wire and the other end was connected to the same Omnetics connector as the rest of the electrodes. Two miniature stainless steel screws (#000-120, Antrin Miniature Specialties, Inc.), pre-soldered to copper wire were implanted bilaterally above the cerebellum and served as the ground for electrophysiological recordings and as anchoring point for the implants. All implants were secured using self-etching, light-curing dental adhesive (OptiBond All-In-One, Kerr), light-curing dental cement (Tetric Evoflow, Ivoclar Vivadent) and autopolymerizing prosthetic resin (Paladur, Heraeus Kulzer). Before the conclusion of the surgery, the skin was sutured (Surgicryl Monofilament USP 5/0) and the edges of the skin were attached to the cemented constructs using tissue adhesive (Vetbond, 3M). Mice were allowed to recover for 7 days before the onset of the experiments, while analgesia (Meloxicam; 5mg/kg) and antibiotics (Enrofloxacin; 5mg/kg) were administered subcutaneously for at least 3 days.

2.4.1 *Olfactory de-afferentiation*

To causally prove the role of respiratory epithelium neurons in driving oscillations in the prefrontal cortex of mice, we induced a selective degeneration of the olfactory epithelium cells by systemic administration of the antithyroid drug methimazole (Bergman et al., 2002). Interestingly, this is a reversible degeneration, since 45 days after the ablation axonal projections to the olfactory bulb are largely reestablished (Blanco-Hernández et al., 2012). Mice were injected intraperitoneally on days 0 and 3 with 50 mg/kg methimazole (5mg/ml solution). Following injection, mice exhibited temporarily reduced activity for the first 48 hours, but at time of testing behavioral activity was normal. Respiratory activity was recorded before and after the ablation of epithelial cells (7 days after the first injection).

2.5 DATA ACQUISITION

Electrodes were connected to RHD2000 chip based amplifier boards (Intan Technologies) with 16-64 channels. Broadband (0.1Hz-7.5kHz) signals were acquired at 30kSps. Signals were digitized at 16bit and multiplexed at the amplifier boards and were transmitted to the OpenEphys recording

controller using thin (1.8mm diameter) 12-wire digital SPI (serial peripheral interface) cables (Intan Technologies). Typically, 32-256 channels were recorded simultaneously. Data acquisition was synchronized across devices using custom-written network synchronization code.

For these studies, the following types of electrodes were used: electrode arrays, optrodes, EEG wires/screws, silicon probes and ECoG arrays. Occasionally, microdrives were used to render the chronically implanted electrode arrays movable. Microelectrodes enable the recording of both LFP and single-unit activity (Adrian and Zotterman, 1926b; Adrian, 1926; Adrian and Zotterman, 1926a; Nicolelis, 2008). Briefly, microelectrode arrays were built using 12.5µm diameter Heavy Polyimide-coated Tungsten wire (California Fine Wire, 100211) (Maynard et al., 2000; Prasad et al., 2012, 2014). Electrodes wires were bundled together and individual wires were carefully de-insulated using fine forceps and tied around the silver-coated pins of micro-connectors (Omnetics, Neuro Nano-Strip). For EEG, stainless-steel miniature screws (#000-120, Antrin Miniature Specialties, Inc.) were used and were connected using copper wire to the micro-connector.

For the electrophysiological monitoring of neuronal activity, the use of high-density silicon probes (Neuronexus) provides an optimal balance between the amount of information gathered and cells recorded and the tissue damage incurred (Csicsvari, 2003). Additionally, the precise spatial arrangement of the electrode sites allows uniform sampling of the laminar profiles of a structure and the accurate current-source density estimation. Individual electrodes or probe sites were electroplated to an impedance of 100-400kΩ (at 1kHZ) using a 75% polyethylene glycol-25% gold solution (Ferguson et al., 2009) or PEDOT (Ludwig et al., 2006, 2011). NanoZ (White Matter LLC) was used to pass the constant electroplating current (0.1-0.5µA) and perform impedance spectroscopy for each electrode site. A reversed-polarity pulse of 1s duration preceded the plating procedure to clean the electrode surface. After electroplating, electrodes were impedance tested in saline (at 1kHz) and were washed with distilled water and checked for any potential short-circuits.

2.6 LOCAL FIELD POTENTIAL ANALYSES

Raw data were converted to binary format, low pass-filtered (0.5-400Hz) to extract local field potential component (LFP) and downsampled to 1kHz (Nyquist, 1928, 1924; Shannon, 1948; Shannon, 1949; Whittaker, 1935). LFP signals were filtered for different frequency bands of interest using zero-phase-distortion sixth-order Butterworth filters. All data analysis was performed using custom-written software (DataSuite, Nikolaos Karalis; `https://github.com/nikolaskaralis/data_suite`). Neuroscope was used to aid with data visualization (Hazan et al., 2006).

LFP power spectrum and LFP–LFP coherence estimations were performed using Thompson's multitaper direct spectral estimates (Thomson, 1982). For respiration frequency analyses, data were padded and a moving window of 3s width and 2.4s overlap was applied to the data. Signals were multiplied with 2 orthogonal taper functions (discrete prolate spheroidal sequences), Fourier transformed and averaged to obtain the spectral estimate (Mitra et al., 1999). For gamma frequency analyses, a window of 100ms with 80ms overlap and 4 tapers was used. For visualizations, gamma frequency power spectra were whitened (Mitra et al., 1999). For some analyses and examples,

to obtain a higher resolution in both time and frequency domain, data were transformed using complex Morlet wavelets (bandwidth parameter: 3, center frequency: 1.5). The cone of influence was calculated for each transformation and data points in this cone were excluded from further analysis. Convolution of the real and imaginary components of the transformed signal enables the extraction of the instantaneous amplitude and phase of the signal for each scale. For some example signal visualizations, we found useful to utilize the real-part of the wavelet transformed signal, which preserves both phase and amplitude information. For the power comodulation analysis, the power profile for each frequency bin in each structure was calculated and the correlation coefficient of every pair was calculated. To characterize the causal relationship between the respiratory signal and the prefrontal LFP, spectrally resolved Granger causality was calculated using the multivariate Granger causality toolbox (Barnett and Seth, 2014). Briefly, unfiltered LFP traces were detrended and normalized. The order of the vector autoregressive (VAR) model to be fitted was calculated using the Akaike information criterion. Signal to noise ratio (SNR) for 4Hz power was calculated as the ratio of the mean power in the 2–6Hz band to the mean power outside this band. Imaginary coherence was calculated as: $iCoh = \frac{|Im(\sum_{bins} S_{xy})|}{\sqrt{\sum_{bins} S_{xx} \times \sum_{bins} S_{yy}}}$ where S_{xy} is the cross-spectrum, $S_{xx}$and S_{yy} are the auto-spectra and summation takes place over the spectrogram bins corresponding to the quantified state (Marzetti et al., 2007; Nolte et al., 2004).

For the detection of heart beats, EMG signals were high-pass filtered (>60Hz) and the signal envelope was calculated from the analytic signal. Local maxima of this signal were detected and the ones that exceeded a specified threshold were selected and corresponded to the heart beats. For the heart beat extraction, only periods of behavioral quiescence and sleep were taken into account, to ensure sufficient signal-to-noise ratio and reliable detection. The threshold was automatically calculated and manually adjusted where necessary. For the automatic calculation, a running window of 1s was used, to calculate the mid-range value for each window and the median of these values was found to provide a good threshold for the detection of heart beats.

2.6.1 *Phase modulation analysis*

For phase analyses, the signal was filtered in the desired narrow frequency band and the complex-valued analytic signal was calculated using the Hilbert transform $r(t) = e^{-if(t)}$. The instantaneous amplitude at each time point was estimated based on the vector length, while the instantaneous phase of the signal based on the four-quadrant inverse tangent of the vector angle. A phase of 0° corresponds to the peak of the oscillation and a phase of 180° to the trough of the oscillation. The waveshape of the respiratory signal and its LFP counterparts is highly asymmetric, resulting in non-uniform phase distribution of this reference signal. This deviation from uniformity is catastrophic for the phase modulation statistics since it biases the phase detection leading to false positive results. To account for this potential bias, the phases of the reference signals, the circular ranks of the phase distribution were computed and the phase distribution was transformed using the inverse of the empirical cumulative density function to return a signal with uniform prior distribution. After this correction, the phases can be assumed to be drawn from a uniform distribution enabling the unbiased application of circular statistics (Siapas et al., 2005; Sirota et al., 2008; Karalis et al., 2016). Point-processes with <200 events

in the periods of interested were excluded from phase analyses, due to the sample-size bias of these analyses. For the quantification of phase modulation, the variance-stabilized statistic log(Z) ($Z = \frac{R^2}{n}$, where R is the resultant length and n the sample size, log is natural logarithm) was used (Siapas et al., 2005; Sirota et al., 2008; Karalis et al., 2016). This statistic quantifies the non-uniformity of a circular distribution against the von Mises distribution.

2.6.2 *Phase-amplitude cross-frequency coupling*

For phase-amplitude cross-frequency coupling, the modulation index (MI), as well as the mean resultant length (MRL), was calculated for each phase and amplitude pair (Tort et al., 2008). Phase was evaluated for 1-20Hz with a bandwidth of 1Hz and step of 0.2Hz using Hilbert transform and correction for non-uniformity as described above. Amplitude was evaluated for 20-120Hz with bandwidth 5Hz and step 3Hz. Shuffling statistics were used to evaluate the statistical significance of the MI and MRL by shuffling the phase and amplitude values.

2.6.3 *Current-source density analysis*

Current-source density analysis was performed using the inverse CSD method (Pettersen et al., 2006) with activity diameter 1mm slow and 0.5mm for fast network events, 0.05 standard deviations, smooth varying using cubic splines and extracellular conductivity σ = 0.3 S/m based on calculations of isotropic and ohmic tissue impedance (Ranck, 1963; Logothetis et al., 2007). Importantly, all results were qualitatively confirmed by exploring the parameter space as well as using the classic second derivative CSD method (Nicholson and Freeman, 1975). Occasional malfunctioning recording sites were interpolated from neighboring sites and all relevant sinks and sources were characterized and quantified from portions of data with no interpolated sites. As an interesting side-note, we investigated the possibility of calculating CSD without the uniform sampling allows by silicon-probes but from the densely but non-uniformly distributed electrode wires. To establish this, we calculated the SWR triggered CSD in a mouse recorded with a dense silicon polytrode (23µm electrode spacing) and for comparison, we sub-sampled the electrodes and added random spatial dislocation for each electrode (46 ± 23µm; mean ± s.e.m.). This procedure was repeated 100 times and the average CSD was calculated. The CSD is qualitatively the same, even when comparing the result between a dense and uniform polytrode and a non-uniform, less dense electrode array. This exemplifies the utility of inverse CSD method for non-uniformly sampled data and the possibility of performing laminar analyses without silicon probes. However, it should be noted that although this result holds for SWRs, events that have high SNR and strong laminar profile, the picture might be different in cases where the events have lower SNR and multiple pairs of closely spaced sinks and sources appear in the data (such as in the case of cortical oscillations).

2.6.4 *Layer identification*

For the hippocampal high-density silicon probe recordings, channel layer assignment was performed based on established electrophysiological patterns of activity for different laminae (Buzsaki, 2002). The middle of the pyramidal layer was assigned to the channel with the

highest amplitude of ripple oscillations (100-250Hz band) and associated complex and bursty spiking activity (Spruston, 2008). Neurons recorded dorsal of the channel with the highest SWR power were characterized as deep CA1 pyramidal neurons (Mizuseki et al., 2011). Conversely, neurons recorded ventral of this reference channel were characterized as superficial CA1 pyramidal neurons. Given that neuronal spikes can be identified in more than one channels of the polytrodes, neurons were assigned to the channel with highest spike amplitude (Csicsvari, 2003). The middle of stratum radiatum was assigned to the channel with the deepest negative sharp wave current-source density sink associated with ripple oscillations (Buzsaki et al., 1983; Ylinen et al., 1995). Stratum oriens was defined as the channels above the pyramidal layer SWR CSD source and below the internal capsule, characterized by the positive component of sharp-waves. Internal capsule is identified as few channels below the neocortex that lack prominent neuronal signals, such as spiking activity. For the identification of dentate layers, we used the CSD and amplitude versus depth profile of dentate spikes (DS) (Bragin et al., 1995). DS are large amplitude events that occur naturally during sleep and reflect synchronized bursts of medial and lateral entorhinal cortex (Bragin et al., 1995). The outer molecular layer was defined as the Type-I dentate spike (DSI) sink, while middle molecular layer was assigned as the channels exhibiting DSII sinks. The inner molecular layer was defined as the channel of the deepest secondary sink in the SWR triggered CSD, which is ventral of the DSII middle molecular layer sink. The source of DSII spikes, which corresponds to a typically more localized source preceding SWR events (Ylinen et al., 1995), together with the polarity reversal of the DSII, which occurs above the granule cell layer (Bragin et al., 1995), enables the precise detection of this layer (Senzai and Buzsaki, 2017). Stratum CA1 lacunosum-moleculare was defined as the difference between the theta-trough triggered CSD sink and the outer molecular DSII sink. This corresponds to approximately the dorsal third of the theta sink. For the neocortex, the polarity of the UP and DOWN states was used as a characteristic of superficial and deep layers (Kandel et al., 1997).

2.6.5 *Network event detection*

Ripples were detected from the CA1 pyramidal layer channel using the instantaneous amplitude of the analytic signal calculated from the band-pass filtered (80-250Hz). The instantaneous amplitude was referenced to the amplitude of a channel typically from the cortex overlying the hippocampus, was convolved with a Gaussian kernel (100ms, 12ms s.d.) and normalized. The mean and s.d. of the referenced amplitude were calculated for periods of quiescent immobility and sleep. Ripples were detected as events exceeding 3 s.d. with a minimum duration of 4 cycles and were aligned on the deepest trough of the band-pass filtered signal. Gamma bursts were detected using a similar procedure, but for the relevant frequency band and behavioral states. Dentate spikes (DS) were detected as large deviations (>3SD) of the envelope of the 2-50Hz band-pass filtered LFP signal from the dentate hilar region, referenced to the CA1 pyramidal layer. Following detection, DS were clustered in two types using k-means clustering on the 2D space defined by the 2 principal components of the CA1/dentate depth profile of each spike.

For the detection of UP and DOWN states, the following algorithm was used. The spike train for each single unit was binned in 10ms windows, normalized and convolved with a 0.5s

wide, 20ms sd Gaussian kernel. The average binned spike histogram was calculated across all simultaneously recorded cells (including PNs and INs). DOWN states were detected as periods longer than 50ms with no spikes across all the cells and the exact onset and offset of DOWN states were detected. UP states were detected as periods contained between two DOWN states, lasting between 100ms and 2000ms, with the average MUA activity during this period exceeding the 70th percentile of the MUA activity throughout the recording.

2.7 SINGLE-UNIT ANALYSES

Raw data were processed to detect spikes and extract single-unit activity (Adrian and Zotterman, 1926b; Adrian, 1926; Adrian and Zotterman, 1926a). Spikes from cells within a radius of 50-100µm (100-1000 cells) can be, in principle, separated by their extracellular waveform features (Buzsaki and Draguhn, 2004; Pettersen and Einevoll, 2008; Neto et al., 2016).

For automated spike sorting, the wide-band signals were band-pass filtered (0.6kHz-6kHz), spatially whitened across channels and thresholded and putative spikes were isolated. Clustering was performed using the ISO-SPLIT method implemented in MountainSort package (Chung et al., 2017) and computed cluster metrics were used to pre-select units for later manual curation. Specifically, only clusters with low overlap with noise (<0.05), low peak noise (<30) and high isolation index (>0.9) were considered for manual curation, using custom-written software. At the manual curation step, only units with clean inter-spike interval (ISI) period, clean waveform, and sufficient amplitude were selected for further analysis. For the data collected with high-density polytrodes, after manual curation, a template of the spike waveform across 10 geometrically adjacent channels was calculated and the unit was re-assigned to the channel with peak waveform amplitude.

Single-unit spike sorting was performed using Off-Line Sorter software (Plexon) for all behavioral sessions. Principal component scores were calculated for unsorted waveforms and plotted in a three-dimensional space defined by principal components and/or timing and voltage features of the waveforms; clusters containing similar valid waveforms were manually defined (Lewicki, 1998). A group of waveforms was considered to be generated from a single neuron if the waveforms formed a discrete, isolated, cluster in the three-dimensional space and did not contain a refractory period less than 1ms, as assessed using inter-spike interval analysis. To avoid analysis of the same neuron recorded on different channels, we computed cross-correlation histograms. If a target neuron presented a peak of activity at a time that the reference neuron fired, only one of the two neurons was considered for further analysis.

The electrophysiological characterization of the extracellularly recorded neurons can be achieved with the examination of the auto-correlogram. For example, bursting cells are characterized by short ISI (peaks at 3-6ms) followed by an exponential decay, while regular-spiking cells have a long mode in their ISI histogram. To classify single-units into putative excitatory and inhibitory cell, a set of parameters based on the waveform shape, firing rate, and autocorrelogram were calculated. The two parameters that offered the best separation, in accordance to what has been reported in the past, were the trough-to-peak duration (Bartho, 2004) and the spike-asymmetry

index (the difference between the pre- and post- depolarization positive peaks of the filtered trace) (Csicsvari et al., 1998), reflecting the duration of action potential repolarization which is shorter in interneurons (Freund and Buzsaki, 1996; Henze et al., 2000). Single-units with <200 spikes in the periods of interest were excluded from all analyses. The Euclidian distance was calculated between all neuron pairs and a clustering algorithm based on Ward's method employing an iterative agglomerative procedure was used to combine neurons into groups based on the matrix of distances such that the total number of groups was reduced to return the smallest possible increase in the within-group sum of square deviation.

2.7.1 *Cofiring analysis*

For the detection of interactions between units recorded in the mPFC and BLA, the spike trains of each simultaneously recorded pair were binned (10ms bin size), the cross-correlation of the binned histograms was calculated over multiple lags (maximum lag, ± 500ms) and the peak cross-correlation coefficient for each pair was determined. For the detection of co-firing property for unit pairs, spike trains were binned as before and the co-firing index was calculated as the ratio of co-occurring (common) spikes to the total number of spikes for the two units. This provides a simple yet direct measure of the co-occurrence of unit spikes on multiple levels of temporal resolution. For the determination of the bin size and the robustness of the method, different bin sizes were tested; they all gave qualitatively similar results. Among those tested, 10ms was selected because it allows the identification of potentially monosynaptic interactions.

2.7.2 *Supervised learning algorithms*

To establish the predictive value of mPFC and BLA 4Hz oscillations for the animal's behavioral state ("freezing" or "not freezing"), we used two distinct machine learning approaches. Specifically, we used the 4Hz signal-to-noise ratio (SNR) of the two structures as features to train a naive Bayes classifier and a support vector machine (SVM). On the basis of the time-resolved spectral decomposition of the signals (spectrograms), we calculated the mean 4Hz SNR across three consecutive time bins (with a bin size of 150ms) and assigned a binary value based on the behavioral state of the animal during the corresponding time (450ms: freezing = 1; mobility = 0). Each formed SNR–binary value pair constitutes a single data point used as an input to the classifier. For this analysis, we considered the total duration of the recordings; that is, all time bins were used in this analysis. SVM projects data into a higher dimensional space and estimates a hyperplane that best separates the data points belonging to distinct classes (Cortes and Vapnik, 1995). Naive Bayes classifiers assume independence of the probability distributions of the features and classify the test data on the basis of the maximal posterior probability of class assignment (Bishop, 2006). The dataset was randomly split into a training dataset containing 70% of the data points, which was used to train the classifiers, and a test dataset containing the remaining 30% of data points, that was used to test the accuracy of the algorithms. To estimate the stability of the algorithms and confidence intervals of the accuracy and receiver operating characteristics (ROC) curves of the classifiers, we implemented a Monte Carlo procedure whereby the dataset was randomly split 10^3 times in mutually exclusive training and test datasets and

the algorithms were trained and tested on the respective datasets. The accuracy, defined as $accuracy = \frac{\#true\ positives + \#\ true\ negatives}{\#\ of\ datapoints}$ and the area under the curve (AUC) of the ROC curve were used to characterize the performance of the classifiers and were compared with the same algorithms trained on shuffled data using the exact same Monte Carlo procedure.

2.8 STATISTICS

For statistical analyses, the normality assumption of the underlying distributions was assessed using the Kolmogorov-Smirnov test, Lilliefors test, and Shapiro-Wilk tests. Further, homoscedasticity was tested using the Levene or Brown-Forsythe tests. If any of the tests rejected their respective null hypothesis, non-parametric statistics were used. When multiple statistical tests were performed, Bonferroni corrections were applied. Where necessary, resampling methods such as bootstrap and permutation tests were used to properly quantify significance.

2.9 ANATOMICAL ANALYSIS

After plating, electrodes and silicon probes were coated with DiI, a red fluorescent lipophilic dye (DiCarlo et al., 1996). Upon insertion in the brain, the dye is slowly incorporated in the cell membranes and diffuses laterally along the membrane, allowing the visualization of the electrode track and the histological verification of the electrode position. After the conclusion of the experiments, selected electrode sites were lesioned by passing anodal current through the electrode (Summerlee et al., 1982). Typically, 10µA current was passed for 5s to produce lesions clearly visible under the microscope. One day was allowed before perfusion, to enable the formation of gliosis. The location of the electrodes was histologically verified. Mice were euthanized and transcardially perfused through the left ventricle with 4% EM-grade paraformaldehyde (PFA) (Electron Microscopy Sciences) in 0.1 M PBS. Histological verification of recording sites was performed with standard light microscopy, while imaging of virus expression or colocalization was performed with confocal microscopy.

3

OSCILLATORY SIGNATURES OF FEAR BEHAVIOR

Fear response to traumatic or threatening situations helps us evade or escape danger. At the same time, fear response is learned in the form of association between stimulus or situation and the presence of a stressor (e.g. physical danger). This association is very powerful and leaves a memory trace that persists for years after a single experience, generating profound structural and functional changes in the brain that can potentially develop into posttraumatic stress and other anxiety-related disorders.

Fear learning requires only a single experience for the association to be formed and each subsequent exposure to the conditioned stimulus leads to the retrieval of the memory. Both the learning and retrieval of fear memory are characterized by a fearful fight-or-flight behavioral state associated with a range of unique physiological correlates, such as sweating, tremor, and increased heart rate. Could it be that this very characteristic state of the body is more than just a response to the stressor or conditioned stimulus? Could it be that the fear-associated state of the body rather parallels a characteristic state of the brain that enables learning and memory retrieval?

Animal research provides the means to tackle these questions. In the laboratory research, this form of learning is referred to as conditioning and is best represented by classical Pavlovian conditioning in which a neutral tone is repeatedly associated with an aversive stimulus. Fear conditioning gives rise to a lasting memory that in rodents manifests as a stereotypical immobilization response (termed freezing), elicited by the presentation of the tone. Decades of research have identified multiple brain regions that are involved in associative fear learning, including the dorsal medial prefrontal cortex (mPFC) and the basolateral amygdala (BLA), which have emerged as two structures critical for the learning and expression of fear.

However, while freezing behavior is widely used as a standard measure of fear memory, little is known about the neural mechanisms supporting this behavior and the functional role of the brain state in the learning and retrieval of fear.

Information transmission between remote brain structures is believed to rely on the synchronization of the neuronal activity between the two structures. Over the past decades, oscillations have emerged as an important mechanism for the organization of collective neural activity and are implicated in both the physiological and pathological functioning of the brain. Oscillatory organization of neuronal circuits is believed to act as a common clock that enables such synchronization between regions directly or indirectly connected. Such patterns of activity have been described in various structures and behaviors and are thought to underlie learning. The exploratory state is associated with distinct internal dynamics known as theta (~8Hz) oscillations, while deep sleep state is characterized by slow (~1Hz) oscillations. Recent evidence suggests that

during fear behavior, neuronal oscillatory activity supports the associative learning and memory expression (Likhtik et al., 2014; Livneh and Paz, 2012).

However, the precise neuronal mechanisms mediating long-range network synchronization during fear behavior remain unknown. Furthermore, a causal role of neuronal synchrony among mPFC and BLA circuits in driving fear behavior has not yet been demonstrated. To fill this important gap, we focused our attention on the study of the neural processes associated with the freezing behavior. To achieve this, we combined electrophysiological recordings of single unit and local field potential activity, as well as optogenetic manipulations of the mPFC and BLA circuits in freely behaving mice.

3.1 INTERNALLY GENERATED FREEZING BEHAVIOR

To investigate these processes, we subjected mice to auditory fear conditioning. In this paradigm, a previously innocuous tone (the conditioned stimulus - CS^+) was repeatedly presented just before the delivery of a mild electric footshock (unconditioned stimulus - US). A different auditory stimulus (CS^-) was never paired with the US and is used as an internal control. Twenty-four hours after conditioning, mice were re-exposed to the conditioned stimuli without the delivery of the US (Figure 3.1a). In response to the CS^+ mice exhibited freezing behavior, while they were able to discriminate between CS^+ and CS^- (Figure 3.1b). Freezing levels were similarly low to both CS^+ and CS^- during the habituation session before the fear conditioning.
When examining the temporal profile of the freezing behavior, we identified long bouts of freezing that occurred after the offset of the CS^+ presentation (Figure 3.1c,d). The periods of freezing outside of CS^+ amount to almost 60% of the total freezing during fear retrieval (Figure 3.1f). The onset of freezing tends to occur after the second pip from the series of 27 pips that comprise one CS^+ presentation (Figure 3.1f) and ~60% of freezing episodes are initiated during CS^+ presentation while the rest are spontaneously initiated outside of tone periods (Figure 3.1e).
These results suggest that in addition to freezing episodes driven by auditory inputs, internally generated mechanisms can initiate and maintain freezing episodes following CS^+ presentations.

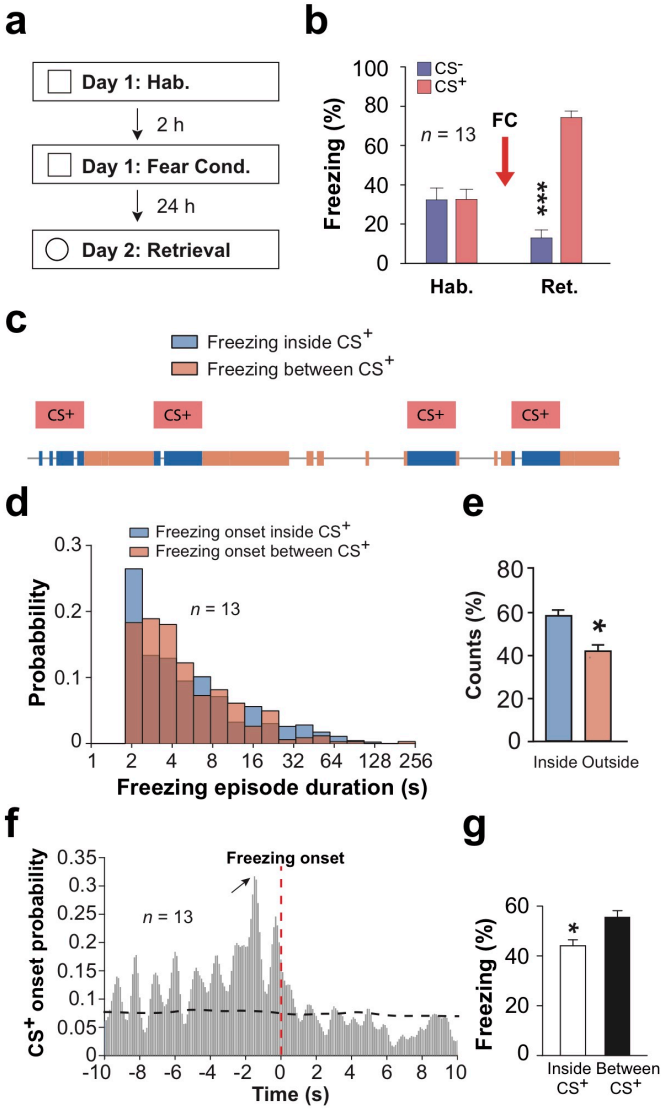

Figure 3.1: **Freezing behavior is triggered by internally generated mechanisms.**
(a) Experimental protocol. *(b)* Behavioral results. During habituation, mice (n = 13) exhibited low freezing during the CS^- and CS^+. After conditioning, the CS^+ induced longer freezing episodes compare to the CS^- (paired t-tests). *(c)* Example behavioral quantification from a single mouse, exhibiting freezing during CS^+ presentations and prolonged freezing episodes between CS^+ presentations. *(d)* Probability distribution of the duration of freezing episodes, for episodes initiated inside or between CS^+ presentations. *(e)* Percentage of freezing episodes initiated inside or between CS^+ presentations (n = 13 mice, paired t-test). *(f)* Cross-correlation analysis performed between freezing and CS^+ onset (n = 13 mice, 100-ms bins). Red vertical dotted line represents freezing onset. Black horizontal dotted line represents significance level. Black arrow indicates the highest probability for CS^+ onset at 1.5 s before freezing onset. *(g)* Percentage of freezing exhibited during and between CS^+ presentations (paired t-test). Error bars: mean ± s.e.m.
Adapted from: Karalis et al., 2016

In order to examine the neural circuits that are potentially involved in the initiation and maintenance of freezing, we performed single-unit and local field potential (LFP) recordings in the mPFC and BLA of freely behaving mice. During freezing periods, the mPFC LFPs are characterized by high-amplitude field oscillations with peak frequency ~4Hz that are sustained throughout the duration of the freezing episode (Figure 3.2a,c,d,e and Figure 3.4b). These oscillations are not present during short episodes of passive immobility in the habituation session (Figure 3.2b,e and Figure 3.4a) or during CS^- related immobility during retrieval (Figure 3.2c,d).

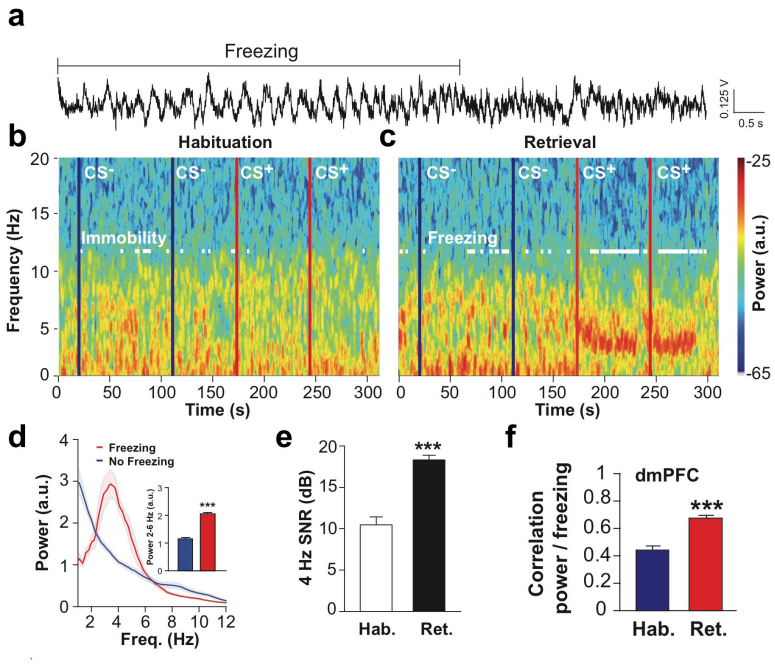

Figure 3.2: **Emergence of mPFC 4Hz oscillations during freezing behavior.**
(a) Example mPFC raw LFP traces recorded during retrieval. 4Hz oscillatory activity is prominent during freezing behavior. (b, c) Example spectrograms of mPFC LFPs during habituation *(b)* and retrieval *(c)* sessions during CS^- and CS^+ presentations (blue lines, CS^- onset; red lines, CS^+ onset; habituation, recording during CS^- 3 and 4; retrieval, recording during CS^+ 1 and 2). White lines on the spectrogram indicate immobility or freezing episodes. Spectral power in log scale. Similar traces were observed for the 13 animals used in these experiments. *(d)* Averaged power spectra of mPFC LFPs recorded during retrieval for freezing and no-freezing periods (n = 13 mice). Inset, averaged mPFC 2-6Hz power during retrieval for freezing and no-freezing periods (paired t-test). *(e)* Averaged SNR of 4Hz oscillation (2-6Hz) during habituation (Hab.) and retrieval (Ret.) (n = 12 mice, paired t-tests). *(f)* Correlation between mPFC 4Hz power and freezing during habituation and retrieval (n = 13 mice, paired t-tests). Error bars: mean ± s.e.m. a.u., arbitrary units. Shaded areas: mean ± s.e.m.
Adapted from: Karalis et al., 2016

To establish the distinction between freezing and passive immobility, we recorded the nuchal muscle EMG and characterized the profile of this signal in response to CS^+ presentations during habituation and retrieval sessions. Freezing can be distinguished from passive immobility based on the EMG response (Figure 3.3a,b).

3.2 MPFC AND BLA 4HZ PREDICT FREEZING BEHAVIOR

The power of these oscillations is positively correlated with the duration of the freezing episodes during retrieval (Figure 3.2f and Figure 3.3c). To establish the utility of 4Hz oscillation presence to predict freezing behavior, we trained two classifiers on a part of the data and used them to predict whether the animals were freezing or not, using only the prefrontal 4Hz power as a predictor. These classifiers predicted correctly the freezing episodes with ~76-79% accuracy (Figure 3.3f,g,h).

To characterize better the relationship between the emergence of 4Hz oscillations and the freezing behavior, we quantified the power profile of the 4Hz oscillations around the onset and offset of freezing behavior. This analysis revealed that 4Hz oscillation power increases ~0.5 s before the onset of the freezing episode and decreases ~0.5 s before the offset (Figure 3.3d,e). These changes suggest a causal role of prefrontal 4Hz oscillations in driving fear behavior.

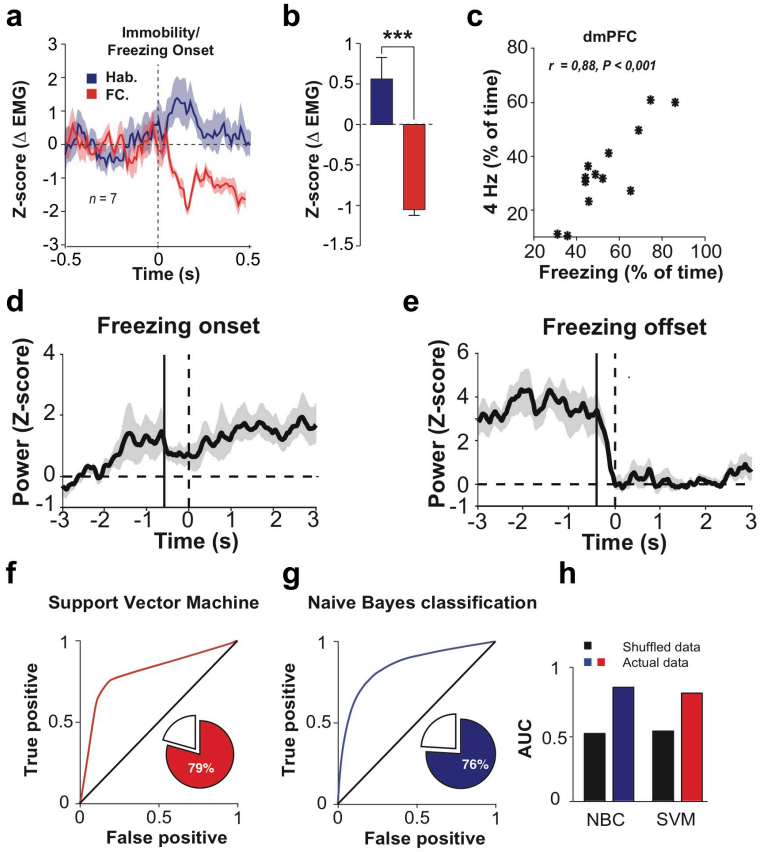

Figure 3.3: **mPFC 4Hz oscillations predict freezing.**
(a) Normalized EMG during immobility or freezing (n = 7 mice). *(b)* Averaged EMG (0-500ms after CS$^+$, Mann-Whitney U test). *(c)* Correlation between freezing and mPFC 4Hz (n = 13 mice; Pearson's r = 0.88, P < 0.001). (d,e) Averaged freezing onset-triggered *(d)* and offset-triggered *(e)* normalized 4Hz power envelope; black lines: first significant bin of 4Hz power changes (f, g) Receiver operating characteristics analysis performed on a naive Bayes classifier (NBC) *(f)* and support vector machine (SVM) classifier *(g)* trained on mPFC 4Hz SNR during freezing. *(h)* Averaged area under the curve for both classifiers versus shuffled data.
Adapted from: Karalis et al., 2016

Interestingly, during fear conditioning, 4Hz oscillations emerged gradually (Figure 3.4c) and the power of these oscillations correlates with the number of CS$^+$ - US pairings and the amount of freezing (Figure 3.4d). To test whether these oscillations are unique to the auditory fear conditioning paradigm, we subjected a different set of mice to contextual fear conditioning (Figure 3.5a,b). The same phenomenon was observed during freezing in this paradigm (Figure 3.5c,d,e) suggesting that prefrontal 4Hz oscillations might constitute a general physiological signature of freezing behavior.

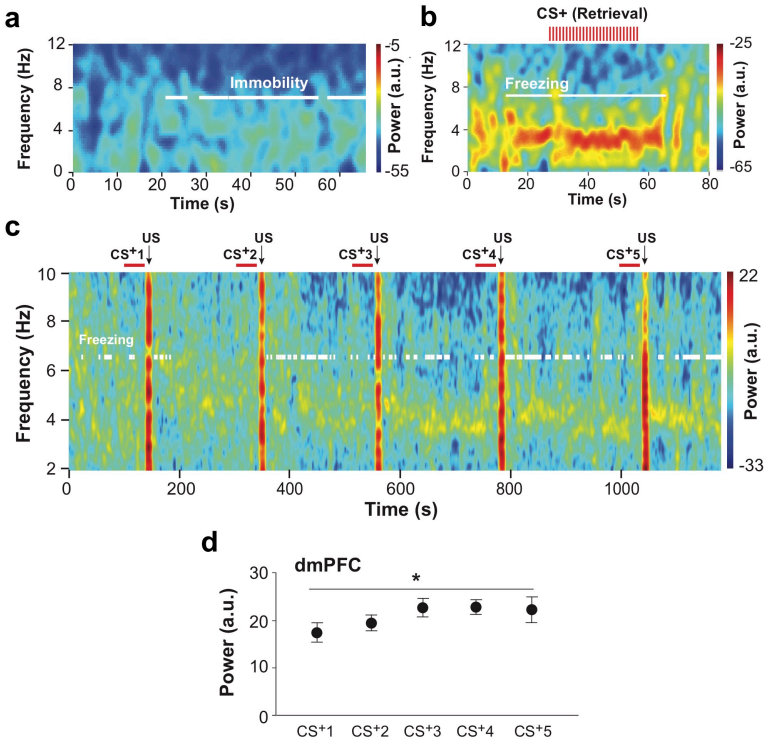

Figure 3.4: **Development of mPFC and BLA 4Hz oscillations during fear conditioning.** *(a)* Spectrograms of mPFC LFP during habituation. White lines indicate immobility. Spectral power in log scale. *(b)* Examplespectrogram of mPFC LFPs at a finer time resolution before, during and after presentation of a CS^+ during retrieval. Each red tick represents a single CS^+ pip. White lines on the spectrogram indicate freezing episodes. *(c)* Example spectrogram of mPFC LFPs recorded during auditory fear conditioning for successive CS^+-US associations (top red lines: CS^+ duration). White lines on the spectrogram indicate immobility/freezing episodes. Similar results were obtained for the 4 animals used in these experiments. Spectral power in log scale. *(d)* Averaged mPFC power during CS^+ presentations throughout the conditioning session (n = 4 mice, one way repeated measures ANOVA). Error bars: mean ± s.e.m. a.u., arbitrary units. Adapted from: Karalis et al., 2016

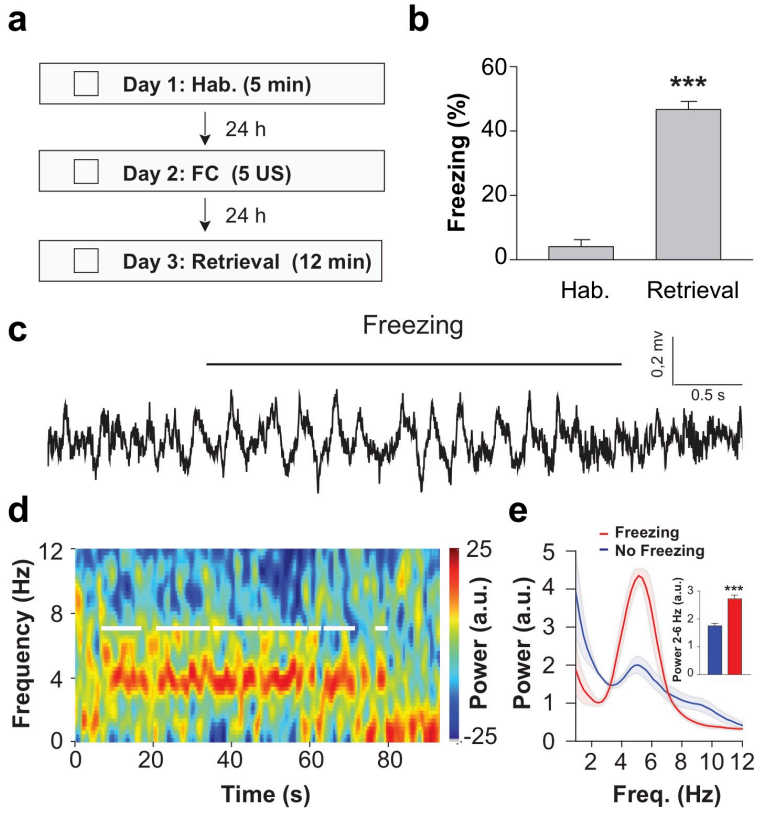

Figure 3.5: **Emergence of mPFC 4Hz oscillations during contextual fear behavior.**
(a) Behavioral protocol *(b)* Behavioral results. During Habituation (Hab.), mice (n = 6) exhibited low freezing whereas following contextual fear conditioning (Day 2: Retrieval), freezing values were significantly increased (paired t-test). *(c)* Example mPFC raw LFP traces recorded during the Retrieval session. 4Hz oscillatory activity is visible during freezing behavior. *(d)* Example spectrogram of mPFC LFPs at a fine time resolution during freezing episodes at Retrieval. White lines on the spectrogram indicate freezing episodes. Similar results were obtained for the 6 animals used in these experiments. Spectral power in log scale. *(e)* Averaged power spectrum of mPFC LFPs recorded during Retrieval for freezing and no freezing periods (n = 6 mice). Inset: Averaged mPFC 2-6Hz power during Retrieval for freezing and no freezing periods (paired t-test). Shaded area and error bars: mean ± s.e.m. a.u.: arbitrary units.
Adapted from: Karalis et al., 2016

3.3 4HZ IS DISTINCT FROM THETA

Past reports have identified the presence of hippocampal theta oscillations in the prefrontal cortex during working memory (Benchenane et al., 2010; Siapas et al., 2005) and fear behavior (Likhtik et al., 2014; Stujenske et al., 2014; Seidenbecher et al., 2003; Lesting et al., 2011). In order to evaluate if 4Hz oscillations correspond to low-theta hippocampal oscillations, we reversibly inactivated the medial septum (MS) which is a prominent generator of hippocampal theta oscillations (Figure 3.6a,b). After pharmacological inactivation with the potent GABAa agonist muscimol, the power of hippocampal and prefrontal theta oscillations was reduced (Figure 3.6c). However, the power of prefrontal 4Hz oscillations during freezing was unaffected (Figure 3.6c,d,e). This manipulation established that the generation of 4Hz oscillation is not dependent on the MS activity.

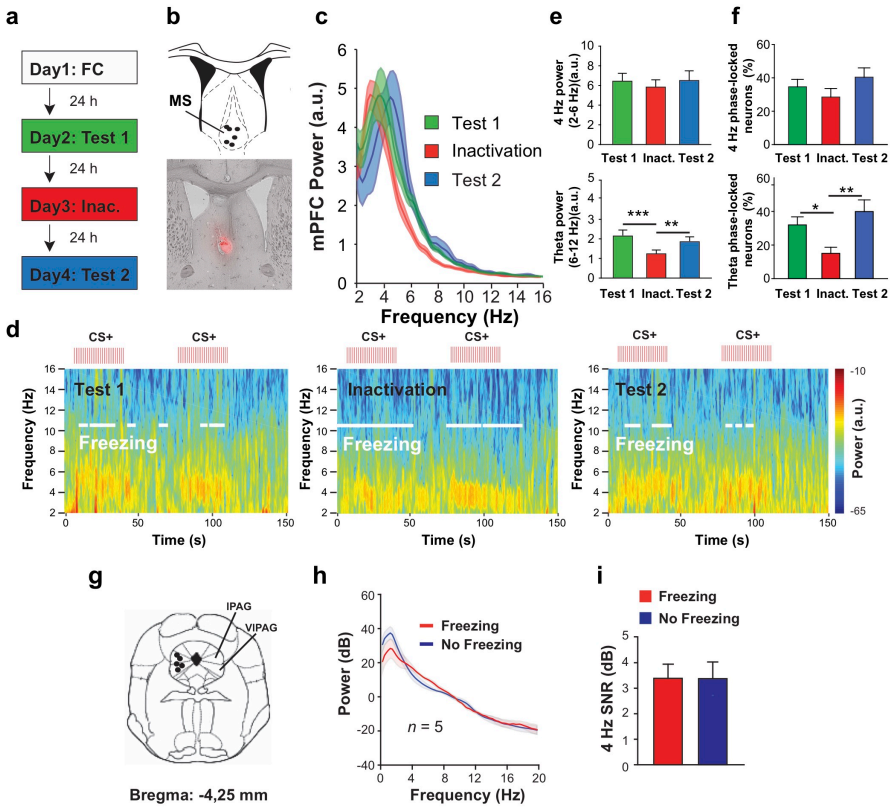

Figure 3.6: **Reversible inactivation of the medial septum does not block mPFC 4Hz oscillations.** *(a)* Experimental strategy *(b)* Location of injections sites in the medial septum (MS) and example diffusion of muscimol covalently bound to a fluorescent tag (bottom, dipyrromethene boron difluoride (BODIPY), red). *(c)* Power spectra of mPFC LFPs before (Day 2: Test 1), following (Day 3: Inact.) and after (Day 4: Test 2) MS inactivation (n = 6). *(d)* Example spectrograms of mPFC LFPs before (Test 1), during (Inactivation) and after (Test 2) MS inactivation (red tick represents single CS^+ pips). White lines on the spectrogram indicate immobility/freezing episodes. *(e)* Top, Quantification of mPFC LFP 4Hz power (2-6Hz) before, during, and after MS inactivation. (n = 6 mice, One-way repeated measure ANOVA). Bottom, Quantification of mPFC LFP theta power (6-12Hz) before, during, and after MS inactivation. MS inactivation significantly reduced mPFC theta power (n = 6 mice). *(f)* Percentage of mPFC neurons phase-locked to 4Hz (*top*), or theta (*bottom*) oscillations (6-12Hz). (Test 1: n = 80 neurons; Inact.: n = 100 neurons; Test 2: n = 120 neurons. One-way repeated measure ANOVA). *(g)* Location of recording sites in the lateral (lPAG) and ventrolateral periaqueductal gray (vlPAG) (n = 5 mice). *(h)* Averaged power spectrum of PAG LFPs recorded during Retrieval for freezing and no freezing periods (n = 5 mice). *(i)* Averaged PAG 2-6Hz power during Retrieval for freezing and no freezing periods (n = 5 mice, paired t-test). Shaded areas: mean ± s.e.m. a.u.: arbitrary units. Error bars: mean ± s.e.m. Adapted from: Karalis et al., 2016

Further, examining the tone-triggered spectrograms and phase locking, we establish that 4Hz oscillations are distinct from the transient, short-lasting (~300ms) prefrontal theta phase resetting induced by the CS^+ presentations (Courtin et al., 2014b; Likhtik and Gordon, 2013)(Figure 3.7). 4Hz oscillations do not exhibit phase resetting nor increased power in response to single CS^+ pip presentations and are in contrast related to the behavioral response to these tones. Finally, to test the possibility of this oscillation being related to motor patterns during freezing, we recorded in the ventrolateral periaqueductal gray (vlPAG), a structure involved in the generation of different aspects of the freezing behavior (Tovote et al., 2016). vlPAG LFPs did not reveal any rhythmicity at 4Hz frequency suggesting that this rhythm is not a global pattern of motor-related activity (Figure 3.6g-i).

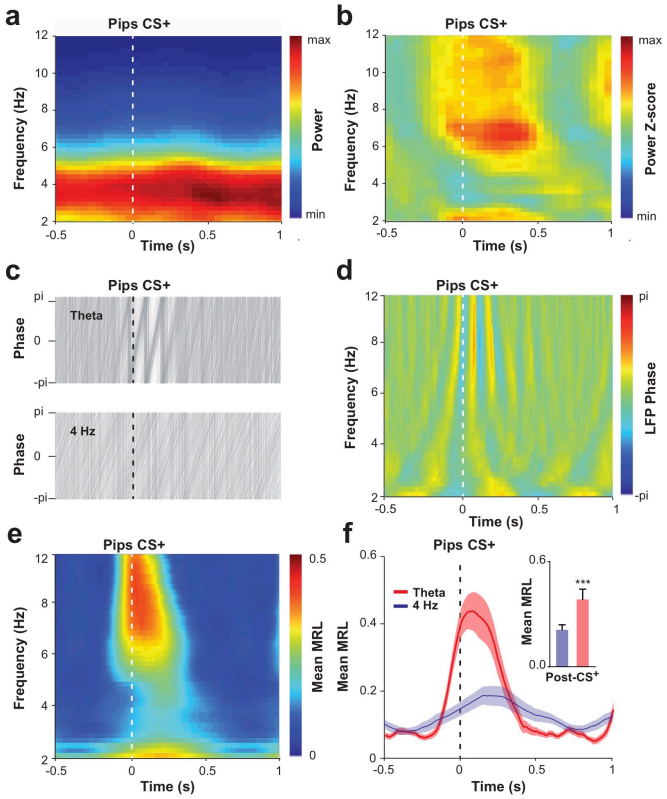

Figure 3.7: **Distinction between tone-evoked theta-resetting and freezing-related 4Hz oscillations.** (a, b) Averaged raw *(a)* and Z-score normalized *(b)* LFP spectrogram in the 2-12Hz frequency band around CS^+ pip presentations during freezing episodes. CS^+-associated theta was observed as a single burst occurring right after CS^+ and spanning ~300ms with frequency between 8 and 12Hz. Spectral power in log scale. *(b)*. On the contrary 4Hz oscillation was present throughout the triggered spectrogram, due to the co- occurring freezing behavior and was not modulated by CS^+ presentation *(a)*. *(c)* Overlaid mPFC local theta and 4Hz phases of CS^+-triggered LFP traces from an example animal, illustrating theta but not 4Hz phase resetting induced by CS^+ pip presentations during freezing episodes. *(d)* LFP phase spectrogram in the 2-12Hz frequency band around CS^+ pip presentations from the same animal as in *(c)* revealing a sharp and stable versus a broad and unstable CS^+-evoked phase for local theta and 4Hz oscillations, respectively. *(e)* Color-coded mean resultant length (MRL) of phases across animal for each time-frequency bin in the 2-12Hz frequency band around CS^+ pip presentations during freezing episodes (n = 13 mice). A low MRL value indicates an unstable phase (no modulation nor resetting of 4Hz oscillations) whereas a high MRL value relates to a consistent phase (8-12Hz theta burst and resetting). *(f)* Mean MRL for mPFC 4Hz (blue line) and 8-12Hz theta (red line) revealing the changes in phase stability triggered by CS^+ pip presentations during freezing episodes (n = 13 mice). Inset: Averaged MRL after (0 to 300ms) CS^+ pip onset (n = 13 mice, 12 CS^+, paired t-test). Shaded areas: mean ± s.e.m. Error bars: mean ± s.e.m.
Adapted from: Karalis et al., 2016

3.4 MPFC 4HZ DRIVE BLA DURING FREEZING

When examining the BLA LFPs, we observe the same 4Hz oscillation during freezing behavior (Figure 3.8a,b,c). The power of the oscillation in this structure is lower than in the prefrontal cortex (Figure 3.8d), a fact that can be explained by the nuclear organization of the BLA that results in mutual canceling of neuronal dipoles, in contrast to the strong lamination of the cortices that supports the amplification of parallel dipoles (Buzsáki et al., 2012; Nunez and Srinivasan, 2006). Nevertheless, during retrieval, the presence of this oscillation is significantly enhanced (Figure 3.8e) and the power of the oscillation correlates with the freezing duration (Figure 3.8f)

while all the qualitative features of this oscillation as described for the mPFC hold for the BLA as well (Figure 3.9).

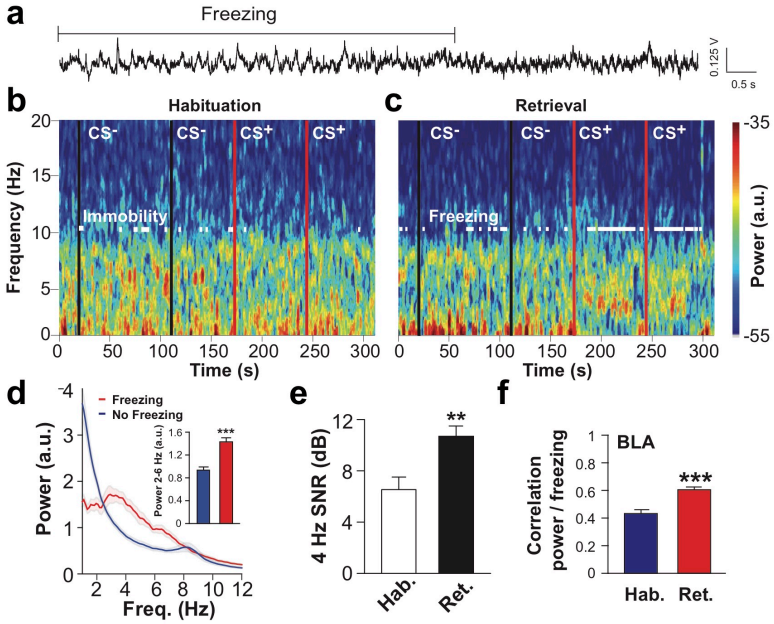

Figure 3.8: **BLA 4Hz oscillations emerge during freezing.**
(a) Example BLA LFP traces recorded during retrieval. (b,c) Spectrograms of BLA LFPs during habituation *(b)* and retrieval *(c)* during CS^- and CS^+ (black lines, CS^- onset; red lines, CS^+ onset). White lines indicate immobility or freezing. *(d)* Averaged power spectrum of BLA LFPs recorded during retrieval for freezing and no freezing (n = 13 mice). Inset, averaged BLA 2-6Hz power during retrieval for freezing and no freezing (paired t-test). *(e)* Averaged 4Hz SNR during habituation (Hab.) and retrieval (Ret.) (n = 12 mice, paired t-tests). *(f)* Correlation coefficient between the power envelope of the 4Hz oscillations (2-6Hz bandpass) recorded in the BLA and immobility/freezing behavior during Habituation (Hab.) and Retrieval sessions (n = 13 mice, paired t-test). Shaded areas: mean ± s.e.m. Error bars: mean ± s.e.m.
Adapted from: Karalis et al., 2016

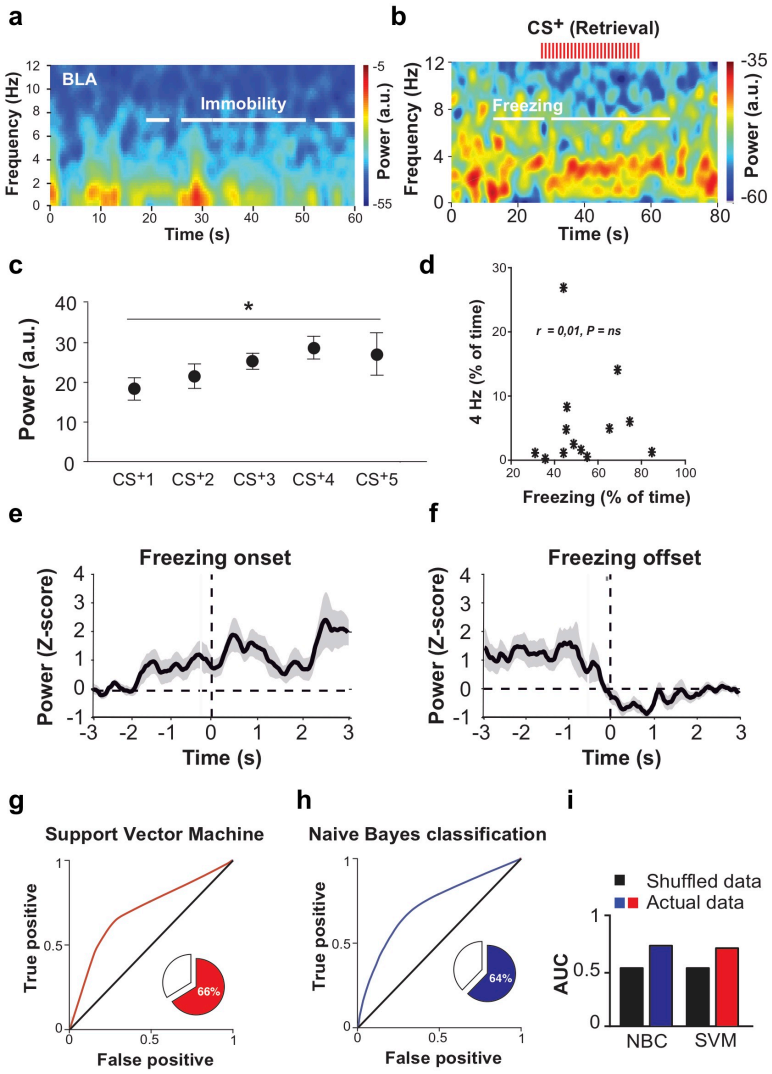

Figure 3.9: **BLA 4Hz oscillations predict fear behavior.**
(a) Example spectrograms of BLA LFPs recorded during Habituation. White lines on the spectrogram indicate immobility periods. Spectral power in log scale. *(b)* Spectrogram of BLA LFPs before, during and after presentation of a CS^+ during retrieval. Red ticks represent single CS^+ pips. White lines indicate freezing. Spectral power in log scale. *(c)* Averaged BLA power during CS^+ presentations throughout the conditioning session (n = 4 mice, one way repeated measures ANOVA). *(d)* Correlation analysis performed between freezing and 4Hz episodes for the BLA (n = 13 mice; BLA: Pearson's r coefficient = 0.01, P = 0.974). (e,f) Averaged freezing onset-triggered *(e)* and offset-triggered *(f)* averaged Z-scored 4Hz power envelope (n = 13 mice). (g,h) Receiver operating characteristics (ROC) analyses performed for Naïve Bayes (NBC) *(g)* and support vector machine (SVM) *(h)* classifiers trained on 4Hz signal to noise ratio (SNR) of the BLA during freezing episodes. Insets: Percentage of accuracy of the NBC *(g)* and SVM *(h)* classifiers to predict freezing behavior based on BLA 4Hz SNR. *(i)* Averaged area under the curve for NBC and SVM classifiers compared to corresponding shuffled data. a.u.: arbitrary units. Error bars: mean ± s.e.m.
Adapted from: Karalis et al., 2016

During freezing behavior, the prefrontal and amygdala 4Hz oscillations are phase-synchronized (Figure 3.10a,c). To exclude the potential of volume conduction between the two structures or from a signal originating in a third structure, we utilized the imaginary coherence. This conservative measure of synchronization eliminates the zero phase-lag signals from consideration and identifies only the phase and amplitude correlation that originates from the non-zero phase lag signals

(Figure 3.10d). Examining the phase difference between the signals we identified a strong phase locking and importantly a clear directionality from the mPFC to the BLA (Figure 3.10b).

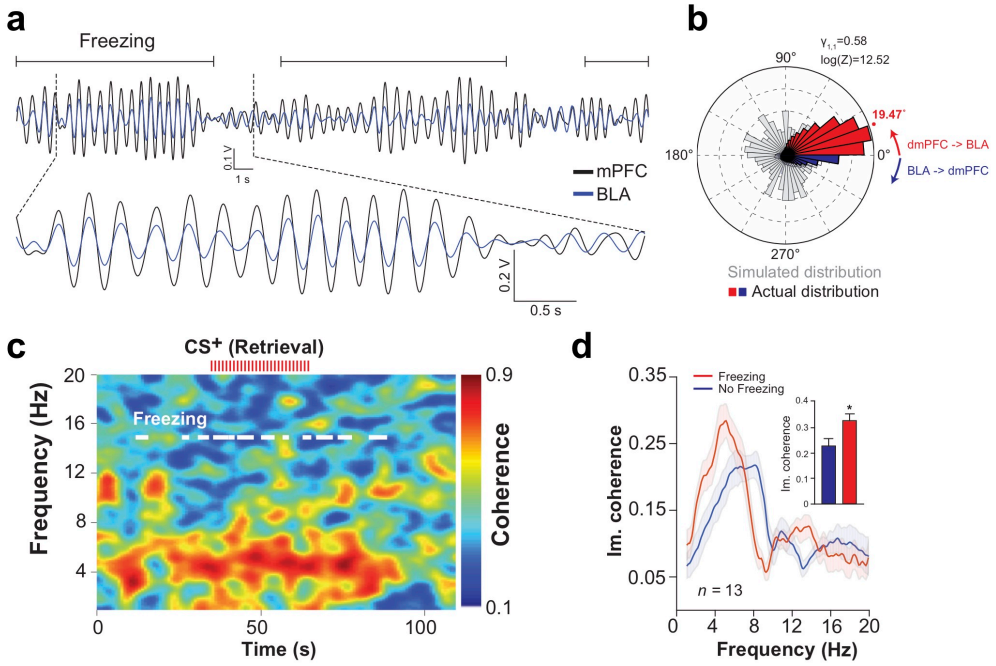

Figure 3.10: **Synchronization of mPFC and BLA 4Hz oscillations during freezing.**
(a) Overlaid filtered (2-6Hz) mPFC and BLA LFP traces illustrating synchronized 4Hz during freezing. *(b)* Circular distribution of the phase differences between mPFC and BLA LFPs recorded for freezing during retrieval compared to a control bootstrap-simulated phase distribution (n = 13 mice). *(c)* Example coherogram for mPFC and BLA LFPs recorded during retrieval during CS^+. Red ticks represent individual CS^+ pips. White lines indicate freezing. *(d)* Averaged mPFC and BLA LFPs imaginary coherence (Im. coherence) for freezing and no freezing during retrieval (n = 13 mice). Inset: Averaged peak of imaginary coherence for freezing and no freezing during retrieval (paired t-test). Shaded area: mean ± s.e.m. Error bars, mean ± s.e.m.
Adapted from: Karalis et al., 2016

To further elaborate on this putative directionality, we resorted to Granger causality analysis, an effective tool for establishing directionality between time-series (Ding et al., 2004; Bressler and Seth, 2011). Using the Granger causality in the spectral domain, we identified a specific directionality from the mPFC to the BLA for the 4Hz oscillation during freezing (Figure 3.11a,c). Analytical perturbations of either the amplitude or the phase of the two signals eliminated the Granger causality, suggesting a dependence on the joint interaction between phase and amplitude for this effect (Figure 3.11c,d,e). Finally, calculating the cross-correlation between the 4Hz oscillation power for both structures revealed a similar directionality and suggested a putative 15ms time-lag between the two oscillations. Together, these results suggest a role of prefrontal 4Hz oscillation in driving BLA LFP activity.

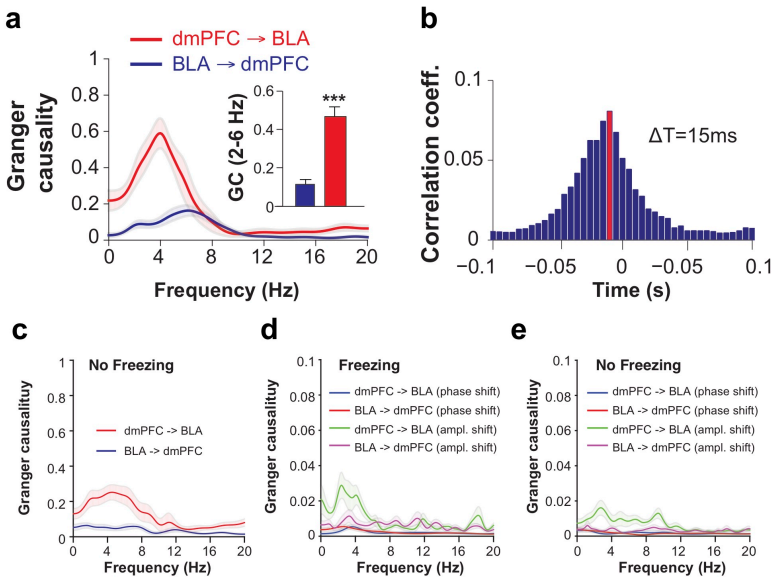

Figure 3.11: **mPFC LFP 4Hz oscillations precede BLA oscillations during freezing.**
(a) Granger causality (GC) analysis performed between mPFC and BLA LFPs during freezing (n = 13 mice). Inset: Averaged GC (2-6Hz) between mPFC and BLA LFPs during freezing (retrieval, paired t-test). *(b)* Averaged cross-correlogram performed between mPFC and BLA LFPs (2-6Hz). The peak (red bar) and negative skewness of the distribution indicate that mPFC 4Hz oscillations lead the BLA oscillatory activity by 15ms (n = 13 mice). *(c)* Granger Causality (GC) analyses performed between mPFC and BLA LFPs during No Freezing periods at retrieval (n = 13 mice). No directional effect was observed in these conditions. (d, e) GC analyses performed between mPFC and BLA LFPs during Freezing *(d)* and No Freezing *(e)* periods at Retrieval and for which the phase or amplitude of 4Hz LFPs was permuted. The absence of directional effect in the freezing condition indicates that the direction of interaction between mPFC and BLA is highly dependent on both 4Hz phase and amplitude (n = 13 mice). Shaded area: mean ± s.e.m. Error bars, mean ± s.e.m.
Adapted from: Karalis et al., 2016

3.5 4HZ ORGANIZE MPFC AND BLA ACTIVITY

To identify the role of 4Hz oscillations in entraining neuronal populations in the prefrontal cortex and the amygdala, we recorded single units in both structures simultaneously (Figure 3.12a,d). Using principal component analysis and clustering, the extracellularly recorded spikes were clustered in single units (Figure 3.12g) and using the firing rate and features of their extracellular waveshape, we separated these units in putative excitatory projection neurons (PNs) and inhibitory interneurons (INs) (Figure 3.12b,i). This separation was confirmed by the few pairs of monosynaptically connected cells that were simultaneously recorded (Figure 3.12h).

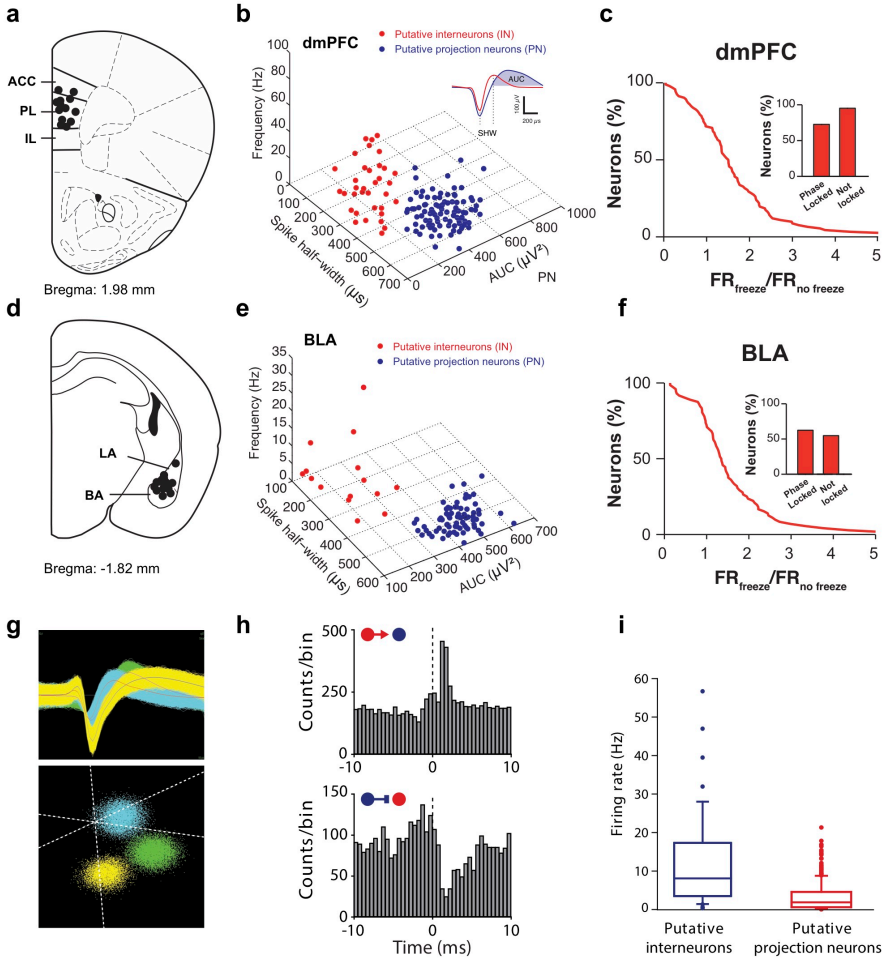

Figure 3.12: **Separation between mPFC and BLA putative principal neurons and putative interneurons.** *(a)* Location of recording sites in the mPFC *(b)* Among mPFC recorded neurons, 27.56% were classified as putative inhibitory neurons (INs, red circle) and 72.44% as putative projection neurons (PNs, blue circle) using an unbiased unsupervised cluster separation algorithm. *(c)* Cumulative distribution of firing rate ratio for freezing and no freezing periods of mPFC putative PNs. Inset, percentage of phase-locked and non phase-locked mPFC neurons to 4Hz oscillations characterized by enhanced firing rate during fear behavior (n = 13 mice, mPFC: 46 cells). *(d)* Location of recording sites in the BLA *(e)* Among BLA recorded neurons, 17.24% were classified as putative inhibitory neurons (INs, red circle) and 82.76% as putative projection neurons (PNs, blue circle) using the same methodology as in *(b)*. *(f)* Cumulative distribution of firing rate ratio for freezing and no freezing periods of BLA putative PNs. Inset, percentage of phase-locked and non phase-locked BLA neurons to 4Hz oscillations characterized by enhanced firing rate during fear behavior (n = 13 mice, BLA: 21 cells). *(g)* Example results from spike-sorting process. Top, individual spike waveforms from three units are superimposed. Bottom, principal component analysis of the waveforms results in clustering of the waveforms belong to each individual unit. *(h)* Cross-correlation analysis identifies putative monosynaptic excitatory (*top*) and inhibitory (*bottom*) interactions between units. Red and blue circles represent PNs and INs. *(i)* Firing rate of all putative PNs (n = 290 in 7 mice) and INs (n = 48 in 7 mice).
Adapted from: Karalis et al., 2016

To identify the phase relationship between the firing of these cells and the 4Hz oscillation, we extracted the phase of each single spike (Figure 3.13a,d,f,i) and calculated the preferred phase and circular statistics for each cell (log-transformed Rayleigh's Z-test) (Figure 3.13b,e,g,h). This analysis identified that more than half of PNs in each structure and ~75% of INs, are significantly entrained by the 4Hz oscillation. Interestingly, when examining the cross-correlation structure of the population by quantifying the correlation coefficient for each pair of cells between structures, as well as the co-firing index for the same pairs of cells, we observed that during freezing pairs of

phase-locked cells in the two structures are significantly more correlated and co-firing in a short time window, compared to the same cell pairs during mobility periods and to non-phase locked cells (Figure 3.13c,h). Together, these results identify the role of 4Hz oscillation in organizing neuronal firing in both structures and its role in temporally coordinating the activity in both mPFC and BLA to enable the simultaneous co-firing in shorter timescales.

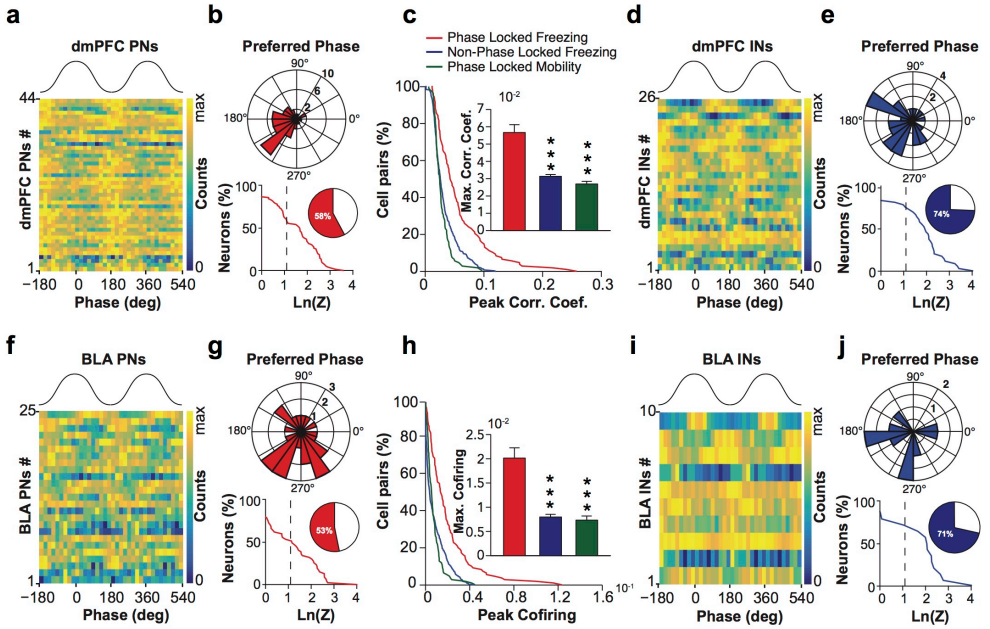

Figure 3.13: **4Hz oscillations synchronize mPFC-BLA spiking activity.**
(a,d,f,i) Color-coded distribution of the 4Hz oscillation phase of spikes from all putative excitatory (a,f) and inhibitory (d,i) neurons recorded in the mPFC (a,d) and BLA (f,i). (b,g,e,j) Circular distribution of the preferred phase of the spiking activity of all mPFC (b,e, top) and BLA (g,j, top) significantly phase-modulated PNs (b,g) and INs (e,j) during freezing (mPFC: 44 PNs and 26 INs; BLA: 25 PNS and 10 INs) and cumulative distribution of log-transformed Rayleigh's test Z of all mPFC (b,e, bottom) and BLA (g,j, bottom) PNs (b,g) and INs (e,j). Inset, percentage of mPFC and BLA neurons significantly phase-modulated by the mPFC 4Hz oscillations. Dashed line, significant 4Hz phase-locking threshold (ln(Z) = 1.097, *P < 0.05, mPFC: 44 of 92 PNs and 26 of 35 INs; BLA: 25 of 72 PNs and 10 of 15 PNs). (c,h) Cumulative distribution of peak correlation coefficient *(c)* and co-firing index *(h)* for pairs of mPFC and BLA phase-locked and non-phase-locked neurons during freezing and mobility. Insets, maximum correlation coefficient *(c)* and co-firing index *(h)* for all pairs of recorded mPFC and BLA neurons (phase-locked pairs, n = 180; non-phase-locked pairs, n = 911; Mann-Whitney U test). Error bars, mean ± s.e.m.
Adapted from: Karalis et al., 2016

3.6 OPTOGENETIC INDUCTION OF MPFC 4HZ DRIVES FEAR BEHAVIOR

In order to establish the causal role of 4Hz oscillations in synchronizing mPFC and BLA PNs and driving fear behavior, we utilized an optogenetic manipulation of the mPFC. Specifically, we expressed the blue-light-gated ion channel Channelrhodopsin-2 onto the PV-expressing interneurons of PV-IRES-Cre mice (Figure 3.14a,b,c). By analog modulation of the laser power intensity, we were able to rhythmically modulate the firing of these cells and consequently rhythmically inhibit and disinhibit the mPFC PN population (Figure 3.14d). This analog stimulation potently entrains prefrontal populations and induces strong field oscillations (Figure 3.14e,f). This manipulation induced freezing behavior during stimulation of naive (non-conditioned) mice, which was specific to 4Hz stimulation and did not occur for other stimulation frequencies or non-sinusoid stimulation with mean 4Hz frequency (Figure 3.14g). Interestingly, 4Hz analog stimulation of

naive mice resulted in contextual conditioning which was evident 24 hours later when mice were re-exposed to the same context in the absence of light stimulation (Figure 3.14h).

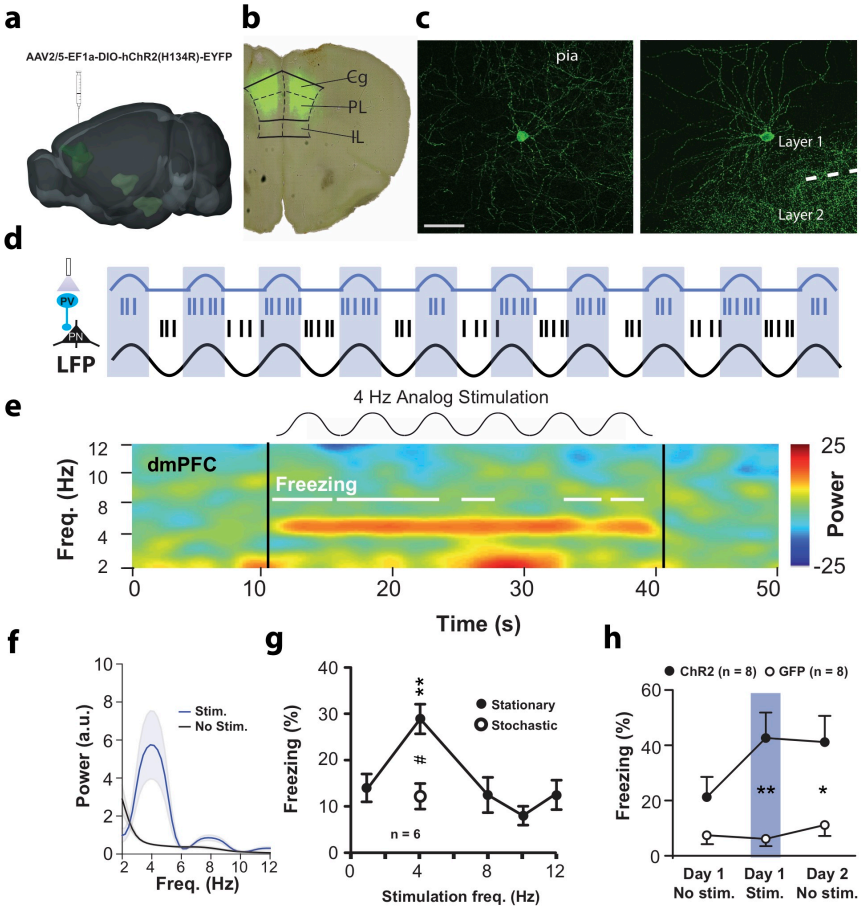

Figure 3.14: **Optogenetic induction of mPFC 4Hz oscillations drives freezing.**
a) PV-IRES-Cre mice were injected in the mPFC with AAV2/5-EF1a-DIO-hChR2-eYFP (n=8) or AAV2/5-EF1a-DIO-GFP (n=8; control). *(b)* Example histological verification of mPFC GFP expression. *(c)* Example labeled mPFC PV+ INs with distinct dendritic arborizations. Left: multipolar neuron with a round soma, corresponding to a putative basket cell. Right: IN with an ovoid soma at the border of layers 1-2, displaying asymmetric and tufted dendrites. Some branches extend towards the pia, bend and follow the pial surface. This neuron corresponds to the typical description of axo-axonic (chandelier) cells in mPFC. *(d)* Experimental design using analog optogenetic stimulation of PV+ INs in the mPFC to induce artificial 4Hz oscillations. *(e)* Spectrogram during 4Hz analog stimulation. *(f)* Averaged normalized LFP power spectra of mPFC LFPs during (Stim.) and outside (No stim.) stimulation (n = 8). *(g)* Percentage of freezing for ChR2 mice (n = 6) during analog stimulation at 1, 4, 8, 10, 12Hz (Stationary) or using a 4Hz stochastic waveform (stationary: one-way repeated measures ANOVA). *(h)* Percentage of freezing for ChR2 (n = 8) or GFP (n = 8) mice before, during and after 4Hz induction (two-way repeated measures ANOVA). Error bars: mean ± s.e.m.
Adapted from: Karalis et al., 2016

Optogenetic analog stimulation resulted in increased cofiring between mPFC and BLA cells during stimulation (Figure 3.15a) and induced strong phase locking of prefrontal PNs and INs (Figure 3.15b) as well as ~20% of BLA PNs and INs (Figure 3.15c). To confirm the specificity of this manipulation for the mPFC and exclude motor or other non-specific effects, we performed the same experiment for the motor cortex instead (Figure 3.15d). This manipulation induced no freezing during stimulation (Figure 3.15e). Similarly, similar manipulation directly at the level

of BLA for conditioned mice led to net inhibition of the structure and reduced freezing during light-stimulation (Figure 3.15f,g).

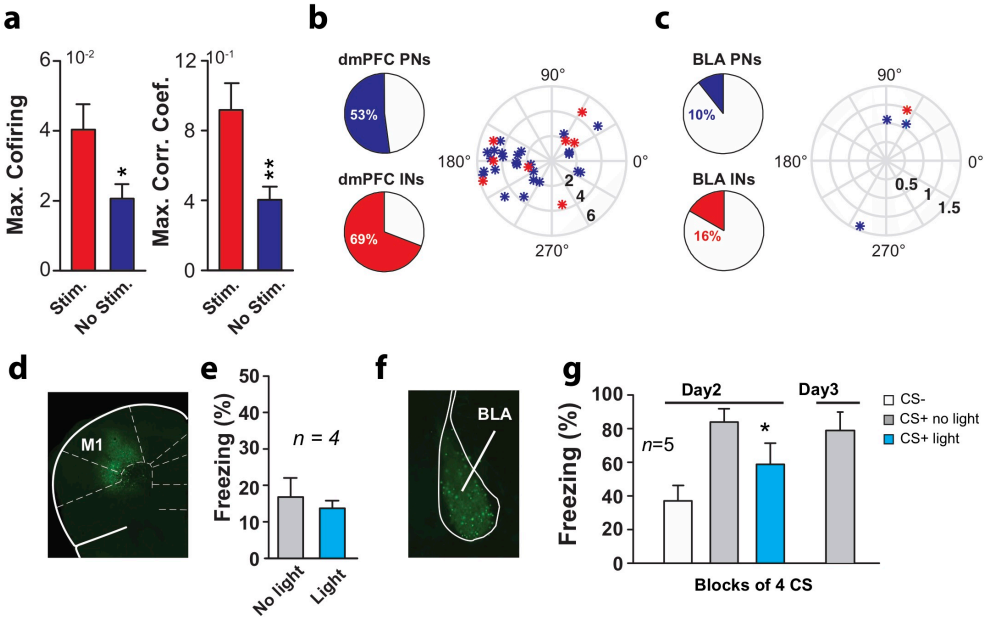

Figure 3.15: **Optogenetic induction of 4Hz entrains neuronal populations.**
(a) Maximum correlation and co-firing index for pairs of mPFC and BLA neurons during and outside stimulation (n = 31 pairs, Mann-Whitney, U = 326 and 278, *P = 0.03; **P = 0.004). (b,c) Percentage of mPFC (b, left) and BLA (c, left) neurons significantly phase-locked to 4Hz oscillations and circular distribution of the 4Hz oscillation preferred phase for populations of mPFC (b, right) and BLA (c, right) phase-locked putative excitatory principal neurons (PNs) and inhibitory interneurons (INs) during mPFC 4Hz analog optogenetic stimulation (mPFC: 25 PNs, 9 INs; BLA: 3 PNs, 1 INs). *(d)* Example micrograph of the motor cortex (M1) in a PV-cre mouse infected with ChR2. Scale bar = 0.5 mm. *(e)* Percentage of freezing displayed by PV-Cre mice infected in the motor cortex with ChR2 during motor cortex 4Hz analog stimulation (n = 4 mice; paired t-test). *(f)* Example micrograph of BLA in a PV-cre mouse infected with ChR2. Scale bar = 0.4 mm. *(g)* Percentage of freezing behavior to CS^- and CS^+ presentations during no-light or light exposure on Day 2 (n = 5 mice, paired t-test). Freezing levels to CS^+ presentations during Day 3 normalized to CS^+ evoked freezing levels during Test 1 (n = 5 mice, paired t-test). Error bars: mean ± s.e.m.
Adapted from: Karalis et al., 2016

3.7 SUMMARY

In summary, these results identified the presence of an intrinsically generated oscillatory mechanism during conditioned fear that organizes the neuronal activity in the prefrontal cortex and the amygdala, resulting in fine timescale assembly organization within and across the structures. The presence of the oscillation and the assembly formation is tightly coupled to freezing behavior and are able to predict the onset and offset of freezing episodes. Optogenetic induction of 4Hz oscillations in the mPFC is sufficient to induce freezing behavior and produce contextual conditioning, while closed-loop phase-specific manipulations of prefrontal activity, conditional on the presence and phase of the oscillation can bidirectionally modulate behavior. These results suggest that this oscillation provides the physiologic substrate for the temporal organization of the prefrontal-amygdala circuit during fear behavior (Figure 3.16a,b).

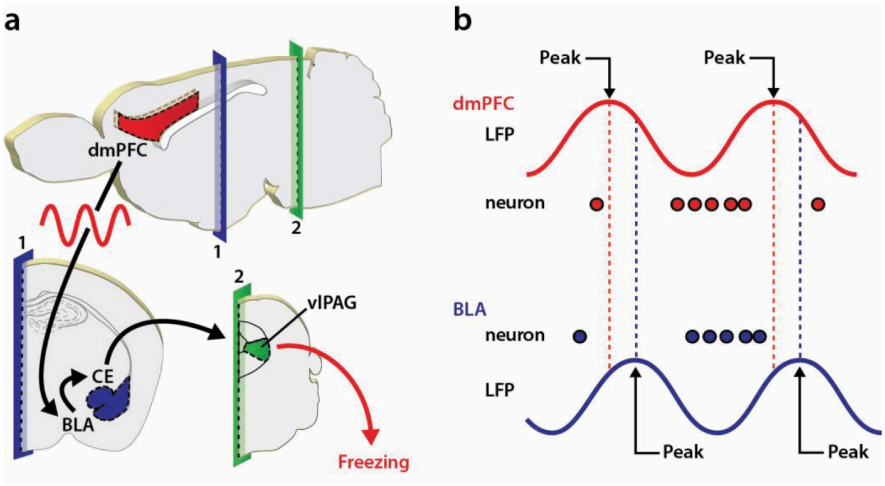

Figure 3.16: **Circuit and potential mechanism of 4Hz-mediated freezing behavior.**
(a) During freezing behavior, mPFC - BLA coupling via 4Hz oscillations allows the expression of conditioned fear behavior, mediated by the recruitment of BLA circuits contacting the central amygdala (CE), which in turn projects to ventrolateral periaqueductal gray (vlPAG). *(b)* 4Hz oscillations promote the fine-scale cofiring of mPFC and BLA neurons in the trough of the oscillation, providing the conditions for fear expression.
Adapted from: Karalis et al., 2016

4

RESPIRATORY ENTRAINMENT OF MEMORY CIRCUITS

Over the past century, cortical and subcortical structures of the limbic circuit and the medial temporal lobe have been identified as critical elements of the memory circuit, involved in emotional regulation and the formation, consolidation, and retrieval of episodic memories (Papez, 1937; Maclean, 1949; Scoville and Milner, 1957). Although the anatomical substrate of these circuits has been elaborated in detail, mechanisms that enable the processing and transfer of information across these distributed circuits are not well understood.

Neuronal dynamics are characterized by oscillatory activity associated with distinct behavioral states and functional roles (Buzsaki and Draguhn, 2004). During active behavioral states, hippocampal theta oscillations dynamically coordinate local activity and information flow between the hippocampus and entorhinal cortex (Buzsaki, 2002; Mizuseki et al., 2009; Fernández-Ruiz et al., 2017), as well as other limbic structures such as the medial prefrontal cortex (mPFC) (Siapas et al., 2005; Benchenane et al., 2010).

During slow-wave sleep, the cortex is in a bistable state, characterized by spontaneous alternations between UP and DOWN states in the membrane potential and action potential firing of neurons (Steriade et al., 1993d; Sirota and Buzsaki, 2005). In parallel, the hippocampal neurons are engaged in transient, fast oscillatory events termed sharp-wave ripples (SWR), during which awake activity is replayed (Wilson and McNaughton, 1993). Such nonlinear dynamics are coordinated between regions (Sirota et al., 2003; Isomura et al., 2006; Maingret et al., 2016) and their interaction is believed to support memory consolidation (Girardeau et al., 2009b; Rothschild et al., 2016a) and the transfer of memories to their permanent cortical storage (Maviel et al., 2004; Kitamura et al., 2017).

While the importance and role of the cortical slow oscillation (SO), hippocampal ripples, and their coordination during sleep have been established, the mechanisms that support this coordination across distributed cortical and limbic circuits during sleep remain elusive and a global pacemaker that ties together distinct network dynamics has not been identified. Recently, a number of studies have identified signatures of respiration in the cortical and hippocampal LFP of rodents (Ito et al., 2014; Yanovsky et al., 2014; Lockmann et al., 2016; Moberly et al., 2018) and humans (Zelano et al., 2016; Herrero et al., 2018), which has been attributed to reafferent olfactory activity. However, the function of these phenomena is not understood and the mechanism and consequences of respiratory modulation have not been established, given the limitations in interpreting LFP signals.

Here we address the hypothesis that the breathing rhythm governs multiregional activity and underlies the coordination of network dynamics across limbic systems during offline states. To this end, using high-density silicon probes we performed a large-scale *in vivo* functional

anatomical characterization of the mPFC, hippocampus, basolateral amygdala (BLA) and nucleus accumbens (NAc). Using this approach, we identified an intracerebral centrifugal respiratory corollary discharge that acts in concert with a respiratory reafference and mediates the inter-regional synchronization of limbic memory circuits. The respiratory modulation is acting as a functional oscillatory scaffold, which together with the underlying anatomical substrate, organizes information flow and systems memory consolidation processes.

4.1 RESPIRATORY ENTRAINMENT OF PREFRONTAL CORTEX ACROSS BRAIN STATES

To investigate the role of breathing in organizing neuronal dynamics in the mPFC, we recorded simultaneously the local electrical activity (electroolfactogram; EOG) (Ottoson, 1955) of the olfactory sensory neurons (OSNs) and single-unit and LFP in the mPFC in freely-behaving mice (Figure 4.1a,b).

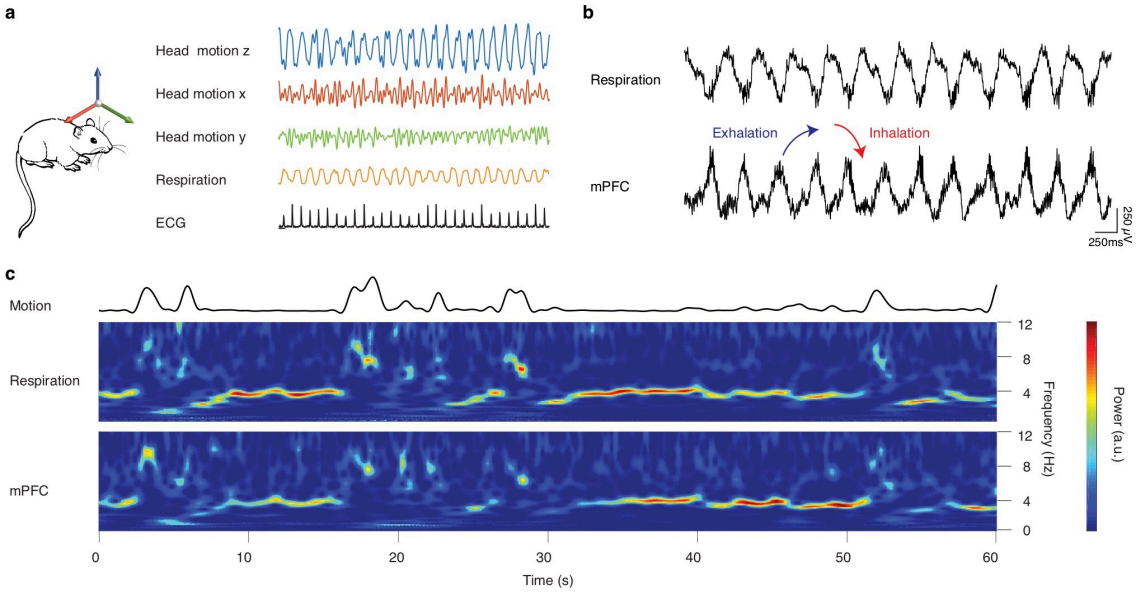

Figure 4.1: **Prefrontal 4Hz oscillations are related to the respiratory rhythm.**
(a) Schematic and example head-motion, respiration, and electrocardiogram (ECG) traces from freely-behaving mice. *(b)* Example traces of simultaneously recorded respiration and medial prefrontal local field potentials (LFP). *(c)* Example time-frequency decomposition of respiratory and mPFC LFP signals, revealing the reliable relationship between the two signals.

The EOG reflected the respiratory activity and exhibited reliable phase relationship to the respiratory cycle, as established by comparing this signal to the airflow from the nostrils (Figure 4.2b-d), and was reflected in rhythmic head-motion (Figure 4.2a).

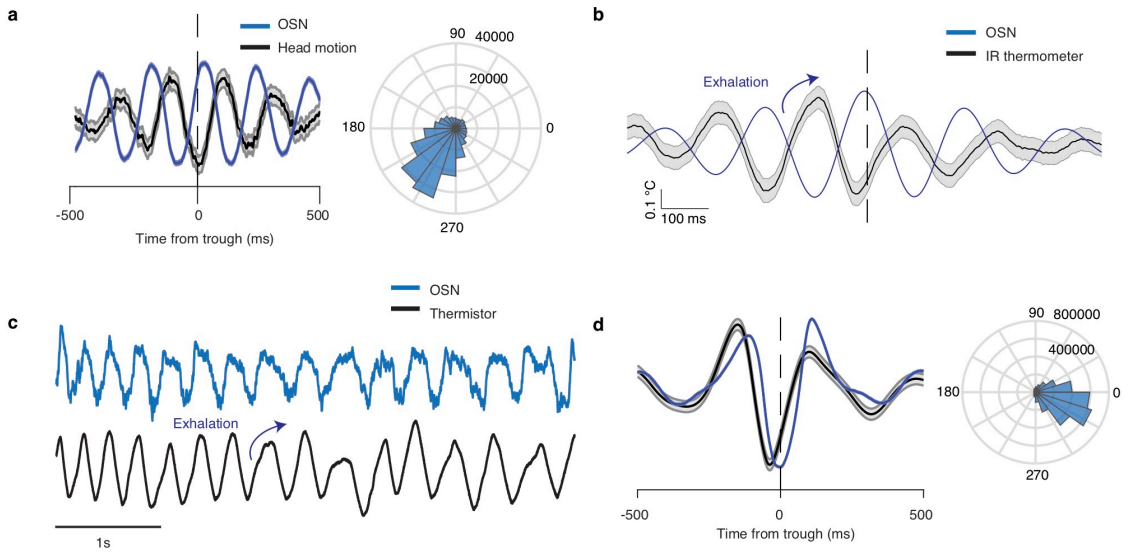

Figure 4.2: **Validation of EOG recordings.**
(a) Left, EOG trough-triggered EOG and head-motion signals during quiescence and sleep. Note the reliable phase relationship between the two signals. *Right*, Distribution of phase differences between EOG and head-motion signals. *(b)* EOG peak-triggered IR thermometer signal in a head-fixed mouse, highlighting the strong relationship of the EOG with the rhythmic airflow from the nostrils. *(c)* Example EOG and simultaneous thermistor trace. *(d) Left*, EOG trough triggered EOG and thermistor traces. *Right*, phase difference distribution between the two signals.

We then segmented behavioral states based on the head micro-motion (Figure 4.3d,e), differentiating slow wave sleep (SWS), REM sleep, quiescence, and awake exploration. Behavioral state changes were associated with changes in the breathing frequency (Figure 4.3a,b) which are accompanied by autonomic changes conferred upon the heart by central regulation and respiratory sinus arrhythmia (RSA), indicative of a generalized role of breathing in coordinating bodily rhythms (Figure 4.4).

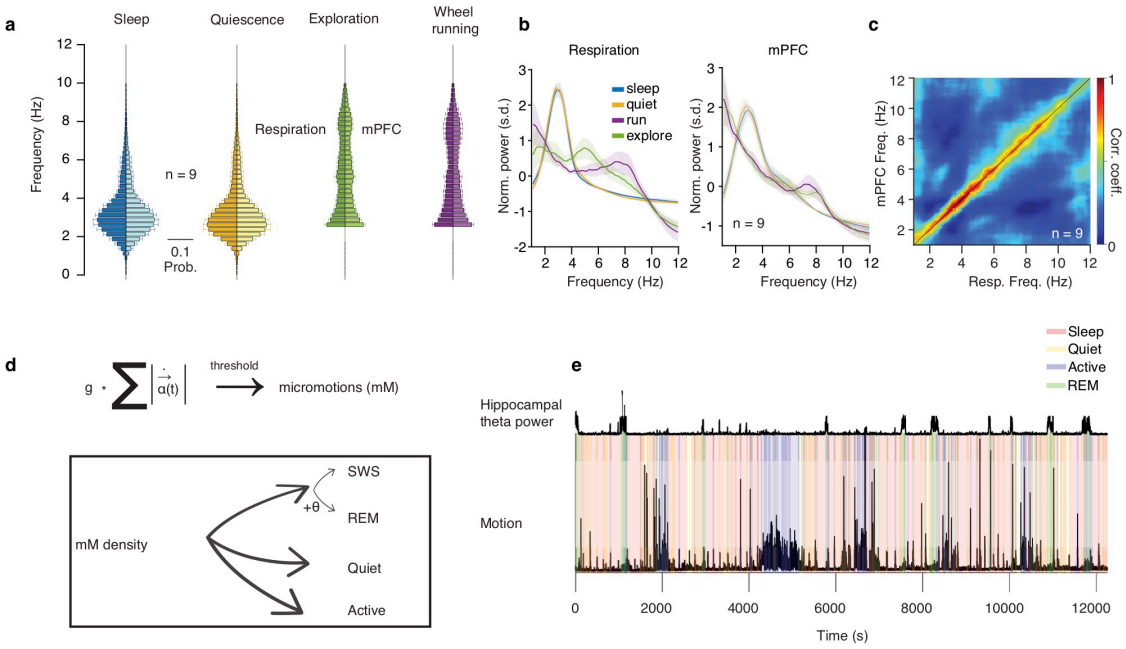

Figure 4.3: **State-resolved relation of breathing and prefrontal LFP.**
(a) Distribution of peak frequency bins of the spectrally decomposed respiration (left; darker colors) and mPFC LFP (right; lighter colors) during sleep, quiescence, exploratory behavior and self-initiated wheel running (n = 9 mice). *(b)* Averaged normalized power spectral density of respiration ((*left*) and mPFC LFP ((*right*) during sleep, quiescence, exploratory behavior and self-initiated wheel running (n = 9 mice). *(c)* Frequency-resolved comodulation of respiration and mPFC LFP oscillation power, across mice and behaviors (n = 9 mice). *(d)* Algorithm for the detection and classification of different behavioral states using only behavioral variables extracted from the head-motion and based on the calculation of micro-motion (mM) density. *(e)* Example classification of behavioral states from a recording in the home cage, using compound motion and hippocampal theta power. a.u., arbitrary units; s.d., standard deviation; corr. coeff., correlation coefficient. Shaded areas, mean ± s.e.m.

Examination of the spectrotemporal characteristics of respiratory activity and the prefrontal LFP revealed a faithful reflection of the respiratory activity in the prefrontal LFP, characterized by a prominent peak in the 2-6Hz range (Figure 4.3a,b), suggesting a potential relationship between these oscillations. The two oscillations were comodulated across a wide frequency range (Figure 4.3c) and this relationship was preserved throughout many active (online) as well as inactive (offline) states in freely-behaving mice (Figure 4.3a-c).

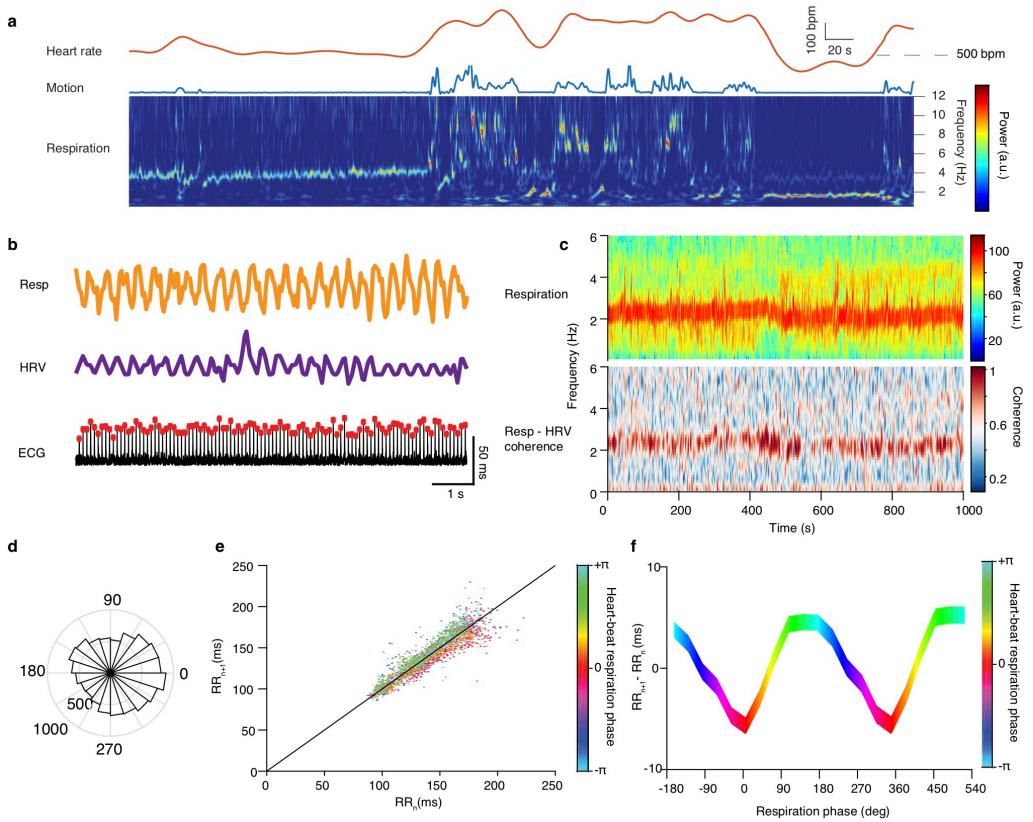

Figure 4.4: **State-dependent cardiac-respiratory dynamics.**
(a) Example heart rate and compound motion traces (*top*) and spectral decomposition of respiration ((*bottom*), from a quiet and sleeping mouse, demonstrating the intricate relationship between heart rate and respiratory frequency during different behavioral states. Dashed horizontal line marks the 500 bpm level. *(b)* Example respiration, heart-rate variability and raw electrocardiogram signals. *(c)* Example spectrogram of respiration (*top*) and coherogram between respiration and heart-rate variability ((*bottom*). Note the almost perfect coherence between the two signals, highlighting the powerful effect of respiration in modulating the heart rhythm. *(d)* Circular distribution of the respiratory phase of each heart-beat reveals a phase preference. *(e)* Poincaré return map of consecutive R-R intervals. R-R intervals are color-coded based on the concurrent respiratory phase. The post-inspiratory events deviating from the diagonal are contributing to the observed relation between heart-rate variability and respiration. *(f)* Color-coded average time difference (variability) between consecutive R-R intervals as a function of the respiratory phase.

Coherence and Granger causality analysis of the respiratory and LFP signals suggested that the respiratory oscillation is tightly locked and likely causally involved in the generation of the prefrontal LFP oscillation signal (Figure 4.5a-d).

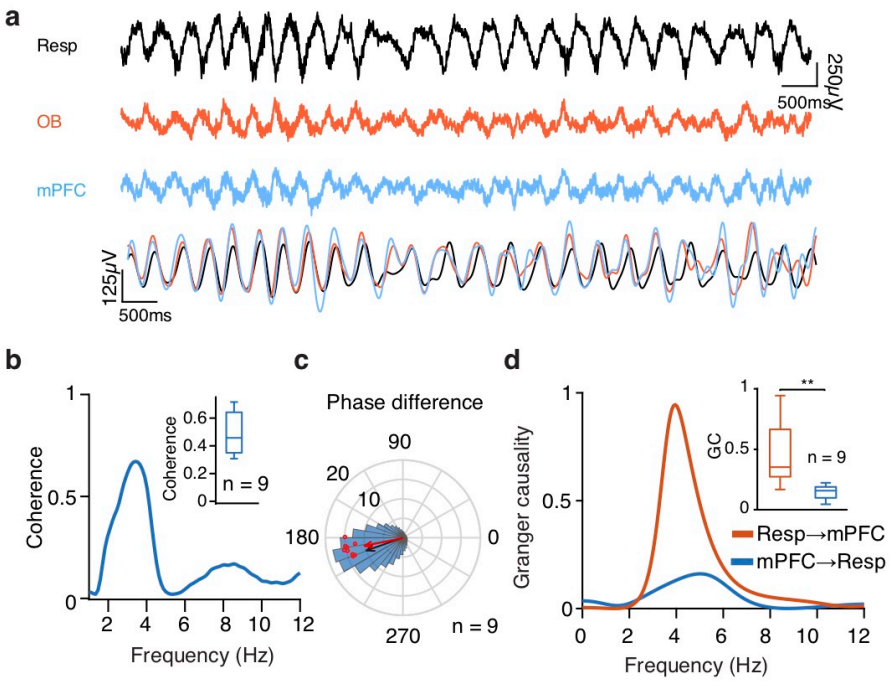

Figure 4.5: **Causality and directionality of prefrontal entrainment.**
(a) Example traces of respiration, olfactory bulb (OB) LFP, and mPFC LFP during quiescence and overlaid filtered (1-6Hz) traces of respiration, olfactory bulb (OB) LFP and mPFC LFP highlight the reliable phase relationship between the three signals. *(b)* Example coherence spectrum between respiration and mPFC LFP. *Inset*, Average coherence value in the 2-5Hz band (n = 9 mice). *(c)* Phase difference of 2-5Hz filtered respiration and mPFC LFP signals for an example animal (blue histogram) and overlaid the log-transformed Rayleigh's test Z (magnitude of phase modulation) and average phase difference for all animals (red dots; n = 9 mice). Black arrow depicts the average phase and log(Z) resultant length for the phase difference for the example and the red arrow for the population. *(d)* Example spectral Granger causality between respiration and mPFC LFP for both causal directions. *Inset*, average Granger causality for the 4Hz band (2 – 5Hz) between respiration and mPFC LFP for both causal directions (n = 9 mice, Wilcoxon signed rank test, $resp \rightarrow mPFC$ versus $mPFC \rightarrow resp$ **P < 0.01). Shaded areas, mean ± s.e.m.

During fear behavior, the mouse mPFC is dominated by a prominent 4 Hz oscillation (Karalis et al., 2016). The similarity in frequency suggests that respiration is the origin of fear-related 4 Hz oscillations, To explicitly test this, we exposed mice to auditory, contextual, and innate fear paradigms (Figure 4.6a). During freezing (Figure 4.6b), the respiratory rhythm changed in a stereotypic manner and matched the rhythmic head-motion and the prefrontal LFP oscillation (Figure 4.6c,d). Interestingly, the respiratory peak frequency was distinct for different types of fear behavior and prefrontal peak frequency faithfully matched it (Figure 4.6e), in support to the generality of the described phenomenon.

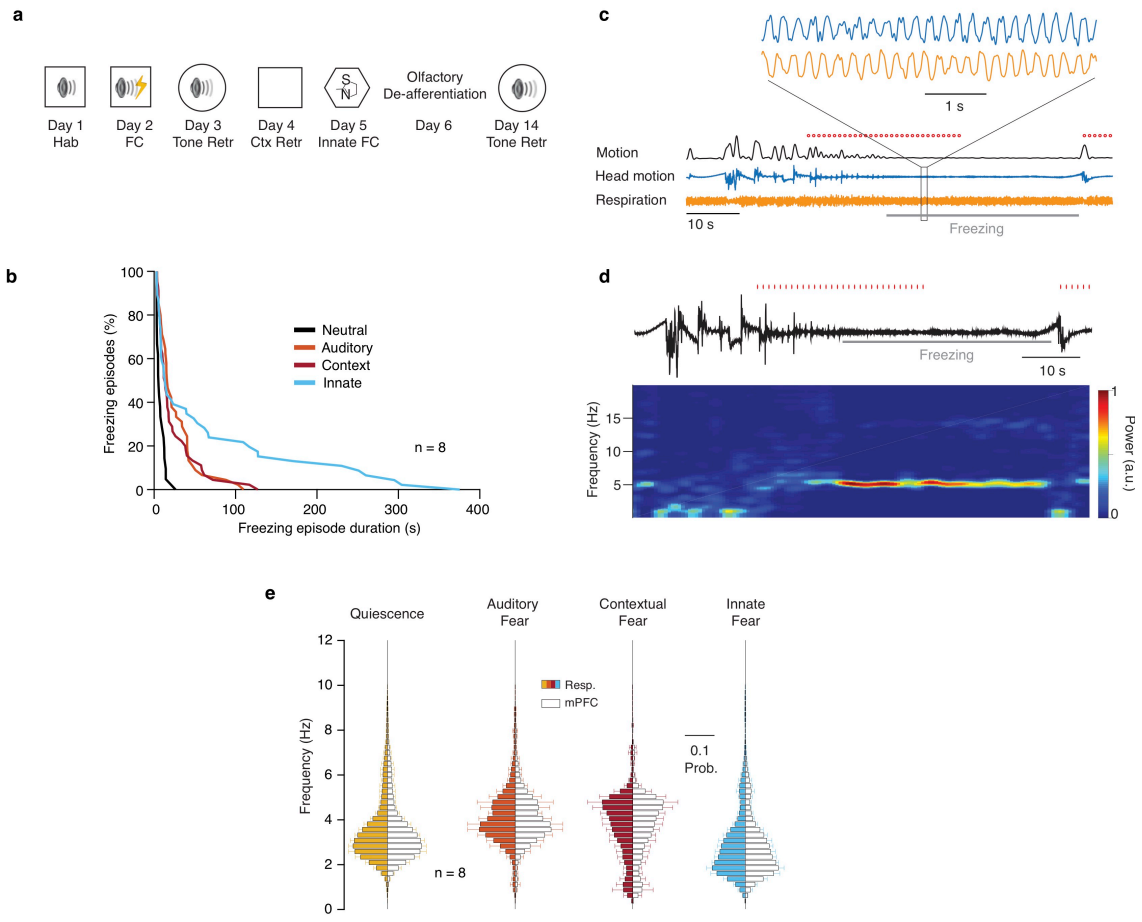

Figure 4.6: **Respiratory dynamics during fear behavior.**
(*a*) Experimental protocol. (*b*) Cumulative distribution of freezing episode duration during neutral context exploration (black trace) and different types of fear behavior for all animals (n = 8 mice). (*c*) Example compound motion, head-motion and respiration traces during tone retrieval (day 3). Red ticks indicate CS presentations and the gray line indicates freezing episode duration. Inset, magnified traces during freezing reveals the presence of ~4 Hz respiration-related oscillatory patterns in EOG and head-motion. (*d*) Example head-motion trace (top) and spectral decomposition of this signal (bottom) during freezing behavior, revealing the presence of strong oscillatory components during freezing behavior. Red ticks indicate CS presentations and gray line indicates freezing episode duration. (*e*) Distribution of peak frequency bins of the spectrally decomposed respiration (left; darker colors) and mPFC LFP (right; lighter colors) during quiescence, auditory fear retrieval, contextual fear retrieval and innate fear (n = 8 mice). Hab., habituation; FC, fear conditioning; Ret., retrieval; Ctx Retr., Context retrieval.

To further investigate the extent of respiratory entrainment of prefrontal circuits, we examined the firing of extracellularly recorded single neurons in mPFC in relation to the respiratory phase (Figure 4.7a). We observed that ~60% of putative prefrontal principal cells (PN) and ~90% of putative inhibitory interneurons (IN), identified based on their extracellular waveform features (Bartho, 2004) (Figure 4.8a,b), were significantly modulated by the phase of respiration cycle (Figure 4.7c).

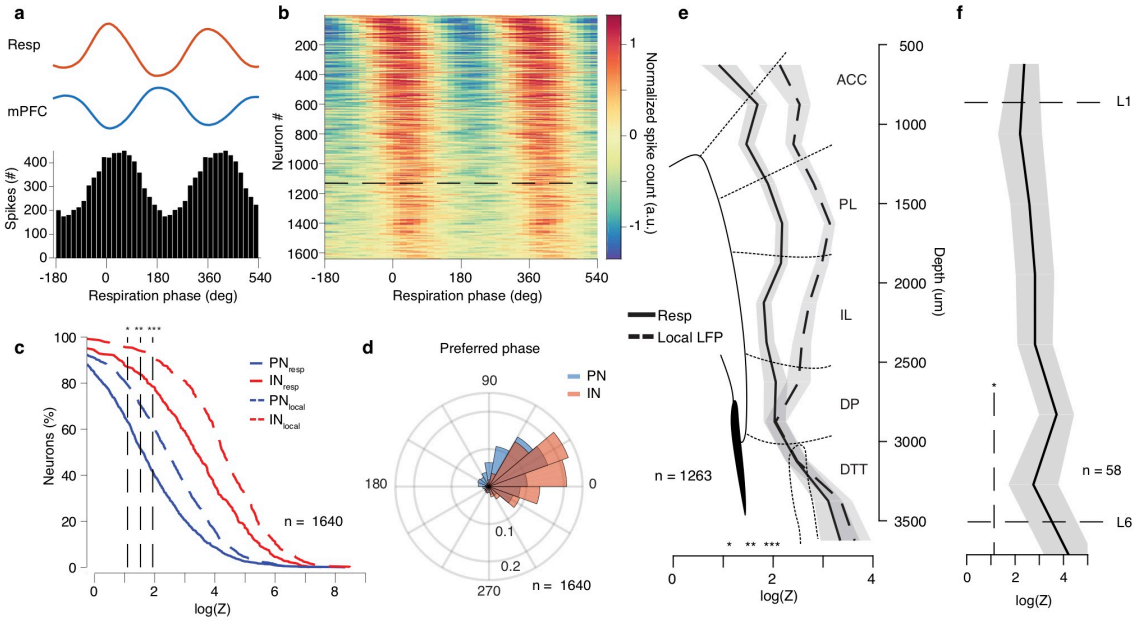

Figure 4.7: **Topography of prefrontal neuronal entrainment by respiration.**
(a) Respiration phase histogram of the spiking activity of one example prefrontal excitatory neuron phase modulated by respiration. *Top*, the associated average respiration (red) and mPFC LFP (blue) traces. *(b)* Color-coded normalized phase histograms of all prefrontal neurons, ordered by phase modulation magnitude (n = 1640 neurons, n = 13 mice). The horizontal dashed line indicated the significance threshold for the log-transformed Rayleigh's test Z. *(c)* Cumulative distribution of the log-transformed Rayleigh's test Z for the non-uniformity of the circular distribution of the spiking activity for each neuron, for all putative prefrontal excitatory principal cells (PN, blue, n = 1250 neurons) and putative inhibitory interneurons (IN, red, n = 390 neurons). Phase modulation is assessed in relation to the respiration (solid lines) and the local prefrontal LFP (dashed lines). *(d)* Circular distribution of the preferred phase for each prefrontal neuron putative principal neurons (blue) and inhibitory interneurons (red). The height of each bar corresponds to the relative number of units. *(e)* Depth-resolved average phase modulation statistics (log-transformed Rayleigh's test Z) and overlaid a schematic of corresponding prefrontal subregions (n = 1263 cells, n = 11 mice). *(f)* Cortical layer-resolved phase modulation statistics (log-transformed Rayleigh's test Z) and overlaid a schematic of corresponding prefrontal subregions (n = 58 cells, n = 6 mice). Dashed vertical lines indicate the significance levels. ACC, anterior cingulate cortex; PL, prelimbic; IL, infralimbic; DP, dorsal peduncular; DTT, dorsal taenia tecta; a.u., arbitrary units; s.d., standard deviation; deg., degrees; L1, layer 1; L6, layer 6. Stars indicate significant phase modulation levels (* P < 0.05; ** P < 0.01; *** P < 0.001).

Most modulated cells fired preferentially in the trough/ascending phase of the local oscillation, corresponding to the inhalation phase (Figure 4.7d, Figure 4.8d) and are even more strongly modulated by the phase of the local oscillation (Figure 4.7c, Figure 4.8c).

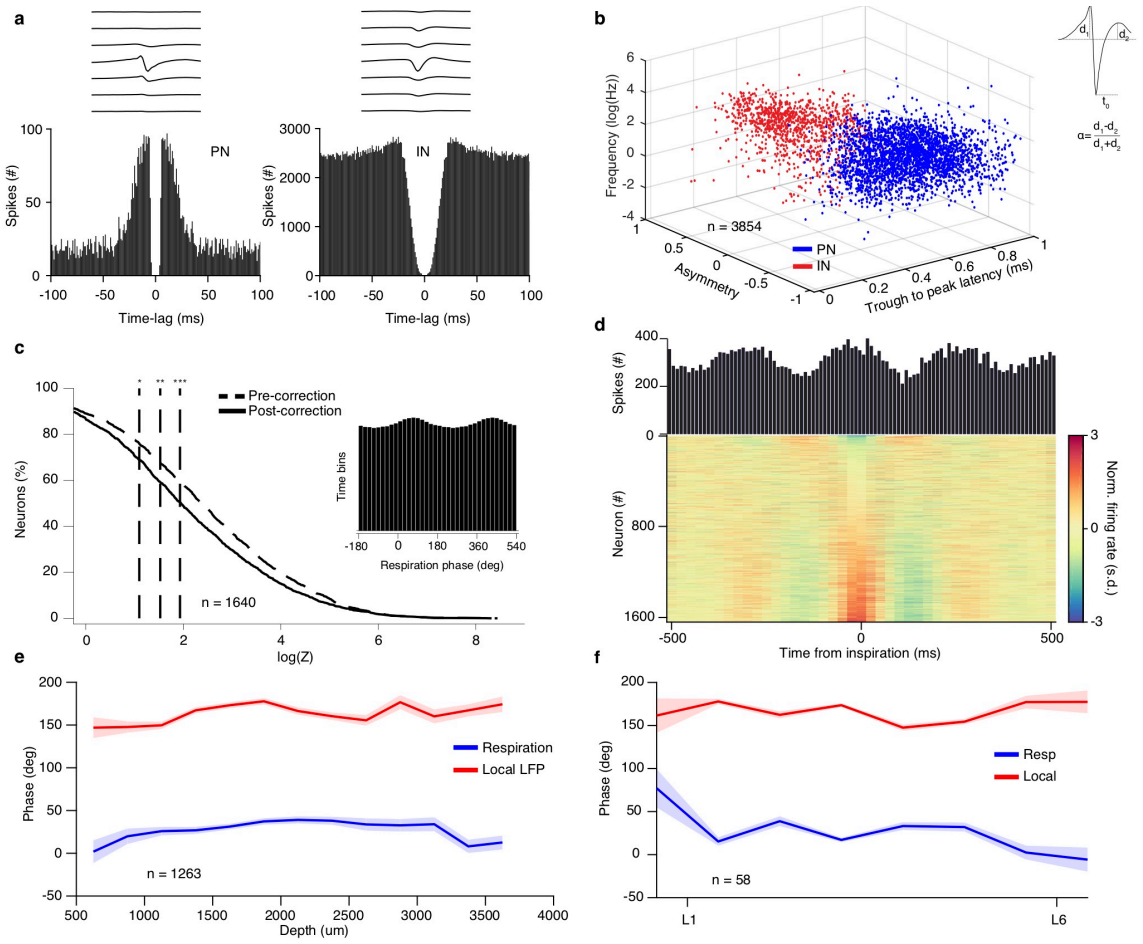

Figure 4.8: **Unit classification and respiratory modulation.**
(a) Average spike waveform polytrode templates ((*top*) and auto-correlation histograms ((*bottom*) for an example prefrontal putative principal neuron (PN) ((*left*) and putative inhibitory interneuron (IN) ((*right*). *(b)* Neurons from all structures were classified as putative principal cells and interneurons using an unsupervised clustering method based on the firing frequency, the trough to peak latency (to) and the waveform asymmetry index (α). *(c)* Cumulative distribution of the log-transformed Rayleigh's test Z for the non-uniformity of the circular distribution of the spiking activity for all prefrontal neurons (n = 1640 cells), before and after correction for the non-uniformity of the respiratory phase. Uncorrected values are artifactually higher. *Inset*, example non-uniform prior distribution of the respiratory phase. *(d) Top*, example inspiration-triggered time histogram for an example prefrontal neuron. *Bottom*, color-coded normalized inspiration-triggered time histograms for all prefrontal neurons (n = 1640 cells), ordered by increasing normalized firing rate. Dashed vertical lines indicate the significance levels. s.d., standard deviation. *(e)* Depth-resolved average preferred phase for all prefrontal neurons (n = 1263 cells; n = 11 mice), assessed in relation to the phase of the respiration and the phase of the local LFP. *(f)* Translaminar average preferred phase for all prefrontal neurons (n = 58 cells; n = 6 mice), assessed in relation to the phase of the respiration and the phase of the local LFP. Stars indicate significant phase modulation levels (* P < 0.05; ** P < 0.01; *** P < 0.001)

Having established the generality of the coupling between respiration and LFP oscillation in the mPFC across distinct states, consistent with previous reports (Moberly et al., 2018; Yanovsky et al., 2014; Biskamp et al., 2017), we focused on the enigmatic and least understood quiescence and slow-wave sleep states. To understand the potential role of breathing in orchestrating the hippocampo-cortical dialogue and supporting memory consolidation, we undertook a detailed investigation of the mechanism and function of the respiratory modulation.

4.2 TOPOGRAPHY OF RESPIRATORY ENTRAINMENT

mPFC consists of multiple subregions along the dorsoventral axis, all of which are characterized by a differential afferent and efferent connectivity and behavioral correlates (Hoover and Vertes, 2007; Herry and Johansen, 2014). To understand the origin and anatomical substrate of the respiratory entrainment of prefrontal circuits, we performed a three-dimensional trans-laminar and trans-regional characterization of the mPFC field potentials using custom-designed high-density silicon probes in freely-behaving and head-fixed mice (Figure 4.9). These recordings revealed a consistent increase from dorsal to ventral mPFC in both the power of the respiration-related oscillation and its coherence with the respiration (Figure 4.9b,c). Similarly, the coherence was stronger in the anterior prefrontal regions (Figure 4.9d).

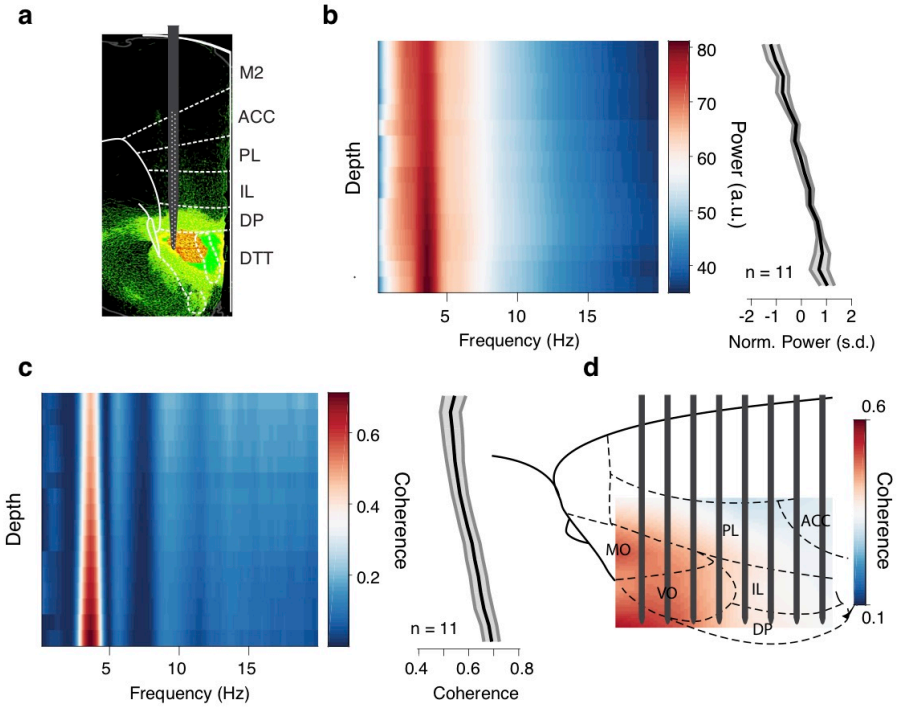

Figure 4.9: **Functional anatomical characterization of prefrontal respiratory entrainment.** *(a)* Schematic depiction of a typical recording using a high-density silicon polytrode inserted in the deep layers of the mPFC, over the projection segmentation of GFP-expression from a two-photon serial section of the mPFC from a mouse injected with anterograde rAAV in the taenia tecta. Image credit: Allen Institute. *(b) Left*, example depth- and frequency-resolved power spectrum across the polytrode channels, spanning all medial prefrontal subregions. *Right*, average depth-resolved normalized power in the 2-5Hz band (n = 11 mice). *(c) Left*, example depth- and frequency-resolved coherence spectrum between the respiration and local prefrontal LFP across the polytrode channels, spanning all medial prefrontal subregions. *Right*, average depth-resolved normalized coherence in the 2-5Hz band (n = 11 mice). *(d)* 2D mapping of coherence between respiration and local LFP throughout the frontal subregions, using an 8x8 silicon probe. Shaded areas, mean ± s.e.m; M2, motor area 2; ACC, anterior cingulate cortex; PL, prelimbic; IL, infralimbic; DP, dorsal peduncular; DTT, dorsal taenia tecta.; MO, medial orbital; VO, ventral orbital

The presence of an oscillation in the mPFC with this particular profile could also be consistent with a volume conducted signal from the high amplitude field potentials generated by bulbar dipoles, since olfactory bulb (OB) LFP is dominated by respiration-related oscillations (Adrian, 1942; Macrides and Chorover, 1972; Fukunaga et al., 2014). To examine this hypothesis, we recorded LFP activity across the prefrontal cortical layers and calculated the current-source

density (CSD) (Figure 4.10,Figure 4.11a). This analysis revealed a prominent pattern of sinks in the deep cortical layers at the inspiration phase giving rise to an increased LFP power and unit-LFP coupling in the deep layers (Figure 4.10b,c), weighing against the hypothesis of volume conduction and suggestive of a synaptic origin of the prefrontal LFP oscillation.

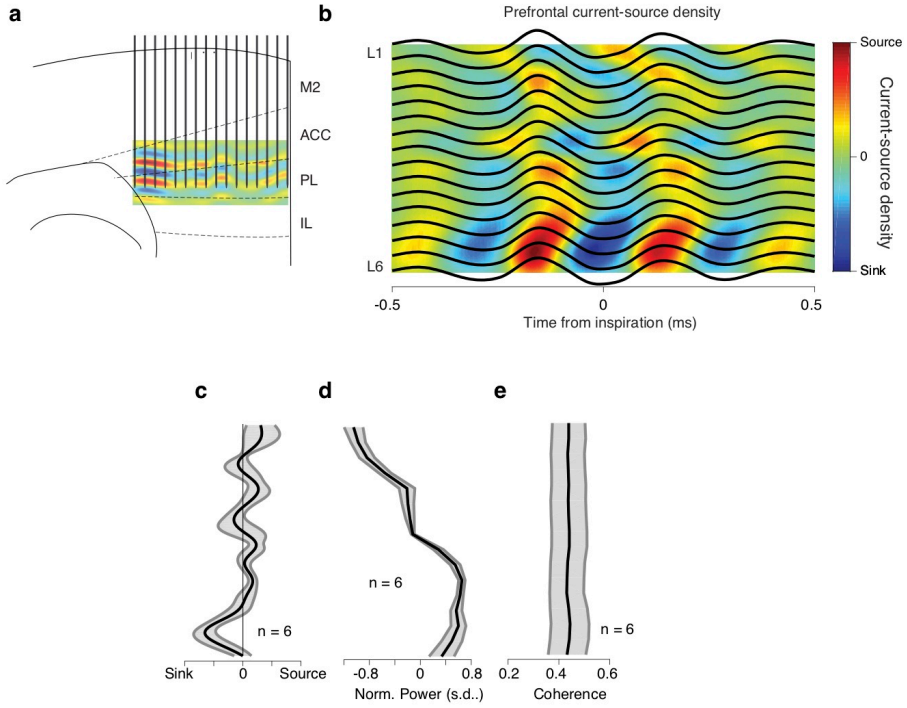

Figure 4.10: **Prefrontal respiratory current-source density.**
(a) Schematic depiction of a 16-shank probe (50µm shank spacing) inserted in the prelimbic region of the mPFC to record simultaneously from all cortical layers and an example inspiration-triggered current-source density profile. *(b)* Example average inspiration-triggered LFP traces and overlaid corresponding translaminar current-source density profile from the dorsal mPFC. *(c)* Average inspiration-triggered translaminar normalized current-source density profile from the dorsal mPFC (n = 6 mice). *(d)* Average cortical layer-resolved profile of the normalized 2-5Hz band local LFP power from the dorsal mPFC (n = 6 mice). *(e)* Average cortical-layer-resolved profile of the 2-5Hz band coherence between respiration and local LFP from the dorsal mPFC (n = 6 mice). M2, motor area 2; ACC, anterior cingulate cortex; PL, prelimbic; IL, infralimbic; a.u., arbitrary units; s.d., standard deviation; L1, layer 1; L6, layer 6. Shaded areas, mean ± s.e.m.

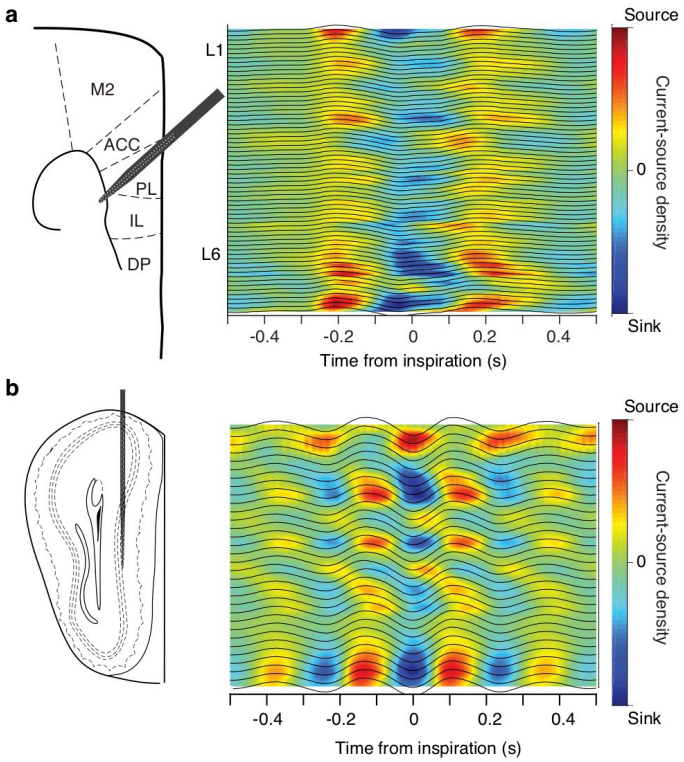

Figure 4.11: **Prefrontal and OB respiratory current-source density.**
(a) Left, schematic of a single-shank angled high-density polytrode inserted in the dorsal mPFC. *Right*, example high-resolution inspiration-triggered current-source density of the mPFC respiration-related oscillation using a single-shank angled polytrode confirms the observations with the multi-shank silicon probe. *(b) Left*, schematic of a high-density polytrode recording across layers of the olfactory bulb. *Right*, example high-resolution inspiration-triggered current-source density of the olfactory bulb. M2, motor area 2; ACC, anterior cingulate cortex; PL, prelimbic; IL, infralimbic; DP, dorsal peduncular; L1, layer 1; L6, layer 6

Harnessing the advantages of spatial information from the silicon probe recordings, we characterized the entrainment of single units across prefrontal subregions and cortical layers. Although cells were phase-modulated throughout the prefrontal subregions, the average modulation strength was increased as a function of distance from the dorsal surface (Figure 4.7e,Figure 4.7e). These results, given the increased density of polysynaptic projections from the OB to ventral mPFC subregions (Moberly et al., 2018), suggest that the bulbar reafferent input to the mPFC is giving rise to the observed LFP signals. Rhythmic air flow could entrain the olfactory sensory neurons (OSNs), that are known to respond both to odors and mechanical stimuli (Grosmaitre et al., 2007), and propagate through the olfactory bulb and the olfactory system to the prefrontal region.

4.3 WIDESPREAD RESPIRATORY MODULATION OF LIMBIC CIRCUITS

Given the prominent modulation of mPFC by respiration, we hypothesized that a concurrent entrainment of other limbic regions could be underlying their generalized long-range interaction, as has been suggested before for theta oscillations (Mizuseki et al., 2009; Buzsaki, 2010). For this, we turned our attention to other limbic structures, reciprocally connected to the mPFC that are known to interact with prefrontal networks in different behaviors. Using large-scale single-unit and laminar LFP recordings from the dorsal hippocampus, we identified that in both dorsal

CA1 and dentate gyrus (DG), ~60% of PNs and 80% CA1 INs were modulated by the phase of respiration, firing preferentially after the inspiration (Figure 4.12), in agreement with previous reports of respiratory entrainment of hippocampal activity (Vanderwolf, 1992; Yanovsky et al., 2014; Nguyen Chi et al., 2016; Lockmann et al., 2016).

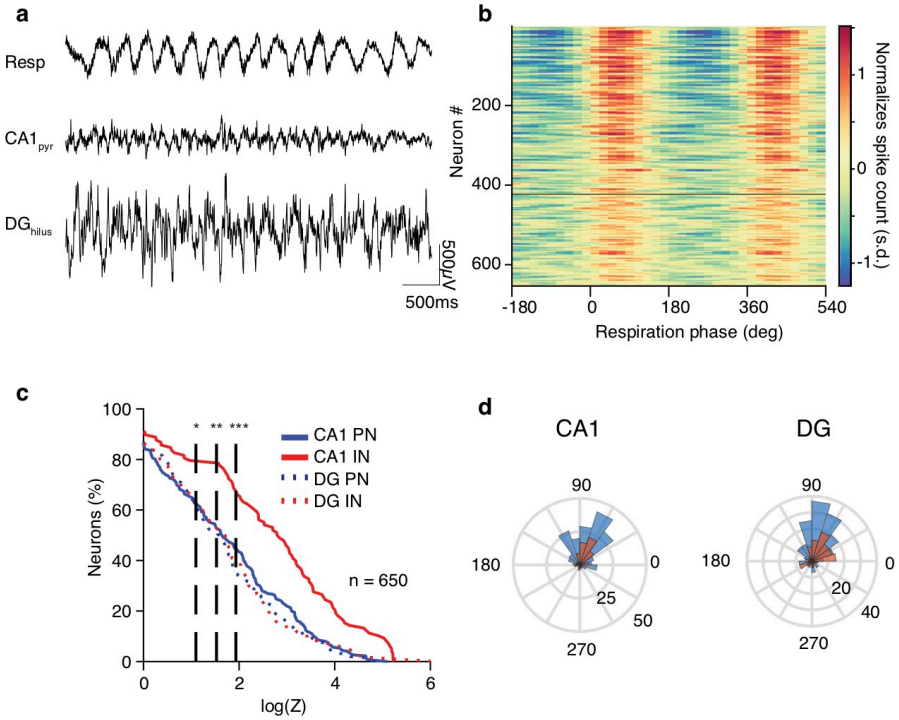

Figure 4.12: **Respiratory inputs entrain hippocampal activity.**
(a) Example simultaneously recorded traces of respiratory activity and CA1 pyramidal layer and DG hilus LFP. *(b)* Color-coded phase histograms of the normalized firing rate of all hippocampal cells (n = 650 cells). *(c)* Cumulative distribution of the log-transformed Rayleigh's test Z for the non-uniformity of the circular distribution of the spiking activity for each neuron, for all putative CA1 and DG excitatory principal cells (PN; CA1, blue solid line, n = 226 cells; DG, blue dashed line, n = 206 cells) and putative inhibitory interneurons (IN; CA1, red solid line, n = 98 cells; DG, red dashed line, n = 120 cells). Dashed vertical lines indicate the significance levels. *(d)* Circular distribution of the preferred phase for each significantly phase locked CA1 ((*left*) and DG ((*right*) cell. s.d., standard deviation; deg., degrees; CA1pyr, str. pyramidale; DGhil, hilus. Dashed vertical lines indicate the significance levels. Stars indicate significance levels (* P < 0.05; ** P < 0.01; *** P < 0.001).

A separation of CA1 PNs based on their relative position within the pyramidal layer into populations with known distinct connectivity patterns (Valero et al., 2015; Mizuseki et al., 2011) did not reveal particular differences in their modulation by respiration, suggesting a generality of this entrainment throughout the CA1 sub-populations (Figure 4.13b).

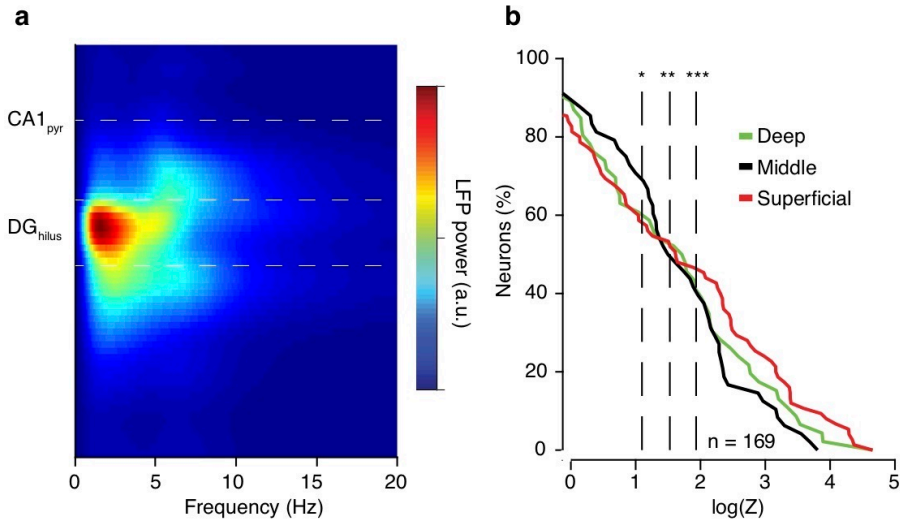

Figure 4.13: **Depth resolved hippocampal modulation.**
(a) Example translaminar spectral decomposition of the hippocampal LFP during quiescence and sleep. *(b)* Cumulative distribution of the log-transformed Rayleigh's test Z for the non-uniformity of the circular distribution of the spiking activity for each neuron, for all CA1 putative pyramidal cells (n = 169 neurons), grouped based on their location within the pyramidal layer into deep (n = 46 cells), middle (n = 48 cells) and superficial (n = 75 cells) cells. Dashed vertical lines indicate the significance levels. Stars indicate significance levels (* P < 0.05; ** P < 0.01; *** P < 0.001).

To understand what afferent pathways are responsible for breathing-related synaptic currents that underlie the modulation of spiking activity, we calculated finely-resolved (23µm resolution) laminar profile of inspiration-triggered dorsal hippocampal current-source density, enabling the identification of synaptic inputs into dendritic sub-compartments. Although the LFP profile only highlights the prominence of the respiratory band in the DG hilus region (Figure 4.13a), high-resolution CSD analysis revealed the presence of two distinct and time-shifted respiratory-related inputs in DG dendritic sub-compartments (Figure 4.14,Figure 4.15). Inspiration was associated with an early sink in the outer molecular layer of DG, indicative of an input from the layer II (LII) of the lateral entorhinal cortex (LEC), followed by a sink in the middle molecular layer of DG, indicative of an input from the layer II of medial entorhinal cortex (MEC) (Figure 4.14).

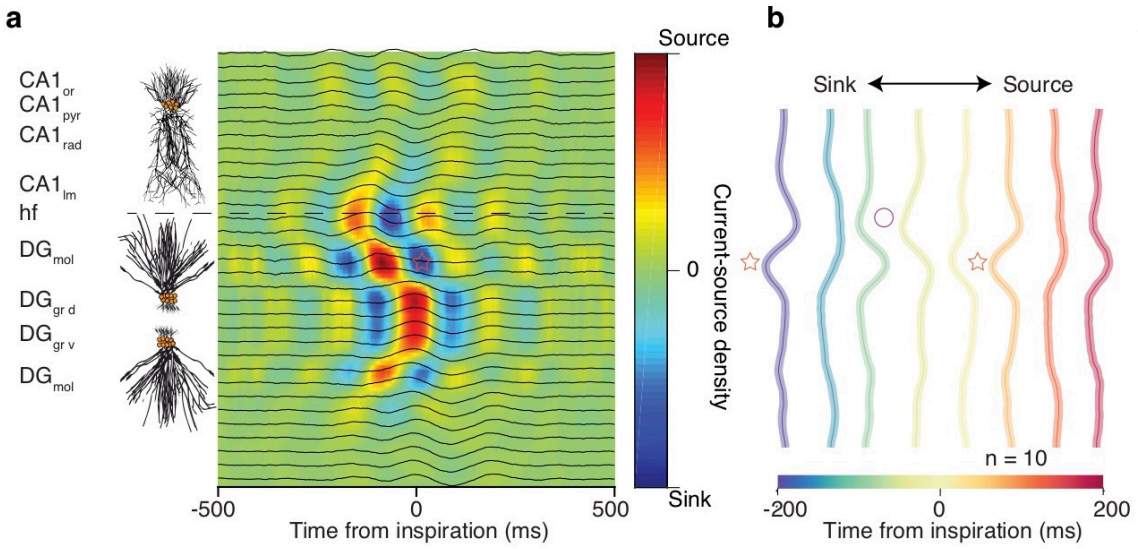

Figure 4.14: **Translaminar profile of respiratory input to the hippocampus.**
(a) Left, schematic depiction of the neuronal alignment of CA1 pyramidal cells and DG granule cells, aligned to the current-source density profiles. *Right*, Example inspiration-triggered high-density current-source density profile of the dorsal hippocampus. Horizontal dashed line indicates the hippocampal fissure. *(b)* Average normalized inspiration-triggered current-source density profile of dorsal hippocampus (n = 10 mice). CA1or, oriens; CA1pyr, str. pyramidale; CA1rad, str. radiatum; CA1lm, str. lacunosum-moleculare; hf, hippocampal fissure; DGmol, dentate gyrus – molecular layer; DGom, outer molecular layer; DGmm, middle molecular layer; DGgr d/v, granule cell layer (dorsal/ventral); DGhil, hilus. Shaded areas, mean ± s.e.m.

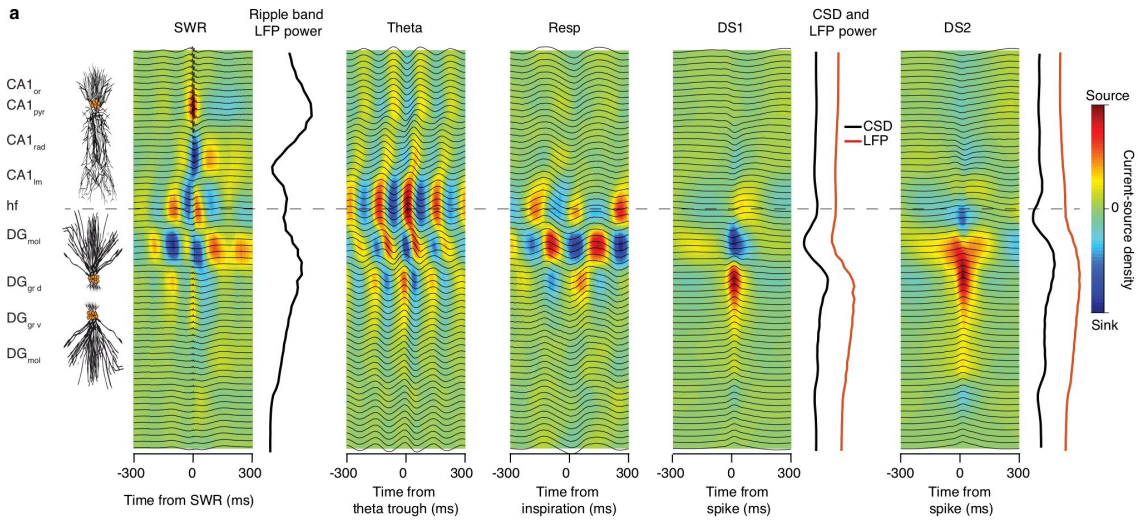

Figure 4.15: **Translaminar profile of hippocampal dynamics.**
(a) Left, schematic depiction of the neuronal alignment of CA1 pyramidal cells and DG granule cells, aligned to the current-source density profiles. *Right*, Example current-source density profiles of the dorsal hippocampus of the same animal, triggered on the peak of sharp-wave ripple (SWR) events, the troughs of theta oscillations, inspiratory events and the two types of dentate spikes (DS1 and DS2). The power of the ripple-band and the CSD magnitude and LFP power for the two types of dentate spikes is aligned to the CSD profiles. Horizontal dashed line indicates the hippocampal fissure. CA1or, oriens; CA1pyr, str. pyramidale; CA1rad, str. radiatum; CA1lm, str. lacunosum-moleculare; hf, hippocampal fissure; DGmol, dentate gyrus – molecular layer; DGom, outer molecular layer; DGmm, middle molecular layer; DGgr d/v, granule cell layer (dorsal/ventral); DGhil, hilus.

To explore the extent of limbic entrainment by respiration, we further recorded LFP and single-unit activity in the BLA (Figure 4.16a), NAc (Figure 4.17a) as well as somatic and midline thalamus (Figure 4.19a). Similar to mPFC, LFP in both BLA and NAc was comodulated with breathing across a range of frequencies, with most prominent modulation at ~4 Hz, the main mode of breathing frequency during quiescence (Figure 4.16a,b,Figure 4.17a,b), and exhibited reliable cycle-to-cycle phase relationship with the respiratory oscillation (Figure 4.18a,b,d,e).

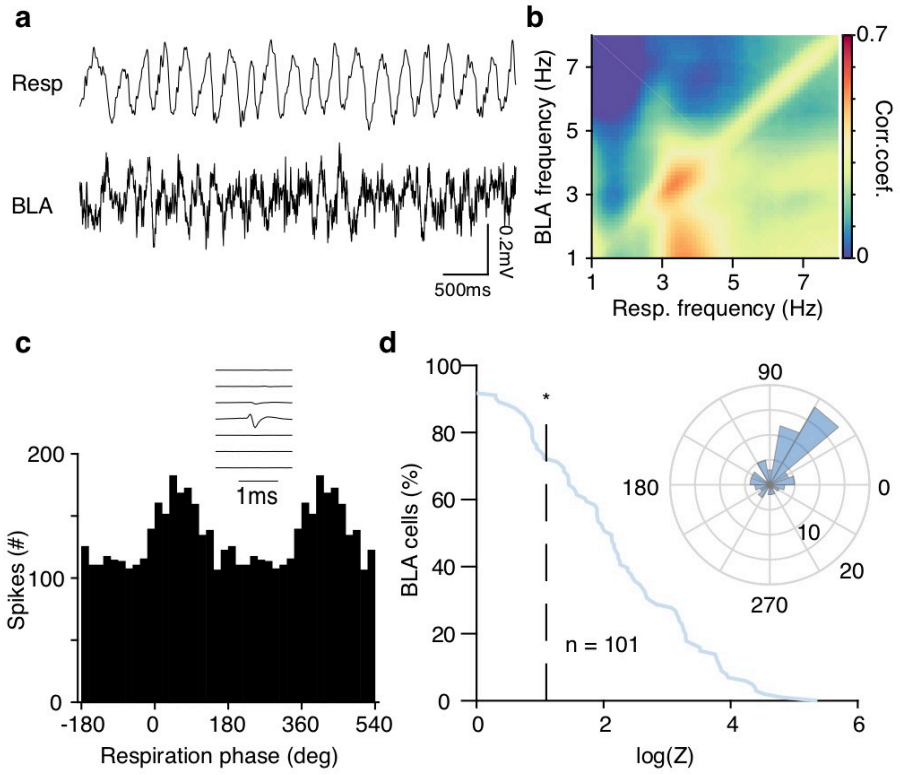

Figure 4.16: **Breathing modulates BLA neuronal dynamics.**
(a) Example simultaneously recorded respiration and BLA LFP trace. *(b)* Frequency-resolved comodulation of respiration and BLA LFP oscillation power for one example animal. *(c)* Respiration phase histogram of the spiking activity of one example BLA neuron phase modulated by respiration. *Inset*, the respective unit spike waveform polytrode template. *(d)* Cumulative distribution of the log-transformed Rayleigh's test Z for the non-uniformity of the circular distribution of the spiking activity for all BLA cells (n = 101 cells). *Inset*, circular distribution of the mean preferred respiration phase for each significantly modulated cell. Dashed vertical line indicates the significance level. Star indicates significance level (* $P < 0.05$). deg., degrees; corr. coeff., correlation coefficient.

Given the nuclear nature and lack of lamination of these structures, which obfuscates the interpretation of slow LFP oscillations, we examined the modulation of single-units by the phase of breathing. Phase-modulation analyses of the spiking activity revealed that a large proportion of BLA (Figure 4.16c,d), NAc (Figure 4.17c,d), and thalamic neurons (Figure 4.19b-d) are modulated by respiration, firing in distinct phases of the breathing cycle.

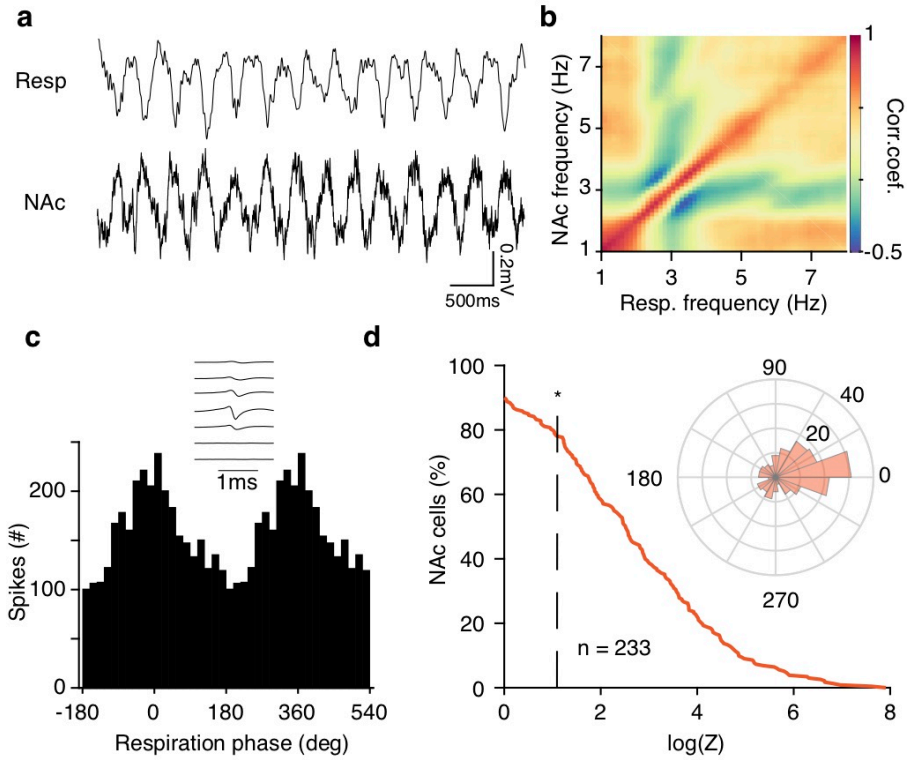

Figure 4.17: **Breathing modulates NAc neuronal dynamics.**
(a) Example simultaneously recorded respiration and NAc LFP trace. *(b)* Frequency-resolved comodulation of respiration and NAc LFP oscillation power for one example animal. *(c)* Respiration phase histogram of the spiking activity of one example NAc neuron phase modulated by respiration. *Inset*, the respective unit spike waveform polytrode template. *(d)* Cumulative distribution of the log-transformed Rayleigh's test Z for the non-uniformity of the circular distribution of the spiking activity for all NAc cells (n = 233 cells). *Inset*, circular distribution of the mean preferred respiration phase for each significantly modulated cell.
Dashed vertical line indicates the significance level. Star indicates significance level (* $P < 0.05$). deg., degrees; corr. coeff., correlation coefficient.

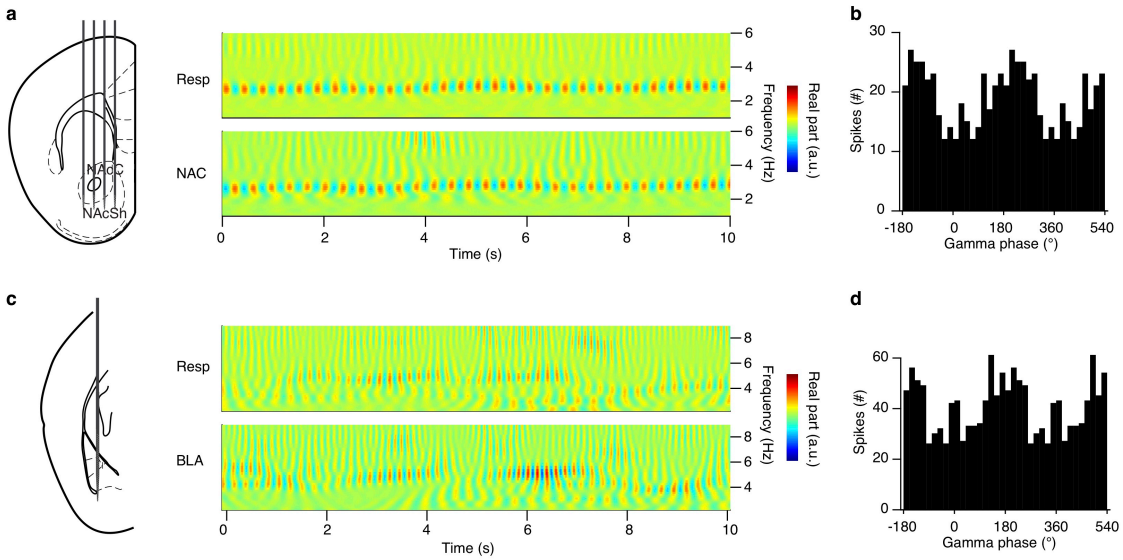

Figure 4.18: **BLA and NAc phase relationship with breathing.**
(a) Left, schematic of a recording from the NAc using a 4 shank silicon polytrode. Right, example spectral representation of the respiration and NAc LFP using the real-part of the wavelet transform highlights the reliable phase relationship between the two signals. *(b)* Gamma phase distribution of the spikes of an example NAc neuron. *(c)* Left, schematic of a high-density polytrode recording from the BLA. Right, example spectral representation of the respiration and BLA LFP using the real-part of the wavelet transform highlights the reliable phase relationship between the two signals. *(d)* Gamma phase distribution of the spikes of an example BLA neuron. a.u., arbitrary units.

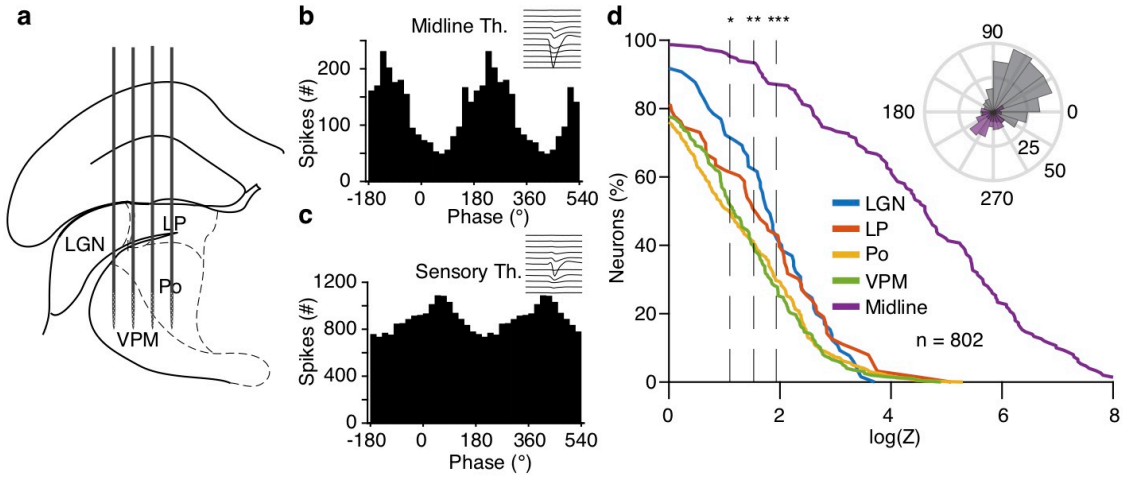

Figure 4.19: **Breathing differentially entrains thalamic nuclei.**
(a) Schematic depiction of multi-shank silicon probe recordings from the sensory thalamus. *(b,c)* Example units from the midline (b) and sensory (c) thalamus, exhibiting strong modulation by the phase of breathing. *(d)* Cumulative distribution of the log-transformed Rayleigh's test Z for the non-uniformity of the circular distribution of the spiking activity for each neuron, for all cells from different thalamic nuclei (n = 802 neurons). *Inset*, circular distribution of the mean preferred phase of all significantly modulated cells from sensory (gray) and midline (purple) thalamus.

4.4 REAFFERENT ORIGIN OF LIMBIC GAMMA OSCILLATIONS

A prominent feature of prefrontal cortex LFP are fast gamma oscillations (~80 Hz) (Sirota et al., 2008; Stujenske et al., 2014) (Figure 4.20a). To investigate the relationship of prefrontal gamma oscillations to the breathing rhythm and well-known OB gamma oscillations of similar frequency (Adrian, 1950; Freeman and Nicholson, 1975; Lepousez and Lledo, 2013; Fukunaga et al., 2014) (Figure 4.21a), we recorded simultaneously from the two structures and calculated the phase-amplitude coupling between breathing and gamma oscillations (Figure 4.20b).

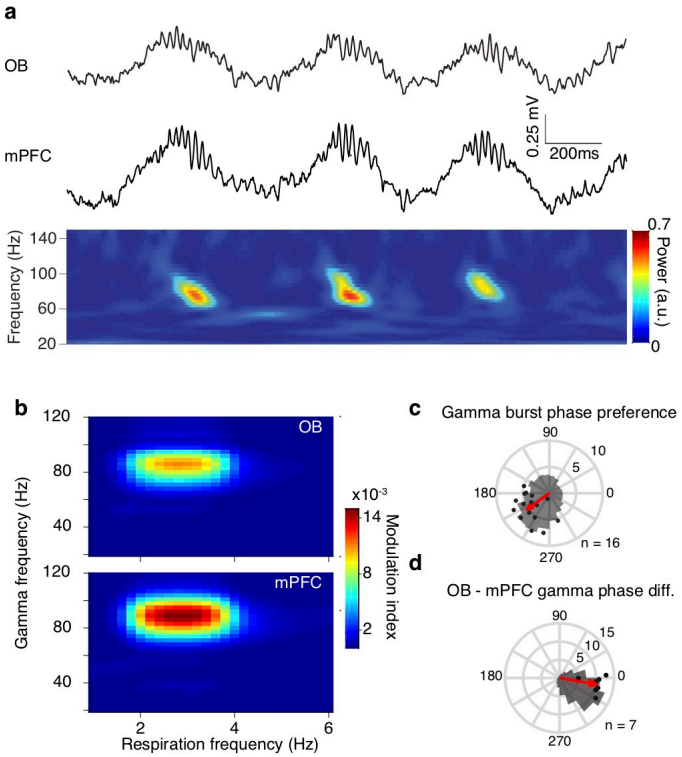

Figure 4.20: **Gamma entrainment and oscillatory coupling between OB and mPFC.**
(a) Example simultaneously recorded LFP traces ((*top*) from OB and mPFC gamma activity and spectral decomposition of mPFC activity ((*bottom*). *(b)* Phase-modulation of OB ((*top*) and mPFC ((*bottom*) gamma activity by respiration for an example animal. *(c)* Phase distribution of mPFC gamma bursts for an example animal (gray histogram) and average preferred phase and phase modulation strength (log-transformed Rayleigh's test Z) for all animals (n = 16 mice). The red arrow indicates the population average preferred phase and log(Z). *(d)* Circular distribution of the phase difference between OB and mPFC gamma filtered traces for one example animal (gray histogram) and average phase difference and phase difference non-uniformity (log(Z)) for all animals (n = 7 mice).

Both OB and mPFC fast gamma oscillations are modulated by respiratory phase and gamma bursts occur predominantly simultaneously and in the descending phase of the local LFP (Figure 4.20c). The simultaneously occurring OB and mPFC gamma oscillations match in frequency and exhibit reliable phase relationship with a phase lag suggesting directionality from the OB to the mPFC (Figure 4.20d, Figure 4.21b).

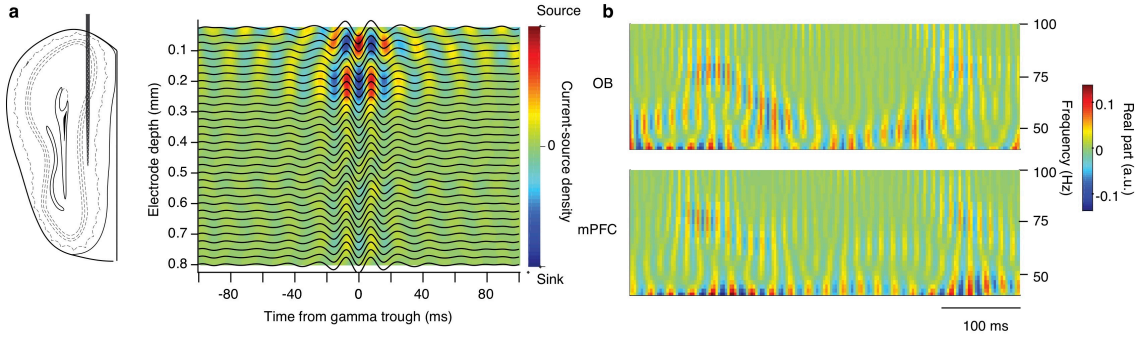

Figure 4.21: **Gamma dynamics in mPFC and OB.**
(a) Left, schematic of a high-density polytrode recording across layers of the olfactory bulb (OB). *Right*, OB gamma trough-triggered LFP traces and corresponding current-source density profile of the OB. *(b)* Example spectral representation of the OB and mPFC gamma-band LFP using the real-part of the wavelet transform highlights the transient phase relation between bursts of gamma oscillations in the two structures. a.u., arbitrary units.

To examine the underlying synaptic inputs mediating the occurrence of these oscillations in the mPFC, we calculated CSD across mPFC layers, triggered on the phase of the OB gamma bursts. This analysis revealed a discrete set of sinks across prefrontal layers associated with OB bursts (Figure 4.22a,b). Similar to the slow time scale LFP signals, these results suggest that fast gamma oscillations in mPFC are generated by OB-gamma rhythmic polysynaptic inputs to mPFC and are not a locally generated rhythm.

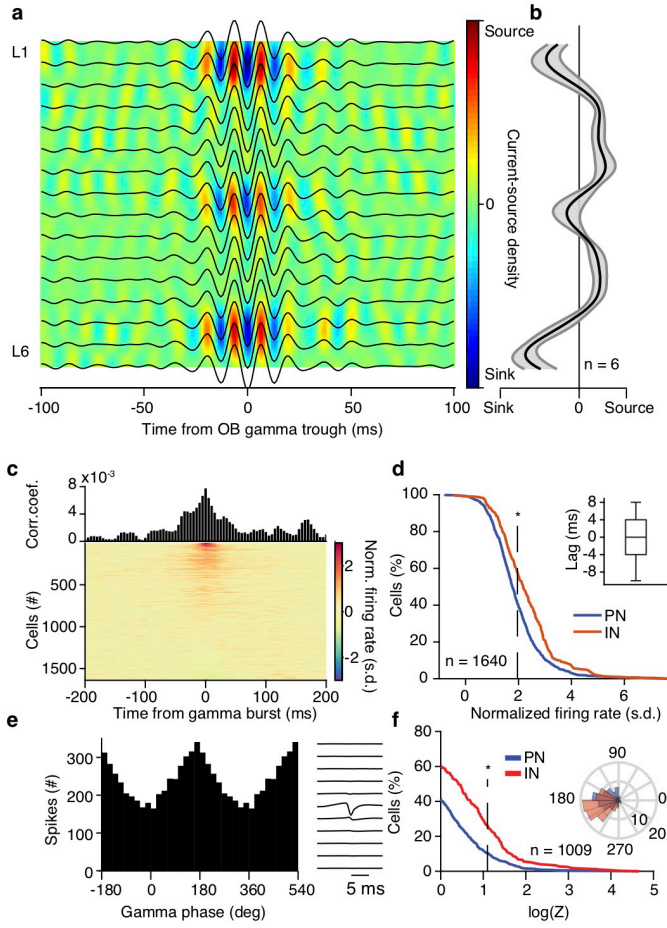

Figure 4.22: **Respiratory gamma relation to prefrontal neuronal activity.**
(a) OB gamma-triggered translaminar current-source density of the dorsal mPFC LFP profile for one example animal. *(b)* Average OB gamma-triggered translaminar current-source density of the dorsal mPFC LFP profile (n = 6 mice). *(c)* Gamma-burst triggered time histogram for one example mPFC cell and color-coded normalized time histograms for all mPFC cells (n = 1640 cells). *(d)* Cumulative distribution of the gamma-triggered normalized firing of mPFC putative principal cells (PN) (n = 1250 cells) and putative inhibitory interneurons (IN) (n = 390 cells). *Inset*, time lag between time from gamma burst and peak firing probability for all significantly responsive cells. *(e)* Example gamma phase histogram of one example mPFC unit ((*left*) and the respective unit spike waveform polytrode template (*right*). *(f)* Cumulative distribution of the log-transformed Rayleigh's test Z for the non-uniformity of the circular distribution of the spiking activity for each neuron, for all putative prefrontal excitatory principal cells (PN, blue, n = 685 neurons) and putative inhibitory interneurons (IN, red, n = 324 neurons). Phase modulation is assessed in relation to the phase of the local prefrontal gamma oscillation. *Inset*, circular distribution of the mean preferred phase of all significantly modulated PN and IN cells. Dashed vertical line indicates the significance level. Star indicates significance level (* P < 0.05). s.d., standard deviation; a.u., arbitrary units; deg., degrees; corr. coeff., correlation coefficient. Shaded areas, mean ± s.e.m.

Examining the OB ~80 Hz gamma-triggered dorsal hippocampal CSD reveals a DG outer molecular layer sink, indicative of an OB gamma propagating to DG via the LEC LII input (Figure 4.23a,b), a profile distinct from the similar frequency $CA1_{lm}$ gamma (Figure 4.23c,d). In parallel, slow BLA gamma (~40 Hz) and fast NAc gamma (~80 Hz) oscillations are modulated by the phase of breathing, occurring predominantly in the trough and ascending phase of breathing respectively (Figure 4.24a-c).

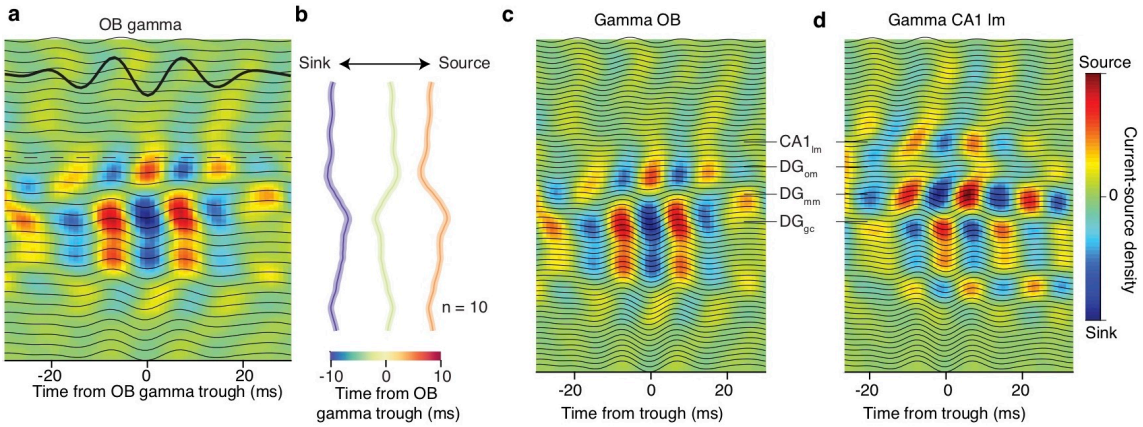

Figure 4.23: **Hippocampal olfactory gamma.**
(a) Left, example OB gamma-triggered current-source density profile of dorsal hippocampus. Horizontal dashed line indicates the hippocampal fissure. Right, average normalized OB-triggered current-source density profile of dorsal hippocampus (n = 10 mice). *(b)* Example olfactory bulb gamma- and CA1lm gamma-triggered LFP traces and translaminar current-source density of the dorsal hippocampus. CA1pyr, str. pyramidale; DGhil, hilus; DGom, outer molecular layer; DGmm, middle molecular layer; DGgc, granule cell layer. Dashed vertical lines indicate the significance levels. Stars indicate significance levels (* P < 0.05; ** P < 0.01; *** P < 0.001).

To examine whether these respiration-modulated OB-mediated gamma oscillations have a functional role in driving local neuronal activity, we quantified coupling of local single units to mPFC gamma signals, revealing that ~40% of principal cells and ~55% of interneurons increased their firing rate in response to local gamma oscillations (Figure 4.22c,d). Interestingly, ~10% of PN and ~30% of IN were significantly phase modulated by gamma oscillations, firing preferentially in the trough of the local oscillation (Figure 4.22e,f). Similarly, ~40% of BLA and ~25% of NAc cells fire preferentially in the trough of the local gamma oscillations (Figure 4.24d,Figure 4.18c,f). Thus OB gamma propagates via several synapses and it recruits and paces cycle-by-cycle the firing in the downstream limbic structures.

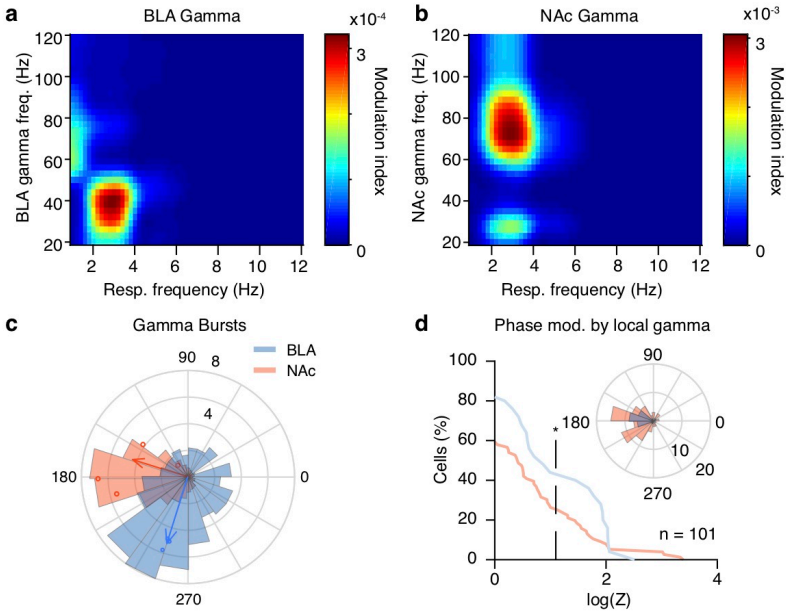

Figure 4.24: **Breathing modulates BLA and NAc gamma.**
(a) Phase-modulation of BLA gamma activity by respiration for an example animal. *(b)* Phase-modulation of NAc gamma activity by respiration for an example animal. *(c)* Circular distribution of the respiratory phase of BLA and NAc gamma bursts for one example animal (histogram) and mean preferred phase of gamma occurrence and log(Z) for all animals (BLA, $n = 3$ mice; NAc, $n = 4$ mice). *(d)* Cumulative distribution of the log-transformed Rayleigh's test Z for the non-uniformity of the circular distribution of the local gamma phase for the spiking activity for all BLA ($n = 25$ cells) and NAc cells ($n = 76$ cells). *Inset*, circular distribution of the mean preferred gamma phase for each significantly modulated BLA and NAc cell. Dashed vertical line indicates the significance level. Star indicates significance level (* $P < 0.05$).

4.5 EFFERENT AND REAFFERENT MECHANISMS OF RESPIRATORY ENTRAINMENT

These results suggest a mechanistic picture in which the OB reafferent gamma and respiration-locked currents are responsible for the observed respiration-associated LFP patterns in the mPFC, consistent with disruption of these LFP patterns after OB lesion or tracheotomy (Ito et al., 2014; Moberly et al., 2018; Biskamp et al., 2017; Tort et al., 2018). However, the distributed and massive modulatory effect that respiration had on unit activity in these regions is at odds with the anatomically-specific synaptic pathways that we identified as responsible for slow and fast currents.

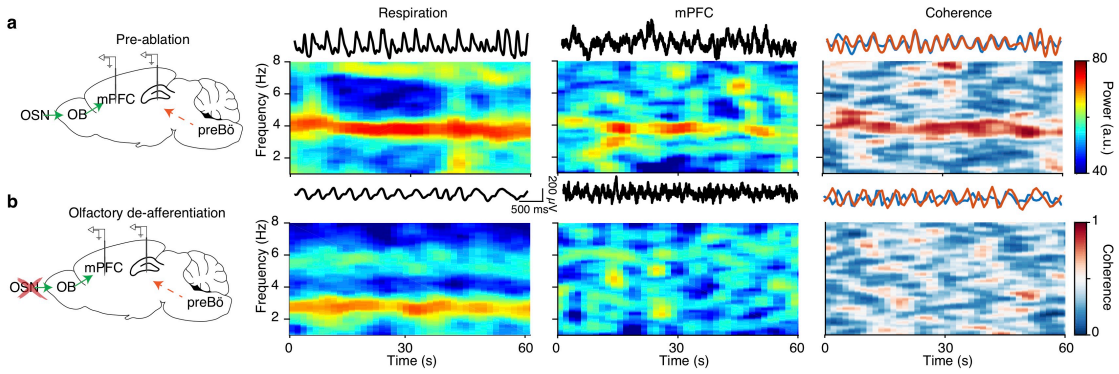

Figure 4.25: **Reafferent respiratory input accounts for LFP oscillations.**
(*a,b*) Left, schematic of the manipulation strategy. Right, example time-frequency decomposition of power and coherence between respiratory and mPFC LFP signals during quiescence before (a) and after (b) OD.

To causally test whether OB reafferent input is the sole origin of the LFP patterns and unit entrainment, we employed a pharmacological approach, that enables selective removal of the reafferent input. A well-characterized effect of systemic methimazole injection is the ablation of the olfactory epithelium that hosts the olfactory sensory neurons (Bergman et al., 2002), that respond to both odors and mechanical stimuli (Grosmaitre et al., 2007). Effectively, this deprives the OB of olfactory and respiratory input, while leaving the bulbar circuits intact, enabling us to study the activity of the de-afferentiated brain in freely-behaving mice. This manipulation eliminated the respiration-coherent prefrontal oscillatory LFP component (Figure 4.25a,b, Figure 4.26a,b, Figure 4.27a-c), consistent with the disappearance of the CSD sink in deep layers (Figure 4.26c), while at the same time abolishing the olfactory-related prefrontal gamma oscillations (Figure 4.26d,e). These results confirm the hypothesis that a respiratory olfactory reafference (ROR) is responsible for the rhythmic cortical LFP, as suggested previously (Ito et al., 2014; Moberly et al., 2018; Biskamp et al., 2017; Tort et al., 2018).

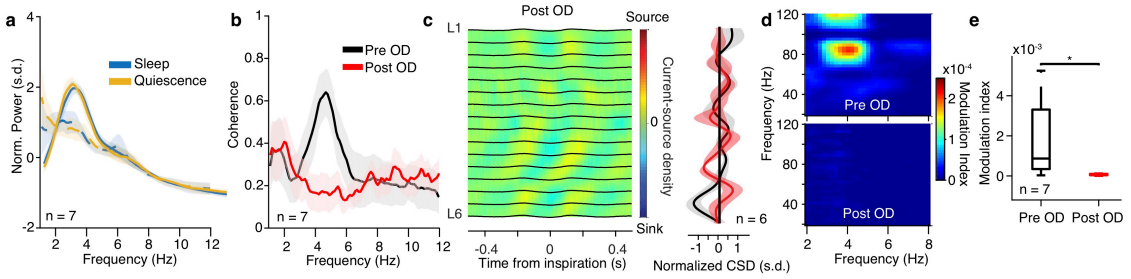

Figure 4.26: **Reafferent origin of gamma oscillations.**
(**a**) Average normalized power spectra before and after OD (n = 7). (**b**) Coherence spectrum between respiration and mPFC LFP before and after OD (n = 7 mice). (**c**) Left, example inspiration-triggered CSD of the mPFC LFP during quiescence and sleep after OD. Right, average normalized CSD at zero lag (n = 6 mice). (**d**) Example power-phase modulation of mPFC gamma oscillations before (top) and after (bottom) OD. (**e**) Average mPFC power-phase modulation strength of ~80 Hz gamma oscillations (n = 7 mice; paired t-test: before vs. after OD).

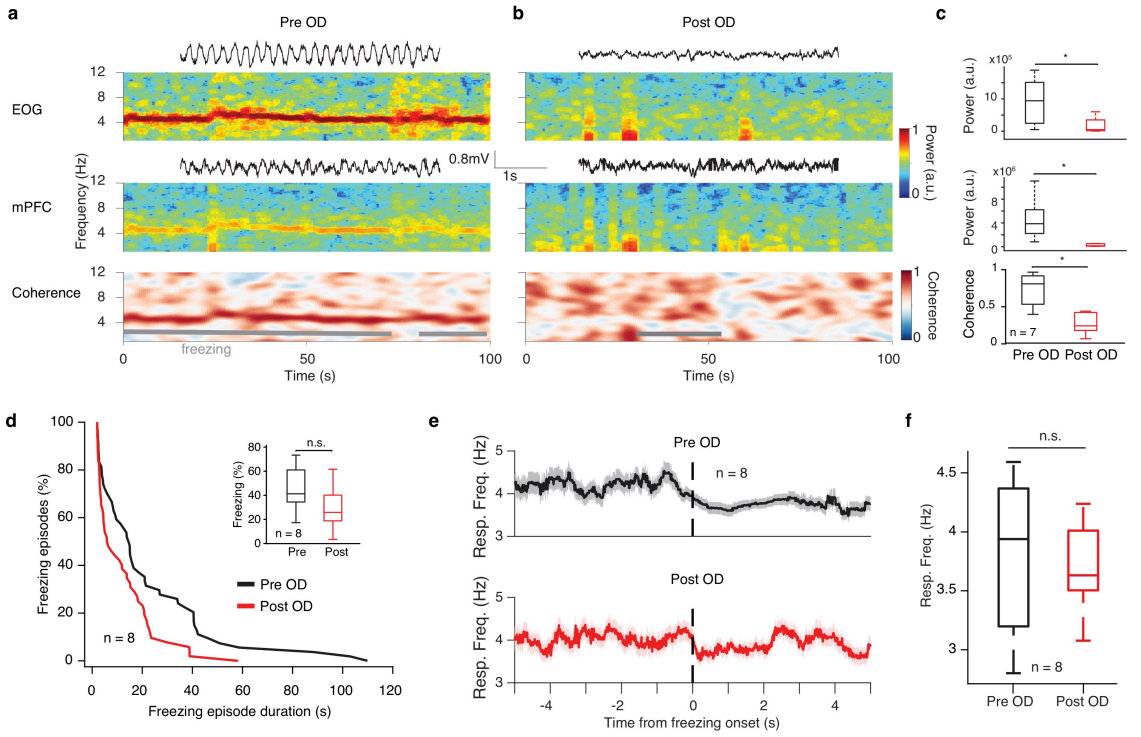

Figure 4.27: **Effect of olfactory de-afferentiation on fear behavior.**
(*a, b*) Example spectral decomposition of the respiration (top) and mPFC LFP (middle) during freezing behavior and coherogram between the two signals (bottom), in baseline conditions (a) and after OD (b). (*c*) Average EOG (top) and mPFC LFP(middle) power and coherence between them (bottom) for the 2-5 Hz band before and after OD (n = 7 mice, Wilcoxon signed-rank tests in all plots, pre- versus post-OD). (*d*) Cumulative distribution of freezing episode duration for tone retrieval before and after OD (n = 8 mice). Inset, average freezing before and after OD (n = 8 mice, Wilcoxon signed-rank test, pre- versus post-OD, P = 0.109). (*e*) Freezing onset triggered respiratory frequency before and after OD (n = 8 mice). (*f*) Average respiratory frequency during freezing, before and after OD (n = 8 mice, Wilcoxon signed-rank test, pre- versus post-OD, P = 0.742). Stars indicate significance levels (* P<0.05; ** P<0.01; *** P<0.001). n.s., not significant; OD, olfactory de-afferentiation.

Surprisingly however, the olfactory de-afferentiation (OD) left most prefrontal and thalamic neurons modulated by breathing, although the strength of modulation was somewhat reduced (Figure 4.28a-c), suggesting that a so-far undescribed ascending respiratory corollary discharge (RCD) signal, likely propagating from the brainstem respiratory rhythm generators, is responsible for the massive entrainment of prefrontal neurons. Interestingly, following OD, mice exhibited intact memory and fear expression, suggesting that the RCD might be underlying the behavioral expression (Figure 4.27d-f). Dorsal hippocampal neurons were somewhat stronger affected by the ablation, yet >40% of cells were still significantly phase locked (Figure 4.28b,c), indicating a differential degree of contribution of RCD and ROR to unit firing across mPFC, HPC, and thalamus. In contrast to the prefrontal CSD, the olfactory de-afferentiation led to a strong reduction of the outer molecular layer current-sink originating in LEC LII in the respiration-locked CSD (Figure 4.28d-e), while leaving MEC LII sink and other non-respiration related CSD patterns intact (Figure 4.28d,Figure 4.35a), suggesting that the LEC input is driven by ROR, while MEC input is driven by RCD.

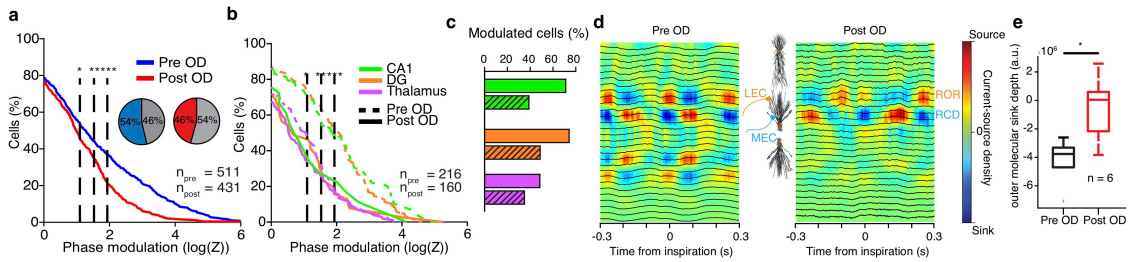

Figure 4.28: **Reafferent respiratory input does not account for neuronal entrainment.**
(*a*) Cumulative distribution of modulation strength for all mPFC neurons pre and post OD (Pre: n = 511 cells; Post: n = 431 cells). Inset, percentage of significantly phase-modulated cells before and after OD. (*b*) Cumulative distribution of modulation strength for CA1, DG and somatic thalamus neurons before and after OD. (*c*) Percentage of significantly phase-modulated cells before and after OD. (*d*) Example inspiration-triggered CSD of the dorsal hippocampus LFP before (left) and after (right) OD. (*e*) Average outer molecular layer sink depth (n = 6 mice; paired t-test: before vs. after OD). Shaded areas, mean ± s.e.m. a.u., arbitrary units; s.d., standard deviations; n.s., not significant. Shaded areas, mean ± s.e.m. Stars indicate significance levels (* P<0.05; ** P<0.01; *** P<0.001). s.d., standard deviations; a.u., arbitrary units; OD, olfactory de-afferentiation.

4.6 HIPPOCAMPAL NETWORK DYNAMICS ARE MODULATED BY BREATHING

From the results so far, it is clear that hippocampal neuronal activity is massively modulated by breathing, by means of entorhinal inputs to the DG. However, during quiescence and slow-wave sleep, hippocampal activity is characterized by recurring nonlinear population events such as dentate spikes (DS) and sharp-wave ripple complexes.

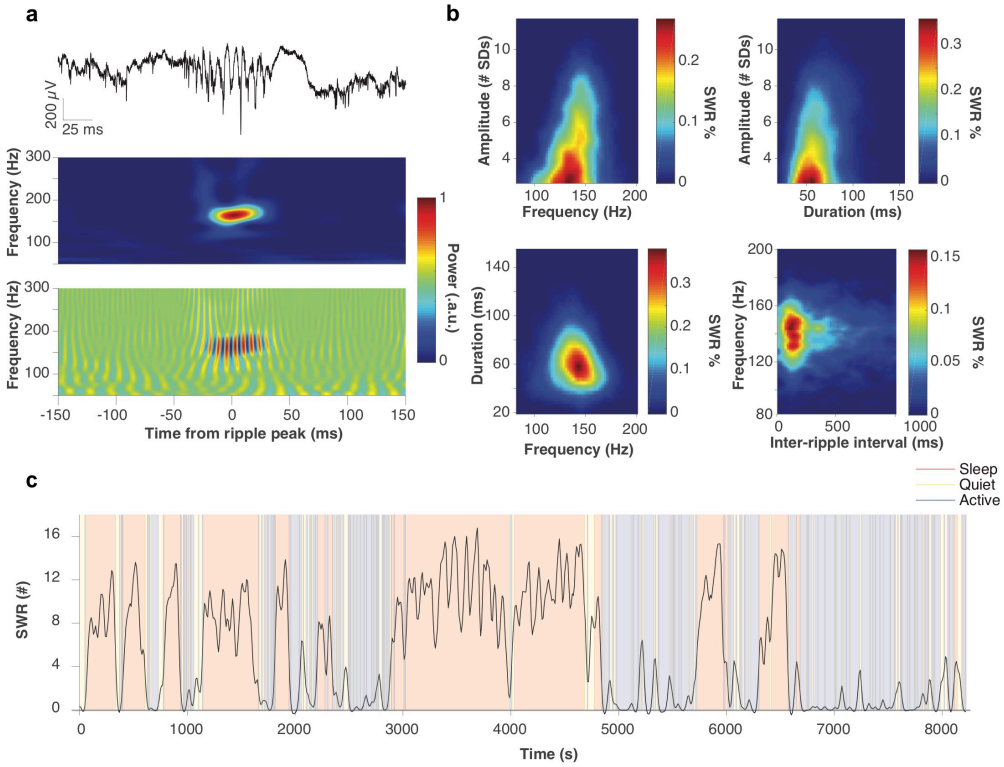

Figure 4.29: **Behavioral and statistical properties of ripples.**
(a) Example trace of ripple oscillation recorded in the pyramidal layer of dCA1 (*top*) and corresponding wavelet decomposition power (*middle*) and real-part (*bottom*). *(b)* Color-coded pairwise joint probability distributions of the properties of ripple events, including the amplitude, frequency, duration and inter-ripple interval. SD, standard deviation. *(c)* Number of ripple events, binned every 10s, as a function of behavioral state, for an example freely-behaving mouse during a 2.5h recording in the homecage.

CA1 ripples are local fast oscillations in the pyramidal layer of CA1, generated by the rhythmic interplay between PNs and INs in response to strong depolarization from CA3 population spikes, identified as sharp negative potentials (sharp-waves) in the CA1 stratum radiatum (Buzsaki and Schomburg, 2015)(Figure 4.29, Figure 4.34a-c). The CA3 population spike is in itself generated due to the low cholinergic tone during quiescence and sleep that enables CA3 recurrent excitation (Vandecasteele et al., 2014), resulting in a characteristic modulation of the ripple occurrence by the behavioral state (Figure 4.29c). Ripples are distinct events but have a tendency to occur in groups of 2 or 3 events (Figure 4.30a), separated by 100-200ms, however the characteristics of each ripple contributing to such burst seem to be independent (Figure 4.30b).

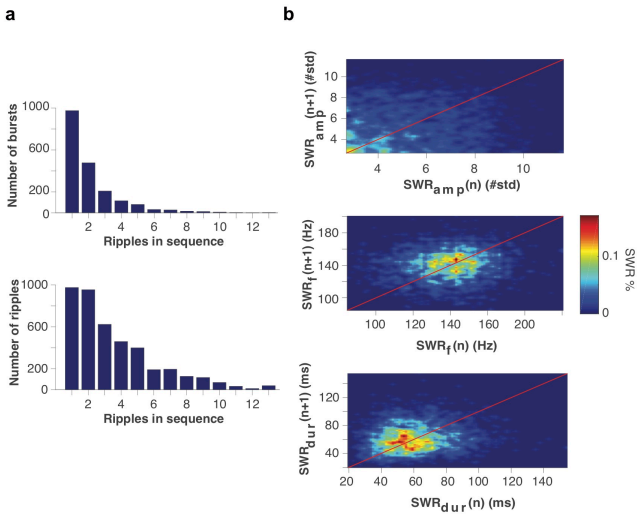

Figure 4.30: **Statistical properties of ripple bursts.**
(a) Histogram of the number of ripple bursts containing 1-12 ripple sequences ((*top*) and histogram of the total number of ripples occurring within sequences with the corresponding number of events. *(b)* Poincaré return map of the properties (*top*, amplitude; *middle*, frequency; *bottom*, duration) of consecutive ripple events within a ripple sequence. std., standard deviation.

Although intrinsic ripple events are generated outside the CA1, optogenetic excitation of the dCA1 pyramidal cells is enough to generate such oscillations locally Stark et al., 2014, 2015 Figure 4.31, which however tend to be of slower frequency compared to the intrinsic events (Figure 4.31e).

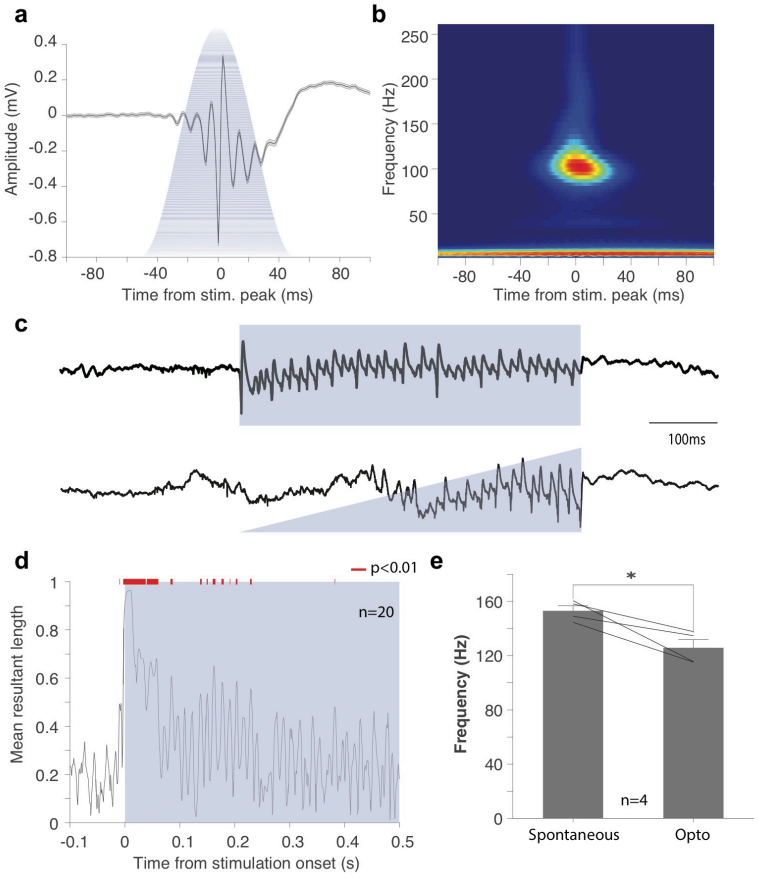

Figure 4.31: **Optogenetic generation of ripples.**
(a) Smooth half-sine-wave light stimulation of dCA1 pyramidal cells, expressing the excitatory opsin ChR2 under the control of the CamKIIa promoter and infected using rAAV1, results in the generation of a fast transient ripple-like oscillation. *(b)* Wavelet decomposition of the optogenetically-induced oscillation in (a) exhibits similar spectral characteristics as the intrinsic ripple oscillations. *(c)* Different stimulation patterns (*top*, continuous light; *bottom*, ramp) result in qualitatively different network pattern. *(d)* Moment-to-moment mean resultant length (MRL) quantification of the phase consistency of the evoked patterns following continuous light stimulation across n = 20 repetitions. Red lights indicate statistically significant periods (p<0.01). *(e)* Average frequency of intrinsic and optogenetically generated ripples (n = 4 mice, mean ± s.e.m., Wilcoxon signed rank test, *P<0.05). Shaded blue areas indicate the duration and amplitude shape of the light stimulation.

The selection of stimulation parameters alters the resulting network pattern. This fact is evident in the case of closed-loop stimulation after online ripple detection (Figure 4.32a). A short light-pulse, results in the termination of the oscillation (Figure 4.32b). This happens potentially because the short strong excitation of the PNs drives feedforward perisomatic inhibition and resets the ongoing oscillation. In contrast, prolonged closed-loop stimulation enables the prolongation of the intrinsic oscillatory pattern (Figure 4.32c).

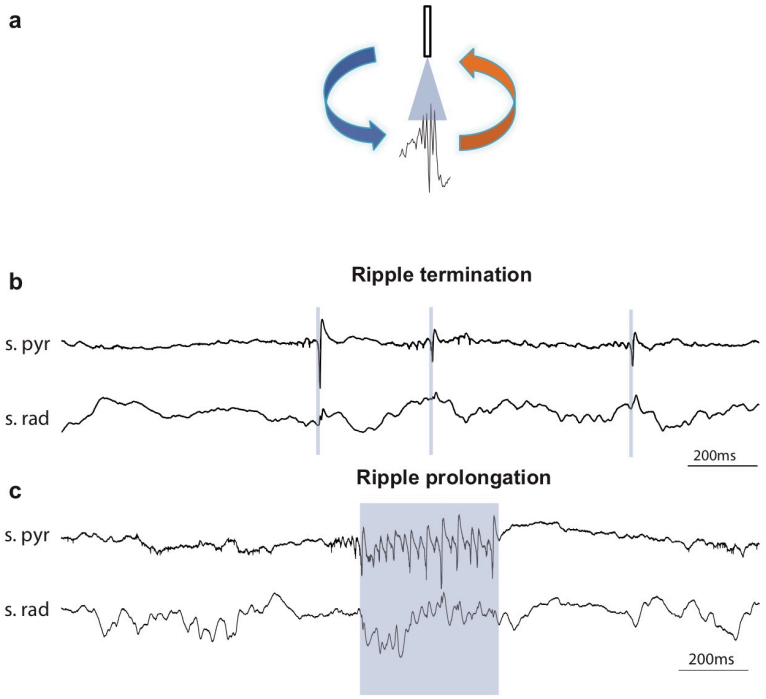

Figure 4.32: **Closed-loop perturbation of ripples.**
(a) Schematic of closed-loop optogenetic perturbation of intrinsic ripples. *(b)* Example traces from the dCA1 stratum pyramidale and radiatum, during the closed-loop short stimulation of pyramidal cells, resulting in the termination of intrinsic ripples. *(c)* Example traces from the dCA1 stratum pyramidale and radiatum, during the closed-loop long stimulation of pyramidal cells, resulting in the prolongation of intrinsic ripples. Shaded blue areas indicate the duration and amplitude shape of the light stimulation.

During ripples, CA1 PN and IN, and to a lesser extent DG cells, were strongly activated (Figure 4.33, Figure 4.34d). Ripple occurrence was strongly modulated by breathing biased towards the post-inspiratory phase, while ripples were suppressed during exhalation (Figure 4.34e-g). Following olfactory de-afferentiation, ripples remained significantly phase modulated by breathing (Figure 4.34h), suggesting that RCD is the main source of their modulation.

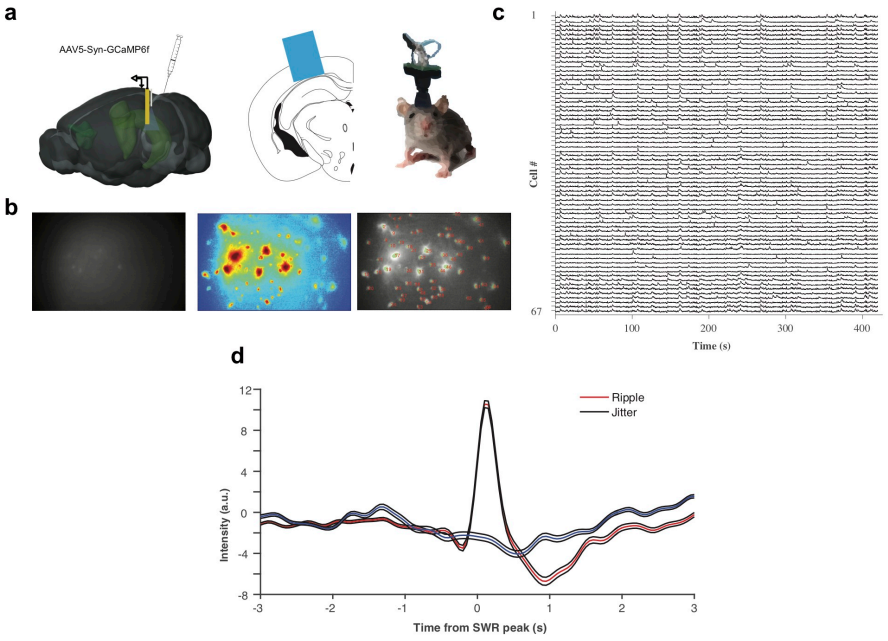

Figure 4.33: **Simultaneous miniscope imaging and electrophysiological recordings.**
(a) Schematic of the injection (*left*), lens implantation in dCA1 (*middle*) and miniscope recording procedure (*right*). *(b)* Example raw image of the dCA1 (*left*), maximum correlation projection (*middle*) and maximum fluorescence projection, overlaid with identified putative cell ROIs (*right*). *(c)* Example Ca^{2+} traces from 67 simultaneously recorded cells in the dCA1. *(d)* Average Ca^{2+} response of all recorded dCA1 cells in response to ripples (red) and shuffle-control (blue). Shaded areas, mean ± s.e.m.

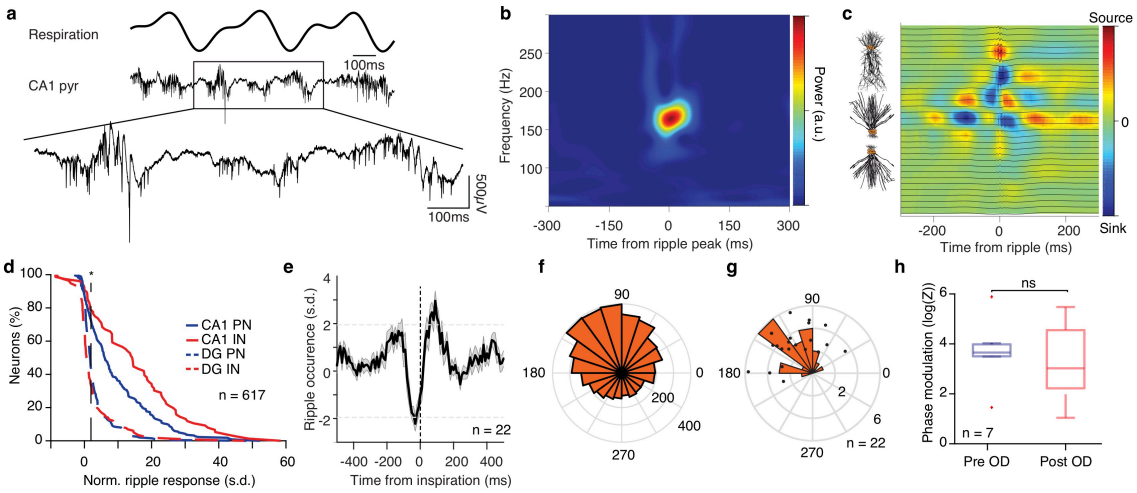

Figure 4.34: **Breathing modulates hippocampal ripples.**
(*a*) Example traces of the respiratory signal and CA1 pyramidal layer LFP. In the magnified LFP signal, ripple events and the associated spiking activity can be observed. (*b*) Average ripple-triggered time-frequency wavelet spectrogram of the CA1 pyramidal layer LFP from one example animal. (*c*) Schematic of the CA1 pyramidal and granular cells somato-dendritic domains aligned to the average ripple-triggered CSD profile of the hippocampal LFP activity for one example animal. (*d*) Cumulative distribution of the ripple-triggered normalized firing of CA1 and DG PNs (CA1, n = 220 cells; DG, n = 202 cells) and INs (CA1, n = 76 cells; DG, n = 119 cells). (*e*) Average cross-correlation between inspiratory events and ripple occurrence (n = 22 mice). Dashed horizontal lines indicate the significance levels. (*f*) Distribution of the respiratory phase of occurrence of individual ripple events for one example animal (n = 4813 ripples). (*g*) Distribution of average phase and modulation strength for ripples (n = 22 mice). (*h*) Phase modulation of ripples before and after OD.

Keeping up with the role of entorhinal input mediating respiratory drive on ripples, we observed a consistent relationship between the magnitude of MEC LII sink directly preceding ripple occurrence and the phase within the respiratory cycle of the ripple occurrence (Figure 4.35b-c).

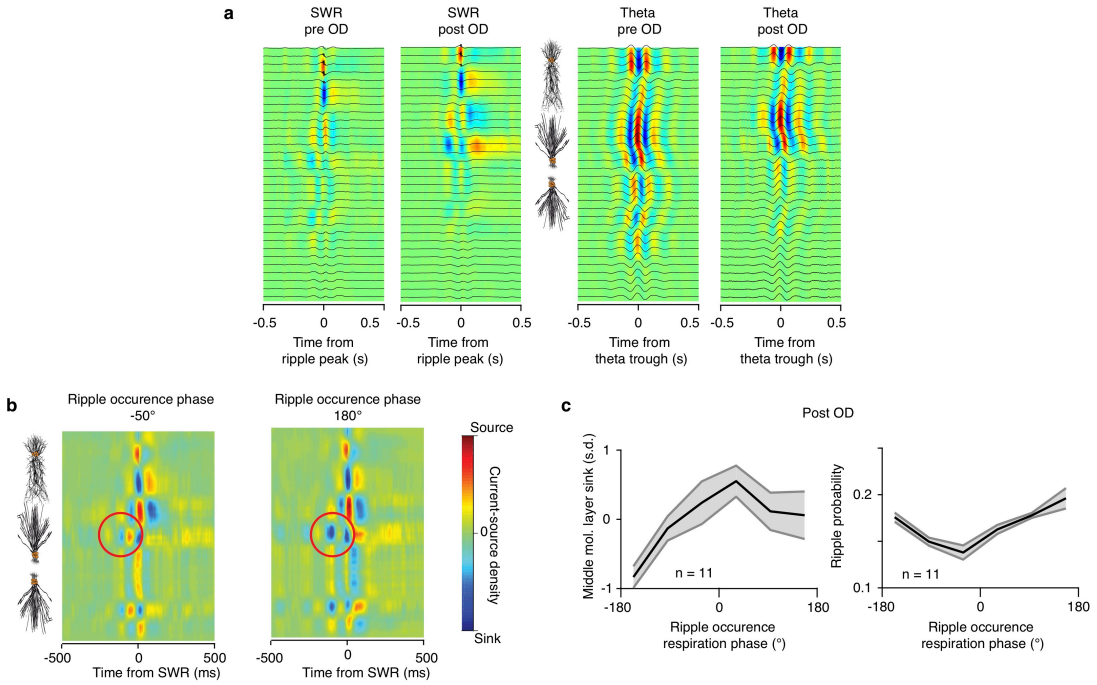

Figure 4.35: **Effect of OD on characteristics of hippocampal respiration-related patterns.** (*a*) Example current-source density profiles of the dorsal hippocampus of the same animal, triggered on the peak of sharp-wave ripple (SWR) events and the troughs of theta oscillations (detected in CA1 pyramidal layer) before and after OD. (*b*) Example ripple-triggered translaminar current-source density profiles of the dorsal hippocampus grouped by the respiratory phase of the ripple occurrence: -50°(left) and 180°(right). Note strong sink at DG middle mol. Layer (red circle) present in the latter but not former. (*c*) Average respiration phase-resolved ripple-triggered middle molecular layer dentate sink magnitude (left) and corresponding phase ripple normalized incidence rate (right).

Another prominent hippocampal offline state-associated pattern are dentate spikes, defined as large positive potentials in the DG hilus region (Bragin et al., 1995) which are believed to occur in response to strong inputs in the molecular layer, such as during entorhinal UP states (Figure 4.36a, Figure 4.15). During DS, both DG (~70% PN and IN), CA1 (~40% PN and ~70% IN) and mPFC (~40% PN and ~70% IN) cells were strongly excited (Figure 4.36b,c). Consistent with respiratory entrainment of the entorhinal inputs, the occurrence of DS was strongly modulated by the breathing phase both before and after OD , with the majority of events occurring after inspiration (Figure 4.36d,e).

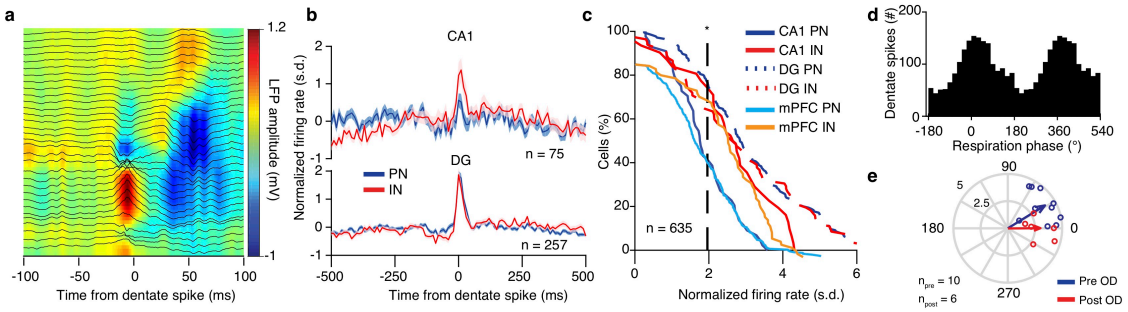

Figure 4.36: **Breathing entrains dentate spikes.**
(a) Color-coded LFP power depth profile and overlaid LFP traces of an example dentate spike. *(b)* Average dentate spike triggered normalized spiking activity for all CA1 ((*top*) and DG ((*bottom*) putative excitatory (PN) and inhibitory (IN) cells. *(c)* Cumulative distribution of the dentate spike-triggered normalized firing of CA1, DG and mPFC putative principal cells and putative inhibitory interneurons. *(d)* Histogram of the occurrence of dentate spike events as a function of the respiratory phase for one example animal. *(e)* Preferred respiratory phase of dentate spike occurrence and phase modulation strength (log(Z)) for all animals and population average (arrow) (n = 10 mice). s.d., standard deviation; Shaded areas, mean ± s.e.m. Dashed vertical lines indicate the significance levels.

4.7 BREATHING ORGANIZES PREFRONTAL UP STATES AND HIPPOCAMPAL OUTPUT

CA1 is projecting to the mPFC (Figure 4.37a-c) and CA1 electrical or optogenetic stimulation drives short-latency mPFC LFP and Ca^{2+} responses (Figure 4.37d-i). Ripple output is known to recruit prefrontal neural activity (Siapas and Wilson, 1998; Peyrache et al., 2011).

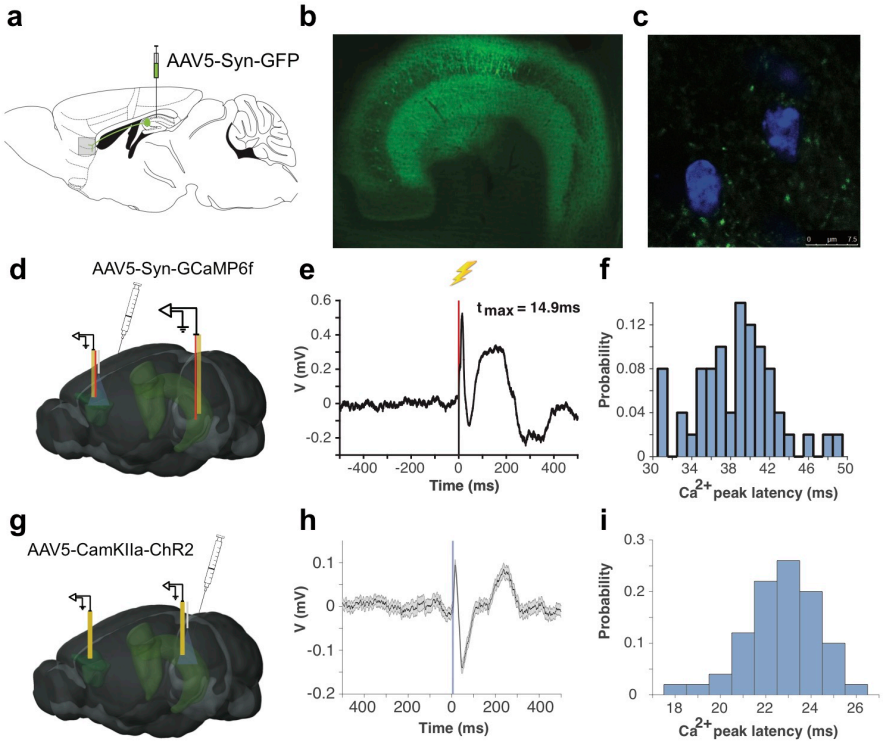

Figure 4.37: **CA1 output to mPFC.**
(a) Schematic depiction of viral tracer injection in the dCA1. *(b)* Fluorescent labeling of the hippocampus following injection as in (a). The image is generated from an artificial imaging plane, reconstructed from whole-brain light-sheet microscope images following tissue clearing with the uDISCO method. *(c)* Confocal microscope images of CA1 axonal terminals (green puncta) in the mPFC, in close proximity to the DAPI fluorescently counterstained prefrontal neuronal nuclei (blue). *(d)* Schematic of virus injection and implantation of optic fibers, recording electrodes and stimulating electrodes for fiber-photometry experiments. *(e)* Prefrontal LFP triggered on the electrical microstimulation of dCA1 region. *(f)* Histogram of prefrontal somatic Ca^{2+} peak latency following CA1 electrical microstimulation. *(g)* Schematic of virus injection and implantation of optic fibers and recording electrodes for optogenetic experiments. *(h)* Prefrontal LFP triggered on short-duration optogenetic stimulation of dCA1 region. *(i)* Histogram of mPFC somatic Ca^{2+} peak latency following local electrical microstimulation. Shaded areas, mean ± s.e.m. Shaded blue areas indicate the duration of the light stimulation.

CA1 ripples evoke a strong response in the mPFC, which is commensurate with the ripple amplitude (Figure 4.38a-b) and can be observed throughout prefrontal subregions, with a prominence in the dorsal mPFC (Figure 4.38e). In agreement with this, hippocampal ripples give rise to an efferent copy of the oscillatory synaptic currents detected as a local increase in fast oscillatory power in the PFC LFP (Khodagholy et al., 2017) (Figure 4.38c), phase-locked to the CA1 ripple (Figure 4.38d).

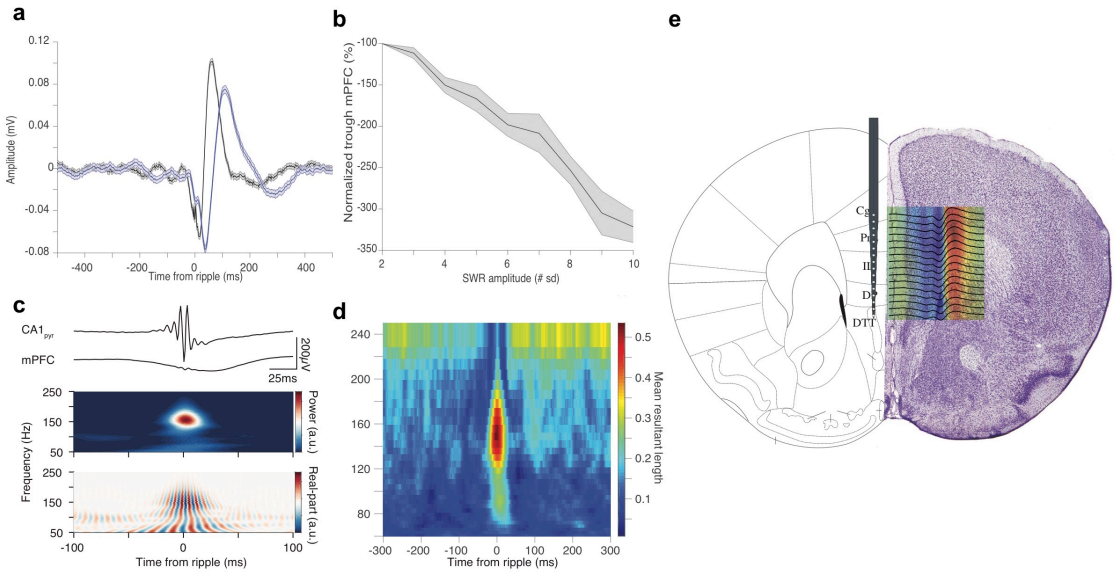

Figure 4.38: **Ripple-evoked prefrontal LFP patterns.**
(a) Ripple-triggered CA1 (black) and mPFC (blue) LFP response. *(b)* Relationship of SWR amplitude and the mPFC evoked response trough magnitude. *(c) Top*, Finer temporal resolution average ripple-triggered CA1pyr and mPFC LFP traces from an example animal. *Bottom*, average ripple triggered wavelet spectral decomposition of mPFC LFP power (upper) and real-part of the wavelet transform (lower) (n = 3162 ripples). *(d)* Color-coded mean resultant length of the phase of mPFC and CA1 wavelet decomposed LFP for each time and frequency bin across ripple events. *(e)* Schematic depiction of a silicon-probe spanning different prefrontal subregions across the dorsal-ventral axis and color-coded ripple-triggered mPFC LFPs from corresponding depth are overlaid on cresyl violet stained brain slice (modified from (Paxinos et al., 2004)). a.u., arbitrary units; sd, standard deviation. Shaded areas, mean ± s.e.m.

In response to ripple events, ~14% of prefrontal PNs and ~42% of INs exhibited increased firing (Figure 4.39, Figure 4.40c). In parallel, ~69% of NAc cells are significantly driven by ripple events (Figure 4.40).

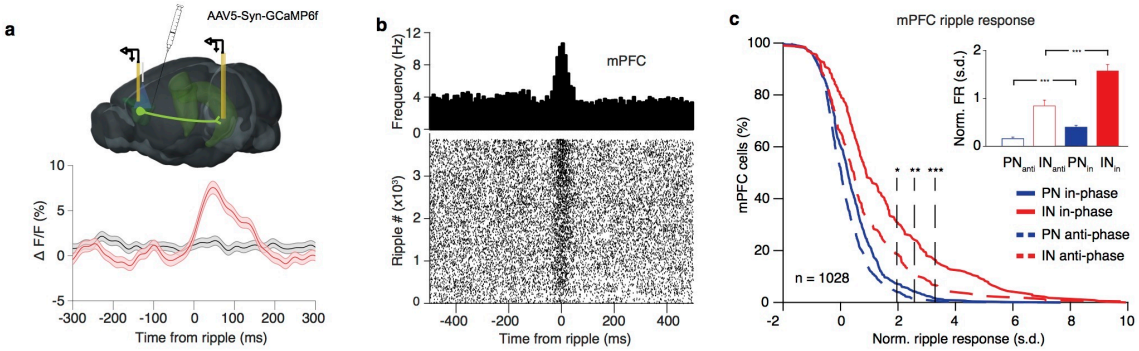

Figure 4.39: **Breathing modulates hippocampal output to mPFC.**
(a) Top, schematic depiction of the experimental design for fiber-photometry of ripple-related prefrontal activity. *Bottom*, ripple-triggered prefrontal somatic Ca^{2+} (red) and shuffle-control (gray). *(b)* Example mPFC unit ripple-triggered spiking activity across individual ripple events ((*bottom*) and average time-histogram (*top*) *(c)* Cumulative distribution of the ripple-triggered normalized firing of mPFC putative principal cells (PN) (n = 791 cells) and putative inhibitory interneurons (IN) (n = 237 cells) in response to ripples occurring in the preferred phase of respiration (in-phase) and the ripples occurring in the least-preferred phase (anti-phase) (n = 11 mice). *Inset*, average ripple-triggered firing rate for PN (n = 791 cells, Wilcoxon signed rank test, in-phase versus anti-phase, ***P<0.001) and IN (n = 237 cells, Wilcoxon signed rank test, in-phase versus anti-phase, ***P<0.001) in response to ripples occurring in the preferred and least-preferred respiratory phase. CA1pyr, str. pyramidale; s.d., standard deviation; a.u., arbitrary units; FR, firing rate. Shaded areas, mean ± s.e.m. Dashed vertical lines indicate the significance levels. Stars indicate significance levels (* P < 0.05; ** P < 0.01; *** P < 0.001).

Interestingly, in both mPFC and NAc there is a great overlap between cells that are phase modulated by breathing and that are responsive to ripples (Figure 4.40c), while ripples occurring in the preferred post-inspiratory phase of ripple occurrence, drive a greater fraction of cells from both structures to fire significantly more compared to anti-preferred phase (Figure 4.39c,Figure 4.40c).

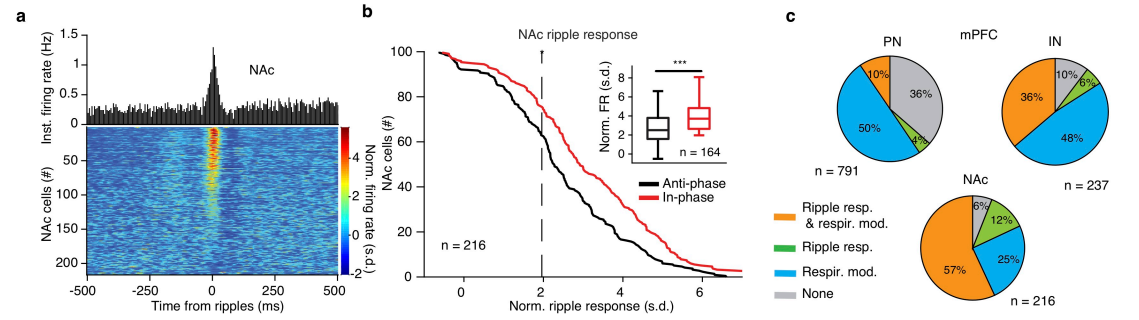

Figure 4.40: **Breathing modulates hippocampal output to NAc.**
(*a*) Cross-correlation of firing with respect to ripple time for one example NAc unit (top) and color-coded cross-correlograms for all NAc cells (n = 216 cells). (*b*) Cumulative distribution of the ripple-triggered normalized firing of NAc cells (n = 216 cells) in response to, as in (l), "in-phase" and "anti-phase" ripples (n = 4 mice). Inset, average ripple-triggered firing rate (n = 164 cells, Wilcoxon signed-rank test, in-phase versus anti-phase). (*c*) Top, pie charts indicating the percentage of all mPFC PNs (left; n = 791 cells) and INs (right; n = 237 cells) that are either phase modulated by respiration (resp. mod), responding significantly to ripples (ripple resp.), being both significantly modulated by breathing and significantly responsive to ripples or neither. Bottom, similarly, for all NAc cells (n = 216 cells).

Similar to the hippocampus, during quiescence and slow-wave sleep neocortical circuits exhibit nonlinear bistable dynamics in the form of DOWN and UP states. We posited that the strong rate modulation of prefrontal neural activity by breathing would bias these dynamics. To test this prediction, we identified prefrontal UP and DOWN states based on the large-scale population activity and characterized their relationship with the phase of the ongoing breathing rhythm (Figure 4.41a). Surprisingly, both UP and DOWN state onsets were strongly modulated by the breathing phase and time from inspiration (Figure 4.41b-d), while the magnitude of UP states followed the profile of UP state onset probability (Figure 4.41e). In agreement with the results on ripples and prefrontal units, UP and DOWN state modulation was not affected by olfactory de-afferentiation, suggesting that RCD is the source of this modulation (Figure 4.41f,g).

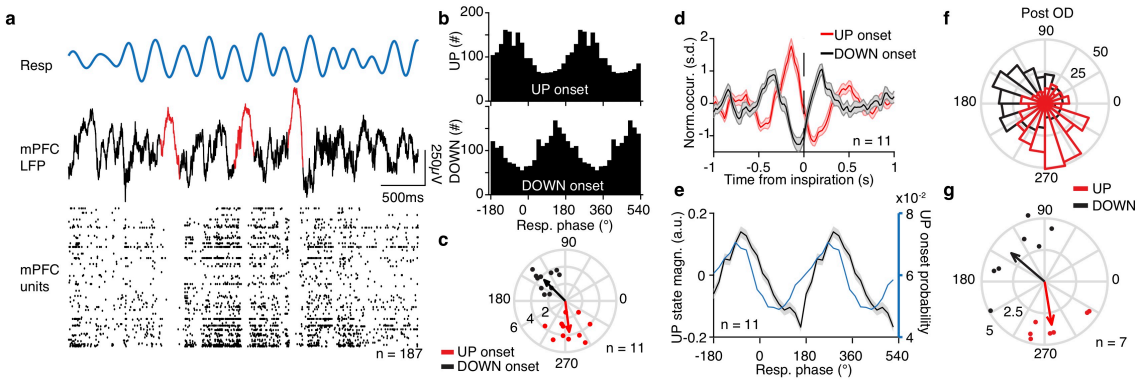

Figure 4.41: **Breathing organizes prefrontal UP states.**
(*a*) Example traces of respiration signal (top), mPFC LFP (middle trace) and spike trains of 183 simultaneously recorded mPFC units during sleep. Three typical delta waves and the corresponding DOWN states of the neuronal population are marked with red. (*b*) Example distributions of the breathing phase of UP (top) and DOWN (bottom) state onsets. (*c*) Distribution of preferred breathing phase of UP and DOWN states (n = 11 mice). (*d*) Cross-correlation of UP and DOWN state onsets with respect to inspiration. (*e*) Normalized power (black) and occurrence probability (blue) for prefrontal UP states (n = 11 mice). (*f, g*) Example (f) and population (g) distribution of preferred breathing phase of UP and DOWN state occurrence after OD (n = 7).

Previous observations during sleep in rats identified a correlation between ripple occurrence and cortical SO (Siapas and Wilson, 1998; Sirota and Buzsaki, 2005; Peyrache et al., 2011). Here, ripples preceded the termination of prefrontal UP states and onset of the DOWN states both before (Figure 4.42a) and after de-afferentation (Figure 4.42b), with ripples contributing to UP state termination occurring in the early post-inspiratory phase (Figure 4.42c). This is in agreenent with the RCD-driven synaptic inputs to the DG middle molecular layer preceding ripple events, which are suggesting an RCD-mediated coordination of SWR occurrence with the MEC UP states (Figure 4.35b,c).

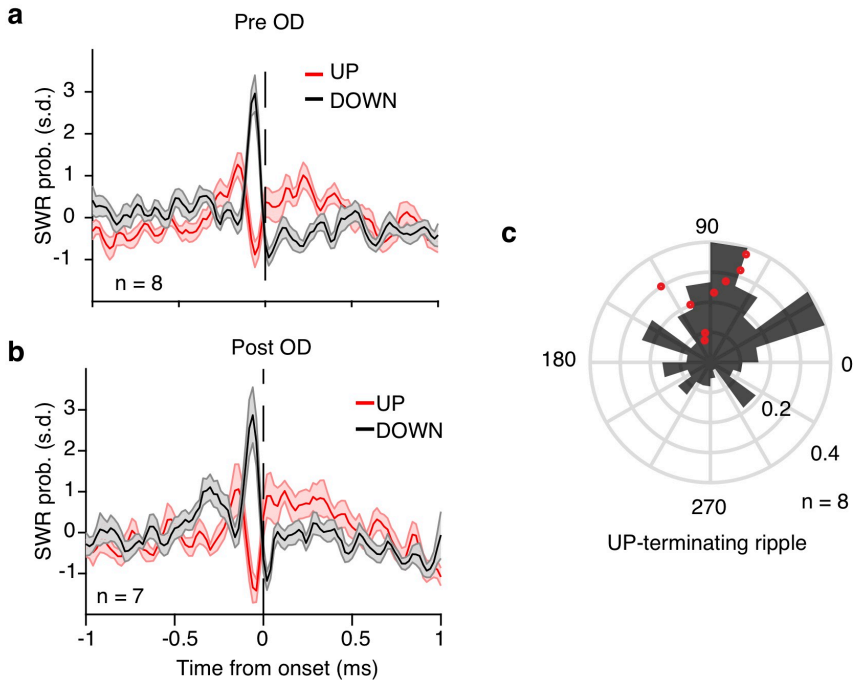

Figure 4.42: **Breathing organizes UP state - ripple interaction.**
(*a*) Probability of SWR occurrence as a function of time from UP or DOWN state onset before OD (n = 8 mice). (*b*) Probability of SWR occurrence as a function of time from UP or DOWN state onset after OD (n = 7 mice). (*c*) Example (black) and distribution of preferred breathing phase of SWR occurrence, for SWRs that are terminating an UP state (red dots, n = 8 mice).

4.8 SUMMARY

In summary, in this work we demonstrate that the respiratory rhythm provides a unifying global temporal coordination of neuronal firing and nonlinear dynamics across cortical and subcortical limbic networks. We identified a joint mechanism of respiratory entrainment, consisting of an efference copy of the brainstem respiratory rhythm (respiratory corollary discharge; RCD) that underlies the neuronal modulation and a respiratory olfactory reafference (ROR) that contributes to the modulation and accounts for LFP phenomena (Figure 4.43a). We further comprehensively characterized the distinct phase relationship between different network events within the breathing cycle across limbic structures, painting the picture of how this organization enables the multiplexing and segregation of information flow across the limbic system and providing the basis for mechanistic theories of memory consolidation processes enabled by the respiratory modulation (Figure 4.43b).

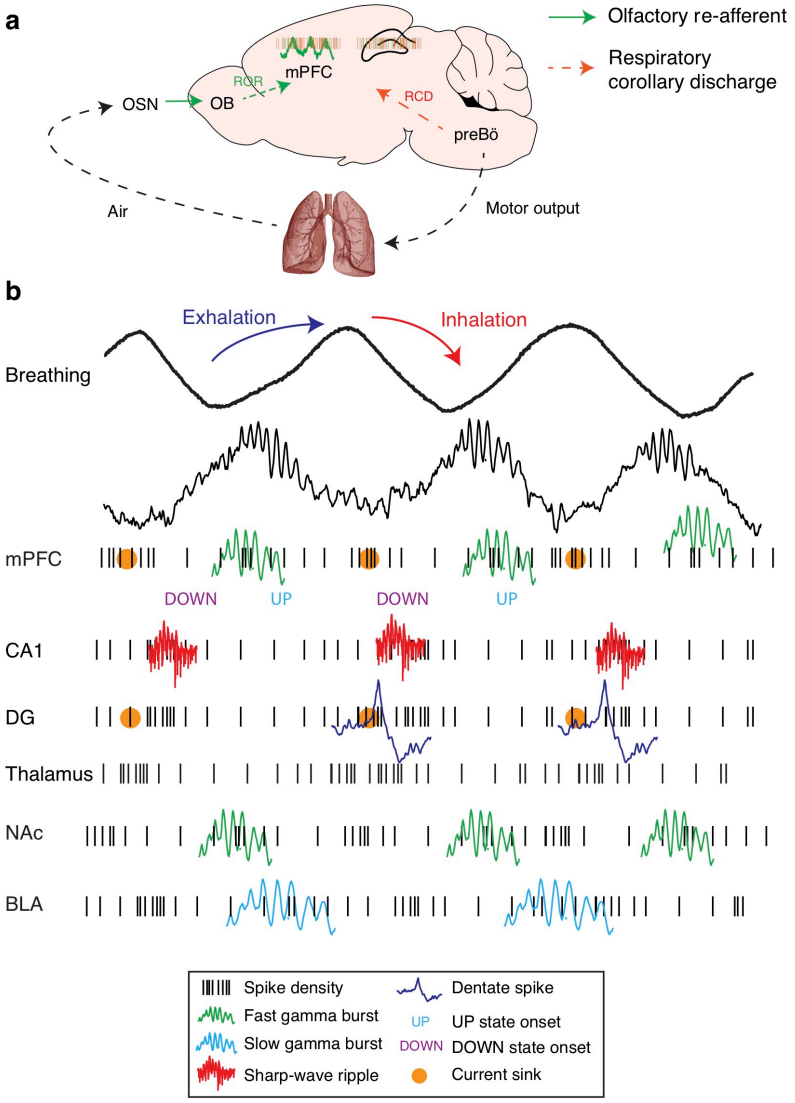

Figure 4.43: **Breathing organizes network dynamics across limbic structures.**
(**a**) Schematic depiction of the efferent copy pathway carrying the respiratory corollary discharge (RCD) signal and the reafferent pathway carrying the respiratory olfactory reafferent (ROR) signal. (**b**) Summary schematic of the network dynamics organized by breathing throughout all structures studied. Black traces: LFPs; Black ticks: neuronal spikes; Green traces: Fast (~80Hz) gamma; Cyan traces: Slow gamma (~40Hz); Red traces: CA1 Ripples; Blue traces: Dentate spikes; Orange dots: CSD sinks (mPFC deep layers and DG middle molecular layer).

5

DISCUSSION

5.1 SUMMARY

In this work, we began by investigating the potential neuronal synchronization between mPFC and BLA during fear behavior, to understand the mechanisms that support the expression of fear memories. We identified that the behavioral expression of fear memories is not only time-locked to the CS presentation but rather is characterized by internally generated freezing episodes, the probability of which is modulated by the presentation of CS. Freezing episodes occur between CS presentations and are potentially a reflection of an induced fearful state after the initial CS-induced retrieval of the fear memory.

We thus investigated the neuronal activity in the mPFC and BLA during freezing, the behavioral expression of fear in mice. We identified that the expression of conditioned fear memories is associated with prominent synchronous 4Hz oscillations in both mPFC and BLA, that organize the spiking activity of local neuronal populations. Our results indicate that internally generated freezing-related 4Hz mPFC oscillations constitute a specific oscillatory mechanism, distinct from the CS-evoked mPFC theta resetting observed previously (Courtin et al., 2014b; Likhtik et al., 2014; Stujenske et al., 2014). Interestingly, the amplitude and synchrony of these oscillations developed during fear conditioning and the length of freezing episodes was also strongly correlated with the duration and power of 4Hz, while we were able to predict the onset and offset of freezing episodes based on this oscillation, using it as a biomarker of the fear state. Our results suggest that the synchronized 4Hz oscillations represent a mechanism for the initiation and maintenance of freezing episodes, inside and outside of CS presentations. The synchronized spiking activity between mPFC and BLA neurons has been implicated in resistance to extinction (Likhtik et al., 2014) and fear discrimination (Livneh and Paz, 2012). Here we mechanistically demonstrate that such synchronization is accomplished by 4Hz oscillations during fear behavior and provide causal evidence for this function.

Optogenetic artificial induction of 4Hz oscillations in the mPFC synchronizes mPFC and BLA neuronal activity and drives freezing behavior in naive mice. This effect was frequency and structure-specific, as mPFC manipulation at other frequencies or 4Hz induction in the motor cortex and BLA did not induce any behavioral effects. Fascinatingly, the 4Hz analog optogenetic stimulation of mPFC induced freezing behavior not only during the stimulation but also 24h later in the same context in which the stimulation took place. This observation suggests that the artificial induction of 4Hz oscillations might be involved in the formation of associative fear memories.

These results leave open the pathway that is involved in the expression of fear behavior in these naive animals. One possibility is a BLA mediated output, while an alternative pathway could be a potential direct functional pathway from the mPFC to the brainstem freezing promoting circuits. Interestingly, pyramidal tract (PT) PAG projecting mPFC neurons exhibit resonance properties at a similar frequency (Ferreira et al., 2015; Dembrow et al., 2010; Dembrow and Johnston, 2014), while they are receiving BLA inputs (Cheriyan et al., 2016). Along these lines, stimulation of the vlPAG, the target of these cells, drives passive coping behaviors (Bandler et al., 2000). This projection has been now shown to be involved in both social defeat (Franklin et al., 2017) and fear expression (Rozeske et al., 2018).

In summary, our data unravel a physiological signature of fear memory and reveal a specific 4Hz oscillatory mechanism that supports the expression of fear memories by organizing prefrontal ensembles and the long-range synchronization of neuronal activity between mPFC and BLA neuronal circuits. These results suggest that blocking oscillations in this circuit might represent a potential therapeutic strategy for pathological conditions such as anxiety disorders.

However, the origin of this oscillation remained opened, as well as the specificity of this oscillation to conditioned fear behavior. The first hypothesis was that 4Hz oscillations might be related to hippocampal theta oscillations. To examine this hypothesis, we transiently inactivated the medial septum, using muscimol, a potent GABA-a agonist. GABAergic projections from the medial septum innervate GABAergic interneurons in the hippocampus and are responsible for the generation of the theta rhythm. The inactivation of medial septum abolished theta oscillations in the hippocampus and reduced the prefrontal theta power, while it had no effect on the freezing related 4Hz power in the prefrontal cortex.

Having established that prefrontal 4Hz is an oscillation distinct from theta, we started from the behavioral definition of freezing, which is defined as the complete absence of movement, with the exception of respiration and heartbeat and we explored the dynamics of micro-motions during freezing. Using ultra-precise head-mounted accelerometers, we identified that during freezing, head micro-motions exhibit rhythmicity with 4Hz frequency. This observation suggested that respiratory rhythm might be coupled or related to prefrontal oscillations. We thus posited that 4Hz oscillation might be related to the respiratory rhythm.

To investigate this hypothesis and further explore the hypothesis that the breathing rhythm governs multiregional activity and underlies the coordination of network dynamics across limbic systems during offline states, we performed a large-scale *in vivo* functional anatomical characterization of the mPFC, hippocampus, basolateral amygdala (BLA) and nucleus accumbens (NAc) using high-density silicon probes.

In this study, we demonstrated that the respiratory rhythm provides a unifying global temporal coordination of neuronal firing and nonlinear dynamics across cortical and subcortical limbic networks. Using recordings of the three-dimensional LFP profile of the mPFC and large-scale unit recordings from the hippocampus, amygdala, nucleus accumbens and thalamus, we identified that during quiescence and slow-wave sleep limbic LFPs are dominated by breathing-related oscillatory activity, while the majority of neurons in each structure are modulated by the phase of

the respiratory rhythm and reafferent gamma oscillations. Using pharmacological manipulations paired with large-scale recordings, we causally identified a joint mechanism of respiratory entrainment, consisting of an efference copy of the brainstem respiratory rhythm (respiratory corollary discharge; RCD) that underlies the neuronal modulation and a respiratory olfactory reafference (ROR) that contributes to the modulation and accounts for LFP phenomena. Hippocampal SWR and dentate spikes, as well as prefrontal UP and DOWN states, were strongly modulated by the respiratory phase with RCD being a sufficient source of modulation. This modulation accounts partially for the coordination of hippocampo-cortical nonlinear dynamics. Finally, we comprehensively characterized the distinct phase relationship between different network events within the breathing cycle across limbic structures, painting the picture of how this organization enables the multiplexing and segregation of information flow across the limbic system and providing the basis for mechanistic theories of memory consolidation processes enabled by the respiratory modulation.

Over the years, mounting evidence have suggested that breathing can entrain frog (Hobson, 1967) and human EEG (Busek and Kemlink, 2005; Yuan et al., 2013a), as well as LFP and spiking activity in the hedgehog OB and cortex (Adrian, 1942), rodent OB (Macrides and Chorover, 1972; Fukunaga et al., 2014; Phillips et al., 2012; Grosmaitre et al., 2007), cortex (Kay and Freeman, 1998; Fontanini et al., 2003; Ito et al., 2014; Biskamp et al., 2017; Zhong et al., 2017; Moberly et al., 2018) and the hippocampus in cats (Poe et al., 1996), rodents (Vanderwolf, 1992; Yanovsky et al., 2014; Nguyen Chi et al., 2016; Lockmann et al., 2016; Liu et al., 2017), and humans (Zelano et al., 2016; Herrero et al., 2018). With this study, we contribute to the ongoing effort to understand the mechanism and role of the respiratory entrainment of brain circuits. Our results extend and provide a mechanistic explanation and interpretation of the previous studies that described respiration-related LFP oscillations in different brain regions. Here, we leverage large-scale recordings from multiple limbic regions and thousands of cells to comprehensively characterize and uncover the underlying mechanisms of the limbic respiratory entrainment and understand the role of this phenomenon in organizing neuronal activity and coordinating network dynamics between remote regions.

In this study, we expanded the characterization of respiratory entrainment to the NAc, BLA, and thalamus for the first time, while we comprehensively characterized the neuronal entrainment across prefrontal layers and subregions. These results highlight the extent and significance of this modulation, given the crucial role of the interaction between these structures for emotional processing and regulation. We further report the reafferent OB origin of local gamma dynamics and their modulation by breathing, as well as the relation between local gamma oscillations and neuronal activity in all structures. This sheds new light onto the origin and role of prefrontal (Sirota et al., 2008; Stujenske et al., 2014; Zhong et al., 2017), BLA (Courtin et al., 2014a), and NAc (Carmichael et al., 2017) gamma oscillations, that might provide a temporally-optimized privileged route for olfactory reafferent input to affect the ongoing activity, in agreement with recent reports in humans (Zelano et al., 2016).

Using a pharmacological olfactory de-afferentiation approach, paired with large-scale recordings, we identified that although cortical LFP signatures of respiration and gamma are mediated by bulbar inputs in the form of a ROR, the bulk entrainment of limbic neuronal activity by breathing is mediated by an intracerebral RCD originating in the brainstem rhythm generators and being unaffected by olfactory de-afferentiation. We suggest that this joint modulation of limbic circuits by respiration is analogous to the predictive signaling employed in a wide range of neural circuits (Crapse and Sommer, 2008), such as those underlying sensory-motor coordination (Straka et al., 2018). Although the pathway of RCD remains unknown, we speculate that ascending long-range somatostatin-expressing interneuron projections from the preBötzinger complex to the thalamus, hypothalamus and basal forebrain (Yang and Feldman, 2018) or the locus coeruleus (Yackle et al., 2017) are probable pathways for this widespread modulation. The global and powerful nature of the RCD calls for future tracing and activity-dependent labeling studies to identify its anatomical substrate. A disinhibition-mediated mechanism of RCD would be consistent with the lack of prominent LFP sources in the absence of ROR, similar to the mechanism of disinhibitory pacing by the medial septum of the entorhinal-hippocampal system during theta oscillations (Buzsaki, 2002). We predict that the functional role of RCD in coordinating activity across the limbic system during offline states extends to other brain structures and brain states. The global outreach of RCD to higher order areas suggests that it might play an important role in the coordination of multi-sensory processing, in sync with orofacial motor output during both passive and active orofacial sampling, thus providing a centrifugal component synchronized with reafferent sensory inputs and respiratory efference copies to orofacial motor centers (Moore et al., 2013).

We provide causal evidence that fear-related 4Hz oscillations (Karalis et al., 2016; Dejean et al., 2016) are a state-specific expression of the limbic respiratory entrainment and originate from the reafferent respiratory entrainment of olfactory sensory neurons by passive airflow (Grosmaitre et al., 2007). Importantly, although prefrontal 4Hz LFP oscillations originate in fear-associated enhanced breathing, the ROR is not necessary for the expression of innate or conditioned fear behavior, in agreement with a recent report (Moberly et al., 2018). This suggests the potential sufficiency of RCD for the behavioral expression. Interestingly, the optogenetic induction of such oscillations is sufficient to drive fear behavior in naïve animals (Karalis et al., 2016), raising the possibility that this effect is mediated by the bidirectional interaction of prefrontal networks with the RCD via top-down projections to PAG. This sets the stage for future investigations of the interaction between the RCD and ROR in limbic networks and in turn the top-down modulation of breathing and emotional responses.

We extend previous work on the hippocampal entrainment (Yanovsky et al., 2014; Nguyen Chi et al., 2016; Lockmann et al., 2016) and provide new evidence for the mechanistic underpinnings of CA1 and DG modulation, by means of joint RCD and ROR inputs. We demonstrate robust modulation of hippocampal ripple occurrence by breathing, in agreement with a previous report (Liu et al., 2017), and its effect on the response of prefrontal (Siapas and Wilson, 1998; Jadhav et al., 2016) and accumbens neurons (Pennartz, 2004) to SWR. Importantly, we provide the first evidence for the role of this global limbic circuit modulation by the respiratory rhythm in coordinating

the interaction between the hippocampus and the downstream structures (i.e. mPFC and NAc), thought to underlie memory consolidation (Buzsaki, 1989; Squire and Alvarez, 1995).

Our results suggest that the respiratory rhythm orchestrates the hippocampo-cortical dialogue, by jointly biasing the neuronal firing and temporally coupling network dynamics across regions. We report for the first time the modulation of prefrontal UP and DOWN states as well as dentate spikes by breathing, which suggests a novel potential mechanism for the large-scale entrainment of thalamocortical excitability during sleep (Headley et al., 2017). Along these lines, an OB-mediated pacing of slow oscillations in olfactory cortices has been demonstrated in the past (Fontanini et al., 2003). Importantly, prefrontal SO entrainment appears to be dominated by the intracerebral RCD, while still receiving synchronous olfactory inputs via the ROR pathway. This highlights olfaction as a royal path to the sleeping brain that via synchronous ROR input reaches the limbic system in sync with RCD-coordinated UP-DOWN state dynamics during slow-wave sleep and could explain the efficacy of manipulations that bias learning (Arzi et al., 2012), consolidation (Rasch et al., 2007) or sleep depth (Perl et al., 2016) using odor presentation during sleep. The intrinsic RCD-mediated comodulation of both SWR and SO by the respiratory phase brings into perspective the mechanistic explanation of studies that improve consolidation using stimulation conditioned on the ongoing phase of the cortical SO (Ngo et al., 2013; Maingret et al., 2016; Latchoumane et al., 2017). Understanding the causal role of respiratory entrainment in the formation, consolidation, and retrieval of memories will require fine time scale closed-loop optogenetic perturbation.

While a causal model of the role of respiration in temporally coordinating hippocampal ripples, dentate spikes, entorhinal cortex inputs, and prefrontal UP and DOWN states remains to be elucidated, their temporal progression and phase relationship with the ongoing respiratory cycle hints to a possible mechanism. ROR-driven gamma-associated waves and RCD lead to differential recruitment of the entorhinal cortex, consistent with the sinks in the dentate molecular layer and the entrainment of dentate spikes. Depending on the strength of the inputs, either feed-forward inhibition of the CA3 (Acsády et al., 1998) or excitation during UP states (Isomura et al., 2006) can suppress or promote respectively SWRs. In parallel, the ripple-driven recruitment of prefrontal neurons likely triggers the resetting of the ongoing UP states by tilting the bias between excitation and inhibition (Shu et al., 2003) and results in a feedback re-entrance to the entorhinal-hippocampal network (Isomura et al., 2006). Further analysis of the SO dynamics across the cortical mantle and their relationship with hippocampal ripples, as well as causal manipulation of the two nonlinear dynamics is required to validate and elucidate the physiological details of this model.

While we show here that the respiratory dynamics bias the prefrontal SO via ROR and RCD, slow oscillations can emerge in isolated cortical slubs (Timofeev et al., 2000a) or slices (Sanchez-Vives and McCormick, 2000). Furthermore, from a mechanistic perspective, the generative mechanism of the two oscillations is potentially comparable. Leading models of the generation of neocortical UP states from DOWN states (Chauvette et al., 2010) or inspiratory bursts from expiratory silence in preBötzinger circuits (Del Negro et al., 2018) suggest that both phenomena

rely on regenerative avalanches due to recurrent connectivity, that are followed by activity-dependent disfacilitation. Given that neocortical slow oscillations can be locally generated (Sirota and Buzsaki, 2005; Vyazovskiy et al., 2011), are globally synchronized by the thalamic input (Lemieux et al., 2015) and propagate across the neocortex (Massimini et al., 2004; Isomura et al., 2006), ROR and RCD biasing of the cortical SO could be considered as an extension of a global system of mutually-coupled nonlinear oscillators. The persistent synchronous output of the respiratory oscillator and its marginal independence of the descending input might provide a widespread asymmetric bias to the slow oscillatory dynamics in the cortical circuits and SWR complexes in the hippocampus across offline states of different depth. It is likely, however, that via descending cortical projections, cortical SO provides feedback to the pontine respiratory rhythm-generating centers (e.g. via mPFC projections to PAG) and thus the interaction between respiratory dynamics and slow oscillations could be bidirectional.

This perpetual limbic rate comodulation by respiration also suggests a potential framework for memory-consolidation processes that do not rely on deep sleep and the associated synchronous K-complexes. This could explain the mechanism and distinctive role of awake replay in memory consolidation (Carr et al., 2011; Jadhav et al., 2012). Given the substantial cross-species differences in respiratory frequency, as well as the effects of sleep depth and recent experience on cortical and hippocampal dynamics, it is conceivable that more synchronized and generalized UP states or awake vs. sleep ripples are differentially modulated by breathing. Further work is required to investigate the role of these parameters on the respiratory biasing of network dynamics and its role in memory consolidation.

Finally, in light of the wide modulation of limbic circuits by breathing during quiescence, we suggest that breathing effectively modulates the default mode network (DMN). To examine this hypothesis future work will be needed to carefully examine the fine temporal structure of neuronal assemblies and their modulation by the RCD and ROR copies of the breathing rhythm throughout cortical and subcortical structures, an endeavor that might uncover functional sub-networks of the DMN.

5.2 BREATHING

In parallel with the cardinal neuronal oscillations described in the introduction, all physiological systems including the mammalian body are characterized by many rhythmic patterns of activity in a wide temporal and spatial scale and with varying degrees of coordination (Holst, 1939). From the cellular and enzymatic level (Walter, 1966) to the circadian rhythms, biological systems exhibit non-linear properties and are often organized far from the thermodynamic equilibrium, giving rise to oscillatory dynamics. The cardiovascular system is exhibiting a host of oscillations, including vascular movements, blood pressure, and heart rate, while the rhythmic patterns of activity of motoneurons are supporting motor patterns and movement supporting different functions, from locomotion to feeding (Marder and Calabrese, 1996).

Among these oscillations, breathing provides the most critical function of an aerobic organism and it comprises the most fundamental and ubiquitous rhythmic activity in life. Respiration is

omnipresent throughout the life and plays a physiological role in homeostasis, delivering oxygen, removing excess carbon dioxide and regulating the extracellular pH. Interestingly, the respiratory system overlaps to a large extent with the olfactory system, that is charged with the sensing of environmental odors.

5.2.1 *Neuronal control of breathing rhythms*

Over the years, it has been established that rhythmically firing heterogeneous populations of the Bötzinger (BötC) and preBötzinger complex (preBötC) in the ventrolateral medulla are the predominant mammalian respiratory pacemakers (Tan et al., 2008; Alsahafi et al., 2015), under the homeostatic control of pulmonary mechanoreceptors and O_2 and CO_2 chemoreceptors (Gonzalez et al., 1994; Hu et al., 2007) and the autonomic nervous system (Chang et al., 2015). The breathing cycle controls the air flow and can be separated into three phases, organized by distinct neuronal cell types: inspiration, post-inspiration, and expiration. Intrinsically bursting glutamatergic cells rhythmically drive inspiratory motor output (Smith et al., 1991). In parallel, glycinergic and GABAergic interneurons provide phasic inspiratory inhibition to the BötC expiratory cells (Sherman et al., 2015), while cells of BötC provide post-inspiratory and expiratory inhibition to the inspiratory cells of preBötC. This creates a feedback loop that supports the rhythmically coordinated alternation between the different phases of breathing. Additionally, projections to orofacial oscillators in the ventral medulla coordinate whisking (Welker, 1964; Ranade et al., 2013; Moore et al., 2013), head-movements (Welker, 1964; Alves et al., 2016), licking (Travers et al., 1997) as well as eye movements (Rittweger and Pöpel, 1998; Rassler and Raabe, 2003), with the respiratory rhythm. The coordination of orofacial sensory inputs has been hypothesized to underlie the temporal binding of distinct sensory elements and their perceptual processing (Moore et al., 2014).

Breathing is under tight control by brain circuits. A unique feature of breathing is the ability to consciously and unconsciously control this function, overriding the default, automated rhythm. This ability serves the pacing of olfactory perception during exploration (Welker, 1964) and active sniffing (Welker, 1964; Mainland and Sobel, 2006; Kepecs et al., 2006), the execution of critical oropharyngeal tasks like chewing and swallowing (Matsuo and Palmer, 2015) as well as the information transfer by means of human speech (Barlow and Estep, 2006; Conrad and Schönle, 1979) and other forms of communication such as vocalization (Sirotin et al., 2014), crying (Magoun et al., 1937; Javorka et al., 1982) , and laughing (Fry and Rader, 1977; Sakuragi et al., 2002) that all rely on precisely timed apneas (Janczewski et al., 2013). Emotional (Boiten, 1998; Suess et al., 1980) and cognitive state (Vlemincx et al., 2011; Huijbers et al., 2014) influence the respiratory rate, while breathing and other bodily functions are modulated as a function of the survival needs of the animal. In the face of danger, fight-or-flight responses impose strict conditions on the coordinated control of many motor and physiologic functions, including respiration rate and depth as well as blood pressure and heart-rate. Fear responses, both innate (Hofer, 1970) and learned (Suess et al., 1980) and anxiety behaviors, including social defeat (Fokkema et al., 1986), result in changes of the respiratory rate in rodents and humans (Suess et al., 1980; Van Diest et al., 2009; Meuret et al., 2009). Interestingly, both behavioral and autonomic (cardiovascular)

conditioned responses depend on the amygdala (Kapp et al., 1979; Smith and DeVito, 1984; LeDoux et al., 1988). The medial and cortical amygdala receive inputs from the VNO via the AOB (Swanson and Petrovich, 1998), as well as from the OB (Canteras et al., 1995).

Respiration is coordinated with other bodily functions and aspects of the autonomic nervous system, potentially by means of central brain control. Blood pressure, under conditions, can be modulated in phase with the respiration (Fokkema et al., 1986) by means of intrathoracic pressure changes due to forced inhalation or exhalation, as is the case with the Valsalva maneuver. Further, heart rate and variability are modulated as a function of the respiratory rate and phase (Clynes, 1960; Sroufe, 1971). During the expiration phase, the parasympathetic system is engaged to reduce the heart frequency, an effect termed respiratory sinus arrhythmia. This source of this modulation is still debated, however, multiple mechanisms are involved, such as the atrial reflex, vagal baroreflex (deBoer et al., 1987), and central motoneuron control (Eckberg, 2003; Eckberg et al., 2016).

The periaqueductal gray (PAG) is a midbrain structure uniquely positioned to integrate high-order sensory and emotional inputs (Bandler and Shipley, 1994; Benarroch, 2012) and is able to modulate bodily functions by means of descending projections to the medulla. The PAG innervates premotor interneurons capable of modulating motor output including respiration (Han et al., 2017; Subramanian et al., 2008) vocalization via laryngeal motoneurons (Kanai and Wang, 1962; Yajima and Hayashi, 1983; Zhang et al., 1994), freezing (Tovote et al., 2016), fight-or-flight responses (Wada et al., 1970; Bandler, 1982), respiration (Huang et al., 2000; Hayward et al., 2003; Subramanian et al., 2008) and cardiovascular control (Huang et al., 2000; Bandler et al., 2000).

The PAG consists of 4 columnar subdivisions that encapsulate the aqueduct, namely the ventrolateral, lateral, dorsolateral and dorsomedial PAG. The lateral and dorsolateral PAG is involved in active coping in the face of danger, such as confrontation and escape responses (Bandler and Carrive, 1988), whereas the ventrolateral PAG (vlPAG) mediates freezing behavior (Tovote et al., 2016; Franklin et al., 2017). Interestingly, the different subdivisions of PAG have distinct modulatory effects on respiratory patterns, suggesting a mechanism that guarantees the appropriate supply of air for the transient metabolic demands.

5.2.2 *Breathing and olfactory input*

The breathing cycle modulates the flow of oxygenated air to the lungs as well as the perception of odors (Adrian, 1942). During inhalation the air enters the nose and passes through the main olfactory neuroepithelium (MOE), a thin layer of neuronal cells (olfactory sensory neurons - OSNs), lining the turbinate walls of the nasal cavity (Chamanza and Wright, 2015) and expressing a single odorant receptor type on their dendritic trees, out of more than a thousand functionally distinct classes (Buck and Axel, 1991). Most mammals, but not teleost fish and higher primates, have two complimentary olfactory systems, the vomeronasal organ (VNO) and the Grüneberg Ganglion (GG), serving to detect chemical signals, volatile odors, and pheromones. Odors bind to multiple of these receptors (Malnic et al., 1999) and initiate an intracellular cyclic adenosine monophosphate (cAMP) cascade (Ma et al., 1999), that leads to the depolarization and action

potential firing of the OSNs (Buck and Axel, 1991; Duchamp-Viret et al., 1999). These cells project to the olfactory bulb (OB) in a topographic manner (Vassar et al., 1994), where the odorant information converge and enable odor perception and representation (Ressler et al., 1994; Spors et al., 2006; Shusterman et al., 2011).

Interestingly, approximately half of the neurons of the olfactory epithelium and of the septal organ exhibit mechanical sensitivity and respond to the mechanical stimulation induced by the air flow in the nose (Grosmaitre et al., 2007). Although a single cell cannot follow stimulation frequencies higher than 0.5Hz, the population of OSNs is able to reliably transmit the rhythmic mechanical stimulation of air flow to the OB, where it paces the spontaneous activity of cells and the rhythmic components of local field potentials that are coupled with respiration even in the absence of odors (Adrian, 1951; Walsh, 1956; Hobson, 1967; Macrides and Chorover, 1972; Chaput and Holley, 1979; Cury and Uchida, 2010).

Sniffing is the voluntary modulation of regular breathing. Consistent evidence highlights the qualitative distinction between odor-free respiration and odor-related, high-frequency sniffing (Bhalla and Bower, 1997; Kay and Laurent, 1999; Pager, 1985), identifying a loss of synchrony between respiratory pacemakers and respiratory movements (Pont, 1987). This is supported by evidence that sniffing can also be modulated in a reflexive, non-voluntary, fashion (Los Cobos Pallares et al., 2016). This is achieved by the projections of the trigeminal system, that innervates the nasal mucosa and is co-activated by most odors (Beidler and Tucker, 1955) to the caudal brainstem (Anton and Peppel, 1991). During sniffing, OB LFPs follow in frequency the respiration (Courtiol et al., 2011; Rojas-Líbano et al., 2014) although a breakdown in the coordination between respiratory cycle and OSN inputs to the OB is observed (Carey et al., 2009), that comes to odds with the understanding that the encoding of odor information is supported by the respiratory-phase specific activity. This suggests a flexible and multimodal encoding of olfactory information that changes as a function of the active or passive sampling of the environment. Interestingly, odor presence activates distinct regions compared to active sniffing, suggesting a distinct functional organization of the two systems (Sobel et al., 1998).

The evidence that OB receives airflow information (Ueki and Domino, 1961; Grosmaitre et al., 2007) and that the firing of OB neurons is phase locked to the nasal airflow, even when decoupled from internal rhythm generators (Macrides and Chorover, 1972; Onoda and Mori, 1980; Sobel and Tank, 1993; Cang and Isaacson, 2003) suggest that this re-afferent signal is serving as a reference of the internally generated respiratory patterns (Kleinfeld et al., 2014), a mode of operation that is observed in many aspects of the nervous and peripheral system (Holst and Mittelstaedt, 1950). It is unknown so-far whether a separate efferent copy of the respiratory signal is distributed to the OB or other cortices, although the possibility of a centrifugal respiratory modulation (Ravel et al., 1987; Ravel and Pager, 1990) or locally generated oscillatory activity (Hayar et al., 2004) cannot be excluded.

The olfactory processing in the brain likely takes place in multiple feedback loops across the olfactory cortices. The respiratory re-afferent signal is reaching further via the lateral olfactory tract (LOT) to the olfactory cortices (Freeman, 1959; Freeman, 1968), comprising the anterior

and posterior piriform cortex (Price and Powell, 1970) and anterior olfactory nucleus. Olfactory cortex neurons are exhibiting olfactory responses (Litaudon et al., 2003) and are modulated by the respiratory rhythm (Fontanini et al., 2003; Fontanini and Bower, 2005; Rennaker et al., 2007; Poo and Isaacson, 2009; Buonviso et al., 2006), while pyramidal cells send axon collaterals back to the OB forming a feedback loop in the olfactory system (Luskin and Price, 1983b; Johnson et al., 2000). The piriform cortex receives diffuse, non-topographic, input from the OB (Miyamichi et al., 2011; Ghosh et al., 2011; Sosulski et al., 2011) and in turn projects widely to olfactory and limbic structures, including the anterior olfactory nucleus, olfactory tubercle, perirhinal cortex, amygdala, lateral entorhinal cortex, nucleus accumbens and striatum as well as the mediodorsal thalamus and ventral medial prefrontal cortex (Johnson et al., 2000; Luskin and Price, 1983b; Price and Slotnick, 1983; Haberly and Price, 1978; Schwabe et al., 2004; Diodato et al., 2016).

5.2.3 *Respiratory entrainment of brain structures*

OB is characterized by respiration-related "olfactory theta" oscillations. Sensory de-afferentiation, by means of tracheotomy, naris occlusion or olfactory nerve lesion abolishes OB theta (Gault and Leaton, 1963; Gray and Skinner, 1988; Courtiol et al., 2011). A prominent oscillatory pattern of the OB is high-frequency gamma oscillations (40-80Hz) (Adrian, 1950). They are known to be generated by inhibitory feedback dendro-dendritic loops between granule and mitral cells (Rall and Shepherd, 1968; Freeman and Nicholson, 1975) and are believed to be involved in olfactory encoding (Laurent and Davidowitz, 1994; Kay et al., 2009). In alternation with gamma oscillations, slower beta oscillations occur in the OB (Robert Heale and Vanderwolf, 1994; Kay and Freeman, 1998). These oscillations can be induced by odors; however, they also spontaneously occur during baseline respiration. Beta oscillations depend critically on centrifugal inputs to the OB (Neville, 2003) and are generated by reciprocal interactions between the OB and the piriform cortex (Gray and Skinner, 1988; Neville, 2003; Martin et al., 2006). Gamma oscillations occur during the transition between inhalation and exhalation, while beta oscillations span the breathing phases (Buonviso et al., 2003). Odor-evoked beta and gamma oscillations are synchronized between the OB and the piriform cortex by means of information transfer via the LOT (Neville, 2003). Odor presence as well as associative reward learning modifies the spiking of OB neurons in relation to the respiratory rhythm during odor sampling but not during baseline breathing (Cenier et al., 2009). This suggests a complex interaction between the centrifugal inputs to the OB and the sensory information reaching the OB from the OSN.

Sparse evidence about respiratory modulation of non-olfactory structures exists in the literature (Zhang et al., 1986; Frysinger and Harper, 1989), however, these interactions have not been systematically studied until recently. A relation between hippocampal theta and whisking frequency has long been posited due to the similar frequency of the two oscillations (Komisaruk, 1970). Although in baseline conditions the two oscillations are not phase locked, suggesting independent generators (Berg et al., 2006), recent evidence suggests that a transient synchronization occurs during a whisking-based texture discrimination task (Grion et al., 2016) and odor discrimination (Gourevitch et al., 2010). Similarly, the relation between sniffing and limbic theta oscillations has been hypothesized and investigated since the first observations of theta

oscillations (Macrides, 1975; Macrides et al., 1982). Further, olfactory responses in the dentate gyrus have been well-established over the years (Vanderwolf, 1992, 2001; Heale et al., 1994; Habets et al., 1980).

A major input of the lateral entorhinal cortex (LEC) consists of the afferent fibers from the olfactory bulb and piriform cortex (Kerr et al., 2007; Biella and Curtis, 2000). LEC exhibits olfactory responses that are accompanied by fast oscillatory activity (Boeijinga and Lopes da Silva, 1988; Eeckman and Freeman, 1990; Uva and De Curtis, 2005). Given the inputs to the LEC from the hippocampus and the amygdala, which also receives olfactory inputs (Sosulski et al., 2011), a further processing and integration takes place and information is being transmitted back to both the olfactory bulb and the piriform cortex through direct projections to these structures from the LEC (Kay and Freeman, 1998; Chapuis et al., 2013).

Olfactory related responses (Hudry et al., 2001) and oscillations (Jung et al., 2006) have been identified in the human amygdala while notably, the phase of the respiration was recently reported to modulate amygdala oscillations and olfactory cortex beta oscillations as well as fear discrimination in humans (Zelano et al., 2016). Neuronal entrainment of the amygdala has been identified in both cats and humans (Zhang et al., 1986; Frysinger and Harper, 1989). Interestingly, stimulation of the amygdala changes respiratory patterns (Dlouhy et al., 2015; Applegate et al., 1983; Anand and Dua, 1956; Harper et al., 1984) Over the years, mounting evidence have suggested that breathing can entrain frog (Hobson, 1967) and human EEG (Busek and Kemlink, 2005; Yuan et al., 2013b), as well as LFP and spiking activity in the hedgehog OB and cortex (Adrian, 1942), rodent OB (Macrides and Chorover, 1972; Fukunaga et al., 2014; Phillips et al., 2012; Grosmaitre et al., 2007), cortex (Kay and Freeman, 1998; Fontanini et al., 2003; Ito et al., 2014; Biskamp et al., 2017; Zhong et al., 2017) and the hippocampus in cats (Poe et al., 1996), rodents (Vanderwolf, 1992; Yanovsky et al., 2014; Nguyen Chi et al., 2016; Lockmann et al., 2016; Liu et al., 2017) and humans (Zelano et al., 2016; Herrero et al., 2018). It is important to note that most of the studies performed so far on the relation of respiration to hippocampal or cortical circuits have been performed under various anesthetic regimes. Although urethane anesthesia has been proposed as a model of natural sleep due to the spontaneous state changes, anesthesia decreases local field potential power and changes both LFP and respiration frequency as well as the intrinsic network dynamics. Furthermore, the role of higher-cortical and memory-related areas such as the prefrontal cortex and the hippocampus can only be studied in relation to the behavior and across different behavioral states. For these reasons, we opted for recording in the awake, freely-behaving mouse and across multiple behavioral states, in an attempt to sample from the wide spectrum of interactions between the prefrontal cortex, the hippocampus, and their respiratory coupling.

With this study, we contribute to the ongoing effort to understand the mechanism and role of the respiratory entrainment of brain circuits. Although most studies have focused on LFP oscillations from a single spot and small numbers of single-units, mPFC comprises multiple subregions with distinct anatomical and functional correlates (Hoover and Vertes, 2007). For this reason, we aimed to comprehensively characterize for the first time the three-dimensional

profile of LFP activity and neuronal entrainment of the mPFC and to quantify the distribution of breathing-related synaptic currents, using large-scale high-density silicon probe recordings from thousands of cells in all structures in freely-behaving and awake head-fixed mice.

Using these techniques, we expand the characterization of limbic respiratory entrainment to the NAc, BLA, and thalamus, and report the re-afferent olfactory origin of local gamma dynamics and their modulation by breathing, as well as the relation between local gamma oscillations and neuronal activity in all structures. This provides new light onto the origin and role of prefrontal (Sirota et al., 2008; Stujenske et al., 2014; Zhong et al., 2017), BLA (Courtin et al., 2014a), and NAc (Meer, 2009) gamma oscillations. Given the importance of the hippocampal-prefrontal and hippocampal – NAc interaction in health and disease, we employed simultaneous recordings to investigate the role of the joint modulation in supporting the functional connectivity of the limbic circuit.

We extend previous work on the hippocampal entrainment (Yanovsky et al., 2014; Nguyen Chi et al., 2016; Lockmann et al., 2016) and provide new evidence for the mechanistic underpinnings of CA1 and DG modulation, by means of olfactory inputs in slow and fast time-scales. In agreement with previous reports, we report the modulation of hippocampal ripple occurrence by breathing (Liu et al., 2017) and the response of prefrontal (Siapas and Wilson, 1998) and accumbens neurons (Pennartz, 2004). We further provide the first evidence for both the underlying mechanism and the role of this joint modulation by breathing in coordinating the interaction between the hippocampus and the downstream structures, thought to underlie memory consolidation (Buzsaki, 1989; Squire and Alvarez, 1995). Importantly, we report for the first time the modulation of ripples, UP states and dentate spikes by breathing, which suggests the potential novel mechanism for the larger scale entrainment of cortical excitability during sleep (Headley et al., 2017). Interestingly, during sleep, slow oscillations can be observed even in the trapezius and upper extremity muscles (Westgaard et al., 2002) which have been associated with the cortical SO. Potentially they are associated with the respiratory input, however, no apparent relationship with heart rate variability was observed (Westgaard et al., 2002). In the future, understanding the causal role of respiratory entrainment in the formation, consolidation, and retrieval of memories will require fine time scale closed-loop optogenetic perturbation.

5.2.4 *Mechanisms of entrainment*

Recently, a few studies reported the presence of breathing-related LFP oscillations in the cortex (Ito et al., 2014; Biskamp et al., 2017; Zhong et al., 2017). During sleep, sharp-waves in the olfactory cortex sharp-wave activity is associated with UP- and DOWN- states in the orbitofrontal cortex (Onisawa et al., 2017). These reports are in agreement with the results of our studies reporting oscillatory entrainment of the neocortex and specifically of the prefrontal cortex. However, the exact mechanism of this entrainment remains to be established. To a large extent, the oscillatory component of the prefrontal LFP that corresponds to the respiration is eliminated after pharmacological olfactory deafferentiation. This argues for the possibility of the respiratory entrainment of prefrontal circuits from the re-afferent signal of respiration, via direct projections from the OB and piriform cortex to the prefrontal cortex (Cinelli et al., 1987; Clugnet and Price,

1987; Price, 1985). However, the possibility of additional entrainment by an efferent copy from the respiratory centers remains open. A few possible routes for such efferent copy are outlined here and remain to be examined and verified.

An interesting possibility lies in the locus coeruleus (LC), a noradrenergic nucleus of the dorsomedial pons that is the primary source of norepinephrine (NA) to the neocortex. LC is known to be involved in the control of arousal (Foote et al., 1983) and the desynchronization of cortical EEG (Berridge and Foote, 1991; Dringenberg and Vanderwolf, 1997). LC has a vastly divergent efferent connectivity, whereas it receives limited inputs, predominantly from the rostral medulla (Aston-Jones et al., 1986). LC neurons are CO2 chemosensors (Pineda and Aghajanian, 1997; Oyamada et al., 1998; Coates et al., 1993) while their activity is modulated by respiration (Oyamada et al., 1998) via the projections of medullar nucleus paragigantocellularis (PGi) (Aston-Jones et al., 1986) and direct projections from preBötzinger complex (Yackle et al., 2017). LC projects robustly to distinct regions of the prefrontal cortex (Chandler et al., 2014) while interestingly the mPFC modulates LC activity via reciprocal projections to regions containing LC dendritic arbors (Jodoj et al., 1998). LC is not only modulated by respiration but it is known to exert a modulatory effect on medullar centers controlling respiration in response to hypercapnia (Carvalho et al., 2014). LC projects to the medial septum (Segal, 1976) which in turn projects widely, including simultaneously to the CA1 and the mPFC (Varela et al., 2014) and modulates oscillatory dynamics (Liljenstrom and Hasselmo, 1995). Interestingly, serotonergic and cholinergic neurons of the basal forebrain are modulated by the respiratory phase (Mason et al., 2007; Manns et al., 2003; Linster and Hasselmo, 2000; Tsanov et al., 2014).

In parallel, an alternative route that potentially supports the modulation of thalamus by breathing comprises the ascending inputs from the brainstem to the thalamus (Chen et al., 1992a; Chen et al., 1992b; Krout et al., 2002; Carstens et al., 1990). We further provide causal evidence that fear-related 4Hz oscillations (Karalis et al., 2016; Dejean et al., 2016) are a state-specific expression of the limbic respiratory entrainment and originate from the re-afferent respiratory entrainment of olfactory sensory neurons by passive airflow (Grosmaitre et al., 2007). Importantly, although prefrontal 4Hz oscillations originate in the breathing, and the optogenetic induction is sufficient to drive fear behavior in naïve animals (Karalis et al., 2016), the re-afferent olfactory input is not necessary for the expression of innate or conditioned fear behavior, as confirmed by an independent study using similar perturbation approach (Moberly et al., 2018). This suggests the potential importance of a separate efference copy of the breathing rhythm for the behavioral expression. Interestingly, prefrontal networks can exert control over autonomic circuits through direct and indirect pathways (Eden and Buijs, 2000). This works sets the stage the future investigation of the interaction between the efference and re-afferent respiratory copy in cortical networks and in turn the top-down modulation of breathing.

Interestingly, mPFC and ACC are involved in the top-down control of autonomic activity and visceral responses. ACC or mPFC lesion diminishes cardiovascular conditioned responses (Buchanan and Powell, 1982) and general autonomic responses (Damasio et al., 1990; Tranel and Damasio, 1994), an effect potentially mediated by intra-prefrontal circuits and the projections of

infralimbic cortex to the solitary nucleus (Van der Kooy and Sawchenko, 1982; Terreberry and Neafsey, 1987). Similarly, stimulation of mPFC elicits autonomic responses (Buchanan et al., 1985; Lofving, 1961; Hardy and Holmes, 1988; Hurley-Gius and Neafsey, 1986).

5.2.5 *Breathing and mental state*

Emotional behavior and emotional disorders are associated with a host of respiratory and general autonomic changes (Smith and DeVito, 1984). Respiratory disorders during sleep and wake have been involved in various bodily and mental disorders. Dyspnea has been related to anxiety disorders (Katon et al., 2004; Gold, 2011) and a subset of panic disorders (Biber and Alkin, 1999), chronic stress and functional somatic syndromes (Mayou and Farmer, 2002), while comorbidity with depression (Neuman et al., 2006) has been reported, however, the directionality of causation is not yet clear. More generally, the cognitive misinterpretation of ambiguous interoceptive cues is believed to underlie many types of anxiety and panic disorders (Beck, 1976; Reiss, 1991) such as in the catastrophic misinterpretation model of panic disorder (Clark, 1986; Austin and Richards, 2001).

In humans, mindfulness meditation and conscious control of breathing exercise powerful control over the mental state of the individual, while targeted interventions are employed in clinical setting to help relieve anxiety disorders. Mind-body techniques, such as mindfulness meditation and yoga have been practiced for millennia and are known to have a positive effect on the mental and bodily health of the practitioners (Chiesa and Serretti, 2010; Hilton et al., 2016). Additionally, meditation exerts powerful short and long-term impact on thought structure and perception, enabling the mental control of otherwise indomitable sensations such as chronic pain (Zeidan and Vago, 2016; Hilton et al., 2016). Although popular, the exact mechanisms that enable these effects on the mind have not been elaborated (Tang et al., 2015). A common aspect of such diverse techniques is the attention to and control of breathing. Typically, meditation results in low respiratory rates (Wielgosz et al., 2016), that is achieved either via the cognitive control of the breathing or through the recitation of mantras or prayers (Bernardi et al., 2001). Importantly, the slow modulation of respiration (e.g. in "Pranayama" breathing exercises) is already enough to affect cognition and perception (Busch et al., 2012; Jerath et al., 2006), even without the cognitive components of meditation. The mental focus on the respiration itself or the mantra that entrains the respiration potentially leads to synchronization of the activity of attention-related frontal cortical regions (Lutz et al., 2004; Street and Wt, 2006; Brefczynski-Lewis et al., 2007; Kerr et al., 2013) and the cardiovascular and cardiorespiratory rhythms (Kubota et al., 2001; Peng et al., 2004; Cysarz and Büssing, 2005; Ditto et al., 2006).

Thus, the study of the relationship between bodily and brain rhythms provides a unique opportunity to understand the oscillatory framework of brain function. In parallel, converging evidence suggests that the timing of heartbeat modulates neural responses and perceptual processing (Park et al., 2014; Garfinkel et al., 2014; Suzuki et al., 2013). The tight relationship between breathing and heart activity suggests a model of neuronal modulation by the joint timing of the heartbeat and respiratory phase.

5.2.6 *Subthreshold and infraslow oscillations*

In light of the wide modulation of limbic circuits by breathing during quiescence, we suggest that breathing effectively modulates the default mode network (DMN). To examine this hypothesis future work will be needed to characterize respiration-related activity throughout cortical and subcortical structures. In parallel, the fine temporal structure of neuronal assemblies across structures should be examined carefully, an endeavor that might uncover functional sub-networks of the DMN.

In the recent years, slow sub-threshold membrane oscillations with frequency 3-5Hz have been detected in multiple cortices and during many behaviors. A growing literature has identified distinct effects of the locomotor behavior to the cortical (Poulet and Petersen, 2008; Niell and Stryker, 2010; Erisken et al., 2014; Fu et al., 2014; Lee et al., 2014; Saleem et al., 2013) and thalamic circuits (Erisken et al., 2014; Polack et al., 2013). Although the main focus has been the gain modulation during the active locomotor state, such slow oscillations were identified during quiet wakefulness in the somatosensory cortex (Poulet and Petersen, 2008), while in the visual cortex (Polack et al., 2013; Bennett et al., 2013) they have been noted to decrease the gain of neurons (Einstein et al., 2017). Similar oscillations have been reported in the auditory cortex (Zhou et al., 2014; Schneider et al., 2014), and motor cortex (Zagha et al., 2015) with a similar effect on behavior. 3-Hz membrane oscillations were recently recorded from hippocampal CA2 cells (Matsumoto et al., 2016) *in vivo*, although such oscillations do not occur *in vitro*. This is suggestive a network dependent generation and relation to inputs from other structures, however, the generation mechanism and relation with the cortical membrane oscillations have not been established.

The effects of locomotion on behavior have begun to be understood as a function of neuromodulatory circuit activation and the corresponding release of neuromodulators such as acetylcholine (ACh) from the medial septum and basal forebrain (Pinto et al., 2013; Fu et al., 2014) and noradrenaline (NA) from the locus coeruleus (LC) (Polack et al., 2013). However, the nature and source of the sub-threshold oscillations remain unknown.

In light of the findings of our studies and the frequency overlap, we suggest that sub-threshold membrane oscillations observed in various cortices and hippocampal regions during quiet immobility are related to respiratory input. The exact pathways of this modulation, however, remain to be resolved.

Similarly, in human studies, neuronal activity fluctuations across the brain have been associated with physiologic breathing (McKay et al., 2003). Infraslow oscillations during sleep have been identified (Aladjalova, 1957; Mantini et al., 2007; Picchioni et al., 2011), the origin of which was not clear, however, their frequency is similar to that of the human resting respiratory rate which is suggestive of a relationship between the two. Although such fluctuations can be, to some extent, attributed to cerebral vasodilation due to changes in arterial CO_2 (Chang and Glover, 2009), the relation between respiration and neuronal activity can be observed at both BOLD fMRI and EEG signals (Yuan et al., 2013a; Zelano et al., 2016) and changes in broadband and frontal

δ-band oscillations at shorter timescales, as a function of the respiratory frequency and phase of respiration, have been reported (Busek and Kemlink, 2005).

5.3 CONCLUSION

In summary, the data provided here suggest that respiration provides a perennial stream of rhythmic input to the brain. In addition to its role as the *condicio sine qua* non for life, we provide evidence that breathing rhythm acts as a global pacemaker for the brain, providing a reference signal that enables the integration of exteroceptive and interoceptive inputs with the internally generated dynamics of the limbic brain during offline states. In this emergent model of respiratory entrainment of limbic circuits, this common reference acts in tandem with the direct anatomical links between brain regions to pace the flow of information.

BIBLIOGRAPHY

Abeles, M (1982). "Role of the cortical neuron: integrator or coincidence detector?" In: *Israel journal of medical sciences* 18.1, pp. 83–92.

Achermann, P and Borbély, A. A. (1997). "Low-frequency (< 1 Hz) oscillations in the human sleep electroencephalogram." In: *Neuroscience* 81.1, pp. 213–222.

Ackley, D. H., Hinton, G. E., and Sejnowski, T. J. (1985). "A learning algorithm for boltzmann machines." In: *Cognitive Science* 9.1, pp. 147–169.

Acsády, L, Kamondi, A, Sík, A, Freund, T, and Buzsáki, G. (1998). "GABAergic cells are the major postsynaptic targets of mossy fibers in the rat hippocampus." In: *Journal of Neuroscience* 18.9, pp. 3386–403.

Adhikari, A., Topiwala, M. A., and Gordon, J. A. (2010). "Synchronized Activity between the Ventral Hippocampus and the Medial Prefrontal Cortex during Anxiety." In: *Neuron* 65.2, pp. 257–269.

Adhikari, A., Topiwala, M. A., and Gordon, J. A. (2011). "Single units in the medial prefrontal cortex with anxiety-related firing patterns are preferentially influenced by ventral hippocampal activity." In: *Neuron* 71.5, pp. 898–910.

Adrian, E. D. (1926). "The impulses produced by sensory nerve endings: Part I." In: *Journal of Physiology* 61.1, pp. 49–72.

Adrian, E. D. (1942). "Olfactory reactions in the brain of the hedgehog." In: *The Journal of Physiology* 100.4, pp. 459–473.

Adrian, E. D. (1944). *Brain rhythms*.

Adrian, E. D. (1950). "The electrical activity of the mammalian olfactory bulb." In: *Electroencephalography and Clinical Neurophysiology* 2.1-4, pp. 377–388.

Adrian, E. D. (1951). "The role of air movement in olfactory stimulation." In: *Journal of Physiology* 114.1-2, 4–5p.

Adrian, E. D. and Zotterman, Y. (1926a). "The impulses produced by sensory nerve endings. II. The response of a single end-organ." In: *Journal of Physiology* 61.1, pp. 151–171.

Adrian, E. D. and Zotterman, Y. (1926b). "The impulses produced by sensory nerve endings: Part 3. Impulses set up by Touch and Pressure." In: *Journal of Physiology* 61.4, pp. 465–483.

Agarwal, G., Stevenson, I. H., Berényi, A., Mizuseki, K., Buzsáki, G., and Sommer, F. T. (2014). "Spatially distributed local fields in the hippocampus encode rat position." In: *Science (New York, N.Y.)* 344.6184, pp. 626–630.

Aggleton, J. P. (2000). *The Amygdala*. A Functional Analysis. Oxford University Press, USA.

Agren, T., Engman, J., Frick, A., Björkstrand, J., Larsson, E. M., Furmark, T., and Fredrikson, M. (2012). "Disruption of reconsolidation erases a fear memory trace in the human amygdala." In: *Science* 337.6101, pp. 1550–1552.

Akil, H, Brenner, S, Kandel, E, Kendler, K. S., King, M. C., Scolnick, E, Watson, J. D., and Zoghbi, H. Y. (2010). "The Future of Psychiatric Research: Genomes and Neural Circuits." In: *Science* 327.5973, pp. 1580–1581.

Aladjalova, N. A. (1957). "Infra-slow rhythmic oscillations of the steady potential of the cerebral cortex." In: *Nature* 179.4567, pp. 957–959.

Alonso, A. and García-Austt, E. (1987a). "Neuronal sources of theta rhythm in the entorhinal cortex of the rat - I. Laminar distribution of theta field potentials." In: *Experimental Brain Research* 67.3, pp. 493–501.

Alonso, A. and García-Austt, E. (1987b). "Neuronal sources of theta rhythm in the entorhinal cortex of the rat - II. Phase relations between unit discharges and theta field potentials." In: *Experimental Brain Research* 67.3, pp. 502–509.

Alonso, A. and Llinás, R. R. (1989). "Subthreshold Na+-dependent theta-like rhythmicity in stellate cells of entorhinal cortex layer II." In: *Nature* 342.6246, pp. 175–177.

Alsahafi, Z., Dickson, C. T., and Pagliardini, S. (2015). "Optogenetic excitation of preBötzinger complex neurons potently drives inspiratory activity in vivo." In: *The Journal of Physiology* 593.16, pp. 3673–3692.

Alvarez, R. P., Biggs, A., Chen, G., Pine, D. S., and Grillon, C. (2008). "Contextual Fear Conditioning in Humans: Cortical-Hippocampal and Amygdala Contributions." In: *Journal of Neuroscience* 28.24, pp. 6211–6219.

Alves, J. A., Boerner, B. C., and Laplagne, D. A. (2016). "Flexible Coupling of Respiration and Vocalizations with Locomotion and Head Movements in the Freely Behaving Rat." In: *Neural Plasticity* 2016.2, pp. 1–16.

Amzica, F and Steriade, M (1995). "Disconnection of intracortical synaptic linkages disrupts synchronization of a slow oscillation." In: *Journal of Neuroscience* 15.6, pp. 4658–77.

Amzica, F. and Steriade, M. M. (1997). "The K-complex: Its slow (<1-Hz) rhythmicity and relation to delta waves." In: *Neurology* 49.4, pp. 952–959.

Amzica, F and Steriade, M. M. (1998). "Cellular substrates and laminar profile of sleep K-complex." In: *Neuroscience* 82.3, pp. 671–686.

Amzica, F. and Steriade, M. (2000). "Neuronal and glial membrane potentials during sleep and paroxysmal oscillations in the neocortex." In: *Journal of Neuroscience* 20.17, pp. 6648–6665.

Anagnostaras, S. G. (2000). "Computer-Assisted Behavioral Assessment of Pavlovian Fear Conditioning in Mice." In: *Learning & Memory* 7.1, pp. 58–72.

Anagnostaras, S. G., Gale, G. D., and Fanselow, M. S. (2001). "Hippocampus and contextual fear conditioning: Recent controversies and advances." In: *Hippocampus* 11.1, pp. 8–17.

Anand, B. K. and Dua, S (1956). "Circulatory and respiratory changes induced by electrical stimulation of limbic system (visceral brain)." In: *Journal of neurophysiology* 19.5, pp. 393–400.

Andersen, P. and Andersson, S. A. (1968). *Physiological Basis of the Alpha Rhythm*. Plenum Publishing Corporation.

Anderson, M. I. and O'Mara, S. M. (2003). "Analysis of recordings of single-unit firing and population activity in the dorsal subiculum of unrestrained, freely moving rats." In: *Journal of neurophysiology* 90.2, pp. 655–665.

Anton, F and Peppel, P (1991). "Central projections of trigeminal primary afferents innervating the nasal mucosa: a horseradish peroxidase study in the rat." In: *Neuroscience* 41.2-3, pp. 617–628.

Applegate, C. D., Kapp, B. S., Underwood, M. D., and McNall, C. L. (1983). "Autonomic and somatomotor effects of amygdala central N. stimulation in awake rabbits." In: *Physiology and Behavior* 31.3, pp. 353–360.

Arnsten, A. F. (2015). *Stress weakens prefrontal networks: Molecular insults to higher cognition*.

Arroyo, S., Lesser, R. P., Gordon, B., Uematsu, S., Jackson, D., and Webber, R. (1993). "Functional significance of the mu rhythm of human cortex: an electrophysiologic study with subdural electrodes." In: *Electroencephalography and Clinical Neurophysiology* 87.3, pp. 76–87.

Arzi, A., Shedlesky, L., Ben-Shaul, M., Nasser, K., Oksenberg, A., Hairston, I. S., and Sobel, N. (2012). "Humans can learn new information during sleep." In: *Nature Neuroscience*.

Aserinsky, E and Kleitman, N (1953). "Regularly occurring periods of eye motility, and concomitant phenomena, during sleep." In: *Science* 118.3062, pp. 273–274.

Aston-Jones, G, Ennis, M, Pieribone, V. A., Nickell, W. T., and Shipley, M. T. (1986). "The brain nucleus locus coeruleus: restricted afferent control of a broad efferent network." In: *Science (New York, N.Y.)* 234.4777, pp. 734–7.

Atkinson, R. C. and Shiffrin, R. M. (1968). "Human Memory: A Proposed System and its Control Processes." In: *Psychology of Learning and Motivation - Advances in Research and Theory* 2.C, pp. 89–195.

Austin, D. W. and Richards, J. C. (2001). "The catastrophic misinterpretation model of panic disorder." In: *Behaviour research and therapy* 39.11, pp. 1277–1291.

Axmacher, N., Elger, C. E., and Fell, J. (2008). "Ripples in the medial temporal lobe are relevant for human memory consolidation." In: *Brain* 131.Pt 7, pp. 1806–1817.

Ball, G. J., Gloor, P., and Schaul, N. (1977). "The cortical electromicrophysiology of pathological delta waves in the electroencephalogram of cats." In: *Electroencephalography and Clinical Neurophysiology* 43.3, pp. 346–361.

Bandler, R (1982). "Induction of 'rage' following microinjections of glutamate into midbrain but not hypothalamus of cats." In: 30.2, pp. 183–188.

Bandler, R and Carrive, P (1988). "Integrated defence reaction elicited by excitatory amino acid microinjection in the midbrain periaqueductal grey region of the unrestrained cat." In: *Brain Research* 439.1-2, pp. 95–106.

Bandler, R and Shipley, M. T. (1994). "Columnar organization in the midbrain periaqueductal gray: modules for emotional expression?" In: *Trends in Neurosciences* 17.9, pp. 379–389.

Bandler, R., Keay, K. A., Floyd, N., and Price, J. (2000). "Central circuits mediating patterned autonomic activity during active vs. passive emotional coping." In: *Brain Research Bulletin* 53.1, pp. 95–104.

Barlow, S. M. and Estep, M. (2006). "Central pattern generation and the motor infrastructure for suck, respiration, and speech." In: *Journal of Communication Disorders* 39.5, pp. 366–380.

Barnes, D. C. and Wilson, D. A. (2014). "Slow-Wave Sleep-Imposed Replay Modulates Both Strength and Precision of Memory." In: *Journal of Neuroscience* 34.15, pp. 5134–5142.

Barnett, L. and Seth, A. K. (2014). "The MVGC multivariate Granger causality toolbox: a new approach to Granger-causal inference." In: *Journal of Neuroscience Methods* 223, pp. 50–68.

Bartho, P. (2004). "Characterization of neocortical principal cells and interneurons by network interactions and extracellular features." In: *Journal of Neurophysiology* 92.1, pp. 600–608.

Bartlett, F. C. (1932). "Remembering : A Study in Experimental and Social Psychology." In: *Cambridge, Social Psychology*, pp. 1–11.

Bassant, M. H. and Poindessous-Jazat, F. (2001). "Ventral tegmental nucleus of Gudden: A pontine hippocampal theta generator?" In: *Hippocampus* 11.6, pp. 809–813.

Bast, T., Zhang, W. N., and Feldon, J. (2003). *Dorsal hippocampus and classical fear conditioning to tone and context in rats: Effects of local NMDA-receptor blockade and stimulation*.

Battaglia, F. P., Sutherland, G. R., and McNaughton, B. L. (2004). "Hippocampal sharp wave bursts coincide with neocortical "up-state" transitions." In: *Learning & Memory* 11.6, pp. 697–704.

Bazhenov, M., Timofeev, I., Steriade, M., and Sejnowski, T. J. (2002). "Model of thalamocortical slow-wave sleep oscillations and transitions to activated States." In: *Journal of Neuroscience* 22.19, pp. 8691–8704.

Beck, A. T. (1976). *Cognitive therapy and the emotional disorders*. New York : International Universities Press.

Beckers, G. J. L. and Rattenborg, N. C. (2015). "An in depth view of avian sleep." In: *Neuroscience & Biobehavioral Reviews* 50, pp. 120–127.

Beckers, G. J. L., Meij, J. van der, Lesku, J. A., and Rattenborg, N. C. (2014). "Plumes of neuronal activity propagate in three dimensions through the nuclear avian brain." In: *BMC Biology* 12, p. 16.

Bédard, C., Kröger, H., and Destexhe, A. (2006a). "Does the 1/f frequency scaling of brain signals reflect self-organized critical states?" In: *Physical Review Letters* 97.11, p. 118102.

Bédard, C., Kröger, H., and Destexhe, A. (2006b). "Model of low-pass filtering of local field potentials in brain tissue." In: *Physical Review E - Statistical, Nonlinear, and Soft Matter Physics* 73.5, p. 51911.

Beidler, L. M. and Tucker, D (1955). "Response of nasal epithelium to odor stimulation." In: *Science* 122.3158, p. 76.

Bellesi, M., Riedner, B. A., Garcia-Molina, G. N., Cirelli, C., and Tononi, G. (2014). "Enhancement of sleep slow waves: underlying mechanisms and practical consequences." In: *Frontiers in systems neuroscience* 8, p. 208.

Beltramo, R., D'Urso, G., Dal Maschio, M., Farisello, P., Bovetti, S., Clovis, Y., Lassi, G., Tucci, V., De Pietri Tonelli, D., and Fellin, T. (2013). "Layer-specific excitatory circuits differentially control recurrent network dynamics in the neocortex." In: *Nature Neuroscience* 16.2, pp. 227–234.

Benarroch, E. E. (2012). *Periaqueductal gray: An interface for behavioral control*.

Benchenane, K., Peyrache, A., Khamassi, M., Tierney, P. L., Gioanni, Y., Battaglia, F. P., and Wiener, S. I. (2010). "Coherent Theta Oscillations and Reorganization of Spike Timing in the Hippocampal- Prefrontal Network upon Learning." In: *Neuron* 66.6, pp. 921–936.

Bendor, D. and Wilson, M. A. (2012). "Biasing the content of hippocampal replay during sleep." In: *Nature neuroscience* 15.10, pp. 1439–1444.

Bennett, C., Arroyo, S., and Hestrin, S. (2013). "Subthreshold mechanisms underlying state-dependent modulation of visual responses." In: *Neuron* 80.2, pp. 350–357.

Berg, R. W., Whitmer, D., and Kleinfeld, D. (2006). "Exploratory Whisking by Rat Is Not Phase Locked to the Hippocampal Theta Rhythm." In: *Journal of Neuroscience* 26.24, pp. 6518–6522.

Berger, H. (1929). "Über das Elektrenkephalogramm des Menschen." In: *Archiv für Psychiatrie und Nervenkrankheiten* 87.1, pp. 527–570.

Bergman, U, Ostergren, A, Gustafson, A.-L., and Brittebo, B (2002). "Differential effects of olfactory toxicants on olfactory regeneration." In: *Archives of toxicology* 76.2, pp. 104–112.

Berke, J. D., Okatan, M., Skurski, J., and Eichenbaum, H. B. (2004). "Oscillatory entrainment of striatal neurons in freely moving rats." In: *Neuron* 43.6, pp. 883–896.

Bernardi, L, Sleight, P, Bandinelli, G, Cencetti, S, Fattorini, L, Wdowczyc-Szulc, J, and Lagi, A (2001). "Effect of rosary prayer and yoga mantras on autonomic cardiovascular rhythms: comparative study." In: *BMJ (Clinical research ed.)* 323.7327, pp. 1446–1449.

Berridge, C. W. and Foote, S. L. (1991). "Effects of locus coeruleus activation on electroencephalographic activity in neocortex and hippocampus." In: *The Journal of Neuroscience* 11.10, pp. 3135–45.

Berry, S. and Thompson, R. (1978). "Prediction of learning rate from the hippocampal electroencephalogram." In: *Science* 200.4347, pp. 1298–1300.

Bhalla, U. S. and Bower, J. M. (1997). "Multiday recordings from olfactory bulb neurons in awake freely moving rats: spatially and temporally organized variability in odorant response properties." In: *Journal of computational neuroscience* 4.3, pp. 221–256.

Biber, B and Alkin, T (1999). "Panic disorder subtypes: differential responses to CO2 challenge." In: *The American journal of psychiatry* 156.5, pp. 739–744.

Biella, G and Curtis, M de (2000). "Olfactory inputs activate the medial entorhinal cortex via the hippocampus." In: *Journal of neurophysiology* 83, pp. 1924–1931.

Bilkey, D. K. and Heinemann, U. (1999). "Intrinsic theta-frequency membrane potential oscillations in layer III/V perirhinal cortex neurons of the rat." In: *Hippocampus* 9.5, pp. 510–518.

Binder, S., Berg, K., Gasca, F., Lafon, B., Parra, L. C., Born, J., and Marshall, L. (2014). "Transcranial slow oscillation stimulation during sleep enhances memory consolidation in rats." In: *Brain Stimulation* 7.4, pp. 508–515.

Bishop, C. M. (2006). *Pattern Recognition and Machine Learning*. Vol. 4. 4, p. 738.

Biskamp, J., Bartos, M., and Sauer, J. F. (2017). "Organization of prefrontal network activity by respiration-related oscillations." In: *Scientific Reports* 7, p. 45508.

Bissière, S., Plachta, N., Hoyer, D., McAllister, K. H., Olpe, H. R., Grace, A. A., and Cryan, J. F. (2008). "The Rostral Anterior Cingulate Cortex Modulates the Efficiency of Amygdala-Dependent Fear Learning." In: *Biological Psychiatry* 63.9, pp. 821–831.

Blake, H.; Gerard, R. W. (1937). "Brain potentials during sleep." In: *American Journal of Physiology* 119, pp. 692–703.

Blanchard, D. C. and Blanchard, R. J. (1972). "Innate and conditioned reactions to threat in rats with amygdaloid lesions." In: *Journal of Comparative and Physiological Psychology* 81.2, pp. 281–290.

Blanchard, R. J. and Blanchard, D. C. (1969). "Crouching as an index of fear." In: *Journal of Comparative and Physiological Psychology* 67.3, pp. 370–375.

Blanchard, R. J., Blanchard, D. C., Weiss, S. M., and Meyer, S. (1990). "The effects of ethanol and diazepam on reactions to predatory odors." In: *Pharmacology, Biochemistry and Behavior* 35.4, pp. 775–780.

Blanco-Hernández, E., Valle-Leija, P., Zomosa-Signoret, V., Drucker-Colín, R., and Vidaltamayo, R. (2012). "Odor memory stability after reinnervation of the olfactory bulb." In: *PLoS ONE* 7.10. Ed. by N. Ravel, e46338.

Bliss, T. V. P. and Lømo, T. (1973). "Long-lasting potentiation of synaptic transmission in the dentate area of the anaesthetized rabbit following stimulation of the perforant path." In: *Journal of Physiology* 232.2, pp. 331–356.

Bliss, T. V. and Gardner-Medwin, a. R. (1973). "Long-lasting potentiation of synaptic transmission in the dentate area of the unanaestetized rabbit following stimulation of the perforant path." In: *Journal of Physiology* 232.2, pp. 357–374.

Boeijinga, P. H. and Lopes da Silva, F. H. (1988). "Differential distribution of beta and theta EEG activity in the entorhinal cortex of the cat." In: *Brain research* 448.2, pp. 272–86.

Boiten, F. A. (1998). "The effects of emotional behaviour on components of the respiratory cycle." In: *Biological Psychology* 49.1-2, pp. 29–51.

Bolles, R. C. and Collier, A. C. (1976). "The effect of predictive cues on freezing in rats." In: 4.1, pp. 6–8.

Bolles, R. C., Holtz, R., Dunn, T., and Hill, W. (1980). "Comparisons of stimulus learning and response learning in a punishment situation." In: *Learning and Motivation* 11.1, pp. 78–96.

Borbély, A. A. and Achermann, P (1999). "Sleep homeostasis and models of sleep regulation." In: *Journal of biological rhythms* 14.6, pp. 557–568.

Both, M., Bähner, F., Halbach, O. von Bohlen und, and Draguhn, A. (2008). "Propagation of specific network patterns through the mouse hippocampus." In: *Hippocampus* 18.9, pp. 899–908.

Bouton, M. E. and Bolles, R. C. (1980). "Conditioned fear assessed by freezing and by the suppression of three different baselines." In:

Bragin, A, Jandó, G, Nádasdy, Z, Landeghem, M van, and Buzsaki, G. (1995). "Dentate EEG spikes and associated interneuronal population bursts in the hippocampal hilar region of the rat." In: *Journal of neurophysiology* 73.4, pp. 1691–705.

Bragin, a, Engel, J, Wilson, C. L., Fried, I, and Buzsaki, G. (1999). "High-frequency oscillations in human brain." In: *Hippocampus* 9.2, pp. 137–142.

Brazier, M. A. B. (1949). "The electrical fields at the surface of the head during sleep." In: *Electroencephalography and clinical neurophysiology* 1.2, pp. 195–204.

Brefczynski-Lewis, J. A., Lutz, A, Schaefer, H. S., Levinson, D. B., and Davidson, R. J. (2007). "Neural correlates of attentional expertise in long-term meditation practitioners." In: *Proceedings of the National Academy of Sciences* 104.27, pp. 11483–11488.

Bremer, F (1935). "Cerveau isole et physiologie du sommeil." In: *Soc Biol* 118, pp. 1235–1241.

Bressler, S. L. and Seth, A. K. (2011). "Wiener-Granger causality: a well established methodology." In: *NeuroImage* 58.2, pp. 323–329.

Brown, R. E., Basheer, R, McKenna, J. T., Strecker, R. E., and McCarley, R. W. (2012). "Control of Sleep and Wakefulness." In: *Physiological Reviews* 92.3, pp. 1087–1187.

Brown, R. M. and Robertson, E. M. (2007). "Inducing motor skill improvements with a declarative task." In: *Nature neuroscience* 10.2, pp. 148–149.

Brunel, N. and Wang, X.-J. (2003). "What Determines the Frequency of Fast Network Oscillations With Irregular Neural Discharges? I. Synaptic Dynamics and Excitation-Inhibition Balance." In: *Journal of Neurophysiology* 90.1, pp. 415–430.

Buchanan, S. L. and Powell, D. A. (1982). "Cingulate damage attenuates conditioned bradycardia." In: *Neuroscience Letters* 29.3, pp. 261–268.

Buchanan, S. L., Valentine, J., and Powell, D. (1985). "Autonomic responses are elicited by electrical stimulation of the medial but not lateral frontal cortex in rabbits." In: *Behavioural Brain Research* 18.1, pp. 51–62.

Buck, L. B. and Axel, R (1991). "A novel multigene family may encode odorant receptors: a molecular basis for odor recognition." In: *Cell* 65.1, pp. 175–187.

Bullock, T. H., Buzsaki, G., and McClune, M. C. (1990). "Coherence of compound field potentials reveals discontinuities in the CA1-subiculum of the hippocampus in freely-moving rats." In: *Neuroscience* 38.3, pp. 609–619.

Buonviso, N, Amat, C, and Litaudon, P (2006). "Respiratory modulation of olfactory neurons in the rodent brain." In: *Chemical Senses* 31.2, pp. 145–154.

Buonviso, N., Amat, C., Litaudon, P., Roux, S., Royet, J. P., Farget, V., and Sicard, G. (2003). "Rhythm sequence through the olfactory bulb layers during the time window of a respiratory cycle." In: *European Journal of Neuroscience* 17.9, pp. 1811–1819.

Burdach, K. F. (1822). *Vom Baue und Leben des Gehirns*.

Burgess, A. P. and Gruzelier, J. H. (1997). "Short duration synchronization of human theta rhythm during recognition memory." In: *NeuroReport* 8.4, pp. 1039–1042.

Burgos-Robles, A., Vidal-Gonzalez, I., and Quirk, G. J. (2009). "Sustained conditioned responses in prelimbic prefrontal neurons are correlated with fear expression and extinction failure." In: *The Journal of neuroscience : the official journal of the Society for Neuroscience* 29.26, pp. 8474–8482.

Busch, V., Magerl, W., Kern, U., Haas, J., Hajak, G., and Eichhammer, P. (2012). "The effect of deep and slow breathing on pain perception, autonomic activity, and mood processing–an experimental study." In: *Pain medicine (Malden, Mass.)* 13.2, pp. 215–228.

Busek, P and Kemlink, D (2005). "The influence of the respiratory cycle on the EEG." In: *Physiological research* 54.3, pp. 327–333.

Bushey, D., Tononi, G., and Cirelli, C. (2011). "Sleep and synaptic homeostasis: structural evidence in Drosophila." In: *Science* 332.6037, pp. 1576–1581.

Buzsáki, G and Buzsaki, G. (1998). "Memory consolidation during sleep: a neurophysiological perspective." In: *Journal of sleep research* 7 Suppl 1, pp. 17–23.

Buzsáki, G., Buhl, D. L., Harris, K. D., Csicsvari, J., Czéh, B., Morozov, A., Buzsaki, G., Buhl, D. L., Harris, K. D., Csicsvari, J., Czéh, B., and Morozov, A. (2003). "Hippocampal network patterns of activity in the mouse." In: *Neuroscience* 116.1, pp. 201–211.

Buzsaki, G. (1984). *Feed-forward inhibition in the hippocampal formation*.

Buzsaki, G. (1989). "Two-stage model of memory trace formation: a role for "noisy" brain states." In: *Neuroscience* 31.3, pp. 551–570.

Buzsaki, G. (1996). "The hippocampo-neocortical dialogue." In: *Cerebral Cortex* 6.2, pp. 81–92.

Buzsaki, G. (2002). "Theta oscillations in the hippocampus." In: *Neuron* 33.3, pp. 325–340.

Buzsáki, G. (2006). *Rhythms of the Brain*. Oxford University Press, pp. 1–464.

Buzsaki, G. (2010). "Neural syntax: cell assemblies, synapsembles, and readers." In: *Neuron* 68.3, pp. 362–385.

Buzsaki, G. (2015). "Hippocampal sharp wave-ripple: A cognitive biomarker for episodic memory and planning." In: *Hippocampus* 25.10. Ed. by H. B. Eichenbaum, pp. 1073–1188.

Buzsáki, G. and Buzsaki, G. (1986). "Hippocampal sharp waves: Their origin and significance." In: *Brain Research* 398.2, pp. 242–252.

Buzsaki, G. and Chrobak, J. J. (1995). "Temporal structure in spatially organized neuronal ensembles: a role for interneuronal networks." In: *Current Opinion in Neurobiology* 5.4, pp. 504–510.

Buzsáki, G. and Draguhn, A. (2004). "Neuronal olscillations in cortical networks." In: *Science* 304.5679, pp. 1926–1929.

Buzsaki, G. and Draguhn, A. (2004). "Neuronal oscillations in cortical networks." In: *Science* 304.5679, pp. 1926–1929.

Buzsaki, G. and Mizuseki, K. (2014). "The log-dynamic brain: How skewed distributions affect network operations." In: *Nature Reviews Neuroscience* 15.4, pp. 264–278.

Buzsaki, G. and Moser, E. I. (2013). "Memory, navigation and theta rhythm in the hippocampal-entorhinal system." In: *Nature Neuroscience* 16.2, pp. 130–138.

Buzsaki, G. and Schomburg, E. W. (2015). "What does gamma coherence tell us about inter-regional neural communication?" In: *Nature Neuroscience* 18.4, pp. 484–489.

Buzsaki, G., Lai-Wo S., L., and Vanderwolf, C. H. (1983). "Cellular bases of hippocampal EEG in the behaving rat." In: *Brain Research Reviews* 6.2, pp. 139–171.

Buzsáki, G., Silva, F. L. da, Buzsaki, G., and Silva, F. L. da (2012a). "High frequency oscillations in the intact brain." In: *Progress in Neurobiology* 98.3, pp. 241–249.

Buzsáki, G., Wang, X.-J., Buzsaki, G., Wang, X.-J., Buzsáki, G., and Wang, X.-J. (2012b). "Mechanisms of Gamma Oscillations." In: *Annual Review of Neuroscience* 35.1, pp. 203–225.

Buzsáki, G., Anastassiou, C. A., and Koch, C. (2012). "The origin of extracellular fields and currents — EEG, ECoG, LFP and spikes." In: *Nature reviews. Neuroscience* 13.6, pp. 407–420.

Cahn, B. R. and Polich, J. (2006). "Meditation states and traits: EEG, ERP, and neuroimaging studies." In: *Psychological Bulletin* 132.2, pp. 180–211.

Cang, J. and Isaacson, J. S. (2003). "In vivo whole-cell recording of odor-evoked synaptic transmission in the rat olfactory bulb." In: *The Journal of Neuroscience* 23.10, pp. 4108–16.

Canolty, R. T., Edwards, E., Dalal, S. S., Soltani, M., Nagarajan, S. S., Kirsch, H. E., Berger, M. S., Barbare, N. M., and Knight, R. T. (2006). "High gamma power is phase-locked to theta oscillations in human neocortex." In: *Science* 313.5793, pp. 1626–1628.

Canolty, R. T. and Knight, R. T. (2010). *The functional role of cross-frequency coupling*.

Canteras, N. S., Simerly, R. B., and Swanson, L. W. (1995). "Organization of projections from the medial nucleus of the amygdala: A PHAL study in the rat." In: *Journal of Comparative Neurology* 360.2, pp. 213–245.

Cantero, J. L., Atienza, M, Stickgold, R, Kahana, M. J., Madsen, J. R., and Kocsis, B (2003). "Sleep-dependent theta oscillations in the human hippocampus and neocortex." In: *Journal of Neuroscience* 23.34, pp. 10897–10903.

Capellini, I., Barton, R. A., McNamara, P., Preston, B. T., and Nunn, C. L. (2008). "Phylogenetic analysis of the ecology and evolution of mammalian sleep." In: *Evolution; international journal of organic evolution* 62.7, pp. 1764–1776.

Carey, R. M., Verhagen, J. V., Wesson, D. W., Pírez, N., and Wachowiak, M. (2009). "Temporal structure of receptor neuron input to the olfactory bulb imaged in behaving rats." In: *Journal of neurophysiology* 101.2, pp. 1073–1088.

Carlén, M., Meletis, K., Siegle, J. H., Cardin, J. A., Futai, K., Vierling-Claassen, D., Rühlmann, C., Jones, S. R., Deisseroth, K., Sheng, M., Moore, C. I., and Tsai, L. H. (2012). "A critical role for NMDA receptors in parvalbumin interneurons for gamma rhythm induction and behavior." In: *Molecular Psychiatry* 17.5, pp. 537–548.

Carmichael, J. E., Gmaz, J. M., and Meer, M. A. van der (2017). "Gamma Oscillations in the Rat Ventral Striatum Originate in the Piriform Cortex." In: *The Journal of Neuroscience* 37.33, pp. 7962–7974.

Carr, M. F., Jadhav, S. P., and Frank, L. M. (2011). "Hippocampal replay in the awake state: A potential substrate for memory consolidation and retrieval." In: *Nature Neuroscience* 14.2, pp. 147–153.

Carr, M. F., Karlsson, M. P., and Frank, L. M. (2012). "Transient slow gamma synchrony underlies hippocampal memory replay." In: *Neuron* 75.4, pp. 700–713.

Carrillo-Reid, L., Yang, W., Bando, Y., Peterka, D. S., and Yuste, R. (2016). "Imprinting and recalling cortical ensembles." In: *Science* 353.6300, pp. 691–694.

Carstens, E, Leah, J, Lechner, J, and Zimmermann, M (1990). "Demonstration of extensive brainstem projections to medial and lateral thalamus and hypothalamus in the rat." In: *Neuroscience* 35.3, pp. 609–26.

Carvalho, D. Ã. bora de, Patrone, L. G. A., Taxini, C. L., Biancardi, V., Vicente, M. C., and Gargaglioni, L. H. (2014). "Neurochemical and electrical modulation of the locus coeruleus: contribution to CO2drive to breathe." In: *Frontiers in physiology* 5.e14746, p. 445.

Cash, S. S. et al. (2009). "The human K-complex represents an isolated cortical down-state." In: *Science* 324.5930, pp. 1084–1087.

Cassell, M. D. and Wright, D. J. (1986). "Topography of projections from the medial prefrontal cortex to the amygdala in the rat." In: *Brain Research Bulletin* 17.3, pp. 321–333.

Caton, R (1875). "Electrical Currents of the Brain." In: *The Journal of Nervous and Mental Disease*.

Cenier, T., David, F., Litaudon, P., Garcia, S., Amat, C., and Buonviso, N. (2009). "Respiration-gated formation of gamma and beta neural assemblies in the mammalian olfactory bulb." In: *European Journal of Neuroscience* 29.5, pp. 921–930.

Chamanza, R and Wright, J. A. (2015). "A Review of the Comparative Anatomy, Histology, Physiology and Pathology of the Nasal Cavity of Rats, Mice, Dogs and Non-human Primates. Relevance to Inhalation Toxicology and Human Health Risk Assessment." In: *Journal of comparative pathology* 153.4, pp. 287–314.

Chandler, D. J., Gao, W.-J., and Waterhouse, B. D. (2014). "Heterogeneous organization of the locus coeruleus projections to prefrontal and motor cortices." In: *Proceedings of the National Academy of Sciences* 111.18, pp. 6816–6821.

Chang, C. and Glover, G. H. (2009). "Relationship between respiration, end-tidal CO2, and BOLD signals in resting-state fMRI." In: *NeuroImage* 47.4, pp. 1381–1393.

Chang, R. B., Strochlic, D. E., Williams, E. K., Umans, B. D., and Liberles, S. D. (2015). "Vagal Sensory Neuron Subtypes that Differentially Control Breathing." In: *Cell* 161.3, pp. 622–633.

Chapman, W. P., Schroeder, H. R., Geyer, G, Brazier, M. A. B., Fager, C, Poppen, J. L., Solomon, H. C., and Yakovlev, P. I. (1954). "Physiological Evidence Concerning Importance of the Amygdaloid Nuclear Region in the Integration of Circulatory Function and Emotion in Man." In: *Science* 120.3127, pp. 949–950.

Chapuis, J., Cohen, Y., He, X., Zhang, Z., Jin, S., Xu, F., and Wilson, D. A. (2013). "Lateral Entorhinal Modulation of Piriform Cortical Activity and Fine Odor Discrimination." In: *Journal of Neuroscience* 33.33, pp. 13449–13459.

Chaput, M and Holley, A (1979). "Spontaneous activity of olfactory bulb neurons in awake rabbits, with some observations on the effects of pentobarbital anaesthesia." In: *Journal de physiologie* 75.8, pp. 939–948.

Chauvette, S., Volgushev, M., and Timofeev, I. (2010). "Origin of active states in local neocortical networks during slow sleep oscillation." In: *Cerebral Cortex* 20.11, pp. 2660–2674.

Chauvette, S., Seigneur, J., and Timofeev, I. (2012). "Sleep Oscillations in the Thalamocortical System Induce Long-Term Neuronal Plasticity." In: *Neuron* 75.6, pp. 1105–1113.

Chen, J, Zeng, S. L., Rao, Z. R., and Shi, J. W. (1992a). "Serotonergic projections from the midbrain periaqueductal gray and nucleus raphe dorsalis to the nucleus parafascicularis of the thalamus." In: *Brain research* 584.1-2, pp. 294–8.

Chen, N., Sugihara, H., and Sur, M. (2015). "An acetylcholine-activated microcircuit drives temporal dynamics of cortical activity." In: *Nature neuroscience* 18.6, pp. 892–902.

Chen, Z, Eldridge, F. L., and Wagner, P. G. (1992b). "Respiratory-associated thalamic activity is related to level of respiratory drive." In: *Respiration physiology* 90.1, pp. 99–113.

Cheng, S. and Frank, L. M. (2008). "New Experiences Enhance Coordinated Neural Activity in the Hippocampus." In: *Neuron* 57.2, pp. 303–313.

Cheriyan, J., Kaushik, M. K., Ferreira, A. N., and Sheets, P. L. (2016). "Specific Targeting of the Basolateral Amygdala to Projectionally Defined Pyramidal Neurons in Prelimbic and Infralimbic Cortex." In: *eneuro* 3.2.

Chiesa, A. and Serretti, A. (2010). "A systematic review of neurobiological and clinical features of mindfulness meditations." In: *Psychological Medicine* 40.8, pp. 1239–1252.

Choi, G. B., Stettler, D. D., Kallman, B. R., and Bhaskar, S. T. (2011). "Driving opposing behaviors with ensembles of piriform neurons." In: *Cell*.

Chrobak, J. J. and Buzsaki, G. (1998). "Gamma oscillations in the entorhinal cortex of the freely behaving rat." In: *Journal of Neuroscience* 18.1, pp. 388–98.

Chung, J. E., Magland, J. F., Barnett, A. H., Felix, S. H., Frank, L. M., Greengard, L. F., Chung, J. E., Magland, J. F., Barnett, A. H., Tolosa, V. M., Tooker, A. C., and Lee, K. Y. (2017). "A fully automated approach to spike sorting." In: *Neuron* 95.6, 1381–1394.e6.

Cinelli, A. R., Ferreyra-Moyano, H., and Barragan, E. (1987). "Reciprocal functional connections of the olfactory bulbs and other olfactory related areas with the prefrontal cortex." In: *Brain Research Bulletin* 19.6, pp. 651–661.

Clark, D. M. (1986). "A cognitive approach to panic." In: *Behaviour research and therapy* 24.4, pp. 461–470.

Clugnet, C and Price, J. L. (1987). "Olfactory Input to the Prefrontal Cortex in the Rat." In: *Annals of the New York Academy of Sciences* 510.1, pp. 231–235.

Clynes, M (1960). "Computer analysis of reflex control and organization: respiratory sinus arrhythmia." In: *Science* 131.3396, pp. 300–302.

Coates, E. L., Li, A, and Nattie, E. E. (1993). "Widespread sites of brain stem ventilatory chemoreceptors." In: *Journal of applied physiology (Bethesda, Md. : 1985)* 75.1, pp. 5–14.

Cohen, N. J. and Squire, L. R. (1980). "Preserved learning and retention of pattern-analyzing skill in amnesia: dissociation of knowing how and knowing that." In: *Science* 210.4466, pp. 207–210.

Cole, S. R. and Voytek, B. (2017). "Brain Oscillations and the Importance of Waveform Shape." In: *Trends in Cognitive Sciences* 21.2, pp. 137–149.

Colgin, L. L. and Moser, E. I. (2010). "Gamma Oscillations in the Hippocampus." In: *Physiology* 25.5, pp. 319–329.

Collins, D. R., Lang, E. J., and Paré, D. (1999). "Spontaneous activity of the perirhinal cortex in behaving cats." In: *Neuroscience* 89.4, pp. 1025–1039.

Colom, L. V., Christie, B. R., and Bland, B. H. (1988). "Cingulate cell discharge patterns related to hippocampal EEG and their modulation by muscarinic and nicotinic agents." In: *Brain Research* 460.2, pp. 329–338.

Conrad, B. and Schönle, P. (1979). "Speech and respiration." In: *Archiv für Psychiatrie und Nervenkrankheiten* 226.4, pp. 251–268.

Constantinople, C. M. and Bruno, R. M. (2011). "Effects and Mechanisms of Wakefulness on Local Cortical Networks." In: *Neuron* 69.6, pp. 1061–1068.

Contreras, D and Steriade, M (1995). "Cellular basis of EEG slow rhythms: a study of dynamic corticothalamic relationships." In: *Journal of Neuroscience* 15.1 Pt 2, pp. 604–622.

Contreras, D. and Steriade, M. M. (1996). "Synchronization of low-frequency rhythms in corticothalamic networks." In: *Neuroscience* 76.1, pp. 11–24.

Conway, B. A., Halliday, D. M., Farmer, S. F., Shahani, U, Maas, P, Weir, A. I., and Rosenberg, J. R. (1995). "Synchronization between motor cortex and spinal motoneuronal pool during the performance of a maintained motor task in man." In: *Journal of Physiology* 489 (Pt 3, pp. 917–924.

Corcoran, K. A. and Quirk, G. J. (2007). "Activity in Prelimbic Cortex Is Necessary for the Expression of Learned, But Not Innate, Fears." In: 27.4, pp. 840–844.

Cortes, C. and Vapnik, V. (1995). "Support-Vector Networks." In: *Machine Learning* 20.3, pp. 273–297.

Cossart, R., Aronov, D., and Yuste, R. (2003). "Attractor dynamics of network UP states in the neocortex." In: *Nature* 423.6937, pp. 283–288.

Courtin, J., Karalis, N., Gonzalez-Campo, C., Wurtz, H., and Herry, C. (2014a). "Persistence of amygdala gamma oscillations during extinction learning predicts spontaneous fear recovery." In: *Neurobiology of Learning and Memory* 113, pp. 82–89.

Courtin, J., Chaudun, F., Rozeske, R. R., Karalis, N., Gonzalez-Campo, C., Wurtz, H., Abdi, A., Baufreton, J., Bienvenu, T. C. M., and Herry, C. (2014b). "Prefrontal parvalbumin interneurons shape neuronal activity to drive fear expression." In: *Nature* 505.7481, pp. 92–96.

Courtiol, E, Hegoburu, C, Litaudon, P, Garcia, S, Fourcaud-Trocme, N, and Buonviso, N (2011). "Individual and synergistic effects of sniffing frequency and flow rate on olfactory bulb activity." In: *Journal of Neurophysiology* 106.6, pp. 2813–2824.

Cousins, J. N., El-Deredy, W., Parkes, L. M., Hennies, N., and Lewis, P. A. (2014). "Cued memory reactivation during slow-wave sleep promotes explicit knowledge of a motor sequence." In: *The Journal of neuroscience : the official journal of the Society for Neuroscience* 34.48, pp. 15870–15876.

Cowan, R. L. and Wilson, C. J. (1994). "Spontaneous firing patterns and axonal projections of single corticostriatal neurons in the rat medial agranular cortex." In: *Journal of neurophysiology* 71.1, pp. 17–32.

Crapse, T. B. and Sommer, M. A. (2008). "Corollary discharge across the animal kingdom." In: *Nature Reviews Neuroscience* 9.8, pp. 587–600.

Crick, F and Mitchison, G (1983). "The function of dream sleep." In: *Nature* 304.5922, pp. 111–114.

Crochet, S. and Petersen, C. C. H. (2006). "Correlating whisker behavior with membrane potential in barrel cortex of awake mice." In: *Nature neuroscience* 9.5, pp. 608–610.

Crunelli, V and Hughes, S. W. (2010). "The slow (< 1 Hz) rhythm of non-REM sleep: a dialogue between three cardinal oscillators." In: *Nature neuroscience*.

Csicsvari, J. (2003). "Massively parallel recording of unit and local field potentials with silicon-based electrodes." In: *Journal of Neurophysiology* 90.2, pp. 1314–1323.

Csicsvari, J, Hirase, H, Czurkó, a, Mamiya, a, and Buzsaki, G. (1999). "Oscillatory coupling of hippocampal pyramidal cells and interneurons in the behaving Rat." In: *Journal of Neuroscience* 19.1, pp. 274–287.

Csicsvari, J., Hirase, H., Czurko, A., and Buzsaki, G. (1998). "Reliability and state dependence of pyramidal cell-interneuron synapses in the hippocampus: An ensemble approach in the behaving rat." In: *Neuron* 21.1, pp. 179–189.

Csicsvari, J., Hirase, H., Mamiya, A., and Buzsaki, G. (2000). "Ensemble Patterns of Hippocampal CA3-CA1 Neurons during Sharp Wave–Associated Population Events." In: *Neuron* 28.2, pp. 585–594.

Csicsvari, J., Jamieson, B., Wise, K. D., and Buzsaki, G. (2003). "Mechanisms of gamma oscillations in the hippocampus of the behaving rat." In: *Neuron* 37.2, pp. 311–322.

Cury, K. M. and Uchida, N. (2010). "Robust odor coding via inhalation-coupled transient activity in the mammalian olfactory bulb." In: *Neuron* 68.3, pp. 570–585.

Curzon, P, Rustay, N. R., and Browman, K. E. (2009). "Cued and contextual fear conditioning for rodents." In:

Cysarz, D. and Büssing, A. (2005). "Cardiorespiratory synchronization during Zen meditation." In: *European journal of applied physiology* 95.1, pp. 88–95.

Damasio, A. R., Tranel, D., and Damasio, H. (1990). "Individuals with sociopathic behavior caused by frontal damage fail to respond autonomically to social stimuli." In: *Behavioural Brain Research* 41.2, pp. 81–94.

Dang-Vu, T. T. et al. (2008). "Spontaneous neural activity during human slow wave sleep." In: *Proceedings of the National Academy of Sciences of the United States of America* 105.39, pp. 15160–15165.

Dave, A. S. and Margoliash, D (2000). "Song replay during sleep and computational rules for sensorimotor vocal learning." In: *Science* 290.5492, pp. 812–816.

Davidson, T. J., Kloosterman, F., and Wilson, M. A. (2009). "Hippocampal Replay of Extended Experience." In: *Neuron* 63.4, pp. 497–507.

Davis, H, Davis, P. A., Loomis, A. L., Hervey, E. N., and Hobart, G (1939). "Electrical reactions of the human brain to auditory stimulation during sleep." In: *Journal of Neurophysiology* 2, pp. 500–514.

Davis, M (1989). "Sensitization of the acoustic startle reflex by footshock." In: *Behavioral Neuroscience* 103.3, pp. 495–503.

Davis, M (1992). "The role of the amygdala in fear and anxiety." In: *Annual Review of Neuroscience*.

deBoer, R. W., Karemaker, J. M., and Strackee, J (1987). "Hemodynamic fluctuations and baroreflex sensitivity in humans: a beat-to-beat model." In: *The American journal of physiology* 253.3 Pt 2, H680–9.

Decharms, R. C. and Zador, A (2000). "Neural representation and the cortical code." In: *Annual Review of Neuroscience* 23.1, pp. 613–647.

Dégenètais, E., Thierry, A.-M., Glowinski, J., Gioanni, Y., and Degenetais, E. (2003). "Synaptic influence of hippocampus on pyramidal cells of the rat prefrontal cortex: an in vivo intracellular recording study." In: *Cerebral cortex (New York, N.Y. : 1991)* 13.7, pp. 782–792.

Deisseroth, K. (2014). "Circuit dynamics of adaptive and maladaptive behaviour." In: *Nature* 505.7483, pp. 309–317.

Dejean, C., Courtin, J., Karalis, N., Chaudun, F., Wurtz, H., Bienvenu, T. C., and Herry, C. (2016). "Prefrontal neuronal assemblies temporally control fear behaviour." In: *Nature* 535.7612, pp. 420–424.

Del Negro, C. A., Funk, G. D., and Feldman, J. L. (2018). "Breathing matters." In: *Nature Reviews Neuroscience* 19.6, pp. 351–367.

Dembrow, N. C., Chitwood, R. A., and Johnston, D. (2010). "Projection-Specific Neuromodulation of Medial Prefrontal Cortex Neurons." In: *Journal of Neuroscience* 30.50, pp. 16922–16937.

Dembrow, N. and Johnston, D. (2014). "Subcircuit-specific neuromodulation in the prefrontal cortex." In: *Frontiers in Neural Circuits* 8, pp. 1–9.

Derégnaucourt, S., Mitra, P. P., Fehér, O., Pytte, C., and Tchernichovski, O. (2005). "How sleep affects the developmental learning of bird song." In: *Nature* 433.7027, pp. 710–716.

Destexhe, A and Bedard, C (2012). "Do neurons generate monopolar current sources?" In: 108.4, pp. 953–955.

Destexhe, A, Contreras, D, and Steriade, M (1999a). "Spatiotemporal analysis of local field potentials and unit discharges in cat cerebral cortex during natural wake and sleep states." In: *The Journal of neuroscience : the official journal of the Society for Neuroscience* 19.11, pp. 4595–4608.

Destexhe, A, Hughes, S. W., Rudolph, M, and Crunelli, V (2007). "Are corticothalamic 'up' states fragments of wakefulness?" In: *Trends in Neurosciences*.

Destexhe, A. and Contreras, D. (2006). "Neuronal computations with stochastic network states." In: *Science* 314.5796, pp. 85–90.

Destexhe, A., Paré, D., Willmore, B. D. B., Cooke, J. E., King, A. J., and Physiol, J (1999b). "Impact of Network Activity on the Integrative Properties of Neocortical Pyramidal Neurons In Vivo Impact of Network Activity on the Integrative Properties of Neocortical Pyramidal Neurons In Vivo." In: *Journal of Neurophysiology* 81.4, pp. 1531–1547.

Destexhe, A., Rudolph, M., and Pare, D. (2003). "The high-conductance state of neocortical neurons in vivo." In: *Nature reviews. Neuroscience* 4.9, pp. 739–751.

Deuker, L., Olligs, J., Fell, J., Kranz, T. A., Mormann, F., Montag, C., Reuter, M., Elger, C. E., and Axmacher, N. (2013). "Memory Consolidation by Replay of Stimulus-Specific Neural Activity." In: *Journal of Neuroscience* 33.49, pp. 19373–19383.

Diamantaki, M., Frey, M., Preston-Ferrer, P., and Burgalossi, A. (2016). "Priming Spatial Activity by Single-Cell Stimulation in the Dentate Gyrus of Freely Moving Rats." In: *Current biology : CB* 26.4, pp. 536–541.

Dias, R., Robbins, T. W., and Roberts, A. C. (1996). "Dissociation in prefrontal cortex of affective and attentional shifts." In: *Nature* 380.6569, pp. 69–72.

Diba, K. and Buzsáki, G. (2007). "Forward and reverse hippocampal place-cell sequences during ripples." In: *Nature neuroscience* 10.10, pp. 1241–1242.

DiCarlo, J. J., Lane, J. W., Hsiao, S. S., and Johnson, K. O. (1996). "Marking microelectrode penetrations with fluorescent dyes." In: *Journal of Neuroscience Methods* 64.1, pp. 75–81.

Diekelmann, S. and Born, J. (2010). "The memory function of sleep." In: *Nature Reviews Neuroscience* 11.2, pp. 114–126.

Diekelmann, S., Biggel, S., Rasch, B., and Born, J. (2012). "Offline consolidation of memory varies with time in slow wave sleep and can be accelerated by cuing memory reactivations." In: *Neurobiology of learning and memory* 98.2, pp. 103–111.

Ding, M, Chen, Y, and Bressler, S. L. (2004). *Granger causality: basic theory and application to neuroscience. 2006*.

Diodato, A., Ruinart de Brimont, M., Yim, Y. S., Derian, N., Perrin, S., Pouch, J., Klatzmann, D., Garel, S., Choi, G. B., and Fleischmann, A. (2016). "Molecular signatures of neural connectivity in the olfactory cortex." In: *Nature Communications* 7, p. 12238.

Ditto, B., Eclache, M., and Goldman, N. (2006). "Short-term autonomic and cardiovascular effects of mindfulness body scan meditation." In: *Annals of behavioral medicine : a publication of the Society of Behavioral Medicine* 32.3, pp. 227–234.

Dlouhy, B. J., Gehlbach, B. K., Kreple, C. J., Kawasaki, H., Oya, H., Buzza, C., Granner, M. A., Welsh, M. J., Howard, M. A., Wemmie, J. A., and Richerson, G. B. (2015). "Breathing Inhibited When Seizures Spread to the Amygdala and upon Amygdala Stimulation." In: *Journal of Neuroscience* 35.28, pp. 10281–10289.

Dossi, R. C., Nuñez, A., and Steriade, M. M. (1992). "Electrophysiology of a slow (0.5-4 Hz) intrinsic oscillation of cat thalamocortical neurones in vivo." In: *Journal of Physiology* 447.1, pp. 215–234.

Dringenberg, H. C. and Vanderwolf, C. H. (1997). "Neocortical activation: Modulation by multiple pathways acting on central cholinergic and serotonergic systems." In: *Experimental Brain Research* 116.1, pp. 160–174.

Duchamp-Viret, P, Chaput, M. A., and Duchamp, A (1999). "Odor response properties of rat olfactory receptor neurons." In: *Science* 284.5423, pp. 2171–2174.

Dudai, Y, Jan, Y. N., and Byers, D (1976). "dunce, a mutant of Drosophila deficient in learning." In: *Proceedings of the ...*

Dudai, Y. (2004). "The Neurobiology of Consolidations, Or, How Stable is the Engram?" In: *Annual review of psychology* 55.1, pp. 51–86.

Dudai, Y. (2012). "The Restless Engram: Consolidations Never End." In: *Annual Review of Neuroscience* 35.1, pp. 227–247.

Dudai, Y., Karni, A., and Born, J. (2015). "The Consolidation and Transformation of Memory." In: *Neuron* 88.1, pp. 20–32.

Durstewitz, D., Vittoz, N. M., Floresco, S. B., and Seamans, J. K. (2010). "Abrupt transitions between prefrontal neural ensemble states accompany behavioral transitions during rule learning." In: *Neuron* 66.3, pp. 438–448.

Eban-Rothschild, A., Rothschild, G., Giardino, W. J., Jones, J. R., and De Lecea, L. (2016). "VTA dopaminergic neurons regulate ethologically relevant sleep-wake behaviors." In: *Nature Neuroscience* 19.10, pp. 1356–1366.

Eccles, J. (1951). "Interpretation of action potentials evoked in the cerebral cortex." In: *Electroencephalography and Clinical Neurophysiology* 3.4, pp. 449–464.

Eckberg, D. L. (2003). "The human respiratory gate." In: *The Journal of Physiology* 548.Pt 2, pp. 339–352.

Eckberg, D. L. et al. (2016). "Respiratory modulation of human autonomic function on Earth." In: *The Journal of Physiology* 594.19, pp. 5611–5627.

Economo, C. V. (1930). "Sleep As a Problem of Localization." In: *The Journal of Nervous and Mental Disease* 71.3, pp. 249–259.

Eden, C. G. van and Buijs, R. M. (2000). "Functional neuroanatomy of the prefrontal cortex: autonomic interactions." In: *Progress in brain research* 126, pp. 49–62.

Eden, C. G. van and Uylings, H. B. (1985). "Cytoarchitectonic development of the prefrontal cortex in the rat." In: *Journal of Comparative Neurology* 241.3, pp. 253–267.

Eeckman, F. H. and Freeman, W. J. (1990). "Correlations between unit firing and EEG in the rat olfactory system." In: *Brain Research* 528.2, pp. 238–244.

Ego-Stengel, V. and Wilson, M. A. (2009). "Disruption of ripple-associated hippocampal activity during rest impairs spatial learning in the rat." In: *Hippocampus*, NA–NA.

Einstein, M. C., Polack, P.-O., Tran, D. T., and Golshani, P. (2017). "Visually Evoked 3–5 Hz Membrane Potential Oscillations Reduce the Responsiveness of Visual Cortex Neurons in Awake Behaving Mice." In: *The Journal of Neuroscience* 37.20, pp. 5084–5098.

Ekstrom, A. D., Caplan, J. B., Ho, E., Shattuck, K., Fried, I., and Kahana, M. J. (2005). "Human hippocampal theta activity during virtual navigation." In: *Hippocampus* 15.7, pp. 881–889.

Engel, A. K., Kreiter, A. K., König, P, and Singer, W (1991). "Synchronization of oscillatory neuronal responses between striate and extrastriate visual cortical areas of the cat." In: *Proc. Natl. Acad. Sci. U. S. A.* 88.14, pp. 6048–6052.

Engel, A. K., Fries, P., and Singer, W. (2001). "Dynamic predictions: Oscillations and synchrony in top–down processing." In: *Nature Reviews Neuroscience* 2.10, pp. 704–716.

English, D. F., Peyrache, A., Stark, E., Roux, L., Vallentin, D., Long, M. A., and Buzsaki, G. (2014). "Excitation and Inhibition Compete to Control Spiking during Hippocampal Ripples: Intracellular Study in Behaving Mice." In: *Journal of Neuroscience* 34.49, pp. 16509–16517.

Erisken, S., Vaiceliunaite, A., Jurjut, O., Fiorini, M., Katzner, S., and Busse, L. (2014). "Effects of locomotion extend throughout the mouse early visual system." In: *Current biology : CB* 24.24, pp. 2899–2907.

Eschenko, O., Magri, C., Panzeri, S., and Sara, S. J. (2012). "Noradrenergic Neurons of the Locus Coeruleus Are Phase Locked to Cortical Up-Down States during Sleep." In: *Cerebral Cortex* 22.2, pp. 426–435.

Esser, S. K., Hill, S., and Tononi, G. (2009). "Breakdown of Effective Connectivity During Slow Wave Sleep: Investigating the Mechanism Underlying a Cortical Gate Using Large-Scale Modeling." In: *Journal of Neurophysiology* 102.4, pp. 2096–2111.

Estes, W. K. and Skinner, B. F. (1941). "Some quantitative properties of anxiety." In: *Journal of experimental Psychology* 29.5, pp. 390–400.

Euston, D. R., Tatsuno, M., and McNaughton, B. L. (2007). "Fast-forward playback of recent memory sequences in prefrontal cortex during sleep." In: *Science* 318.5853, pp. 1147–1150.

Euston, D. R., Gruber, A. J., and McNaughton, B. L. (2012). "The Role of Medial Prefrontal Cortex in Memory and Decision Making." In: *Neuron* 76.6, pp. 1057–1070.

Fanselow, M. S., Lester, L. S., and Helmstetter, F. J. (1988). "Changes in feeding and foraging patterns as an antipredator defensive strategy: a laboratory simulation using aversive stimulation in a closed economy." In: *Journal of the experimental analysis of behavior* 50.3, pp. 361–374.

Fanselow, M. S. (1990). "Factors governing one-trial contextual conditioning." In: *Animal Learning & Behavior* 18.3, pp. 264–270.

Fenno, L., Yizhar, O., and Deisseroth, K. (2011). "The Development and Application of Optogenetics." In: *Annual Review of Neuroscience* 34.1, pp. 389–412.

Ferguson, J. E., Boldt, C., and Redish, A. D. (2009). "Creating low-impedance tetrodes by electroplating with additives." In: *Sensors and Actuators, A: Physical* 156.2, pp. 388–393.

Fernández-Ruiz, A., Oliva, A., Nagy, G. A., Maurer, A. P., Berényi, A., and Buzsáki, G. (2017). "Entorhinal-CA3 dualinput control of spike timing in the hippocampus by theta-gamma Coupling." In: *Neuron* 93.5, 1213–1226.e5.

Fernandez, L. M. J., Comte, J.-C., Le Merre, P., Lin, J.-S., Salin, P.-A., and Crochet, S. (2016). "Highly Dynamic Spatiotemporal Organization of Low-Frequency Activities During Behavioral States in the Mouse Cerebral Cortex." In: *Cerebral Cortex*.

Ferreira, A. N., Yousuf, H., Dalton, S., and Sheets, P. L. (2015). "Highly differentiated cellular and circuit properties of infralimbic pyramidal neurons projecting to the periaqueductal gray and amygdala." In: *Frontiers in Cellular Neuroscience* 9, p. 161.

File, S. E. (1980). "The use of social interaction as a method for detecting anxiolytic activity of chlordiazepoxide-like drugs." In: *Journal of Neuroscience Methods* 2.3, pp. 219–238.

Finelli, L. A., Borbély, A. A., and Achermann, P. (2001). "Functional topography of the human nonREM sleep electroencephalogram." In: *European Journal of Neuroscience* 13.12, pp. 2282–2290.

Floresco, S. B., Seamans, J. K., and Phillips, a. G. (1997). "Selective roles for hippocampal, prefrontal cortical, and ventral striatal circuits in radial-arm maze tasks with or without a delay." In: *Journal of Neuroscience* 17.5, pp. 1880–1890.

Fogel, S. M. and Smith, C. T. (2006). "Learning-dependent changes in sleep spindles and Stage 2 sleep." In: *Journal of sleep research* 15.3, pp. 250–255.

Fokkema, D. S., Koolhaas, J. M., Meulen, J van der, and Schoemaker, R (1986). "Social stress induced pressure breathing and consequent blood pressure oscillation." In: *Life sciences* 38.6, pp. 569–75.

Fontanini, A. and Bower, J. M. (2005). "Variable coupling between olfactory system activity and respiration in ketamine/xylazine anesthetized rats." In: *Journal of neurophysiology* 93.6, pp. 3573–81.

Fontanini, A., Spano, P., and Bower, J. M. (2003). "Ketamine–Xylazine-Induced Slow (?1.5 Hz) Oscillations in the Rat Piriform (Olfactory) Cortex Are Functionally Correlated with Respiration." In: *Journal of Neuroscience* 23.22, pp. 7993–8001.

Foote, S. L., Bloom, F. E., and Aston-Jones, G (1983). "Nucleus locus ceruleus: new evidence of anatomical and physiological specificity." In: *Physiological reviews* 63.3, pp. 844–914.

Foster, D. J. and Wilson, M. A. (2006). "Reverse replay of behavioural sequences in hippocampal place cells during the awake state." In: *Nature* 440.7084, pp. 680–683.

Fourment, A, Hirsch, J. C., Chastanet, M, and Guidet, C (1983). "The effect of midbrain reticular stimulation upon perigeniculate neurons activity during different states of the sleep-waking cycle in the cat." In: *Brain Research* 259.2, pp. 301–307.

Frankland, P. W. and Bontempi, B. (2005). "The organization of recent and remote memories." In: *Nature Reviews Neuroscience* 6.2, pp. 119–130.

Frankland, P. W., Bontempi, B., Talton, L. E., Kaczmarek, L., and Silva, A. J. (2004). "The Involvement of the Anterior Cingulate Cortex in Remote Contextual Fear Memory." In: *Science* 304.5672, pp. 881–883.

Franklin, T. B. et al. (2017). "Prefrontal cortical control of a brainstem social behavior circuit." In: *Nature Neuroscience* 20.2, pp. 260–270.

Freeman, J. A. and Nicholson, C (1975). "Experimental optimization of current source-density technique for anuran cerebellum." In: *Journal of neurophysiology* 38.2, pp. 369–382.

Freeman, W. J. (1968). "Effects of surgical isolation and tetanization on prepyriform cortex in cats." In: *Journal of neurophysiology* 31.3, pp. 349–57.

Freeman, W. J. (1959). "Distribution in time and space of prepyriform electrical activity." In: *Journal of neurophysiology* 2, pp. 644–65.

Freeman, W. J. (1975). *Mass action in the nervous system : examination of the neurophysiological basis of adaptive behavior through the EEG*. Academic Press, p. 489.

Freemon, F. R. and Walter, R. D. (1970). "Electrical activity of human limbic system during sleep." In: *Comprehensive psychiatry* 11.6, pp. 544–551.

Freemon, F. R., McNew, J. J., and Adey, W. R. (1969). "Sleep of unrestrained chimpanzee: cortical and subcortical recordings." In: *Experimental neurology* 25.1, pp. 129–137.

Freund, T. F. and Buzsaki, G. (1996). "Interneurons of the hippocampus." In: *Hippocampus* 6.4, pp. 347–470.

Fries, P., Reynolds, J. H., Rorie, A. E., and Desimone, R. (2001). "Modulation of oscillatory neuronal synchronization by selective visual attention." In: *Science* 291.5508, pp. 1560–1563.

Fries, P. (2015). "Rhythms for Cognition: Communication through Coherence." In: *Neuron* 88.1, pp. 220–235.

Fry, W. F. and Rader, C (1977). "The respiratory components of mirthful laughter." In: *Journal of Biological Psychology* 19.2, pp. 39–50.

Frysinger, R. C. and Harper, R. M. (1989). "Cardiac and respiratory correlations with unit discharge in human amygdala and hippocampus." In: *Electroencephalography and clinical neurophysiology* 72.6, pp. 463–70.

Frysztak, R. J. and Neafsey, E. J. (1991). "The Effect of Medial Frontal Cortex Lesions on Respiration, "Freezing," and Ultrasonic Vocalizations during Conditioned Emotional Responses in Rats." In: *Cerebral Cortex* 1.5, pp. 418–425.

Fu, Y., Tucciarone, J. M., Espinosa, J. S., Sheng, N., Darcy, D. P., Nicoll, R. A., Huang, Z. J., and Stryker, M. P. (2014). "A cortical circuit for gain control by behavioral state." In: *Cell* 156.6, pp. 1139–1152.

Fuentemilla, L., Barnes, G. R., Düzel, E., and Levine, B. (2014). "Theta oscillations orchestrate medial temporal lobe and neocortex in remembering autobiographical memories." In: *NeuroImage* 85, pp. 730–737.

Fuentemilla, L., Miró, J., Ripollés, P., Vilà-Balló, A., Juncadella, M., Castañer, S., Salord, N., Monasterio, C., Falip, M., and Rodríguez-Fornells, A. (2013). "Hippocampus-dependent strengthening of targeted memories via reactivation during sleep in humans." In: *Current biology : CB* 23.18, pp. 1769–1775.

Fujisawa, S. and Buzsaki, G. (2011). "A 4 Hz Oscillation Adaptively Synchronizes Prefrontal, VTA, and Hippocampal Activities." In: *Neuron* 72.1, pp. 153–165.

Fukunaga, I., Herb, J. T., Kollo, M., Boyden, E. S., and Schaefer, A. T. (2014). "Independent control of gamma and theta activity by distinct interneuron networks in the olfactory bulb." In: *Nature Neuroscience* 17.9, pp. 1208–1216.

Fuster, J. (2015). *The Prefrontal Cortex*. Academic Press.

Gabbott, P. L., Warner, T. A., and Busby, S. J. (2006). "Amygdala input monosynaptically innervates parvalbumin immunoreactive local circuit neurons in rat medial prefrontal cortex." In: *Neuroscience* 139.3, pp. 1039–1048.

Gais, S. and Born, J. (2004). "Low acetylcholine during slow-wave sleep is critical for declarative memory consolidation." In: *Proceedings of the National Academy of Sciences* 101.7, pp. 2140–2144.

Gale, G. D., Anagnostaras, S. G., and Godsil, B. P. (2004). "Role of the basolateral amygdala in the storage of fear memories across the adult lifetime of rats." In:

Garfinkel, S. N., Minati, L., Gray, M. A., Seth, A. K., Dolan, R. J., and Critchley, H. D. (2014). "Fear from the Heart: Sensitivity to Fear Stimuli Depends on Individual Heartbeats." In: *Journal of Neuroscience* 34.19, pp. 6573–6582.

Garner, A. R., Rowland, D. C., Hwang, S. Y., Baumgaertel, K., Roth, B. L., Kentros, C., and Mayford, M. (2012). "Generation of a synthetic memory trace." In: *Science* 335.6075, pp. 1513–1516.

Gastaut, H. J. and Bert, J (1954). "EEG changes during cinematographic presentation (Moving picture activation of the EEG)." In: *Electroencephalography and clinical neurophysiology*.

Gaudreau, H and Pare, D (1996). "Projection neurons of the lateral amygdaloid nucleus are virtually silent throughout the sleep–waking cycle." In: *J.Neurophysiol.* 75.0022-3077 (Print), pp. 1301–1305.

Gault, F. and Leaton, R. (1963). "Electrical activity of the olfactory system." In: *Electroencephalography and Clinical Neurophysiology* 15.2, pp. 299–304.

Gentet, L. J., Avermann, M., Matyas, F., Staiger, J. F., and Petersen, C. C. (2010). "Membrane Potential Dynamics of GABAergic Neurons in the Barrel Cortex of Behaving Mice." In: *Neuron* 65.3, pp. 422–435.

Genzel, L., Kroes, M. C. W., Dresler, M., and Battaglia, F. P. (2014). "Light sleep versus slow wave sleep in memory consolidation: A question of global versus local processes?" In: *Trends in Neurosciences* 37.1, pp. 10–19.

Gerard, R. W. (1955). "Biological roots of psychiatry." In: *Science* 122.3162, pp. 225–230.

Gerstein, G. L. and Perkel, D. H. (1969). "Simultaneously recorded trains of action potentials: analysis and functional interpretation." In: *Science* 164.0036-8075 (Print), pp. 828–830.

Ghosh, S., Larson, S. D., Hefzi, H., Marnoy, Z., Cutforth, T., Dokka, K., and Baldwin, K. K. (2011). "Sensory maps in the olfactory cortex defined by long-range viral tracing of single neurons." In: *Nature* 472.7342, pp. 217–220.

Girardeau, G, Cei, A, and Zugaro, M (2014). "Learning-Induced Plasticity Regulates Hippocampal Sharp Wave-Ripple Drive." In: 34.15, pp. 5176–5183.

Girardeau, G., Benchenane, K., Wiener, S. I., Buzsáki, G., and Zugaro, M. B. (2009a). "Selective suppression of hippocampal ripples impairs spatial memory." In: *Nature neuroscience* 12.10, pp. 1222–1223.

Girardeau, G., Benchenane, K., Wiener, S. I., Buzsáki, G., Zugaro, M. B., Buzsaki, G., Zugaro, M. B., Buzsáki, G., and Zugaro, M. B. (2009b). "Selective suppression of hippocampal ripples impairs spatial memory." In: *Nature Neuroscience* 12.10, pp. 1222–1223.

Givens, B. S. and Olton, D. S. (1990). "Cholinergic and GABAergic Modulation of Medial Septal Area: Effect on Working Memory." In: *Behavioral Neuroscience* 104.6, pp. 849–855.

Glenn, L. L. and Steriade, M (1982). "Discharge rate and excitability of cortically projecting intralaminar thalamic neurons during waking and sleep states." In: *Journal of Neuroscience* 2.10, pp. 1387–1404.

Gloor, P, Ball, G, and Schaul, N (1977). "Brain lesions that produce delta waves in the EEG." In: *Neurology* 27.4, pp. 326–333.

Godsil, B. P., Kiss, J. P., Spedding, M., and Jay, T. M. (2013). "The hippocampal-prefrontal pathway: the weak link in psychiatric disorders?" In: *European neuropsychopharmacology : the journal of the European College of Neuropsychopharmacology* 23.10, pp. 1165–1181.

Gold, A. R. (2011). "Functional somatic syndromes, anxiety disorders and the upper airway: a matter of paradigms." In: *Sleep Medicine Reviews* 15.6, pp. 389–401.

Gold, C (2006). "On the Origin of the Extracellular Action Potential Waveform: A Modeling Study." In: 95.5, pp. 3113–3128.

Goldman, R. I., Stern, J. M., Engel, J., and Cohen, M. S. (2002). "Simultaneous EEG and fMRI of the alpha rhythm." In: *NeuroReport* 13.18, pp. 2487–2492.

Gomes, J.-M., Bédard, C., Valtcheva, S., Nelson, M., Khokhlova, V., Pouget, P., Venance, L., Bal, T., and Destexhe, A. (2016). "Intracellular Impedance Measurements Reveal Non-ohmic Properties of the Extracellular Medium around Neurons." In: *Biophysical Journal* 110.1, pp. 234–246.

Gonzalez, C, Almaraz, L, Obeso, A, and Rigual, R (1994). "Carotid body chemoreceptors: from natural stimuli to sensory discharges." In: *Physiological Reviews* 74.4, pp. 829–898.

Goto, Y and O'Donnell, P (2001). "Synchronous activity in the hippocampus and nucleus accumbens in vivo." In: *Journal of Neuroscience* 21.4, RC131.

Gourevitch, B., Kay, L. M., Martin, C., Gourévitch, B., Kay, L. M., and Martin, C. (2010). "Directional Coupling From the Olfactory Bulb to the Hippocampus During a Go/No-Go Odor Discrimination Task." In: *Journal of Neurophysiology* 103.5, pp. 2633–2641.

Gouty-Colomer, L. A., Hosseini, B, Marcelo, I. M., Schreiber, J, Slump, D. E., Yamaguchi, S, Houweling, A. R., Jaarsma, D, Elgersma, Y, and Kushner, S. A. (2015). "Arc expression identifies the lateral amygdala fear memory trace." In: *Molecular psychiatry* 21.November 2014, pp. 1–12.

Grastyán, E., Lissák, K., Madarász, I., and Donhoffer, H. (1959). "Hippocampal electrical activity during the development of conditioned reflexes." In: *Electroencephalography and Clinical Neurophysiology* 11.3, pp. 409–430.

Graves, L. A. (2003). "Sleep Deprivation Selectively Impairs Memory Consolidation for Contextual Fear Conditioning." In: *Learning & Memory* 10.3, pp. 168–176.

Gray, C. M. and McCormick, D. A. (1996). "Chattering cells: superficial pyramidal neurons contributing to the generation of synchronous oscillations in the visual cortex." In: *Science* 274.5284, pp. 109–113.

Gray, C. M. and Skinner, J. E. (1988). "Centrifugal regulation of neuronal activity in the olfactory bulb of the waking rabbit as revealed by reversible cryogenic blockade." In: *Experimental brain research* 69.2, pp. 378–86.

Gray, C. M., König, P., Engel, A. K., and Singer, W. (1989). "Oscillatory responses in cat visual cortex exhibit inter-columnar synchronization which reflects global stimulus properties." In: *Nature* 338.6213, pp. 334–337.

Green, J. D. and Arduini, A. A. (1954). "Hippocampal Electrical Activity in Arousal." In: *Journal of Neurophysiology* 17.6, pp. 533–57.

Griffin, A. L., Asaka, Y., Darling, R. D., and Berry, S. D. (2004). "Theta-Contingent Trial Presentation Accelerates Learning Rate and Enhances Hippocampal Plasticity during Trace Eyeblink Conditioning." In: *Behavioral Neuroscience* 118.2, pp. 403–411.

Grion, N., Akrami, A., Zuo, Y., Stella, F., and Diamond, M. E. (2016). "Coherence between Rat Sensorimotor System and Hippocampus Is Enhanced during Tactile Discrimination." In: *PLoS Biology* 14.2, e1002384.

Groenewegen, H. J. and Berendse, H. W. (1994). "The specificity of the 'nonspecific' midline and intralaminar thalamic nuclei." In: *Trends in Neurosciences* 17.2, pp. 52–57.

Grosmaitre, X., Santarelli, L. C., Tan, J., Luo, M., and Ma, M. (2007). "Dual functions of mammalian olfactory sensory neurons as odor detectors and mechanical sensors." In: *Nature Neuroscience* 10.3, pp. 348–354.

Guerrien, A, Dujardin, K, Mandai, O, Sockeel, P, and Leconte, P (1989). "Enhancement of memory by auditory stimulation during postlearning REM sleep in humans." In: *Physiology & behavior* 45.5, pp. 947–950.

Gulyás, A. I., Freund, T. F., and Káli, S. (2016). "The Effects of Realistic Synaptic Distribution and 3D Geometry on Signal Integration and Extracellular Field Generation of Hippocampal Pyramidal Cells and Inhibitory Neurons." In: *Frontiers in neural circuits* 10, p. 88.

Gulyás, A. I., Freund, T. F., and Káli, S. (2016). "The Effects of Realistic Synaptic Distribution and 3D Geometry on Signal Integration and Extracellular Field Generation of Hippocampal Pyramidal Cells and Inhibitory Neurons." In: *Frontiers in Neural Circuits* 10, p. 88.

Haberly, L. B. and Price, J. L. (1978). "Association and commissural fiber systems of the olfactory cortex of the rat." In: *Journal of Comparative Neurology* 178.4, pp. 711–740.

Habets, A. M., Lopes Da Silva, F. H., and Mollevanger, W. J. (1980). "An olfactory input to the hippocampus of the cat: Field potential analysis." In: *Brain Research* 182.1, pp. 47–64.

Hahn, T. T. G., Sakmann, B., and Mehta, M. R. (2007). "Differential responses of hippocampal subfields to cortical up-down states." In: *Proceedings of the National Academy of Sciences* 104.12, pp. 5169–5174.

Hahn, T. T. G., Sakmann, B., and Mehta, M. R. (2006). "Phase-locking of hippocampal interneurons' membrane potential to neocortical up-down states." In: *Nature neuroscience* 9.11, pp. 1359–1361.

Haider, B. (2006). "Neocortical Network Activity In Vivo Is Generated through a Dynamic Balance of Excitation and Inhibition." In: *Journal of Neuroscience* 26.17, pp. 4535–4545.

Hajos, N. (2004). "Spike Timing of Distinct Types of GABAergic Interneuron during Hippocampal Gamma Oscillations In Vitro." In: *Journal of Neuroscience* 24.41, pp. 9127–9137.

Halasz, P, Pal, I, and Rajna, P (1985). "K-complex formation of the EEG in sleep. A survey and new examinations." In: *Acta Physiol Hung* 65.1, pp. 3–35.

Halgren, E., Babb, T. L., Rausch, R., and Crandall, P. H. (1977). "Neurons in the human basolateral amygdala and hippocampal formation do not respond to odors." In: *Neuroscience Letters* 4.6, pp. 331–335.

Han, J.-H. H., Kushner, S. A., Yiu, A. P., Cole, C. J., Matynia, A., Brown, R. A., Neve, R. L., Guzowski, J. F., Silva, A. J., and Josselyn, S. A. (2007). "Neuronal competition and selection during memory formation." In: *Science* 316.5823, pp. 457–460.

Han, J.-H., Kushner, S. A., Yiu, A. P., Hsiang, H.-L. L., Buch, T., Waisman, A., Bontempi, B., Neve, R. L., Frankland, P. W., and Josselyn, S. A. (2009). "Selective erasure of a fear memory." In: *Science* 323.5920, pp. 1492–1496.

Han, W., Tellez, L. A., Rangel, M. J., Motta, S. C., Zhang, X., Perez, I. O., Canteras, N. S., Shammah-Lagnado, S. J., Pol, A. N. van den, and Araujo, I. E. de (2017). "Integrated Control of Predatory Hunting by the Central Nucleus of the Amygdala." In: *Cell* 168.1-2, 311–324.e18.

Hardy, S. G. and Holmes, D. E. (1988). "Prefrontal stimulus-produced hypotension in rat." In: *Experimental brain research* 73.2, pp. 249–55.

Harper, R., Frysinger, R., Trelease, R., and Marks, J. (1984). "State-dependent alteration of respiratory cycle timing by stimulation of the central nucleus of the amygdala." In: *Brain Research* 306.1-2, pp. 1–8.

Harris, K., Csicsvari, J., Hirase, H., Dragoi, G., and Buzsaki, G. (2003). "Organization of cell assemblies in the hippocampus." In: *Nature* 424.July, pp. 552–556.

Hars, B., Hennevin, E., and Pasques, P. (1985). "Improvement of learning by cueing during postlearning paradoxical sleep." In: *Behavioural brain research* 18.3, pp. 241–250.

Hasselmo, M. E. (1999). "Neuromodulation: Acetylcholine and memory consolidation." In: *Trends in Cognitive Sciences* 3.9, pp. 351–359.

Hasselmo, M. E. (2005). *What is the function of hippocampal theta rhythm? - Linking bahavioral data to phasic properties of field potential and unit recording data*.

Hasselmo, M. E. (2006). "The role of acetylcholine in learning and memory." In: *Current Opinion in Neurobiology* 16.6, pp. 710–715.

Hasselmo, M. E. and McGaughy, J. (2004). "High acetylcholine levels set circuit dynamics for attention and encoding and low acetylcholine levels set dynamics for consolidation." In: *Progress in Brain Research* 145, pp. 207–231.

Hasselmo, M. E., Bodelón, C., and Wyble, B. P. (2002). "A Proposed Function for Hippocampal Theta Rhythm: Separate Phases of Encoding and Retrieval Enhance Reversal of Prior Learning." In: *Neural Computation* 14.4, pp. 793–817.

Havekes, R., Vecsey, C. G., and Abel, T. (2013). "The impact of sleep deprivation on neuronal and glial signalling pathways important for memory and synaptic plasticity." In: *Cell Signal* 24.6, pp. 1251–1260.

Hayar, A., Karnup, S., Shipley, M. T., and Ennis, M. (2004). "Olfactory bulb glomeruli: external tufted cells intrinsically burst at theta frequency and are entrained by patterned olfactory input." In: *The Journal of neuroscience : the official journal of the Society for Neuroscience* 24.5, pp. 1190–1199.

Hayward, L. F., Swartz, C. L., and Davenport, P. W. (2003). "Respiratory response to activation or disinhibition of the dorsal periaqueductal gray in rats." In: *Journal of Applied Physiology* 94.3, pp. 913–922.

Hazan, L., Zugaro, M., and Buzsáki, G. (2006). "Klusters, NeuroScope, NDManager: a free software suite for neurophysiological data processing and visualization." In: *Journal of Neuroscience Methods* 155.2, pp. 207–216.

Headley, D. B. and Pare, D. (2017). "Common oscillatory mechanisms across multiple memory systems." In: *npj Science of Learning* 2.1, p. 1.

Headley, D. B., Kanta, V., and Paré, D. (2017). "Intra- and interregional cortical interactions related to sharp-wave ripples and dentate spikes." In: *Journal of Neurophysiology* 117.2, pp. 556–565.

Heale, V. R., Vanderwolf, C. H., and Kavaliers, M. (1994). "Components of weasel and fox odors elicit fast wave bursts in the dentate gyrus of rats." In: *Behavioural Brain Research* 63.2, pp. 159–165.

Hebb, D. O. (1946). "On the nature of fear." In: *Psychological review*.

Hebb, D. O. (1949). "The Organization of Behavior: A Neuropsychological Approach." In: *The Organization of Behavior* 911.1, p. 335.

Hediger, H (1969). "Comparative observations on sleep." In: *Proceedings of the Royal Society of Medicine* 62.2, pp. 153–156.

Henry, C. E. and Scoville, W. B. (1952). "Suppression-burst activity from isolated cerebral cortex in man." In: *Electroencephalography and clinical ...*

Henze, D. A., Borhegyi, Z, Csicsvari, J, Mamiya, A, Harris, K. D., and Buzsaki, G. (2000). "Intracellular features predicted by extracellular recordings in the hippocampus in vivo." In: 84.1, pp. 390–400.

Herrero, J. L., Khuvis, S., Yeagle, E., Cerf, M., and Mehta, A. D. (2018). "Breathing above the brainstem: Volitional control and attentional modulation in humans." In: *Journal of Neurophysiology* 119.1, pp. 145–159.

Herry, C. and Johansen, J. P. (2014). "Encoding of fear learning and memory in distributed neuronal circuits." In: *Nature Neuroscience* 17.12, pp. 1644–1654.

Herry, C. and Mons, N. (2004). "Resistance to extinction is associated with impaired immediate early gene induction in medial prefrontal cortex and amygdala." In: *European Journal of Neuroscience* 20.3, pp. 781–790.

Hilton, L., Hempel, S., Ewing, B. A., Apaydin, E., Xenakis, L., Newberry, S., Colaiaco, B., Maher, A. R., Shanman, R. M., Sorbero, M. E., and Maglione, M. A. (2016). "Mindfulness Meditation for Chronic Pain: Systematic Review and Meta-analysis." In: *Annals of behavioral medicine : a publication of the Society of Behavioral Medicine*.

Hiltunen, T., Kantola, J., Abou Elseoud, A., Lepola, P., Suominen, K., Starck, T., Nikkinen, J., Remes, J., Tervonen, O., Palva, S., Kiviniemi, V., and Palva, J. M. (2014). "Infra-slow EEG fluctuations are correlated with resting-state network dynamics in fMRI." In: *The Journal of neuroscience : the official journal of the Society for Neuroscience* 34.2, pp. 356–362.

Hinton, G., Dayan, P, Frey, B., and Neal, R. (1995). "The "wake-sleep" algorithm for unsupervised neural networks." In: *Science* 268.5214, pp. 1158–1161.

Hinton, G. G., Osindero, S., and Teh, Y. Y. (2006). "A fast learning algorithm for deep belief nets." In: *Neural computation* 18.7, pp. 1527–1554.

Hobson, J. A. (1967). "Respiration and EEG synchronization in the frog." In: *Nature* 213.5080, pp. 988–989.

Hobson, J. A. and Pace-Schott, E. F. (2002). "The cognitive neuroscience of sleep: Neuronal systems, consciousness and learning." In: *Nature Reviews Neuroscience* 3.9, pp. 679–693.

Hobson, J., McCarley, R., and Wyzinski, P. (1975). "Sleep cycle oscillation: reciprocal discharge by two brainstem neuronal groups." In: *Science* 189.4196, pp. 55–58.

Hofer, M. A. (1970). "Cardiac and respiratory function during sudden prolonged immobility in wild rodents." In: *Psychosomatic Medicine* 32.6, pp. 633–47.

Hoffman, K. L. and McNaughton, B. L. (2002). "Coordinated reactivation of distributed memory traces in primate neocortex." In: *Science* 297.5589, pp. 2070–2073.

Hölscher, C, Anwyl, R, and Rowan, M. J. (1997). "Stimulation on the positive phase of hippocampal theta rhythm induces long-term potentiation that can Be depotentiated by stimulation on the negative phase in area CA1 in vivo." In: *Journal of Neuroscience* 17.16, pp. 6470–6477.

Holsheimer, J and Feenstra, B. W. (1977). "Volume conduction and EEG measurements within the brain: a quantitative approach to the influence of electrical spread on the linear relationship of activity measured at different locations." In: *Electroencephalography and clinical neurophysiology* 43.1, pp. 52–58.

Holst, E. v (1939). "Die relative Koordination als Phänomen und als Methode zentralnervöser Funktionsanalyse." In: *Ergebnisse der Physiologie Biologischen Chemie und Experimentellen Pharmakologie* 42.1, pp. 228–306.

Holst, E. von and Mittelstaedt, H. (1950). "Das Reafferenzprinzip - Wechselwirkungen zwischen Zentralnervensystem und Peripherie." In: *Die Naturwissenschaften* 37.20, pp. 464–476.

Hoover, W. B. and Vertes, R. P. (2007). "Anatomical analysis of afferent projections to the medial prefrontal cortex in the rat." In: *Brain Structure and Function* 212.2, pp. 149–179.

Hopfield, J. J. (1982). "Neural networks and physical systems with emergent collective computational abilities." In: *Proceedings of the National Academy of Sciences* 79.8, pp. 2554–2558.

Hopfield, J. J., Feinstein, D. I., and Palmer, R. G. (1983). "'Unlearning' has a stabilizing effect in collective memories." In: *Nature* 304.5922, pp. 158–159.

Hu, J., Zhong, C., Ding, C., Chi, Q., Walz, A., Mombaerts, P., Matsunami, H., and Luo, M. (2007). "Detection of near-atmospheric concentrations of CO2 by an olfactory subsystem in the mouse." In: *Science* 317.5840, pp. 953–957.

Huang, Z. G., Subramanian, S. H., Balnave, R. J., Turman, a. B., and Moi Chow, C (2000). "Roles of periaqueductal gray and nucleus tractus solitarius in cardiorespiratory function in the rat brainstem." In: *Respiration physiology* 120.3, pp. 185–195.

Huber, R., Ghilardi, M. F., Massimini, M., and Tononi, G. (2004). "Local sleep and learning." In: *Nature* 430.6995, pp. 78–81.

Hudry, J, Ryvlin, P, Royet, J. P., and Mauguière, F (2001). "Odorants elicit evoked potentials in the human amygdala." In: *Cerebral Cortex* 11.7, pp. 619–627.

Huerta, P. T. and Lisman, J. E. (1995). "Bidirectional synaptic plasticity induced by a single burst during cholinergic theta oscillation in CA1 in vitro." In: *Neuron* 15.5, pp. 1053–1063.

Hughes, S. W., Lőrincz, M. L., Parri, H. R., and Crunelli, V. (2011). "Infra-slow (<0.1 Hz) oscillations in thalamic relay nuclei: basic mechanisms and significance to health and disease states." In: *Progress in brain research* 193, pp. 145–162.

Huijbers, W., Pennartz, C. M. A., Beldzik, E., Domagalik, A., Vinck, M, Hofman, W. F., Cabeza, R., and Daselaar, S. M. (2014). "Respiration phase-locks to fast stimulus presentations: implications for the interpretation of posterior midline "deactivations"." In: *Human brain mapping* 35.9, pp. 4932–4943.

Hunt, M. J., Falinska, M, Łęski, S, and Wójcik, D. K. (2011). "Differential effects produced by ketamine on oscillatory activity recorded in the rat hippocampus, dorsal striatum and nucleus accumbens." In:

Hurley-Gius, K. M. and Neafsey, E. J. (1986). "The medial frontal cortex and gastric motility: microstimulation results and their possible significance for the overall pattern of organization of rat frontal and parietal cortex." In: *Brain research* 365.2, pp. 241–8.

Hyman, J. M., Wyble, B. P., Goyal, V., Rossi, C. A., and Hasselmo, M. E. (2003). "Stimulation in hippocampal region CA1 in behaving rats yields long-term potentiation when delivered to the peak of theta and long-term depression when delivered to the trough." In: *The Journal of neuroscience : the official journal of the Society for Neuroscience* 23.37, pp. 11725–11731.

Hyman, J. M., Zilli, E. A., Paley, A. M., and Hasselmo, M. E. (2005). "Medial prefrontal cortex cells show dynamic modulation with the hippocampal theta rhythm dependent on behavior." In: *Hippocampus* 15.6, pp. 739–749.

Hyman, J. M., Zilli, E. A., Paley, A. M., and Hasselmo, M. E. (2010). "Working memory performance correlates with prefrontal-hippocampal theta interactions but not with prefrontal neuron firing rates." In: *Frontiers in Integrative Neuroscience* 4, p. 2.

Ikegaya, Y., Aaron, G., Cossart, R., Aronov, D., Lampl, I., Ferster, D., and Yuste, R. (2004). "Synfire Chains and Cortical Songs: Temporal Modules of Cortical Activity." In: *Science* 304.5670, pp. 559–564.

Ishikawa, D., Matsumoto, N., Sakaguchi, T., Matsuki, N., and Ikegaya, Y. (2014). "Operant Conditioning of Synaptic and Spiking Activity Patterns in Single Hippocampal Neurons." In: *Journal of Neuroscience* 34.14, pp. 5044–53.

Isomura, Y., Sirota, A., Özen, S., Montgomery, S., Mizuseki, K., Henze, D. A., and Buzsáki, G. (2006). "Integration and Segregation of Activity in Entorhinal-Hippocampal Subregions by Neocortical Slow Oscillations." In: *Neuron* 52.5, pp. 871–882.

Isosaka, T., Matsuo, T., Yamaguchi, T., Funabiki, K., Nakanishi, S., Kobayakawa, R., and Kobayakawa, K. (2015). "Htr2a-expressing cells in the central amygdala control the hierarchy between innate and learned fear." In: *Cell* 163.5, pp. 1153–1164.

Ito, J., Roy, S., Liu, Y., Cao, Y., Fletcher, M., Lu, L., Boughter, J. D., Grün, S., and Heck, D. H. (2014). "Whisker barrel cortex delta oscillations and gamma power in the awake mouse are linked to respiration." In: *Nature Communications* 5, p. 3572.

Iwanir, S., Tramm, N., Nagy, S., Wright, C., Ish, D., and Biron, D. (2013). "The microarchitecture of C. elegans behavior during lethargus: homeostatic bout dynamics, a typical body posture, and regulation by a central neuron." In: *Sleep* 36.3, pp. 385–395.

Izaki, Y., Takita, M., and Akema, T. (2008). "Specific role of the posterior dorsal hippocampus-prefrontal cortex in short-term working memory." In: *European Journal of Neuroscience* 27.11, pp. 3029–3034.

Jackson, J. C., Johnson, A, and Redish, A. D. (2006). "Hippocampal sharp waves and reactivation during awake states depend on repeated sequential experience." In: *Journal of Neuroscience*.

Jackson, J., Goutagny, R., and Williams, S. (2011). "Fast and Slow Gamma Rhythms Are Intrinsically and Independently Generated in the Subiculum." In: *Journal of Neuroscience* 31.34, pp. 12104–12117.

Jackson, J., Amilhon, B., Goutagny, R., Bott, J. B., Manseau, F., Kortleven, C., Bressler, S. L., and Williams, S. (2014). "Reversal of theta rhythm flow through intact hippocampal circuits." In: *Nature Neuroscience* 17.10, pp. 1362–1370.

Jadhav, S. P. P., Rothschild, G., Roumis, D. K. K., and Frank, L. M. M. (2016). "Coordinated excitation and inhibition of prefrontal ensem- bles during awake hippocampal sharp-wave ripple events." In: *Neuron* 90.1, pp. 113–127.

Jadhav, S. P., Kemere, C., German, P. W., and Frank, L. M. (2012). "Awake hippocampal sharp-wave ripples support spatial memory." In: *Science* 336.6087, pp. 1454–1458.

James, W. (1884). "What is an Emotion?" In: *Mind* 9.34, pp. 188–205.

Janczewski, W. A., Tashima, A., Hsu, P., Cui, Y., and Feldman, J. L. (2013). "Role of inhibition in respiratory pattern generation." In: *The Journal of neuroscience : the official journal of the Society for Neuroscience* 33.13, pp. 5454–5465.

Jarosiewicz, B. and Skaggs, W. E. (2004). "Level of Arousal During the Small Irregular Activity State in the Rat Hippocampal EEG." In: *Journal of Neurophysiology* 91.6, pp. 2649–2657.

Jasper, H (1949). "Diffuse projection systems: the integrative action of the thalamic reticular system." In: *Electroencephalography and clinical neurophysiology* 1.4, 405–19–discussion 419–20.

Javorka, K, Tomori, Z, and Zavarská, L (1982). "Mechanics of breathing during sneezing and crying in premature newborns." In: *European journal of respiratory diseases* 63.5, pp. 442–8.

Jay, T. M. and Witter, M. P. (1991). "Distribution of hippocampal CA1 and subicular efferents in the prefrontal cortex of the rat studied by means of anterograde transport of Phaseolus vulgaris-leucoagglutinin." In: *Journal of Comparative Neurology* 313.4, pp. 574–586.

Jenkins, J. G. and Dallenbach, K. M. (1924). "Obliviscence during sleep and waking." In: *The American Journal of Psychology*.

Jerath, R., Edry, J. W., Barnes, V. A., and Jerath, V. (2006). "Physiology of long pranayamic breathing: neural respiratory elements may provide a mechanism that explains how slow deep breathing shifts the autonomic nervous system." In: *Medical hypotheses* 67.3, pp. 566–571.

Ji, D. and Wilson, M. A. (2006). "Coordinated memory replay in the visual cortex and hippocampus during sleep." In: *Nature neuroscience* 10.1, pp. 100–107.

Jin, J. and Maren, S. (2015). "Prefrontal-Hippocampal Interactions in Memory and Emotion." In: *Frontiers in systems neuroscience* 9, p. 170.

Jodoj, E, Chiang, C, Aston-Jones, G, Jodo, E, Chiang, C, and Aston-Jones, G (1998). "Potent excitatory influence of prefrontal cortex activity on noradrenergic locus coeruleus neurons." In: *Neuroscience* 83.1, pp. 63–79.

Johansen, J. P., Fields, H. L., and Manning, B. H. (2001). "The affective component of pain in rodents: direct evidence for a contribution of the anterior cingulate cortex." In: *Proceedings of the National Academy of Sciences of the United States of America* 98.14, pp. 8077–8082.

Johansen, J. P. and Fields, H. L. (2004). "Glutamatergic activation of anterior cingulate cortex produces an aversive teaching signal." In: *Nature Neuroscience* 7.4, pp. 398–403.

Johnson, D. M. G., Illig, K. R., Behan, M., and Haberly, L. B. (2000). "New Features of Connectivity in Piriform Cortex Visualized by Intracellular Injection of Pyramidal Cells Suggest that "Primary" Olfactory Cortex Functions Like "Association" Cortex in Other Sensory Systems." In: *Journal of Neuroscience* 20.18, pp. 6974–6982.

Johnson, L. A., Euston, D. R., Tatsuno, M., and McNaughton, B. L. (2010). "Stored-Trace Reactivation in Rat Prefrontal Cortex Is Correlated with Down-to-Up State Fluctuation Density." In: *Journal of Neuroscience* 30.7, pp. 2650–2661.

Jones, E. G. (1985). "Principles of Thalamic Organization." In: *The Thalamus*. Boston, MA: Springer US, pp. 85–149.

Jones, M. W. and Wilson, M. A. (2005a). "Phase precession of medial prefrontal cortical activity relative to the hippocampal theta rhythm." In: *Hippocampus* 15.7, pp. 867–873.

Jones, M. W. and Wilson, M. A. (2005b). "Theta rhythms coordinate hippocampal-prefrontal interactions in a spatial memory task." In: *PLoS Biology* 3.12, pp. 1–13.

Jones, S. R., Kerr, C. E., Wan, Q., Pritchett, D. L., Hamalainen, M., and Moore, C. I. (2010). "Cued Spatial Attention Drives Functionally Relevant Modulation of the Mu Rhythm in Primary Somatosensory Cortex." In: *Journal of Neuroscience* 30.41, pp. 13760–13765.

Jouvet, M (1962). *Recherches sur les structures nerveuses et les mécanismes responsables des différentes phases du sommeil physiologique*. Arch Ital Biol.

Jouvet, M. (1969). "Biogenic Amines and the States of Sleep." In: *Science* 163.3862, pp. 32–41.

Jung, J., Hudry, J., Ryvlin, P., Royet, J.-P., Bertrand, O., and Lachaux, J.-P. (2006). "Functional significance of olfactory-induced oscillations in the human amygdala." In: *Cerebral Cortex* 16.1, pp. 1–8.

Jung, R. and Kornmüller, A. E. (1938). "Eine Methodik der Ableitung Iokalisierter Potentialschwankungen aus subcorticalen Hirngebieten." In: *Archiv für Psychiatrie und Nervenkrankheiten* 109.1, pp. 1–30.

Jürgens, U. (2009). *The Neural Control of Vocalization in Mammals: A Review*.

Jutras, M. J., Fries, P., and Buffalo, E. A. (2009). "Gamma-Band Synchronization in the Macaque Hippocampus and Memory Formation." In: *Journal of Neuroscience* 29.40, pp. 12521–12531.

Kajikawa, Y. and Schroeder, C. E. (2011). "How local is the local field potential?" In: *Neuron* 72.5, pp. 847–858.

Kanai, T. and Wang, S. C. (1962). "Localization of the central vocalization mechanism in the brain stem of the cat." In: *Experimental neurology* 6.5, pp. 426–434.

Kanamori, N., Sakai, K., and Jouvet, M. (1980). "Neuronal activity specific to paradoxical sleep in the ventromedial medullary reticular formation of unrestrained cats." In: *Brain Research* 189.1, pp. 251–255.

Kandel, a, Buzsáki, G, and Buzsaki, G. (1997). "Cellular-synaptic generation of sleep spindles, spike-and-wave discharges, and evoked thalamocortical responses in the neocortex of the rat." In: *Journal of Neuroscience* 17.17, pp. 6783–6797.

Kaplan, R., Adhikari, M. H., Hindriks, R., Mantini, D., Murayama, Y., Logothetis, N. K., and Deco, G. (2016). "Hippocampal Sharp-Wave Ripples Influence Selective Activation of the Default Mode Network." In: *Current biology : CB* 26.5, pp. 686–691.

Kapp, B. S., Frysinger, R. C., Gallagher, M., and Haselton, J. R. (1979). "Amygdala central nucleus lesions: Effect on heart rate conditioning in the rabbit." In: *Physiology and Behavior* 23.6, pp. 1109–1117.

Karalis, N. and Sirota, A. (2018). "Breathing coordinates limbic network dynamics underlying memory consolidation." In: *bioRxiv*.

Karalis, N., Dejean, C., Chaudun, F., Khoder, S., R Rozeske, R., Wurtz, H., Bagur, S., Benchenane, K., Sirota, A., Courtin, J., and Herry, C. (2016). "4-Hz oscillations synchronize prefrontal-amygdala circuits during fear behavior." In: *Nature Neuroscience* 19.4, pp. 605–612.

Karlsson, M. P. and Frank, L. M. (2009). "Awake replay of remote experiences in the hippocampus." In: *Nature neuroscience* 12.7, pp. 913–918.

Katon, W. J., Richardson, L., Lozano, P., and McCauley, E. (2004). "The relationship of asthma and anxiety disorders." In: *Psychosomatic medicine* 66.3, pp. 349–355.

Katzner, S., Nauhaus, I., Benucci, A., Bonin, V., Ringach, D. L., and Carandini, M. (2009). "Local Origin of Field Potentials in Visual Cortex." In: *Neuron* 61.1, pp. 35–41.

Kay, L. M. and Laurent, G (1999). "Odor- and context-dependent modulation of mitral cell activity in behaving rats." In: *Nature neuroscience* 2.11, pp. 1003–1009.

Kay, L. M. and Freeman, W. J. (1998). "Bidirectional processing in the olfactory-limbic axis during olfactory behavior." In: *Behavioral Neuroscience* 112.3, pp. 541–553.

Kay, L. M., Beshel, J., Brea, J., Martin, C., Rojas-Líbano, D., and Kopell, N. (2009). "Olfactory oscillations: the what, how and what for." In: *Trends in neurosciences* 32.4, pp. 207–214.

Kepecs, A., Uchida, N., and Mainen, Z. F. (2006). "The sniff as a unit of olfactory processing." In: 31.2, pp. 167–179.

Kerr, C. E., Sacchet, M. D., Lazar, S. W., Moore, C. I., and Jones, S. R. (2013). "Mindfulness starts with the body: somatosensory attention and top-down modulation of cortical alpha rhythms in mindfulness meditation." In: *Frontiers in Human Neuroscience* 7, p. 12.

Kerr, K. M., Agster, K. L., Furtak, S. C., and Burwell, R. D. (2007). "Functional neuroanatomy of the parahippocampal region: the lateral and medial entorhinal areas." In: *Hippocampus* 17.9, pp. 697–708.

Khodagholy, D., Gelinas, J. N., and Buzsaki, G. (2017). "Learning-enhanced coupling between ripple oscillations in association cortices and hippocampus." In: *Science* 358.6361, pp. 369–372.

Kim, H., Ährlund-Richter, S., Wang, X., Deisseroth, K., and Carlén, M. (2016). "Prefrontal Parvalbumin Neurons in Control of Attention." In: *Cell* 164.1-2, pp. 208–218.

Kim, J. and Fanselow, M. (1992). "Modality-specific retrograde amnesia of fear." In: *Science* 256.5057, pp. 675–677.

Kim, S. and Lee, D. (2011). "Prefrontal cortex and impulsive decision making." In: *Biological Psychiatry* 69.12, pp. 1140–1146.

Kim, S. D., Rivers, S., Bevins, R. A., and Ayres, J. J. (1996). "Conditioned stimulus determinants of conditioned response form in pavlovian fear conditioning." In: *Journal of Experimental Psychology: Animal Behavior Processes* 22.1, pp. 87–104.

Kitamura, T., Ogawa, S. K., Roy, D. S., Okuyama, T., Morrissey, M. D., Smith, L. M., Redondo, R. L., and Tonegawa, S. (2017). "Engrams and circuits crucial for systems consolidation of a memory." In: *Science* 356.6333, pp. 73–78.

Klausberger, T., Magill, P. J., Márton, L. F., Roberts, J. D. B., Cobden, P. M., Buzsáki, G., Somogyi, P., Buzsaki, G., and Somogyi, P. (2003). "Brain-state- and cell-type-specific firing of hippocampal interneurons in vivo." In: *Nature* 421.6925, pp. 844–848.

Klavir, O., Genud-Gabai, R., and Paz, R. (2012). "Low-Frequency Stimulation Depresses the Primate Anterior-Cingulate-Cortex and Prevents Spontaneous Recovery of Aversive Memories." In: *Journal of Neuroscience* 32.25, pp. 8589–8597.

Kleinfeld, D., Deschênes, M., Wang, F., and Moore, J. D. (2014). "More than a rhythm of life: breathing as a binder of orofacial sensation." In: *Nature Publishing Group* 17.5, pp. 647–651.

Klimesch, W. (2012). "Alpha-band oscillations, attention, and controlled access to stored information." In: *Trends in Cognitive Sciences* 16.12, pp. 606–617.

Knapska, E., Macias, M., Mikosz, M., Nowak, A., Owczarek, D., Wawrzyniak, M., Pieprzyk, M., Cymerman, I. A., Werka, T., Sheng, M., Maren, S., Jaworski, J., and Kaczmarek, L. (2012). "Functional anatomy of neural circuits regulating fear and extinction." In: *Proceedings of the National Academy of Sciences* 109.42, pp. 17093–17098.

Knapska, E. and Maren, S. (2009). "Reciprocal patterns of c-Fos expression in the medial prefrontal cortex and amygdala after extinction and renewal of conditioned fear." In: *Learning & memory (Cold Spring Harbor, N.Y.)* 16.8, pp. 486–493.

Ko, H., Hofer, S. B., Pichler, B., Buchanan, K. A., Sjöström, P. J., and Mrsic-Flogel, T. D. (2011). "Functional specificity of local synaptic connections in neocortical networks." In: *Nature* 473.7345, pp. 87–91.

Ko, H., Cossell, L., Baragli, C., Antolik, J., Clopath, C., Hofer, S. B., and Mrsic-Flogel, T. D. (2013). "The emergence of functional microcircuits in visual cortex." In: *Nature* 496.7443, pp. 96–100.

Kobayakawa, K., Kobayakawa, R., Matsumoto, H., Oka, Y., Imai, T., Ikawa, M., Okabe, M., Ikeda, T., Itohara, S., Kikusui, T., Mori, K., and Sakano, H. (2007). "Innate versus learned odour processing in the mouse olfactory bulb." In: *Nature* 450.7169, pp. 503–508.

Koch, M (1999). "The neurobiology of startle." In: *Progress in neurobiology* 59.2, pp. 107–128.

Kocsis, B and Vertes, R. P. (1994). "Characterization of neurons of the supramammillary nucleus and mammillary body that discharge rhythmically with the hippocampal theta rhythm in the rat." In: *Journal of Neuroscience* 14.11 Pt 2, pp. 7040–7052.

Kocsis, B and Vertes, R. P. (1992). "Dorsal raphe neurons: synchronous discharge with the theta rhythm of the hippocampus in the freely behaving rat." In: *Journal of neurophysiology* 68.4, pp. 1463–7.

Kocsis, B., Di Prisco, G. V., and Vertes, R. P. (2001). "Theta synchronization in the limbic system: The role of Gudden's tegmental nuclei." In: *European Journal of Neuroscience* 13.2, pp. 381–388.

Komisaruk, B. R. (1970). "Synchrony between limbic system theta activity and rhythmical behavior in rats." In: *Journal of comparative and physiological psychology* 70.3, pp. 482–492.

König, P., Engel, A. K., and Singer, W. (1996). "Integrator or coincidence detector? The role of the cortical neuron revisited." In: *Trends in Neurosciences* 19.4, pp. 130–137.

Krech, D, Rosenzweig, M. R., and Bennett, E. L. (1964). "Chemical and anatomical plasticity of brain." In: *Science*.

Kreiter, A. K. and Singer, W. (1996). "Stimulus-Dependent Synchronization of Neuronal Responses in the Visual Cortex of the Awake Macaque Monkey." In: *Journal of Neuroscience* 76.7, pp. 2381–2396.

Krieger, J. (2005). "Respiratory Physiology: Breathing in Normal Subjects BT - Principles and Practice of Sleep Medicine." In: *Principles and Practice of Sleep Medicine*. Elsevier, pp. 232–244.

Krout, K. E., Belzer, R. E., and Loewy, A. D. (2002). "Brainstem projections to midline and intralaminar thalamic nuclei of the rat." In: *The Journal of comparative neurology* 448.1, pp. 53–101.

Kubota, Y., Sato, W., Toichi, M., Murai, T., Okada, T., Hayashi, A., and Sengoku, A. (2001). "Frontal midline theta rhythm is correlated with cardiac autonomic activities during the performance of an attention demanding meditation procedure." In: *Cognitive Brain Research* 11.2, pp. 281–287.

Kuhlman, W. N. (1978). "Functional topography of the human mu rhythm." In: *Electroencephalography and Clinical Neurophysiology* 44.1, pp. 83–93.

Kwag, J. and Paulsen, O. (2009). "The timing of external input controls the sign of plasticity at local synapses." In: *Nature Neuroscience* 12.10, pp. 1219–1221.

Lancel, M., Riezen, H. van, and Glatt, A. (1992). "The time course of σ activity and slow-wave activity during NREMS in cortical and thalamic EEG of the cat during baseline and after 12 hours of wakefulness." In: *Brain Research* 596.1-2, pp. 285–295.

Lansink, C. S., Jackson, J. C., Lankelma, J. V., Ito, R., Robbins, T. W., Everitt, B. J., and Pennartz, C. M. A. (2012). "Reward Cues in Space: Commonalities and Differences in Neural Coding by Hippocampal and Ventral Striatal Ensembles." In: *Journal of Neuroscience* 32.36, pp. 12444–12459.

Lasztóczi, B. and Klausberger, T. (2014). "Layer-specific GABAergic control of distinct gamma oscillations in the CA1 hippocampus." In: *Neuron* 81.5, pp. 1126–1139.

Latchoumane, C. F. V., Ngo, H. V. V., Born, J., and Shin, H. S. (2017). "Thalamic spindles promote memory formation during sleep through triple phase-locking of cortical, thalamic, and hippocampal rhythms." In: *Neuron*.

Laurent, G and Davidowitz, H (1994). "Encoding of olfactory information with oscillating neural assemblies." In: *Science* 265.5180, pp. 1872–1875.

Laurent, V and Westbrook, R. F. (2009). "Inactivation of the infralimbic but not the prelimbic cortex impairs consolidation and retrieval of fear extinction." In: *Learning & Memory*.

Leaf, R. C. and Muller, S. A. (1965). "Simple Method for Cer Conditioning and Measurement." In: *Psychological Reports* 17.1, pp. 211–215.

Lechner, H. A., Squire, L. R., and Byrne, J. H. (1999). "100 Years of Consolidation— Remembering Müller and Pilzecker." In: *Learning & Memory* 6, pp. 77–87.

LeDoux, J. E. (2000). "Emotion circuits in the brain." In: *Annual Review of Neuroscience* 23.1, pp. 155–184.

LeDoux, J. E., Farb, C, and Ruggiero, D. a. (1990). "Topographic organization of neurons in the acoustic thalamus that project to the amygdala." In: *Journal of Neuroscience* 10.4, pp. 1043–1054.

LeDoux, J. E., Iwata, J, Cicchetti, P, and Reis, D. J. (1988). "Different projections of the central amygdaloid nucleus mediate autonomic and behavioral correlates of conditioned fear." In: *The Journal of Neuroscience* 8.7, pp. 2517–2529.

Lee, A. M., Hoy, J. L., Bonci, A., Wilbrecht, L., Stryker, M. P., and Niell, C. M. (2014). "Identification of a brainstem circuit regulating visual cortical state in parallel with locomotion." In: *Neuron* 83.2, pp. 455–466.

Lee, A. K. and Wilson, M. A. (2002). "Memory of sequential experience in the hippocampus during slow wave sleep." In: *Neuron* 36.6, pp. 1183–1194.

Leemburg, S., Vyazovskiy, V. V., Olcese, U., Bassetti, C. L., Tononi, G., and Cirelli, C. (2010). "Sleep homeostasis in the rat is preserved during chronic sleep restriction." In: *Proceedings of the National Academy of Sciences of the United States of America* 107.36, pp. 15939–15944.

Lega, B. C., Jacobs, J., and Kahana, M. (2012). "Human hippocampal theta oscillations and the formation of episodic memories." In: *Hippocampus* 22.4, pp. 748–761.

Lemieux, M., Chauvette, S., and Timofeev, I. (2015). "Neocortical inhibitory activities and long-range afferents contribute to the synchronous onset of silent states of the neocortical slow oscillation." In: *Journal of Neurophysiology* 113.3, pp. 768–779.

Leonard, T. K., Mikkila, J. M., Eskandar, E. N., Gerrard, J. L., Kaping, D, Patel, S. R., Womelsdorf, T, and Hoffman, K. L. (2015). "Sharp Wave Ripples during Visual Exploration in the Primate Hippocampus." In: *Journal of Neuroscience* 35.44, pp. 14771–14782.

Leonard, T. K. and Hoffman, K. L. (2016). "Sharp-Wave Ripples in Primates Are Enhanced near Remembered Visual Objects." In: *Current biology : CB*.

Lepousez, G. and Lledo, P.-M. (2013). "Odor discrimination requires proper olfactory fast oscillations in awake mice." In: *Neuron* 80.4, pp. 1010–1024.

Lesburguères, E., Gobbo, O. L., Alaux-Cantin, S., Hambucken, A., Trifilieff, P., and Bontempi, B. (2011). "Early tagging of cortical networks is required for the formation of enduring associative memory." In: *Science* 331.6019, pp. 924–928.

Lesting, J., Narayanan, R. T., Kluge, C., Sangha, S., Seidenbecher, T., and Pape, H. C. (2011). "Patterns of coupled theta activity in amygdala-hippocampal-prefrontal cortical circuits during fear extinction." In: *PLoS ONE* 6.6, e21714.

Lesting, J., Daldrup, T., Narayanan, V., Himpe, C., Seidenbecher, T., and Pape, H. C. (2013). "Directional Theta Coherence in Prefrontal Cortical to Amygdalo-Hippocampal Pathways Signals Fear Extinction." In: *PLoS ONE* 8.10, e77707.

Leung, L. W. S. and Borst, J. G. G. (1987). "Electrical activity of the cingulate cortex. I. Generating mechanisms and relations to behavior." In: *Brain research* 407.1, pp. 68–80.

Leutgeb, S and Leutgeb, J. K. (2007). "Pattern separation, pattern completion, and new neuronal codes within a continuous CA3 map." In: *Learning & Memory* 14.11, pp. 745–757.

Levy, W. B. and Steward, O. (1983). "Temporal contiguity requirements for long-term associative potentiation/depression in the hippocampus." In: *Neuroscience* 8.4, pp. 791–797.

Lewicki, M. (1998). "A review of methods for spike sorting: the detection and classification of neural action potentials." In: *Network: Computation in Neural Systems* 9.4, R53–R78.

Liberzon, I. and Abelson, J. L. (2016). "Context Processing and the Neurobiology of Post-Traumatic Stress Disorder." In: *Neuron* 92.1, pp. 14–30.

Likhtik, E. and Gordon, J. A. (2013). "A Surprised Amygdala Looks to the Cortex for Meaning." In: *Neuron* 80.5, pp. 1109–1111.

Likhtik, E. and Gordon, J. A. (2014). *Circuits in sync: Decoding theta communication in fear and safety*.

Likhtik, E., Stujenske, J. M., Topiwala, M. A., Harris, A. Z., and Gordon, J. A. (2014). "Prefrontal entrainment of amygdala activity signals safety in learned fear and innate anxiety." In: *Nature Neuroscience* 17.1, pp. 106–113.

Liljenstrom, H and Hasselmo, M. E. (1995). "Cholinergic modulation of cortical oscillatory dynamics." In: *J Neurophysiol* 74.1, pp. 288–297.

Lindén, H., Tetzlaff, T., Potjans, T. C., Pettersen, K. H., Grün, S., Diesmann, M., and Einevoll, G. T. (2011). "Modeling the Spatial Reach of the LFP." In: *Neuron* 72.5, pp. 859–872.

Linster, C and Hasselmo, M. E. (2000). "Neural activity in the horizontal limb of the diagonal band of broca can be modulated by electrical stimulation of the olfactory bulb and cortex in rats." In: *Neuroscience letters* 282.3, pp. 157–60.

Lisman, J. E. (1997). "Bursts as a unit of neural information: Making unreliable synapses reliable." In: *Trends in Neurosciences* 20.1, pp. 38–43.

Lisman, J. E. and Jensen, O. (2013). "The Theta-Gamma Neural Code." In: *Neuron* 77.6, pp. 1002–1016.

Lisman, J. (2010). "Working memory: The importance of theta and gamma oscillations." In: *Current Biology* 20.11.

Litaudon, P, Amat, C, and Bertrand, B (2003). "Piriform cortex functional heterogeneity revealed by cellular responses to odours." In: *European Journal of Neuroscience* 17.11, pp. 2457–2461.

Liu, Y., McAfee, S. S., and Heck, D. H. (2017). "Hippocampal sharp-wave ripples in awake mice are entrained by respiration." In: *Scientific reports* 7.1, p. 8950.

Livneh, U. and Paz, R. (2012). "Amygdala-prefrontal synchronization underlies resistance to extinction of aversive memories." In: *Neuron* 75.1, pp. 133–142.

Llinas, R. R., Grace, A. A., and Yarom, Y. (1991). "In vitro neurons in mammalian cortical layer 4 exhibit intrinsic oscillatory activity in the 10- to 50-Hz frequency range." In: *Proceedings of the National Academy of Sciences* 88.3, pp. 897–901.

Llinas, R. (1988). "The intrinsic electrophysiological properties of mammalian neurons: insights into central nervous system function." In: *Science* 242.4886, pp. 1654–1664.

Llinas, R. and Ribary, U. (1993). "Coherent 40-Hz oscillation characterizes dream state in humans." In: *Proceedings of the National Academy of Sciences* 90.5, pp. 2078–2081.

Lockmann, A. L. V., Laplagne, D. A., Leão, R. N., and Tort, A. B. L. (2016). "A respiration-coupled rhythm in the rat hippocampus independent of theta and slow oscillations." In: *Journal of Neuroscience* 36.19, pp. 5338–5352.

Lofving, B (1961). "Cardiovascular adjustments induced from the rostral cingulate gyrus with special reference to sympatho-inhibitory mechanisms." In: *Acta physiologica Scandinavica. Supplementum* 53.184, pp. 1–82.

Logothetis, N. K., Eschenko, O., Murayama, Y., Augath, M., Steudel, T., Evrard, H. C., Besserve, M., and Oeltermann, A. (2012). "Hippocampal-cortical interaction during periods of subcortical silence." In: *Nature* 491.7425, pp. 547–553.

Logothetis, N. K., Kayser, C., and Oeltermann, A. (2007). "In vivo measurement of cortical impedance spectrum in monkeys: implications for signal propagation." In: *Neuron* 55.5, pp. 809–823.

Loomis, A. L., Harvey, E. N., and Hobart, G. A. (1938). "Distribution of disturbance-patterns in the human electroencephalogram with special reference to sleep." In: *Journal of Neurophysiology*.

Lopes da Silva, F. H., Lierop, T. H. van, Schrijer, C. F., and Storm van Leeuwen, W. (1973). "Organization of thalamic and cortical alpha rhythms: Spectra and coherences." In: *Electroencephalography and Clinical Neurophysiology* 35.6, pp. 627–639.

Lopes da Silva, F. H., Vos, J. E., Mooibroek, J., and Rotterdam, A. van (1980). "Relative contributions of intracortical and thalamo-cortical processes in the generation of alpha rhythms, revealed by partial coherence analysis." In: *Electroencephalography and Clinical Neurophysiology* 50.5-6, pp. 449–456.

Lopes, G., Bonacchi, N., FrazÃ£o, J., Neto, J. P., Atallah, B. V., Soares, S., Moreira, L., Matias, S., Itskov, P. M., Correia, P. A., Medina, R. E., Calcaterra, L., Dreosti, E., Paton, J. J., and Kampff, A. R. (2015). "Bonsai: an event-based framework for processing and controlling data streams." In: *Frontiers in Neuroinformatics* 9.

López-Aguado, L, Ibarz, J. M., and Herreras, O (2001). "Activity-dependent changes of tissue resistivity in the CA1 region in vivo are layer-specific: modulation of evoked potentials." In: *Neuroscience* 108.2, pp. 249–262.

Lorente de No, R (1947). "Analysis of the distribution of the action currents of nerve in volume conductors." In: *Studies from the Rockefeller institute for medical research. Reprints. Rockefeller Institute for Medical Research* 132, pp. 384–477.

Lörincz, a and Buzsaki, G. (2000). "Two-phase computational model training long-term memories in the entorhinal-hippocampal region." In: *Annals of the New York Academy of Sciences* 911, pp. 83–111.

Los Cobos Pallares, F. Pérez de, Bautista, T. G., Stanić, D., Egger, V., and Dutschmann, M. (2016). "Brainstem-mediated sniffing and respiratory modulation during odor stimulation." In: *Respiratory physiology & neurobiology* 233, pp. 17–24.

Lu, J., Sherman, D., Devor, M., and Saper, C. B. (2006). "A putative flip-flop switch for control of REM sleep." In: *Nature* 441.7093, pp. 589–594.

Luczak, A., Bartho, P., Marguet, S. L., Buzsaki, G., and Harris, K. D. (2007). "Sequential structure of neocortical spontaneous activity in vivo." In: *Proceedings of the National Academy of Sciences* 104.1, pp. 347–352.

Luczak, A., Bartho, P., and Harris, K. D. (2013). "Gating of Sensory Input by Spontaneous Cortical Activity." In: *Journal of Neuroscience* 33.4, pp. 1684–1695.

Luczak, A., Barthó, P., and Harris, K. D. (2009). "Spontaneous Events Outline the Realm of Possible Sensory Responses in Neocortical Populations." In: *Neuron* 62.3, pp. 413–425.

Ludwig, K. A., Uram, J. D., Yang, J., Martin, D. C., and Kipke, D. R. (2006). "Chronic neural recordings using silicon microelectrode arrays electrochemically deposited with a poly(3,4-ethylenedioxythiophene) (PEDOT) film." In: *Journal of Neural Engineering* 3.1, pp. 59–70.

Ludwig, K. A., Langhals, N. B., Joseph, M. D., Richardson-Burns, S. M., Hendricks, J. L., and Kipke, D. R. (2011). "Poly(3,4-ethylenedioxythiophene) (PEDOT) polymer coatings facilitate smaller neural recording electrodes." In: *Journal of Neural Engineering* 8.1.

Luo, L., Callaway, E. M., and Svoboda, K. (2008). "Genetic Dissection of Neural Circuits." In: *Neuron* 57.5, pp. 634–660.

Luskin, M. B. and Price, J. L. (1983a). "The laminar distribution of intracortical fibers originating in the olfactory cortex of the rat." In: *Journal of Comparative Neurology* 216.3, pp. 292–302.

Luskin, M. B. and Price, J. L. (1983b). "The topographic organization of associational fibers of the olfactory system in the rat, including centrifugal fibers to the olfactory bulb." In: *Journal of Comparative Neurology* 216.3, pp. 264–291.

Lutz, A., Greischar, L. L., Rawlings, N. B., Ricard, M., and Davidson, R. J. (2004). "Long-term meditators self-induce high-amplitude gamma synchrony during mental practice." In: *Proceedings of the National Academy of Sciences* 101.46, pp. 16369–16373.

Lyamin, O. I., Manger, P. R., Ridgway, S. H., Mukhametov, L. M., and Siegel, J. M. (2008). "Cetacean sleep: an unusual form of mammalian sleep." In: *Neuroscience & Biobehavioral Reviews* 32.8, pp. 1451–1484.

Ma, M, Chen, W. R., and Shepherd, G. M. (1999). "Electrophysiological characterization of rat and mouse olfactory receptor neurons from an intact epithelial preparation." In: *J.Neurosci.Methods* 92.0165-0270, pp. 31–40.

MacLean, J. N., Watson, B. O., Aaron, G. B., and Yuste, R. (2005). "Internal dynamics determine the cortical response to thalamic stimulation." In: *Neuron* 48.5, pp. 811–823.

Maclean, P. D. (1949). "Psychosomatic disease and the visceral brain; recent developments bearing on the Papez theory of emotion." In: *Psychosomatic medicine* 11.6, pp. 338–353.

MacLeod, K, Bäcker, A, and Laurent, G (1998). "Who reads temporal information contained across synchronized and oscillatory spike trains?" In: *Nature* 395.6703, pp. 693–698.

Macrides, F and Chorover, S. L. (1972). "Olfactory bulb units: activity correlated with inhalation cycles and odor quality." In: *Science* 175.4017, pp. 84–87.

Macrides, F. (1975). "Temporal relationships between hippocampal slow waves and exploratory sniffing in hamsters." In: *Behavioral Biology* 14.3, pp. 295–308.

Macrides, F., Eichenbaum, H. B., and Forbes, W. B. (1982). "Temporal Relationship Between Sniffing and the Limbic 8 Rhythm During Odor Discrimination Reversal Learning'." In: *Journal of Neuroscience* 2.12, pp. 1705–1717.

Magee, J. C. (2000). "Dendritic integration of excitatory synaptic input." In: *Nature Reviews Neuroscience* 1.3, pp. 1–10.

Magoun, H. W., Atlas, D., Ingersoll, E. H., and Ranson, S. W. (1937). "Associated facial, vocal and respiratory components of emotional expression: An experimental study." In: *Journal of Neurology, Neurosurgery and Psychiatry* S1-17.67, pp. 241–255.

Maingret, N., Girardeau, G., Todorova, R., Goutierre, M., and Zugaro, M. (2016). "Hippocampo-cortical coupling mediates memory consolidation during sleep." In: *Nature Neuroscience* 19.7, pp. 959–964.

Mainland, J. and Sobel, N. (2006). "The sniff is part of the olfactory percept." In: 31.2, pp. 181–196.

Makeig, S., J. Bell., A., Jung, T.-P., and Sejnowski, T. J. (1996). "Independent Component Analysis of Electroencephalographic Data." In: *Advances in Neural Information Processing Systems* 8, pp. 145–151.

Malnic, B, Hirono, J, Sato, T, and Buck, L. B. (1999). "Combinatorial receptor codes for odors." In: *Cell* 96.5, pp. 713–723.

Manns, I. D., Alonso, A., and Jones, B. E. (2003). "Rhythmically Discharging Basal Forebrain Units Comprise Cholinergic, GABAergic, and Putative Glutamatergic Cells." In: *Journal of Neurophysiology* 89.2, pp. 1057–1066.

Mansouri, F. A., Tanaka, K., and Buckley, M. J. (2009). *Conflict-induced behavioural adjustment: A clue to the executive functions of the prefrontal cortex*.

Mantini, D, Perrucci, M. G., Del Gratta, C, Romani, G. L., and Corbetta, M (2007). "Electrophysiological signatures of resting state networks in the human brain." In: *Proceedings of the National Academy of Sciences* 104.32, pp. 13170–13175.

Maquet, P, Laureys, S, Peigneux, P, and Fuchs, S (2000). "Experience-dependent changes in cerebral activation during human REM sleep." In: *Nature.*

Marder, E. and Calabrese, R. L. (1996). "Principles of rhythmic motor pattern generation." In: *Physiological Reviews* 76.3, pp. 687–717.

Maren, S. and Quirk, G. J. (2004). "Neuronal signalling of fear memory." In: *Nature Reviews Neuroscience* 5.11, pp. 844–852.

Maren, S., Phan, K. L., and Liberzon, I. (2013). "The contextual brain: Implications for fear conditioning, extinction and psychopathology." In: *Nature Reviews Neuroscience* 14.6, pp. 417–428.

Markram, H., Lübke, J., Frotscher, M., and Sakmann, B. (1997). "Regulation of synaptic efficacy by coincidence of postsynaptic APs and EPSPs." In: *Science* 275.5297, pp. 213–215.

Márquez-Ruiz, J. and Escudero, M. (2008). "Tonic and phasic phenomena underlying eye movements during sleep in the cat." In: *Journal of Physiology* 586.14, pp. 3461–3477.

Marr, D (1971). "Simple memory: a theory for archicortex." In: *Philosophical Transactions of the Royal Society B: Biological Sciences* 262.841, pp. 23–81.

Marrosu, F., Portas, C., Mascia, M. S., Casu, M. A., Fà, M., Giagheddu, M., Imperato, A., and Gessa, G. L. (1995). "Microdialysis measurement of cortical and hippocampal acetylcholine release during sleep-wake cycle in freely moving cats." In: *Brain Research* 671.2, pp. 329–332.

Marschner, A., Kalisch, R., Vervliet, B., Vansteenwegen, D., and Buchel, C. (2008). "Dissociable Roles for the Hippocampus and the Amygdala in Human Cued versus Context Fear Conditioning." In: *Journal of Neuroscience* 28.36, pp. 9030–9036.

Marshall, L., Mölle, M., Hallschmid, M., and Born, J. (2004). "Transcranial direct current stimulation during sleep improves declarative memory." In: *The Journal of neuroscience : the official journal of the Society for Neuroscience* 24.44, pp. 9985–9992.

Marshall, L., Helgadóttir, H., Mölle, M., and Born, J. (2006). "Boosting slow oscillations during sleep potentiates memory." In: *Nature* 444.7119, pp. 610–613.

Martin, C., Gervais, R., Messaoudi, B., and Ravel, N. (2006). "Learning-induced oscillatory activities correlated to odour recognition: A network activity." In: *European Journal of Neuroscience* 23.7, pp. 1801–1810.

Marzetti, L, Della Penna, S, Nolte, G, Franciotti, R, Stefanics, G, and Romani, G. L. (2007). "A cartesian time–frequency approach to reveal brain interaction dynamics." In: *Brain topography* 19.3, pp. 147–154.

Mason, P., Gao, K., and Genzen, J. R. (2007). "Serotonergic Raphe Magnus Cell Discharge Reflects Ongoing Autonomic and Respiratory Activities." In: *Journal of Neurophysiology* 98.4, pp. 1919–1927.

Massimini, M (2004). "The Sleep Slow Oscillation as a Traveling Wave." In: 24.31, pp. 6862–6870.

Massimini, M and Amzica, F (2001). "Extracellular calcium fluctuations and intracellular potentials in the cortex during the slow sleep oscillation." In: *Journal of Neurophysiology* 85.3, pp. 1346–1350.

Massimini, M., Huber, R., Ferrarelli, F., Hill, S., and Tononi, G. (2004). "The Sleep Slow Oscillation as a Traveling Wave." In: *Journal of Neuroscience* 24.31, pp. 6862–6870.

Matsumoto, K., Ishikawa, T., Matsuki, N., and Ikegaya, Y. (2013). "Multineuronal spike sequences repeat with millisecond precision." In: *Frontiers in neural circuits* 7, p. 112.

Matsumoto, N., Okamoto, K., Takagi, Y., and Ikegaya, Y. (2016). "3-Hz subthreshold oscillations of CA2 neurons In vivo." In: *Hippocampus* 26.12, pp. 1570–1578.

Matsuo, K. and Palmer, J. B. (2015). "Coordination of oro-pharyngeal food transport during chewing and respiratory phase." In: *Physiology and Behavior* 142, pp. 52–56.

Matyas, F., Lee, J., Shin, H.-S., and Acsády, L. (2014). "The fear circuit of the mouse forebrain: connections between the mediodorsal thalamus, frontal cortices and basolateral amygdala." In: *European Journal of Neuroscience* 39.11, pp. 1810–1823.

Maviel, T., Durkin, T. P., Menzaghi, F., and Bontempi, B. (2004). "Sites of neocortical reorganization critical for remote spatial memory." In: *Science* 305.5680, pp. 96–99.

Maynard, E. M., Fernandez, E., and Normann, R. A. (2000). "A technique to prevent dural adhesions to chronically implanted microelectrode arrays." In: *Journal of Neuroscience Methods* 97.2, pp. 93–101.

Mayou, R and Farmer, A (2002). "Functional somatic symptoms and syndromes." In: *British Medical Journal*.

McAfee, S. S., Ogg, M. C., Ross, J. M., Liu, Y., Fletcher, M. L., and Heck, D. H. (2016). "Minimally invasive highly precise monitoring of respiratory rhythm in the mouse using an epithelial temperature probe." In: *Journal of Neuroscience Methods* 263, pp. 89–94.

McCarley, R. W. and Hobson, J. A. (1975). "Neuronal excitability modulation over the sleep cycle: a structural and mathematical model." In: *Science* 189.4196, pp. 58–60.

McClelland, J. L., McNaughton, B. L., and O'Reilly, R. C. (1995). "Why there are complementary learning systems in the hippocampus and neocortex: Insights from the successes and failures of connectionist models of learning and memory." In: *Psychological review* 102.3, pp. 419–57.

McDonald, A. J. (1991). "Organization of amygdaloid projections to the prefrontal cortex and associated striatum in the rat." In: *Neuroscience* 44.1, pp. 1–14.

McDonald, A. J. (1998). "Cortical pathways to the mammalian amygdala." In: *Progress in neurobiology* 55.3, pp. 257–332.

McGaugh, J. L. (2000). "Memory–a Century of Consolidation." In: *Science* 287.5451, pp. 248–251.

McGaugh, J. L. (1999). *The perseveration-consolidation hypothesis: Mueller and Pilzecker, 1900*.

McGaugh, J. L. (2015). "Consolidating memories." In: *Annual review of psychology* 66, pp. 1–24.

McGinley, M. J., Vinck, M., Reimer, J., Batista-Brito, R., Zagha, E., Cadwell, C. R., Tolias, A. S., Cardin, J. A., and McCormick, D. A. (2015). "Waking State: Rapid Variations Modulate Neural and Behavioral Responses." In: *Neuron* 87.6, pp. 1143–1161.

McGinty, D. J. and Sterman, M. B. (1968). "Sleep suppression after basal forebrain lesions in the cat." In: *Science* 160.3833, pp. 1253–1255.

McKay, L. C., Evans, K. C., Frackowiak, R. S. J., and Corfield, D. R. (2003). "Neural correlates of voluntary breathing in humans." In: *Journal of Applied Physiology* 95.3, pp. 1170–1178.

McNaughton, B. L. and Morris, R. (1987). "Hippocampal synaptic enhancement and information storage within a distributed memory system." In: *Trends in Neurosciences*.

Meddis, R (1975). "On the function of sleep." In: *Animal Behaviour* 23.3, pp. 676–691.

Meer, M. A. van der (2009). "Low and high gamma oscillations in rat ventral striatum have distinct relationships to behavior, reward, and spiking activity on a learned spatial decision task." In: *Frontiers in Integrative Neuroscience* 3, p. 9.

Meuret, A. E., Rosenfield, D., Hofmann, S. G., Suvak, M. K., and Roth, W. T. (2009). "Changes in respiration mediate changes in fear of bodily sensations in panic disorder." In: *Journal of Psychiatric Research* 43.6, pp. 634–641.

Meynert, T (1868). *Der Bau der Gross-Hirnrinde: und seine örtlichen Verschiedenheiten, nebst einem pathologisch-anatomischen Corollarium*.

Milad, M. R. and Quirk, G. J. (2002). "Neurons in medial prefrontal cortex signal memory for fear extinction." In: *Nature* 420.6911, pp. 70–74.

Miller, E. K. (2000). "The prefrontal cortex and cognitive control." In: *Nature Reviews Neuroscience* 1.1, pp. 59–65.

Milner, B (1963). "Effects of different brain lesions on card sorting: The role of the frontal lobes." In: *Arch Neurol* 9.1, pp. 90–100.

Milstein, A. D., Bloss, E. B., Apostolides, P. F., Vaidya, S. P., Dilly, G. A., Zemelman, B. V., and Magee, J. C. (2015). "Inhibitory Gating of Input Comparison in the CA1 Microcircuit." In: *Neuron* 87.6, pp. 1274–1289.

Milstein, J. N. and Koch, C. (2008). "Dynamic Moment Analysis of the Extracellular Electric Field of a Biologically Realistic Spiking Neuron." In: *Neural Computation* 20.8, pp. 2070–2084.

Mitchell, S. J. and Ranck, J. B. (1980). "Generation of theta rhythm in medial entorhinal cortex of freely moving rats." In: *Brain Research* 189.1, pp. 49–66.

Mitra, P. P., Pesaran, B, and Kleinfeld, D (1999). "Analysis of dynamic optical imaging data." In: *Imaging: a laboratory manual (...* 76.2, pp. 691–708.

Mitzdorf, U. (1985). "Current source-density method and application in cat cerebral cortex: investigation of evoked potentials and EEG phenomena." In: *Physiological Reviews* 65.1, pp. 37–100.

Miyamichi, K., Amat, F., Moussavi, F., Wang, C., Wickersham, I., Wall, N. R., Taniguchi, H., Tasic, B., Huang, Z. J., He, Z., Callaway, E. M., Horowitz, M. A., and Luo, L. (2011). "Cortical representations of olfactory input by trans-synaptic tracing." In: *Nature* 472.7342, pp. 191–199.

Miyawaki, H. and Diba, K. (2016). "Regulation of Hippocampal Firing by Network Oscillations during Sleep." In: *Current Biology* 26.7, pp. 893–902.

Mizuseki, K., Sirota, A., Pastalkova, E., and Buzsaki, G. (2009). "Theta oscillations provide temporal windows for local circuit computation in the entorhinal-hippocampal loop." In: *Neuron* 64.2, pp. 267–280.

Mizuseki, K., Diba, K., Pastalkova, E., and Buzsaki, G. (2011). "Hippocampal CA1 pyramidal cells form functionally distinct sublayers." In: *Nature Neuroscience* 14.9, pp. 1174–1183.

Moberly, A. H., Schreck, M., Bhattarai, J. P., Zweifel, L. S., Luo, W., and Ma, M. (2018). "Olfactory inputs modulate respiration-related rhythmic activity in the prefrontal cortex and freezing behavior." In: *Nature Communications*.

Mohajerani, M. H., McVea, D. A., Fingas, M., and Murphy, T. H. (2010). "Mirrored Bilateral Slow-Wave Cortical Activity within Local Circuits Revealed by Fast Bihemispheric Voltage-Sensitive Dye Imaging in Anesthetized and Awake Mice." In: *Journal of Neuroscience* 30.10, pp. 3745–3751.

Mohajerani, M. H., Chan, A. W., Mohsenvand, M., Ledue, J., Liu, R., McVea, D. A., Boyd, J. D., Wang, Y. T., Reimers, M., and Murphy, T. H. (2013). "Spontaneous cortical activity alternates between motifs defined by regional axonal projections." In: *Nature Neuroscience* 16.10, pp. 1426–1435.

Mokeichev, A., Okun, M., Barak, O., Katz, Y., Ben-Shahar, O., and Lampl, I. (2007). "Stochastic Emergence of Repeating Cortical Motifs in Spontaneous Membrane Potential Fluctuations In Vivo." In: *Neuron* 53.3, pp. 413–425.

Molle, M., Marshall, L., Gais, S., and Born, J. (2004). "Learning increases human electroencephalographic coherence during subsequent slow sleep oscillations." In: *Proceedings of the National Academy of Sciences* 101.38, pp. 13963–13968.

Mölle, M., Yeshenko, O., Marshall, L., Sara, S. J., and Born, J. (2006). "Hippocampal sharp wave-ripples linked to slow oscillations in rat slow-wave sleep." In: 96.1, pp. 62–70.

Mölle, M., Eschenko, O., Gais, S., Sara, S. J., and Born, J. (2009). "The influence of learning on sleep slow oscillations and associated spindles and ripples in humans and rats." In: *European Journal of Neuroscience* 29.5, pp. 1071–1081.

Monaco, J. D., Rao, G., Roth, E. D., and Knierim, J. J. (2014). "Attentive scanning behavior drives one-trial potentiation of hippocampal place fields." In: *Nature Neuroscience* 17.5, pp. 725–731.

Monckton, J. E. and McCormick, D. A. (2002). "Neuromodulatory role of serotonin in the ferret thalamus." In: *Journal of neurophysiology* 87.4, pp. 2124–36.

Montgomery, S. M. and Buzsaki, G. (2007). "Gamma oscillations dynamically couple hippocampal CA3 and CA1 regions during memory task performance." In: *Proceedings of the National Academy of Sciences* 104.36, pp. 14495–14500.

Moore, J. D., Deschênes, M., Furuta, T., Huber, D., Smear, M. C., Demers, M., and Kleinfeld, D. (2013). "Hierarchy of orofacial rhythms revealed through whisking and breathing." In: *Nature* 497.7448, pp. 205–210.

Moore, J. D., Kleinfeld, D., and Wang, F. (2014). "How the brainstem controls orofacial behaviors comprised of rhythmic actions." In: *Trends in Neurosciences* 37.7, pp. 370–380.

Morison, R. S. and Bassett, D. L. (1945). "Electrical Activity of the Thalamus and Basal Ganglia in Decorticate Cats." In: *Journal of Neurophysiology* 8.5, pp. 309–314.

Morison, R. S. and Dempsey, E. W. (1943). "Mechanism of thalamocortical augmentation and repetition." In: *American Journal of Physiology*.

Moroni, F., Nobili, L., Curcio, G., De Carli, F., Fratello, F., Marzano, C., De Gennaro, L., Ferrillo, F., Cossu, M., Francione, S., Russo, G. L., Bertini, M., and Ferrara, M. (2007). "Sleep in the human hippocampus: A stereo-EEG study." In: *PLoS ONE* 2.9.

Moroni, F., Nobili, L., Iaria, G., Sartori, I., Marzano, C., Tempesta, D., Proserpio, P., Lo Russo, G., Gozzo, F., Cipolli, C., De Gennaro, L., and Ferrara, M. (2014). "Hippocampal slow EEG frequencies during NREM sleep are involved in spatial memory consolidation in humans." In: *Hippocampus* 24.10, pp. 1157–1168.

Morris, R. G., Garrud, P, Rawlins, J. N., and O'Keefe, J (1982). "Place navigation impaired in rats with hippocampal lesions." In: *Nature* 297.5868, pp. 681–683.

Moyer, J. R., Thompson, L. T., and Disterhoft, J. F. (1996). "Trace eyeblink conditioning increases CA1 excitability in a transient and learning-specific manner." In: *Journal of Neuroscience* 16.17, pp. 5536–5546.

Muir, G. M. and Bilkey, D. K. (1998). "Synchronous modulation of perirhinal cortex neuronal activity during cholinergically mediated (Type II) hippocampal theta." In: *Hippocampus* 8.5, pp. 526–532.

Muir, G. M. and Bilkey, D. K. (2003). *Theta- and movement velocity-related firing of hippocampal neurons is disrupted by lesions centered on the perirhinal cortex*.

Muller, L., Piantoni, G., Koller, D., Cash, S. S., Halgren, E., and Sejnowski, T. J. (2016). "Rotating waves during human sleep spindles organize global patterns of activity that repeat precisely through the night." In: *eLife* 5.NOVEMBER2016, p. 1195.

Murphy, M., Riedner, B. A., Huber, R., Massimini, M., Ferrarelli, F., and Tononi, G. (2009). "Source modeling sleep slow waves." In: *Proceedings of the National Academy of Sciences of the United States of America* 106.5, pp. 1608–1613.

Murthy, V. N. and Fetz, E. E. (1992). "Coherent 25- to 35-Hz oscillations in the sensorimotor cortex of awake behaving monkeys." In: *Proceedings of the National Academy of Sciences* 89.12, pp. 5670–5674.

Nadasdy, Z, Hirase, H, Czurko, A, Csicsvari, J, and Buzsáki, G (1999). "Replay and time compression of recurring spike sequences in the hippocampus." In: *The Journal of neuroscience : the official journal of the Society for Neuroscience* 19.21, pp. 9497–9507.

Nadel, L. and Moscovitch, M. (1997). "Memory consolidation, retrograde amnesia and the hippocampal complex." In: *Current Opinion in Neurobiology* 7.2, pp. 217–227.

Narayanan, N. S. and Laubach, M. (2006). "Top-Down Control of Motor Cortex Ensembles by Dorsomedial Prefrontal Cortex." In: *Neuron* 52.5, pp. 921–931.

Natsume, K., Hallworth, N. E., Szgatti, T. L., and Bland, B. H. (1999). "Hippocampal theta-related cellular activity in the superior colliculus of the urethane-anesthetized rat." In: *Hippocampus* 9.5, pp. 500–509.

Neto, J. P., Lopes, G., Frazão, J., Nogueira, J., Lacerda, P., Baião, P., Aarts, A., Andrei, A., Musa, S., Fortunato, E., Barquinha, P., and Kampff, A. R. (2016). "Validating silicon polytrodes with paired juxtacellular recordings: method and dataset." In: *Journal of Neurophysiology* 116.2, pp. 892–903.

Neuman, A., Gunnbjörnsdottir, M., Tunsäter, A., Nyström, L., Franklin, K. A., Norrman, E., and Janson, C. (2006). "Dyspnea in relation to symptoms of anxiety and depression: A prospective population study." In: *Respiratory medicine* 100.10, pp. 1843–1849.

Neville, K. R. (2003). "Beta and Gamma Oscillations in the Olfactory System of the Urethane-Anesthetized Rat." In: *Journal of Neurophysiology* 90.6, pp. 3921–3930.

Ngo, H.-V. V., Miedema, A., Faude, I., Martinetz, T., Molle, M., and Born, J. (2015). "Driving Sleep Slow Oscillations by Auditory Closed-Loop Stimulation–A Self-Limiting Process." In: *Journal of Neuroscience* 35.17, pp. 6630–6638.

Ngo, H.-V. V., Claussen, J. C., Born, J., and Mölle, M. (2013). "Induction of slow oscillations by rhythmic acoustic stimulation." In: *Journal of sleep research* 22.1, pp. 22–31.

Nguyen Chi, V., Muller, C., Wolfenstetter, T., Yanovsky, Y., Draguhn, A., Tort, A. B. L., and Branka k, J. (2016). "Hippocampal respiration-driven rhythm distinct from theta Oscillations in awake mice." In: *Journal of Neuroscience* 36.1, pp. 162–177.

Nicholson, C. and Freeman, J. A. (1975). "Theory of current source-density analysis and determination of conductivity tensor for anuran cerebellum." In: *Journal of Neurophysiology* 38.2, pp. 356–368.

Nicholson, P. W. (1965). "Specific impedance of cerebral white matter." In: *Experimental Neurology* 13.4, pp. 386–401.

Nicolelis, M., Baccala, L., Lin, R., and Chapin, J. (1995). "Sensorimotor encoding by synchronous neural ensemble activity at multiple levels of the somatosensory system." In: *Science* 268.5215, pp. 1353–1358.

Nicolelis, M. A. L. (2008). *Methods for neural ensemble recordings*. CRC Press, p. 269.

Niedermeyer, E. (1997). "Alpha rhythms as physiological and abnormal phenomena." In: *International Journal of Psychophysiology*. Vol. 26. 1-3, pp. 31–49.

Niell, C. M. and Stryker, M. P. (2010). "Modulation of Visual Responses by Behavioral State in Mouse Visual Cortex." In: *Neuron* 65.4, pp. 472–479.

Nir, Y., Staba, R. J., Andrillon, T., Vyazovskiy, V. V., Cirelli, C., Fried, I., and Tononi, G. (2011). "Regional Slow Waves and Spindles in Human Sleep." In: *Neuron* 70.1, pp. 153–169.

Nokia, M. S., Penttonen, M, and Wikgren, J (2010). "Hippocampal Ripple-Contingent Training Accelerates Trace Eyeblink Conditioning and Retards Extinction in Rabbits." In: 30.34, pp. 11486–11492.

Nokia, M. S., Penttonen, M., Korhonen, T., and Wikgren, J. (2008). "Hippocampal theta (3-8Hz) activity during classical eyeblink conditioning in rabbits." In: *Neurobiology of learning and memory* 90, pp. 62–70.

Nokia, M. S., Mikkonen, J. E., Penttonen, M., and Wikgren, J. (2012). "Disrupting neural activity related to awake-state sharp wave-ripple complexes prevents hippocampal learning." In: *Frontiers in behavioral neuroscience* 6, p. 84.

Nolte, G., Bai, O., Wheaton, L., Mari, Z., Vorbach, S., and Hallett, M. (2004). "Identifying true brain interaction from EEG data using the imaginary part of coherency." In: *Clinical Neurophysiology* 115.10, pp. 2292–2307.

Nuñez, A., Amzica, F., and Steriade, M. M. (1992). "Voltage-dependent fast (20-40 Hz) oscillations in long-axoned neocortical neurons." In: *Neuroscience* 51.1, pp. 7–10.

Nunez, P. L. (1998). "Neocortical dynamics of macroscopic-scale EEG measurements." In: *IEEE engineering in medicine and biology magazine : the quarterly magazine of the Engineering in Medicine & Biology Society* 17.5, pp. 110–117.

Nunez, P. L. and Srinivasan, R. (2006). *Electric Fields of the Brain*. The Neurophysics of EEG. Oxford University Press, USA.

Nyberg, L, McIntosh, A. R., Houle, S, and Nilsson, L. G. (1996). "Activation of medial temporal structures during episodic memory retrieval." In: *Nature*.

Nyquist, H. (1924). "Certain Factors Affecting Telegraph Speed." In: *Bell System Technical Journal* 3.2, pp. 324–346.

Nyquist, H. (1928). "Certain Topics in Telegraph Transmission Theory." In: *Transactions of the American Institute of Electrical Engineers* 47.2, pp. 617–644.

Oakson, G and Steriade, M (1982). "Slow rhythmic rate fluctuations of cat midbrain reticular neurons in synchronized sleep and waking." In: *Brain Research* 247.2, pp. 277–288.

Oakson, G and Steriade, M (1983). "Slow rhythmic oscillations of EEG slow-wave amplitudes and their relations to midbrain reticular discharge." In: *Brain Research* 269.2, pp. 386–390.

Obál, F., Rubicsek, G., Alföldi, P., and Sáry, G. (1985). "Changes in the brain and core temperatures in relation to the various arousal states in rats in the light and dark periods of the day." In: *Pflügers Archiv European Journal of Physiology* 404.1, pp. 73–79.

O'Donnell, P. and Grace, A. a. (1995). "Synaptic interactions among excitatory afferents to nucleus accumbens neurons: hippocampal gating of prefrontal cortical input." In: *Journal of Neuroscience* 15.5, pp. 3622–3639.

O'Keefe, J (1976). "Place units in the hippocampus of the freely-moving rat." In: *Experimental Neurobiology* 51.1, pp. 78–109.

O'Keefe, J and Conway, D. H. (1978). "Hippocampal place units in the freely moving rat: why they fire where they fire." In: *Experimental Brain Research* 31.4, pp. 573–590.

O'Keefe, J and Dostrovsky, J (1971). "The hippocampus as a spatial map. Preliminary evidence from unit activity in the freely-moving rat." In: *Brain Research* 34.1, pp. 171–175.

Okun, M, Nain, A, and Lampl, I (2010). "The subthreshold relationship between cortical local field potential and neuronal firing unveiled by intracellular recordings in awake rats." In: *Journal of Neuroscience* 20.12, pp. 4440–4448.

Olton, D. S. and Samuelson, R. J. (1976). "Remembrance of places passed: Spatial memory in rats." In: *Journal of Experimental Psychology: Animal ...*

O'Neill, J., Senior, T., and Csicsvari, J. (2006). "Place-selective firing of CA1 pyramidal cells during sharp wave/ripple network patterns in exploratory behavior." In: *Neuron* 49.1, pp. 143–155.

O'Neill, J., Senior, T. J., Allen, K., Huxter, J. R., and Csicsvari, J. (2008). "Reactivation of experience-dependent cell assembly patterns in the hippocampus." In: *Nature Neuroscience* 11.2, pp. 209–215.

O'Neill, P.-K., Gordon, J. A., and Sigurdsson, T. (2013). "Theta Oscillations in the Medial Prefrontal Cortex Are Modulated by Spatial Working Memory and Synchronize with the Hippocampus through Its Ventral Subregion." In: *Journal of Neuroscience* 33.35, pp. 14211–14224.

Onisawa, N., Manabe, H., and Mori, K. (2017). "Temporal coordination of olfactory cortex sharp-wave activity with up- and downstates in the orbitofrontal cortex during slow-wave sleep." In: *Journal of Neurophysiology* 117.1, pp. 123–135.

Onoda, N and Mori, K (1980). "Depth distribution of temporal firing patterns in olfactory bulb related to air-intake cycles." In: *Journal of Neurophysiology* 44.1, pp. 29–39.

Orr, G, Rao, G, Houston, F. P., McNaughton, B. L., and Barnes, C. A. (2001). "Hippocampal synaptic plasticity is modulated by theta rhythm in the fascia dentata of adult and aged freely behaving rats." In: *Hippocampus* 11.6, pp. 647–654.

Ottoson, D (1955). "Analysis of the electrical activity of the olfactory epithelium." In: *Acta physiologica Scandinavica. Supplementum* 35.122, pp. 1–83.

Ottoson, D. (1960). "Comparison of Slow Potentials Evoked in the Frog's Nasal Mucosa and Olfactory Bulb by Natural Stimulation." In: *Acta Physiologica Scandinavica* 47.2-3, pp. 149–159.

Oyamada, Y, Ballantyne, D, Mückenhoff, K, and Scheid, P (1998). "Respiration-modulated membrane potential and chemosensitivity of locus coeruleus neurones in the in vitro brainstem-spinal cord of the neonatal rat." In: *The Journal of physiology* 513 (Pt 2, pp. 381–98.

Pabba, M. (2013). "Evolutionary development of the amygdaloid complex." In: *Frontiers in neuroanatomy* 7, p. 27.

Pace-Schott, E. F. and Hobson, J. A. (2002). "The neurobiology of sleep: genetics, cellular physiology and subcortical networks." In: *Nature reviews. Neuroscience* 3.8, pp. 591–605.

Padilla-Coreano, N., Bolkan, S. S., Pierce, G. M., Blackman, D. R., Hardin, W. D., Garcia-Garcia, A. L., Spellman, T. J., and Gordon, J. A. (2016). "Direct Ventral Hippocampal-Prefrontal Input Is Required for Anxiety-Related Neural Activity and Behavior." In: *Neuron* 89.4, pp. 857–866.

Pager, J (1985). "Respiration and olfactory bulb unit activity in the unrestrained rat: statements and reappraisals." In: *Behavioural brain research* 16.2-3, pp. 81–94.

Pape, H. C. and Pare, D. (2010). "Plastic Synaptic Networks of the Amygdala for the Acquisition, Expression, and Extinction of Conditioned Fear." In: *Physiological Reviews* 90.2, pp. 419–463.

Pape, H. C., Narayanan, R. T., Smid, J., Stork, O., and Seidenbecher, T. (2005). "Theta activity in neurons and networks of the amygdala related to long-term fear memory." In: *Hippocampus* 15.7, pp. 874–880.

Papez, J. W. (1937). "A proposed mechanism of emotions." In: *Archives of Neurology & Psychiatry* 38.March 5, pp. 725–743.

Paré, D and Collins, D. R. (2000). "Neuronal correlates of fear in the lateral amygdala: multiple extracellular recordings in conscious cats." In: *Journal of Neuroscience* 20.7, pp. 2701–10.

Paré, D and Gaudreau, H (1996). "Projection cells and interneurons of the lateral and basolateral amygdala: distinct firing patterns and differential relation to theta and delta rhythms in conscious cats." In: *Journal of Neuroscience* 16.10, pp. 3334–3350.

Pare, D., Collins, D. R., Pelletier, J. G., Paré, D., Collins, D. R., and Pelletier, J. G. (2002). "Amygdala oscillations and the consolidation of emotional memories." In: *Trends in Cognitive Sciences* 6.7, pp. 306–314.

Park, H.-D., Correia, S., Ducorps, A., and Tallon-Baudry, C. (2014). "Spontaneous fluctuations in neural responses to heartbeats predict visual detection." In: *Nature neuroscience* 17.4, pp. 612–618.

Park, S., Kramer, E. E., Mercaldo, V., Rashid, A. J., Insel, N., Frankland, P. W., and Josselyn, S. A. (2016). "Neuronal Allocation to a Hippocampal Engram." In: *Neuropsychopharmacology* 41.13, pp. 2987–2993.

Parker, K. L., Chen, K.-H., Kingyon, J. R., Cavanagh, J. F., and Narayanan, N. S. (2014). "D1-Dependent 4 Hz Oscillations and Ramping Activity in Rodent Medial Frontal Cortex during Interval Timing." In: *Journal of Neuroscience* 34.50, pp. 16774–16783.

Pavlides, C and Winson, J (1989). "Influences of hippocampal place cell firing in the awake state on the activity of these cells during subsequent sleep episodes." In: *Journal of Neuroscience* 9.8, pp. 2907–2918.

Pavlides, C, Greenstein, Y. J., Grudman, M, and Winson, J (1988). "Long-term potentiation in the dentate gyrus is induced preferentially on the positive phase of theta-rhythm." In: *Brain Research* 439.1-2, pp. 383–387.

Paxinos, G., Franklin, K. B. J., Paxinos, G and Franklin, K., Paxinos, G., and Franklin, K. B. J. (2004). *Mouse Brain in Stereotaxic Coordinates*. Vol. 2nd.

Pedemonte, M, Peña, J. L., and Velluti, R. a. (1996). "Firing of inferior colliculus auditory neurons is phase-locked to the hippocampus theta rhythm during paradoxical sleep and waking." In: *Experimental brain research. Experimentelle Hirnforschung. Expérimentation cérébrale* 112.1, pp. 41–6.

Peigneux, P., Laureys, S., Fuchs, S., Collette, F., Perrin, F., Reggers, J., Phillips, C., Degueldre, C., Del Fiore, G., Aerts, J., Luxen, A., and Maquet, P. (2004). "Are spatial memories strengthened in the human hippocampus during slow wave sleep?" In: *Neuron* 44.3, pp. 535–545.

Penfield, W. and Rasmussen, T. (1950). *The Cerebral Cortex of Man: Clinical Study of Localization of Function*.

Peng, C.-K., Henry, I. C., Mietus, J. E., Hausdorff, J. M., Khalsa, G., Benson, H., and Goldberger, A. L. (2004). "Heart rate dynamics during three forms of meditation." In: *International journal of cardiology* 95.1, pp. 19–27.

Pennartz, C. M. A. (2004). "The ventral striatum in off-line processing: ensemble reactivation during sleep and modulation by hippocampal ripples." In: *Journal of Neuroscience* 24.29, pp. 6446–6456.

Perl, O., Arzi, A., Sela, L., Secundo, L., Holtzman, Y., Samnon, P., Oksenberg, A., Sobel, N., and Hairston, I. S. (2016). "Odors enhance slow-wave activity in non-rapid eye movement sleep." In: *Journal of Neurophysiology*.

Peters, A and Sethares, C (1991). "Organization of pyramidal neurons in area 17 of monkey visual cortex." In: *The Journal of comparative neurology* 306.1, pp. 1–23.

Petsche, H., Pockberger, H., and Rappelsberger, P. (1984). "On the search for the sources of the electroencephalogram." In: *Neuroscience* 11.1, pp. 1–27.

Pettersen, K. H. and Einevoll, G. T. (2008). "Amplitude variability and extracellular low-pass filtering of neuronal spikes." In: *Biophysical Journal* 94.3, pp. 784–802.

Pettersen, K. H., Devor, A., Ulbert, I., Dale, A. M., and Einevoll, G. T. (2006). "Current-source density estimation based on inversion of electrostatic forward solution: Effects of finite extent of neuronal activity and conductivity discontinuities." In: *Journal of Neuroscience Methods* 154.1-2, pp. 116–133.

Peyrache, A., Battaglia, F. P., and Destexhe, A. (2011). "Inhibition recruitment in prefrontal cortex during sleep spindles and gating of hippocampal inputs." In: *Proceedings of the National Academy of Sciences* 108.41, pp. 17207–17212.

Peyrache, A., Khamassi, M., Benchenane, K., Wiener, S. I., and Battaglia, F. P. (2009). "Replay of rule-learning related neural patterns in the prefrontal cortex during sleep." In: *Nature Neuroscience* 12.7, pp. 919–926.

Peyrache, A., Lacroix, M. M., Petersen, P. C., and Buzsaki, G. (2015). "Internally organized mechanisms of the head direction sense." In: *Nature Neuroscience* 18.4, pp. 569–575.

Phillips, M. E., Sachdev, R. N. S., Willhite, D. C., and Shepherd, G. M. (2012). "Respiration drives network activity and modulates synaptic and circuit processing of lateral inhibition in the olfactory bulb." In: *Journal of Neuroscience* 32.1, pp. 85–98.

Phillips, R. G. and LeDoux, J. E. (1992). "Differential contribution of amygdala and hippocampus to cued and contextual fear conditioning." In: *Behavioral Neuroscience* 106.2, pp. 274–285.

Picchioni, D., Horovitz, S. G., Fukunaga, M., Carr, W. S., Meltzer, J. A., Balkin, T. J., Duyn, J. H., and Braun, A. R. (2011). "Infraslow EEG oscillations organize large-scale cortical-subcortical interactions during sleep: a combined EEG/fMRI study." In: *Brain Research* 1374, pp. 63–72.

Pinault, D. and Deschenes, M. (1992). "Voltage-dependent 40-Hz oscillations in rat reticular thalamic neurons in vivo." In: *Neuroscience* 51.2, pp. 245–258.

Pineda, J and Aghajanian, G. K. (1997). "Carbon dioxide regulates the tonic activity of locus coeruleus neurons by modulating a proton- and polyamine-sensitive inward rectifier potassium current." In: *Neuroscience* 77.3, pp. 723–43.

Pinto, L., Goard, M. J., Estandian, D., Xu, M., Kwan, A. C., Lee, S. H., Harrison, T. C., Feng, G., and Dan, Y. (2013). "Fast modulation of visual perception by basal forebrain cholinergic neurons." In: *Nature Neuroscience* 16.12, pp. 1857–1863.

Pitman, R. K., Rasmusson, A. M., Koenen, K. C., Shin, L. M., Orr, S. P., Gilbertson, M. W., Milad, M. R., and Liberzon, I. (2012). "Biological studies of post-traumatic stress disorder." In: *Nature reviews. Neuroscience* 13.11, pp. 769–787.

Plonsey, R. and Heppner, D. B. (1967). "Considerations of quasi-stationarity in electrophysiological systems." In: *The Bulletin of Mathematical Biophysics* 29.4, pp. 657–664.

Poe, G. R., Kristensen, M. P., Rector, D. M., and Harper, R. M. (1996). "Hippocampal activity during transient respiratory events in the freely behaving cat." In: *Neuroscience* 72.1, pp. 39–48.

Polack, P. O., Friedman, J., and Golshani, P. (2013). "Cellular mechanisms of brain state-dependent gain modulation in visual cortex." In: *Nature Neuroscience* 16.9, pp. 1331–1339.

Pont, J. S. du (1987). "Firing patterns of bulbar respiratory neurones during sniffing in the conscious, non-paralyzed rabbit." In: *Brain Research* 414.1, pp. 163–168.

Poo, C. and Isaacson, J. S. (2009). "Odor representations in olfactory cortex: "sparse" coding, global inhibition, and oscillations." In: *Neuron* 62.6, pp. 850–861.

Popa, D., Duvarci, S., Popescu, A. T., Lena, C., and Pare, D. (2010). "Coherent amygdalocortical theta promotes fear memory consolidation during paradoxical sleep." In: *Proceedings of the National Academy of Sciences* 107.14, pp. 6516–6519.

Popescu, A. T., Popa, D., and Paré, D. (2009). "Coherent gamma oscillations couple the amygdala and striatum during learning." In: *Nature Neuroscience* 12.6, pp. 801–807.

Poulet, J. F. A. and Petersen, C. C. H. (2008). "Internal brain state regulates membrane potential synchrony in barrel cortex of behaving mice." In: *Nature* 454.7206, pp. 881–885.

Poulet, J. F. A., Fernandez, L. M. J., Crochet, S., and Petersen, C. C. H. (2012). *Thalamic control of cortical states*.

Poulos, A. M., Mehta, N., Lu, B., Amir, D., Livingston, B., Santarelli, A., Zhuravka, I., and Fanselow, M. S. (2016). "Conditioning- and time-dependent increases in context fear and generalization." In: *Learning & Memory* 23.7, pp. 379–385.

Power, A. E. (2004). "Slow-wave sleep, acetylcholine, and memory consolidation." In: *Proceedings of the National Academy of Sciences* 101.7, pp. 1795–1796.

Prasad, A., Xue, Q. S., Sankar, V., Nishida, T., Shaw, G., Streit, W. J., and Sanchez, J. C. (2012). "Comprehensive characterization and failure modes of tungsten microwire arrays in chronic neural implants." In: *Journal of Neural Engineering* 9.5, p. 056015.

Prasad, A., Xue, Q.-S., Dieme, R., Sankar, V., Mayrand, R. C., Nishida, T., Streit, W. J., and Sanchez, J. C. (2014). "Abiotic-biotic characterization of Pt/Ir microelectrode arrays in chronic implants." In: *Frontiers in Neuroengineering* 7, p. 2.

Preston, A. R. and Eichenbaum, H. B. (2013). *Interplay of hippocampus and prefrontal cortex in memory*.

Price, J. L. and Powell, T. P. S. (1970). "The mitral and short axon cells of the olfactory bulb." In: *Journal of Cell Science*.

Price, J. L. (1985). "Beyond the primary olfactory cortex: olfactory-related areas in the neocortex, thalamus and hypothalamus." In: *Chemical Senses* 10.2, pp. 239–258.

Price, J. L. and Slotnick, B. M. (1983). "Dual olfactory representation in the rat thalamus: An anatomical and electrophysiological study." In: *Journal of Comparative Neurology* 215.1, pp. 63–77.

Prut, Y, Vaadia, E, Bergman, H, Haalman, I, Slovin, H, and Abeles, M. (1998). "Spatiotemporal structure of cortical activity: properties and behavioral relevance." In: *Journal of neurophysiology* 79.6, pp. 2857–2874.

Raghavachari, S, Kahana, M. J., Rizzuto, D. S., Caplan, J. B., Kirschen, M. P., Bourgeois, B, Madsen, J. R., and Lisman, J. E. (2001). "Gating of human theta oscillations by a working memory task." In: *Journal of Neuroscience* 21.9, pp. 3175–3183.

Rajasethupathy, P., Sankaran, S., Marshel, J. H., Kim, C. K., Ferenczi, E., Lee, S. Y., Berndt, A., Ramakrishnan, C., Jaffe, A., Lo, M., Liston, C., and Deisseroth, K. (2015). "Projections from neocortex mediate top-down control of memory retrieval." In: *Nature* 526.7575, pp. 653–659.

Rall, W and Shepherd, G. M. (1968). "Theoretical reconstruction of field potentials and dendrodendritic synaptic interactions in olfactory bulb." In: *Journal of neurophysiology* 31.6, pp. 884–915.

Ramanathan, D. S., Gulati, T., and Ganguly, K. (2015). "Sleep-Dependent Reactivation of Ensembles in Motor Cortex Promotes Skill Consolidation." In: *PLoS Biology* 13.9. Ed. by J. Ashe, e1002263.

Ramirez-Villegas, J. F., Logothetis, N. K., and Besserve, M. (2015). "Diversity of sharp-wave–ripple LFP signatures reveals differentiated brain-wide dynamical events." In: *Proceedings of the National Academy of Sciences* 112.46, E6379–E6387.

Ramm, P. and Smith, C. T. (1990). "Rates of cerebral protein synthesis are linked to slow wave sleep in the rat." In: *Physiology and Behavior* 48.5, pp. 749–753.

Ranade, S., Hangya, B., and Kepecs, A. (2013). "Multiple modes of phase locking between sniffing and whisking during active exploration." In: *The Journal of neuroscience : the official journal of the Society for Neuroscience* 33.19, pp. 8250–8256.

Ranck, J. B. (1963). "Specific impedance of rabbit cerebral cortex." In: *Experimental neurology* 7, pp. 144–152.

Ranck, J. B. (1973). "Studies on single neurons in dorsal hippocampal formation and septum in unrestrained rats. I. Behavioral correlates and firing repertoires." In: *Experimental neurology* 41.2, pp. 461–531.

Rasch, B. and Born, J. (2013). "About sleep's role in memory." In: *Physiological reviews* 93.2, pp. 681–766.

Rasch, B., Büchel, C., Gais, S., and Born, J. (2007). "Odor cues during slow-wave sleep prompt declarative memory consolidation." In: *Science* 315.5817, pp. 1426–1429.

Rassler, B. and Raabe, J. (2003). "Co-ordination of breathing with rhythmic head and eye movements and with passive turnings of the body." In: *European journal of applied physiology* 90.1-2, pp. 125–130.

Rattenborg, N. C., Lima, S. L., and Amlaner, C. J. (1999). "Half-awake to the risk of predation." In: *Nature* 397.6718, pp. 397–398.

Ravel, N and Pager, J (1990). "Respiratory patterning of the rat olfactory bulb unit activity: nasal versus tracheal breathing." In: *Neuroscience Letters* 115.2-3, pp. 213–218.

Ravel, N, Caille, D, and Pager, J (1987). "A centrifugal respiratory modulation of olfactory bulb unit activity: a study on acute rat preparation." In: *Experimental Brain Research* 65.3, pp. 623–628.

Reimer, J., Froudarakis, E., Cadwell, C. R., Yatsenko, D., Denfield, G. H., and Tolias, A. S. (2014). "Pupil Fluctuations Track Fast Switching of Cortical States during Quiet Wakefulness." In: *Neuron* 84.2, pp. 355–362.

Reiss, S. (1991). "Expectancy model of fear, anxiety, and panic." In: *Clinical Psychology Review* 11.2, pp. 141–153.

Remondes, M. and Wilson, M. A. (2015). "Slow-γ Rhythms Coordinate Cingulate Cortical Responses to Hippocampal Sharp-Wave Ripples during Wakefulness." In: *Cell Reports* 13.7, pp. 1327–1335.

Rennaker, R. L., Chen, C.-F. F., Ruyle, A. M., Sloan, A. M., and Wilson, D. A. (2007). "Spatial and Temporal Distribution of Odorant-Evoked Activity in the Piriform Cortex." In: *Journal of Neuroscience* 27.7, pp. 1534–1542.

Rescorla, R. A. (1968). "Probability of shock in the presence and absence of CS in fear conditioning." In: *Journal of comparative and physiological psychology* 66.1, pp. 1–5.

Rescorla, R. A. (1988). "Pavlovian conditioning: It's not what you think it is." In: *American Psychologist*.

Rescorla, R. A. and Wagner, A. R. (1972). *A theory of Pavlovian conditioning: Variations in the effectiveness of reinforcement and nonreinforcement*. ... conditioning II: Current research and theory.

Ressler, K. J., Sullivan, S. L., and Buck, L. B. (1994). "Information coding in the olfactory system: evidence for a stereotyped and highly organized epitope map in the olfactory bulb." In: *Cell* 79.7, pp. 1245–1255.

Rex, C. S., Colgin, L. L., Jia, Y., Casale, M., Yanagihara, T. K., Debenedetti, M., Gall, C. M., Kramar, E. A., and Lynch, G. (2009). "Origins of an intrinsic hippocampal EEG pattern." In: *PLoS ONE* 4.11. Ed. by C. T. Dickson, e7761.

Ribot, T (1882). *Diseases of memory: An essay in the positive psychology*. 46, p. 232.

Richardson, G. S., Moore-Ede, M. C., Czeisler, C. A., and Dement, W. C. (1985). "Circadian rhythms of sleep and wakefulness in mice: analysis using long-term automated recording of sleep." In: *The American journal of physiology* 248.3 Pt 2, R320–30.

Riera, J. J., Ogawa, T., Goto, T., Sumiyoshi, A., Nonaka, H., Evans, A., Miyakawa, H., and Kawashima, R. (2012). "Pitfalls in the dipolar model for the neocortical EEG sources." In: *Journal of Neurophysiology* 108.4, pp. 956–975.

Rittweger, J and Pöpel, A (1998). "Respiratory-like periodicities in slow eye movements during sleep onset." In: *Clinical physiology (Oxford, England)* 18.5, pp. 471–478.

Robert Heale, V. and Vanderwolf, C. H. (1994). "Dentate gyrus and olfactory bulb responses to olfactory and noxious stimulation in urethane anaesthetized rats." In: *Brain Research* 652.2, pp. 235–242.

Robertson, E. M., Pascual-Leone, A., and Miall, R. C. (2004). "Current concepts in procedural consolidation." In: *Nature reviews. Neuroscience* 5.7, pp. 576–582.

Robinson, D. A. (1968). "The electrical properties of metal microelectrodes." In: *Proceedings of the IEEE*.

Rojas-Líbano, D., Frederick, D. E., Egaña, J. I., and Kay, L. M. (2014). "The olfactory bulb theta rhythm follows all frequencies of diaphragmatic respiration in the freely behaving rat." In: *Frontiers in behavioral neuroscience* 8, p. 214.

Roth, M., Shaw, J., and Green, J. (1956). "The form, voltage distribution and physiological significance of the K-complex." In: *Electroencephalography and Clinical Neurophysiology* 8.3, pp. 385–402.

Rothschild, G., Eban, E., and Frank, L. M. (2016a). "A cortical – hippocampal – cortical loop of information processing during memory consolidation." In: *Nature Neuroscience* 20.December, pp. 1–12.

Rothschild, G., Eban, E., and Frank, L. M. (2016b). "A cortical–hippocampal–cortical loop of information processing during memory consolidation." In: *Nature neuroscience*.

Rozeske, R. R., Jercog, D., Karalis, N., Chaudun, F., Khoder, S., Girard, D., Winke, N., and Herry, C. (2018). "Prefrontal-Periaqueductal Gray-Projecting Neurons Mediate Context Fear Discrimination." In: *Neuron* 97.4, pp. 898–910.

Rudoy, J. D., Voss, J. L., Westerberg, C. E., and Paller, K. A. (2009). "Strengthening Individual Memories by Reactivating Them During Sleep." In: *Science* 326.5956, pp. 1079–1079.

Russell, W. R. and Nathan, P. W. (1946). "Traumatic amnesia." In: *Brain* 69.4, pp. 280–300.

Rutishauser, U., Ross, I. B., Mamelak, A. N., and Schuman, E. M. (2010). "Human memory strength is predicted by theta-frequency phase-locking of single neurons." In: *Nature* 464.7290, pp. 903–907.

Sacco, T. and Sacchetti, B. (2010). "Role of secondary sensory cortices in emotional memory storage and retrieval in rats." In: *Science* 329.5992, pp. 649–656.

Sah, P, Faber, E. S. L., Lopez De Armentia, M, and Power, J (2003). "The amygdaloid complex: anatomy and physiology." In: *Physiological Reviews* 83.3, pp. 803–834.

Sakai, K. and Crochet, S. (2001). "Differentiation of presumed serotonergic dorsal raphe neurons in relation to behavior and wake-sleep states." In: *Neuroscience* 104.4, pp. 1141–1155.

Sakata, S. and Harris, K. D. (2009). "Laminar Structure of Spontaneous and Sensory-Evoked Population Activity in Auditory Cortex." In: *Neuron* 64.3, pp. 404–418.

Sakuragi, S., Sugiyama, Y., and Takeuchi, K. (2002). "Effects of laughing and weeping on mood and heart rate variability." In: *Journal of physiological anthropology and applied human science* 21.3, pp. 159–165.

Saleem, A. B., Ayaz, A., Jeffery, K. J., Harris, K. D., and Carandini, M. (2013). "Integration of visual motion and locomotion in mouse visual cortex." In: *Nature Neuroscience* 16.12, pp. 1864–1869.

Salinas, E. and Sejnowski, T. J. (2001). "Correlated neuronal activity and the flow of neural information." In: *Nature Reviews Neuroscience* 2.8, pp. 539–550.

Sanchez-Vives, M. V. and McCormick, D. A. (2000). "Cellular and network mechanisms of rhytmic recurrent activity in neocortex." In: *Nature Neuroscience* 3.10, pp. 1027–1034.

Saper, C. B., Scammell, T. E., and Lu, J. (2005). "Hypothalamic regulation of sleep and circadian rhythms." In: *Nature* 437.7063, pp. 1257–1263.

Sara, S. J. (2015). *Locus Coeruleus in time with the making of memories*.

Sasaki, K (1975). "Electrophysiological studies on thalamo-cortical projections." In: *International anesthesiology clinics* 13.1, pp. 1–35.

Scheeringa, R., Fries, P., Petersson, K.-M., Oostenveld, R., Grothe, I., Norris, D. G., Hagoort, P., and Bastiaansen, M. C. M. (2011). "Neuronal dynamics underlying high- and low-frequency EEG oscillations contribute independently to the human BOLD signal." In: *Neuron* 69.3, pp. 572–583.

Schendan, H. E., Searl, M. M., Melrose, R. J., and Stern, C. E. (2003). "An FMRI study of the role of the medial temporal lobe in implicit and explicit sequence learning." In: *Neuron* 37.6, pp. 1013–1025.

Schneider, D. M., Nelson, A., and Mooney, R. (2014). "A synaptic and circuit basis for corollary discharge in the auditory cortex." In: *Nature* 513.7517, pp. 189–194.

Schwabe, K, Ebert, U, and Löscher, W (2004). "The central piriform cortex: anatomical connections and anticonvulsant effect of GABA elevation in the kindling model." In: *Neuroscience* 126.3, pp. 727–741.

Scoville, W. B. and Milner, B. (1957). "Loss of recent memory after bilateral hippocampal lesions." In: *Journal of Neurology, Neurosurgery & Psychiatry* 20.1, pp. 11–21.

Seager, M. A., Johnson, L. D., Chabot, E. S., Asaka, Y., and Berry, S. D. (2002). "Oscillatory brain states and learning: Impact of hippocampal theta-contingent training." In: *Proceedings of the National Academy of Sciences* 99.3, pp. 1616–1620.

Segal, M. (1976). "Brain stem afferents to the rat medial septum." In: *The Journal of Physiology* 261.3, pp. 617–631.

Seidenbecher, T., Laxmi, T. R., Stork, O., and Pape, H.-C. C. (2003). "Amygdalar and hippocampal theta rhythm synchronization during fear memory retrieval." In: *Science* 301.5634, pp. 846–850.

Sejnowski, T. J. (1995). "Time for a new neural code?" In: *Nature* 376.6535, pp. 21–22.

Senn, V., Wolff, S. B. E., Herry, C., Grenier, F., Ehrlich, I., Gründemann, J., Fadok, J. P., Müller, C., Letzkus, J. J., and LUthi, A. (2014). "Long-range connectivity defines behavioral specificity of amygdala neurons." In: *Neuron* 81.2, pp. 428–437.

Senzai, Y. and Buzsaki, G. (2017). "Physiological properties and behavioral correlates of hippocampal granule cells and mossy cells." In: *Neuron* 93.3, 691–704.e5.

Shannon, C. E. (1948). "A mathematical theory of communication." In: *The Bell System Technical Journal* 27.July 1928, pp. 379–423.

Shannon, C. E. (1949). "Communication in the Presence of Noise." In: *Proceedings of the IRE* 37.1, pp. 10–21.

Shaw, P. J., Tononi, G., Greenspan, R. J., and Robinson, D. F. (2002). "Stress response genes protect against lethal effects of sleep deprivation in Drosophila." In: *Nature* 417.6886, pp. 287–291.

Shein-Idelson, M., Ondracek, J. M., Liaw, H.-P., Reiter, S., and Laurent, G. (2016). "Slow waves, sharp waves, ripples, and REM in sleeping dragons." In: *Science* 352.6285, pp. 590–595.

Sherman, D., Worrell, J. W., Cui, Y., and Feldman, J. L. (2015). "Optogenetic perturbation of preBötzinger complex inhibitory neurons modulates respiratory pattern." In: *Nature Publishing Group* 18.3, pp. 408–414.

Sherman, M. T., Kanai, R., Seth, A. K., and VanRullen, R. (2016). "Rhythmic Influence of Top-Down Perceptual Priors in the Phase of Prestimulus Occipital Alpha Oscillations." In: *Journal of Cognitive Neuroscience* 28.9, pp. 1318–1330.

Shi, C and Davis, M (2001). "Visual pathways involved in fear conditioning measured with fear-potentiated startle: behavioral and anatomic studies." In: *The Journal of neuroscience : the official journal of the Society for Neuroscience* 21.24, pp. 9844–9855.

Shin, L. M. (2006). "Amygdala, Medial Prefrontal Cortex, and Hippocampal Function in PTSD." In: *Annals of the New York Academy of Sciences* 1071.1, pp. 67–79.

Shu, Y., Hasenstaub, A., and McCormick, D. A. (2003). "Turning on and off recurrent balanced cortical activity." In: *Nature* 423.6937, pp. 288–293.

Shusterman, R., Smear, M. C., Koulakov, A. A., and Rinberg, D. (2011). "Precise olfactory responses tile the sniff cycle." In: *Nature Neuroscience* 14.8, pp. 1039–1044.

Siapas, A. G. and Wilson, M. A. (1998). "Coordinated interactions between hippocampal ripples and cortical spindles during slow-wave sleep." In: *Neuron* 21.5, pp. 1123–1128.

Siapas, A. G., Lubenov, E. V., and Wilson, M. A. (2005). "Prefrontal phase locking to hippocampal theta oscillations." In: *Neuron* 46.1, pp. 141–151.

Siegel, J. M., Wheeler, R. L., and McGinty, D. J. (1979). "Activity of medullary reticular formation neurons in the unrestrained cat during waking and sleep." In: *Brain Research* 179.1, pp. 49–60.

Siegel, M., Donner, T. H., and Engel, A. K. (2012). "Spectral fingerprints of large-scale neuronal interactions." In: *Nature Reviews Neuroscience* 13.2, pp. 121–134.

Siegle, J. H. and Wilson, M. A. (2014). "Enhancement of encoding and retrieval functions through theta phase-specific manipulation of hippocampus." In: *eLife* 3, e03061.

Sierra-Mercado, D., Padilla-Coreano, N., and Quirk, G. J. (2010). "Dissociable Roles of Prelimbic and Infralimbic Cortices, Ventral Hippocampus, and Basolateral Amygdala in the Expression and Extinction of Conditioned Fear." In: *Neuropsychopharmacology : official publication of the American College of Neuropsychopharmacology* 36.2, pp. 529–538.

Sigurdsson, T., Stark, K. L., Karayiorgou, M., Gogos, J. A., and Gordon, J. A. (2010). "Impaired hippocampal-prefrontal synchrony in a genetic mouse model of schizophrenia." In: *Nature* 464.7289, pp. 763–767.

Singer, W (1993). "Synchronization of Cortical Activity and Its Putative Role in Information Processing and Learning." In: *Annual Review of Physiology* 55.1, pp. 349–374.

Singer, W (1999). "Neuronal Synchrony: A Versatile Code Review for the Definition of Relations?" In: *Neuron* 24.1, pp. 49–65.

Singer, W and Gray, C. M. (1995). "Visual Feature Integration and the Temporal Correlation Hypothesis." In: *Annual Review of Neuroscience* 18, pp. 555–586.

Sirota, A., Csicsvari, J., Buhl, D. L., and Buzsaki, G. (2003). "Communication between neocortex and hippocampus during sleep in rodents." In: *Proceedings of the National Academy of Sciences* 100.4, pp. 2065–2069.

Sirota, A. and Buzsaki, G. (2005). "Interaction between neocortical and hippocampal networks via slow oscillations." In: *Thalamus and Related Systems* 3.4, pp. 245–259.

Sirota, A., Montgomery, S., Fujisawa, S., Isomura, Y., Zugaro, M. B., and Buzsaki, G. (2008). "Entrainment of neocortical neurons and gamma oscillations by the hippocampal theta rhythm." In: *Neuron* 60.4, pp. 683–697.

Sirotin, Y. B., Costa, M. E., and Laplagne, D. A. (2014). "Rodent ultrasonic vocalizations are bound to active sniffing behavior." In: *Frontiers in behavioral neuroscience* 8.25, p. 399.

Skaggs, W. E. and McNaughton, B. L. (1996). "Replay of Neuronal Firing Sequences in Rat Hippocampus During Sleep Following Spatial Experience." In: *Science* 271.5257, pp. 1870–1873.

Smith, J. C., Ellenberger, H. H., Ballanyi, K, Richter, D. W., and Feldman, J. L. (1991). "Pre-Bötzinger complex: a brainstem region that may generate respiratory rhythm in mammals." In: *Science* 254.5032, pp. 726–729.

Smith, M. a., Banerjee, S, Gold, P. W., and Glowa, J (1992). "Induction of c-fos mRNA in rat brain by conditioned and unconditioned stressors." In: *Brain research* 578.1-2, pp. 135–141.

Smith, O. A. and DeVito, J. L. (1984). "Central neural integration for the control of autonomic responses associated with emotion." In: *Annual Review of Neuroscience* 7.1, pp. 43–65.

Sobel, E. C. and Tank, D. W. (1993). "Timing of odor stimulation does not alter patterning of olfactory bulb unit activity in freely breathing rats." In: *Journal of Neurophysiology*.

Sobel, N., Prabhakaran, V., Desmond, J. E., Glover, G. H., Goode, R. L., Sullivan, E. V., and Gabriell, J. D. (1998). "Sniffing and smelling: Separate subsystems in the human olfactory cortex." In: *Nature* 392.6673, pp. 282–286.

Somers, D. and Kopell, N. (1993). "Rapid synchronization through fast threshold modulation." In: *Biological Cybernetics* 68.5, pp. 393–407.

Somers, D. and Kopell, N. (1995). "Waves and synchrony in networks of oscillators of relaxation and non-relaxation type." In: *Physica D: Nonlinear Phenomena* 89.1-2, pp. 169–183.

Sosulski, D. L., Bloom, M. L., Cutforth, T., Axel, R., and Datta, S. R. (2011). "Distinct representations of olfactory information in different cortical centres." In: *Nature* 472.7342, pp. 213–216.

Sotres-Bayon, F., Sierra-Mercado, D., Pardilla-Delgado, E., and Quirk, G. J. (2012). "Gating of fear in prelimbic cortex by hippocampal and amygdala inputs." In: *Neuron* 76.4, pp. 804–812.

Spellman, T., Rigotti, M., Ahmari, S. E., Fusi, S., Gogos, J. A., and Gordon, J. A. (2015). "Hippocampal–prefrontal input supports spatial encoding in working memory." In: *Nature* 522.7556, pp. 309–314.

Spiers, H. J., Burgess, N, Maguire, E. A., Baxendale, S. A., Hartley, T, Thompson, P. J., and O'Keefe, J (2001). "Unilateral temporal lobectomy patients show lateralized topographical and episodic memory deficits in a virtual town." In: *Brain* 124.Pt 12, pp. 2476–2489.

Spocter, M. A., Hopkins, W. D., Barks, S. K., Bianchi, S., Hehmeyer, A. E., Anderson, S. M., Stimpson, C. D., Fobbs, A. J., Hof, P. R., and Sherwood, C. C. (2012). "Neuropil distribution in the cerebral cortex differs between humans and chimpanzees." In: *Journal of Comparative Neurology* 520.13, pp. 2917–2929.

Spors, H., Wachowiak, M., Cohen, L. B., and Friedrich, R. W. (2006). "Temporal dynamics and latency patterns of receptor neuron input to the olfactory bulb." In: *Journal of Neuroscience* 26.4, pp. 1247–59.

Spruston, N and Johnston, D (1992). "Perforated patch-clamp analysis of the passive membrane properties of three classes of hippocampal neurons." In: *Journal of Neurophysiology* 67.3, pp. 508–529.

Spruston, N. (2008). "Pyramidal neurons: dendritic structure and synaptic integration." In: *Nature Reviews Neuroscience* 9.3, pp. 206–221.

Squire, L. R. and Alvarez, P (1995). "Retrograde amnesia and memory consolidation: a neurobiological perspective." In: *Current opinion in neurobiology* 5.2, pp. 169–177.

Squire, L. R. and Cohen, N (1979). "Memory and amnesia: resistance to disruption develops for years after learning." In: *Behavioral and neural biology* 25.1, pp. 115–125.

Squire, L. R. and Zola, S. M. (1996). "Structure and function of declarative and nondeclarative memory systems." In: *Proceedings of the National Academy of Sciences* 93.24, pp. 13515–13522.

Squire, L. R. (1975). "A stable impairment in remote memory following electroconvulsive therapy." In: *Neuropsychologia* 13.1, pp. 51–58.

Squire, L. R. (2004). "Memory systems of the brain: A brief history and current perspective." In: *Neurobiology of Learning and Memory* 82.3, pp. 171–177.

Srinivasan, R, Nunez, P. L., Tucker, D. M., Silberstein, R. B., and Cadusch, P. J. (1996). "Spatial sampling and filtering of EEG with spline laplacians to estimate cortical potentials." In: *Brain topography* 8.4, pp. 355–366.

Sroufe, L. A. (1971). "Effects of Depth and Rate of Breathing on Heart Rate and Heart Rate Variability." In: *Psychophysiology* 8.5, pp. 648–655.

Staresina, B. P., Alink, A., Kriegeskorte, N., and Henson, R. N. (2013). "Awake reactivation predicts memory in humans." In: *Proceedings of the National Academy of Sciences* 110.52, pp. 21159–21164.

Stark, E., Roux, L., Eichler, R., Senzai, Y., Royer, S., and Buzsaki, G. (2014). "Pyramidal cell-interneuron interactions underlie hippocampal ripple oscillations." In: *Neuron* 83.2, pp. 467–480.

Stark, E., Roux, L., Eichler, R., and Buzsáki, G. (2015). "Local generation of multineuronal spike sequences in the hippocampal CA1 region." In: *Proceedings of the National Academy of Sciences* 112.33, pp. 10521–10526.

Steenland, H. W., Li, X.-Y., and Zhuo, M. (2012). "Predicting aversive events and terminating fear in the mouse anterior cingulate cortex during trace fear conditioning." In: *The Journal of neuroscience : the official journal of the Society for Neuroscience* 32.3, pp. 1082–1095.

Stefanelli, T., Bertollini, C., Lüscher, C., Muller, D., and Mendez, P. (2016). "Hippocampal Somatostatin Interneurons Control the Size of Neuronal Memory Ensembles." In: *Neuron* 89.5, pp. 1–20.

Steriade, M, Nuñez, a, and Amzica, F (1993a). "A novel slow (< 1 Hz) oscillation of neocortical neurons in vivo: depolarizing and hyperpolarizing components." In: *Journal of Neuroscience* 13.8, pp. 3252–3265.

Steriade, M, Amzica, F, and Nuñez, A (1993b). "Cholinergic and noradrenergic modulation of the slow (approximately 0.3 Hz) oscillation in neocortical cells." In: *Journal of Neurophysiology* 70.4, pp. 1385–1400.

Steriade, M, Nunez, A, and Amzica, F (1993c). "Intracellular analysis of relations between the slow (< 1 Hz) neocortical oscillation and other sleep rhythms of the electroencephalogram." In: *Journal of Neuroscience* 13.8, pp. 3266–3283.

Steriade, M, Timofeev, I, and Grenier, F (2001). "Natural waking and sleep states: a view from inside neocortical neurons." In: *Journal of Neurophysiology* 85.5, pp. 1969–1985.

Steriade, M. M. (1997). "Synchronized activities of coupled oscillators in the cerebral cortex and thalamus at different levels of vigilance." In: *Cerebral Cortex* 7.6, pp. 583–588.

Steriade, M. M. (2000). "Corticothalamic resonance, states of vigilance and mentation." In: *Neuroscience* 101.2, pp. 243–276.

Steriade, M. M. (2006). "Grouping of Brain Rhythms in Corticothalamic Systems." In: *Neuroscience* 137.4, pp. 1087–1106.

Steriade, M. M. and Amzica, F. (1996). "Intracortical and corticothalamic coherency of fast spontaneous oscillations." In: *Proceedings of the National Academy of Sciences* 93.6, pp. 2533–2538.

Steriade, M. M. and Amzica, F (1998a). "Coalescence of sleep rhythms and their chronology in corticothalamic networks." In: *Sleep research online : SRO* 1.1, pp. 1–10.

Steriade, M. M. and Amzica, F (1998b). "Slow sleep oscillation, rhythmic K-complexes, and their paroxysmal developments." In: *Journal of sleep research* 7 Suppl 1.S1, pp. 30–35.

Steriade, M. M. and Deschenes, M. (1984). *The thalamus as a neuronal oscillator*.

Steriade, M. M. and McCarley, R. W. (2013). *Brainstem Control of Wakefulness and Sleep*. Springer Science & Business Media.

Steriade, M. M., Oakson, G, and Ropert, N (1982). "Firing rates and patterns of midbrain reticular neurons during steady and transitional states of the sleep-waking cycle." In: *Experimental Brain Research* 46.1, pp. 37–51.

Steriade, M. M., Gloor, P., Llinás, R. R., Lopes da Silva, F. H., and Mesulam, M. M. (1990). "Basic mechanisms of cerebral rhythmic activities." In: *Electroencephalography and Clinical Neurophysiology* 76.6, pp. 481–508.

Steriade, M. M., McCormick, D. A, and Sejnowski, T. J (1993d). "Thalamocortical oscillations in the sleeping and aroused brain." In: *Science* 262.5134, pp. 679–685.

Steriade, M. and McCarley, R. W. (1990). *Brainstem Control of Wakefulness and Sleep*. Boston, MA: Springer US.

Steriade, M. and Pare, D. (2009). *Gating in Cerebral Networks*. Cambridge: Cambridge University Press.

Stern, E. A., Jaeger, D., and Wilson, C. J. (1998). "Membrane potential synchrony of simultaneously recorded striatal spiny neuronsin vivo." In: *Nature* 394.6692, pp. 475–478.

Stewart, M. and Fox, S. E. (1991). "Hippocampal theta activity in monkeys." In: *Brain Research* 538.1, pp. 59–63.

Stickgold, R. (2005). "Sleep-dependent memory consolidation." In: *Nature* 437.7063, pp. 1272–1278.

Stiedl, O., Birkenfeld, K., Palve, M., and Spiess, J. (2000). "Impairment of conditioned contextual fear of C57BL/6J mice by intracerebral injections of the NMDA receptor antagonist APV." In: *Behavioural Brain Research* 116.2, pp. 157–168.

Straka, H., Simmers, J., and Chagnaud, B. P. (2018). "A new perspective on predictive motor signaling." In: *Current Biology* 28.5, R193–R194.

Street, M. and Wt, L. (2006). "Cross-Sectional and Longitudinal Study of Effects of Transcendental Meditation Practice on Interhemispheric of Effects of Transcendental Meditation." In: *Consciousness and Cognition* 116.788715756, pp. 1519–1538.

Stroh, A., Adelsberger, H., Groh, A., Rühlmann, C., Fischer, S., Schierloh, A., Deisseroth, K., and Konnerth, A. (2013). "Making Waves: Initiation and Propagation of Corticothalamic Ca2+ Waves In Vivo." In: *Neuron* 77.6, pp. 1136–1150.

Stujenske, J. M., Likhtik, E., Topiwala, M. A., and Gordon, J. A. (2014). "Fear and safety engage competing patterns of theta-gamma coupling in the basolateral amygdala." In: *Neuron* 83.4, pp. 919–933.

Stumpf, C. (1965). "The fast component in the electrical activity of rabbit's hippocampus." In: *Electroencephalography and Clinical Neurophysiology* 18.5, pp. 477–486.

Subramanian, H. H., Balnave, R. J., and Holstege, G. (2008). "The Midbrain Periaqueductal Gray Control of Respiration." In: *Journal of Neuroscience* 28.47, pp. 12274–12283.

Suess, W. M., Alexander, A. B., Smith, D. D., Sweeney, H. W., and Marion, R. J. (1980). "The Effects of Psychological Stress on Respiration: A Preliminary Study of Anxiety and Hyperventilation." In: *Psychophysiology* 17.6, pp. 535–540.

Summerlee, A. J. S., Paisley, A. C., and Goodall, C. L. (1982). "A method for determining the position of chronically implanted platinum microwire electrodes." In: *Journal of Neuroscience Methods* 5.1-2, pp. 7–11.

Suzuki, K., Garfinkel, S. N., Critchley, H. D., and Seth, A. K. (2013). "Multisensory integration across exteroceptive and interoceptive domains modulates self-experience in the rubber-hand illusion." In: *Neuropsychologia* 51.13, pp. 2909–2917.

Swanson, L. W. and Petrovich, G. D. (1998). "What is the amygdala?" In: *Trends Neuroscience* 21.8, pp. 323–31.

Takeuchi, T., Duszkiewicz, A. J., Sonneborn, A., Spooner, P. A., Yamasaki, M., Watanabe, M., Smith, C. C., Fernández, G., Deisseroth, K., Greene, R. W., and Morris, R. G. (2016). "Locus coeruleus and dopaminergic consolidation of everyday memory." In: *Nature* 537.7620, pp. 357–362.

Tambini, A., Ketz, N., and Davachi, L. (2010). "Enhanced Brain Correlations during Rest Are Related to Memory for Recent Experiences." In: *Neuron* 65.2, pp. 280–290.

Tan, W., Janczewski, W. A., Yang, P., Shao, X. M., Callaway, E. M., and Feldman, J. L. (2008). "Silencing preBötzinger Complex somatostatin-expressing neurons induces persistent apnea in awake rat." In: *Nature neuroscience* 11.5, pp. 538–540.

Tang, J., Ko, S., Ding, H.-K., Qiu, C.-S., Calejesan, A. A., and Zhuo, M. (2005). "Pavlovian fear memory induced by activation in the anterior cingulate cortex." In: *Molecular pain* 1, p. 6.

Tang, Y.-Y., Hölzel, B. K., and Posner, M. I. (2015). "The neuroscience of mindfulness meditation." In: *Nature Reviews Neuroscience* 16.4, pp. 213–225.

Taxidis, J., Anastassiou, C. A., Diba, K., and Koch, C. (2015). "Local Field Potentials Encode Place Cell Ensemble Activation during Hippocampal Sharp Wave Ripples." In: *Neuron* 87.3, pp. 590–604.

Teixeira, C. M., Pomedli, S. R., Maei, H. R., Kee, N., and Frankland, P. W. (2006). "Involvement of the Anterior Cingulate Cortex in the Expression of Remote Spatial Memory." In: *Journal of Neuroscience* 26.29, pp. 7555–7564.

Terreberry, R. R. and Neafsey, E. J. (1987). "The rat medial frontal cortex projects directly to autonomic regions of the brainstem." In: *Brain Research Bulletin* 19.6, pp. 639–649.

Terzano, M. G., Parrino, L., and Spaggiari, M. C. (1988). "The cyclic alternating pattern sequences in the dynamic organization of sleep." In: *Electroencephalography and clinical neurophysiology* 69.5, pp. 437–447.

Teyler, T. J. and DiScenna, P. (1986). "The Hippocampal Memory Indexing Theory." In: *Behavioral Neuroscience* 100.2, pp. 147–154.

Theunissen, F and Miller, J. P. (1995). "Temporal encoding in nervous systems: a rigorous definition." In: *Journal of computational neuroscience* 2.2, pp. 149–162.

Thompson, E and Varela, F. J. (2001). "Radical embodiment: neural dynamics and consciousness." In: *Trends in Cognitive Sciences*.

Thompson, L. T., Moyer, J. R., and Disterhoft, J. F. (1996). "Transient changes in excitability of rabbit CA3 neurons with a time course appropriate to support memory consolidation." In: *Journal of Neurophysiology* 76.3, pp. 1836–1849.

Thomson, D. (1982). "Spectrum estimation and harmonic analysis." In: *Proceedings of the IEEE* 70.9, pp. 1055–1096.

Thut, G., Nietzel, A., Brandt, S. A., and Pascual-Leone, A. (2006). "Alpha-band electroencephalographic activity over occipital cortex indexes visuospatial attention bias and predicts visual target detection." In: *The Journal of neuroscience : the official journal of the Society for Neuroscience* 26.37, pp. 9494–9502.

Timofeev, I and Steriade, M. M. (1996). "Low-frequency rhythms in the thalamus of intact-cortex and decorticated cats." In: *Journal of neurophysiology* 76.6, pp. 4152–4168.

Timofeev, I., Grenier, F, Bazhenov, M, Sejnowski, T. J., and Steriade, M (2000a). "Origin of slow cortical oscillations in deafferented cortical slabs." In: *Cerebral Cortex* 10.12, pp. 1185–1199.

Timofeev, I, Grenier, F, and Steriade, M (2001). "Disfacilitation and active inhibition in the neocortex during the natural sleep-wake cycle: An intracellular study." In: *Proceedings of the National Academy of Sciences* 98.4, pp. 1924–1929.

Timofeev, I., Grenier, F., and Steriade, M. M. (2000b). "Impact of intrinsic properties and synaptic factors on the activity of neocortical networks in vivo." In: *Journal of Physiology*. Vol. 94. 5-6, pp. 343–355.

Tolman, E. C. (1948). "Cognitive maps in rats and men." In: *Psychological Review* 55.4, pp. 189–208.

Tononi, G. and Cirelli, C. (2014). "Sleep and the Price of Plasticity: From Synaptic and Cellular Homeostasis to Memory Consolidation and Integration." In: *Neuron* 81.1, pp. 12–34.

Tononi, G. and Sporns, O. (2003). "Measuring information integration." In: *BMC Neuroscience* 4.

Tort, A. B. L., Kramer, M. A., Thorn, C, Gibson, D. J., Kubota, Y, Graybiel, A. M., and Kopell, N. J. (2008). "Dynamic cross-frequency couplings of local field potential oscillations in rat striatum and hippocampus during performance of a T-maze task." In: *Proceedings of the National Academy of Sciences* 105.51, pp. 20517–20522.

Tort, A. B. L., Komorowski, R. W., Manns, J. R., Kopell, N. J., and Eichenbaum, H. B. (2009). "Theta-gamma coupling increases during the learning of item-context associations." In: *Proceedings of the National Academy of Sciences* 106.49, pp. 20942–20947.

Tort, A. B., Brankačk, J., and Draguhn, A. (2018). "Respiration-entrained brain rhythms are global but often overlooked." In: *Trends in Neurosciences* 41.4, pp. 186–197.

Tovote, P., Fadok, J. P., and Lüthi, A. (2015). "Neuronal circuits for fear and anxiety." In: *Nature Reviews Neuroscience* 16.6, pp. 317–331.

Tovote, P., Esposito, M. S., Botta, P., Chaudun, F., Fadok, J. P., Markovic, M., Wolff, S. B., Ramakrishnan, C., Fenno, L., Deisseroth, K., Herry, C., Arber, S., and Lüthi, A. (2016). "Midbrain circuits for defensive behaviour." In: *Nature* 534.7606, pp. 206–212.

Tranel, D. and Damasio, H. (1989). "Intact electrodermal skin conductance responses after bilateral amygdala damage." In: *Neuropsychologia* 27.4, pp. 381–390.

Tranel, D. and Damasio, H. (1994). "Neuroanatomical correlates of electrodermal skin conductance responses." In: *Psychophysiology* 31.5, pp. 427–438.

Traub, R. D., Whittington, M. A., Stanford, I. M., and Jefferys, J. G. (1996). "A mechanism for generation of long-range synchronous fast oscillations in the cortex." In: *Nature* 383.6601, pp. 621–224.

Traub, R. D. and Bibbig, A. (2000). "A model of high-frequency ripples in the hippocampus based on synaptic coupling plus axon-axon gap junctions between pyramidal neurons." In: *Journal of Neuroscience* 20.6, pp. 2086–2093.

Traub, R. D., Spruston, N., Soltesz, I., Konnerth, A., Whittington, M. A., and Jefferys, J. G. R. (1998). *Gamma-frequency oscillations: A neuronal population phenomenon, regulated by synaptic and intrinsic cellular processes, and inducing synaptic plasticity*.

Travers, J. B., Dinardo, L. A., and Karimnamazi, H. (1997). "Motor and premotor mechanisms of licking." In: *Neuroscience and Biobehavioral Reviews* 21.5, pp. 631–647.

Treves, A. and Rolls, E. T. (1994). "Computational analysis of the role of the hippocampus in memory." In: *Hippocampus* 4.3, pp. 374–391.

Treves, A, Tashiro, A, Witter, M. P., and Moser, E. I. (2008). "What is the mammalian dentate gyrus good for? [Neuroscience. 2008] - PubMed Result." In: *Neuroscience*.

Tsanov, M., Chah, E., Wright, N., Vann, S. D., Reilly, R., Erichsen, J. T., Aggleton, J. P., and O'Mara, S. M. (2011a). "Oscillatory Entrainment of Thalamic Neurons by Theta Rhythm in Freely Moving Rats." In: *Journal of Neurophysiology* 105.1, pp. 4–17.

Tsanov, M., Chah, E., Vann, S. D., Reilly, R. B., Erichsen, J. T., Aggleton, J. P., and O'Mara, S. M. (2011b). "Theta-Modulated Head Direction Cells in the Rat Anterior Thalamus." In: *Journal of Neuroscience* 31.26, pp. 9489–9502.

Tsanov, M., Chah, E., Reilly, R., and O'Mara, S. M. (2014). "Respiratory cycle entrainment of septal neurons mediates the fast coupling of sniffing rate and hippocampal theta rhythm." In: *European Journal of Neuroscience* 39.6, pp. 957–974.

Tse, D., Langston, R. F., Kakeyama, M., Bethus, I., Spooner, P. A., Wood, E. R., Witter, M. P., and Morris, R. G. M. (2007). "Schemas and memory consolidation." In: *Science* 316.5821, pp. 76–82.

Tulving, E (2002). "Episodic memory: From mind to brain." In: *Annual review of psychology*.

Tye, K. M. and Deisseroth, K. (2012). "Optogenetic investigation of neural circuits underlying brain disease in animal models." In: *Nature reviews. Neuroscience* 13.4, pp. 251–266.

Uchida, S, Maehara, T, Hirai, N, Okubo, Y, and Shimizu, H (2001). "Cortical oscillations in human medial temporal lobe during wakefulness and all-night sleep." In: *Brain research* 891.1-2, pp. 7–19.

Uchida, S., Atsumi, Y., and Kojima, T. (1994). "Dynamic relationships between sleep spindles and delta waves during a NREM period." In: *Brain Research Bulletin* 33.3, pp. 351–355.

Ueki, S and Domino, E. F. (1961). "Some evidence for a mechanical receptor in olfactory function." In: *Journal of Neurophysiology* 24, pp. 12–25.

Ulanovsky, N. and Moss, C. F. (2007). "Hippocampal cellular and network activity in freely moving echolocating bats." In: 10.2, pp. 224–233.

Uva, L. and De Curtis, M. (2005). "Polysynaptic olfactory pathway to the ipsi- and contralateral entorhinal cortex mediated via the hippocampus." In: *Neuroscience* 130.1, pp. 249–258.

Uylings, H. B. and Eden, C. G. van (1990). "Qualitative and quantitative comparison of the prefrontal cortex in rat and in primates, including humans." In: *Progress in brain research* 85, pp. 31–62.

Uylings, H. B. M., Groenewegen, H. J., and Kolb, B. (2003). "Do rats have a prefrontal cortex?" In: *Behavioural brain research* 146.1-2, pp. 3–17.

Valero, M., Cid, E., Averkin, R. G., Aguilar, J., Sanchez-Aguilera, A., Viney, T. J., Gomez-Dominguez, D., Bellistri, E., and De La Prida, L. M. (2015). "Determinants of different deep and superficial CA1 pyramidal cell dynamics during sharp-wave ripples." In: *Nature Neuroscience* 18.9, pp. 1281–1290.

Valero, M., Averkin, R. G., Fernandez-Lamo, I., Aguilar, J., Lopez-Pigozzi, D., Brotons-Mas, J. R., Cid, E., Tamas, G., and Menendez de la Prida, L. (2017). "Mechanisms for Selective Single-Cell Reactivation during Offline Sharp-Wave Ripples and Their Distortion by Fast Ripples." In: *Neuron* 94.6, 1234–1247.e7.

Van der Kooy, D. and Sawchenko, P. E. (1982). "Characterization of serotonergic neurons using concurrent fluorescent retrograde axonal tracing and immunohistochemistry." In: *Journal of Histochemistry and Cytochemistry* 30.8, pp. 794–798.

Van Diest, I., Bradley, M. M., Guerra, P., Van den Bergh, O., and Lang, P. J. (2009). "Fear-conditioned respiration and its association to cardiac reactivity." In: *Biological Psychology* 80.2, pp. 212–217.

Van Dongen, H. P. A., Maislin, G., Mullington, J. M., and Dinges, D. F. (2003). "The cumulative cost of additional wakefulness: dose-response effects on neurobehavioral functions and sleep physiology from chronic sleep restriction and total sleep deprivation." In: *Sleep* 26.2, pp. 117–126.

Van Twyver, H. (1969). "Sleep patterns of five rodent species." In: *Physiology & behavior* 4.6, pp. 901–905.

Vandecasteele, M., Varga, V., Berényi, A., Papp, E., Barthó, P., Venance, L., Freund, T. F., and Buzsaki, G. (2014). "Optogenetic activation of septal cholinergic neurons suppresses sharp wave ripples and enhances theta oscillations in the hippocampus." In: *Proceedings of the National Academy of Sciences* 111.37, pp. 13535–13540.

Vanderwolf, C. H. (1992). "Hippocampal activity, olfaction, and sniffing: an olfactory input to the dentate gyrus." In: *Brain Research* 593.2, pp. 197–208.

Vanderwolf, C. H. (2001). "The hippocampus as an olfacto-motor mechanism: Were the classical anatomists right after all?" In: *Behavioural Brain Research*. Vol. 127. 1-2, pp. 25–47.

Vanderwolf, C. (1969). "Hippocampal electrical activity and voluntary movement in the rat." In: *Electroencephalography and Clinical Neurophysiology* 26.4, pp. 407–418.

Varela, C., Kumar, S., Yang, J. Y., and Wilson, M. A. (2014). "Anatomical substrates for direct interactions between hippocampus, medial prefrontal cortex, and the thalamic nucleus reuniens." In: *Brain Structure and Function* 219.3, pp. 911–929.

Varela, F., Lachaux, J. P., Rodriguez, E., and Martinerie, J. (2001). "The brainweb: Phase synchronization and large-scale integration." In: *Nature Reviews Neuroscience* 2.4, pp. 229–239.

Vargha-Khadem, F, Gadian, D. G., Watkins, K. E., Connelly, A, Van Paesschen, W, and Mishkin, M (1997). "Differential effects of early hippocampal pathology on episodic and semantic memory." In: *Science* 277.5324, pp. 376–380.

Vassar, R, Chao, S. K., Sitcheran, R, Nuñez, J. M., Vosshall, L. B., and Axel, R (1994). "Topographic organization of sensory projections to the olfactory bulb." In: *Cell* 79.6, pp. 981–991.

Veasey, S. C., Valladares, O, Fenik, P, Kapfhamer, D, Sanford, L, Benington, J, and Bucan, M (2000). "An automated system for recording and analysis of sleep in mice." In: *Sleep* 23.8, pp. 1025–1040.

Vertes, R. P., Albo, Z., and Viana Di Prisco, G. (2001). "Theta-rhythmically firing neurons in the anterior thalamus: Implications for mnemonic functions of Papez's circuit." In: *Neuroscience* 104.3, pp. 619–625.

Vertes, R. P. (2006). "Interactions among the medial prefrontal cortex, hippocampus and midline thalamus in emotional and cognitive processing in the rat." In: *Neuroscience* 142.1, pp. 1–20.

Verzeano, M and Negishi, K (1960). "Neuronal activity in cortical and thalamic networks." In: *The Journal of general physiology* 43(6)Suppl, pp. 177–195.

Vidal-Gonzalez, I., Vidal-Gonzalez, B., Rauch, S. L., and Quirk, G. J. (2006). "Microstimulation reveals opposing influences of prelimbic and infralimbic cortex on the expression of conditioned fear." In: *Learning & Memory* 13.6, pp. 728–733.

Vinck, M., Batista-brito, R., Cardin, J. A., Vinck, M., Batista-brito, R., Knoblich, U., and Cardin, J. A. (2015). "Arousal and Locomotion Make Distinct Contributions to Cortical Activity Patterns and Visual Encoding Article Arousal and Locomotion Make Distinct Contributions to Cortical Activity Patterns and Visual Encoding." In: *Neuron* 86.3, pp. 1–15.

Vlemincx, E., Taelman, J., De Peuter, S., Van Diest, I., and Bergh, O. Van den (2011). "Sigh rate and respiratory variability during mental load and sustained attention." In: *Psychophysiology* 48.1, pp. 117–120.

Voirin, B., Cruz, S. M., Tisdale, R., Omo, G. D. r., Lipp, H.-P., Wikelski, M., Rattenborg, N. C., and Vyssotski, A. L. (2016). "Evidence that birds sleep in mid-flight." In: *Nature Communications* 7, pp. 1–9.

Volgushev, M. (2006). "Precise Long-Range Synchronization of Activity and Silence in Neocortical Neurons during Slow-Wave Sleep." In: *Journal of Neuroscience* 26.21, pp. 5665–5672.

Vyazovskiy, V. V., Olcese, U., Lazimy, Y. M., Faraguna, U., Esser, S. K., Williams, J. C., Cirelli, C., and Tononi, G. (2009). "Cortical Firing and Sleep Homeostasis." In: *Neuron* 63.6, pp. 865–878.

Vyazovskiy, V. V., Olcese, U., Hanlon, E. C., Nir, Y., Cirelli, C., and Tononi, G. (2011). "Local sleep in awake rats." In: *Nature* 472.7344, pp. 443–447.

Wada, J. A., Matsuda, M., Jung, E., and Hamm, A. E. (1970). "Mesencephalically induced escape behavior and avoidance performance." In: *Experimental Neurology* 29.2, pp. 215–220.

Walsh, R. R. (1956). "Single cell spike activity in the olfactory bulb." In: *The American journal of physiology* 186.2, pp. 255–257.

Walter, C. (1966). "Oscillation in Enzyme Reactions." In: *Nature* 209.5021, pp. 404–405.

Wamsley, E. J., Tucker, M, Paine, J, Bonavides, A, and Stickgold, R (2010). "Dreaming of a learning task is associated with enhanced sleep-dependant memory consolidation." In: *Current Biology* 20.9, pp. 850–855.

Wang, D. V. and Ikemoto, S. (2016). "Coordinated Interaction between Hippocampal Sharp-Wave Ripples and Anterior Cingulate Unit Activity." In: *Journal of Neuroscience* 36.41, pp. 10663–10672.

Wang, D. V., Yau, H. J., Broker, C. J., Tsou, J. H., Bonci, A., and Ikemoto, S. (2015). "Mesopontine median raphe regulates hippocampal ripple oscillation and memory consolidation." In: *Nature Neuroscience* 18.5, pp. 728–735.

Wang, G.-W. and Cai, J.-X. (2006). "Disconnection of the hippocampal–prefrontal cortical circuits impairs spatial working memory performance in rats." In: *Behavioural Brain Research* 175.2, pp. 329–336.

Wang, S.-H. and Morris, R. G. (2010). "Hippocampal-Neocortical Interactions in Memory Formation, Consolidation, and Reconsolidation." In: *Annual Review of Psychology* 61.1, pp. 49–79.

Wang, S. H., Teixeira, C. M., Wheeler, A. L., and Frankland, P. W. (2009). "The precision of remote context memories does not require the hippocampus." In: *Nature Neuroscience* 12.3, pp. 253–255.

Wang, T. and Samworth, R. J. (2016). "High-dimensional changepoint estimation via sparse projection." In: *arXiv.org*.

Waterhouse, I. K. (1957). "Effects of prefrontal lobotomy on conditioned fear and food responses in monkeys." In: *Journal of comparative and physiological psychology* 50.1, pp. 81–88.

Watson, J. B. and Rayner, R (1920). "Conditioned emotional reactions." In: *Journal of experimental Psychology*.

Weber, F. and Dan, Y. (2016). *Circuit-based interrogation of sleep control*.

Weber, F., Chung, S., Beier, K. T., Xu, M., Luo, L., and Dan, Y. (2015). "Control of REM sleep by ventral medulla GABAergic neurons." In: *Nature* 526.7573, pp. 435–438.

Weible, A. P., Rowland, D. C., Monaghan, C. K., Wolfgang, N. T., and Kentros, C. G. (2012). "Neural Correlates of Long-Term Object Memory in the Mouse Anterior Cingulate Cortex." In: *Journal of Neuroscience* 32.16, pp. 5598–5608.

Weinberger, N. M. (2004). "Specific long-term memory traces in primary auditory cortex." In: *Nature Reviews Neuroscience* 5.4, pp. 279–290.

Welker, W. I. (1964). "Analysis of Sniffing of the Albino Rat." In: *Behaviour*.

Westgaard, R., Bonato, P., and Holte, K. (2002). "Low-frequency oscillations (<0.3 Hz) in the electromyographic (EMG) activity of the human trapezius muscle during sleep." In: *Journal of Neurophysiology* 88.3, pp. 1177–1184.

Whittaker, J (1935). *Interpolatory Function Theory.* Cambridge University Press.

Whittington, M. A., Traub, R. D., and Jefferys, J. G. R. (1995). "Synchronized oscillations in interneuron networks driven by metabotropic glutamate receptor activation." In: *Nature* 373.6515, pp. 612–615.

Wiech, K., Kalisch, R., Weiskopf, N., Pleger, B., Stephan, K. E., and Dolan, R. J. (2006). "Anterolateral Prefrontal Cortex Mediates the Analgesic Effect of Expected and Perceived Control over Pain." In: *Journal of Neuroscience* 26.44, pp. 11501–11509.

Wielgosz, J., Schuyler, B. S., Lutz, A., and Davidson, R. J. (2016). "Long-term mindfulness training is associated with reliable differences in resting respiration rate." In: *Scientific reports* 6, p. 27533.

Wierzynski, C. M., Lubenov, E. V., Gu, M., and Siapas, A. G. (2009). "State-Dependent Spike-Timing Relationships between Hippocampal and Prefrontal Circuits during Sleep." In: *Neuron* 61.4, pp. 587–596.

Wilhelm, I., Diekelmann, S., Molzow, I., Ayoub, A., Molle, M., and Born, J. (2011). "Sleep Selectively Enhances Memory Expected to Be of Future Relevance." In: *Journal of Neuroscience* 31.5, pp. 1563–1569.

Wilson, C. J. (1993). "The generation of natural firing patterns in neostriatal neurons." In: *Progress in brain research*.

Wilson, C. J. and Groves, P. M. (1981). "Spontaneous firing patterns of identified spiny neurons in the rat neostriatum." In: *Brain Research* 220.1, pp. 67–80.

Wilson, M. and McNaughton, B. (1993). "Dynamics of the hippocampal ensemble code for space." In: *Science* 261.5124, pp. 1055–1058.

Wilson, M. and McNaughton, B. (1994). "Reactivation of hippocampal ensemble memories during sleep." In: *Science* 265.5172, pp. 676–679.

Wiltgen, B. J., Brown, R. A. M., Talton, L. E., and Silva, A. J. (2004). *New circuits for old memories: The role of the neocortex in consolidation*.

Windels, F., Crane, J. W., and Sah, P. (2010). "Inhibition dominates the early phase of up-states in the basolateral amygdala." In: *Journal of neurophysiology* 104.6, pp. 3433–3438.

Winocur, G., Moscovitch, M., and Bontempi, B. (2010). "Memory formation and long-term retention in humans and animals: Convergence towards a transformation account of hippocampal-neocortical interactions." In: *Neuropsychologia* 48.8, pp. 2339–2356.

Winson, J (1974). "Patterns of hippocampal theta rhythm in the freely moving rat." In: *Electroencephalography and clinical neurophysiology* 36.3, pp. 291–301.

Winson, J (1978). "Loss of hippocampal theta rhythm results in spatial memory deficit in the rat." In: *Science* 201.4351, pp. 160–163.

Wolansky, T., Clement, E. A., Peters, S. R., Palczak, M. A., and Dickson, C. T. (2006). "Hippocampal slow oscillation: a novel EEG state and its coordination with ongoing neocortical activity." In: *The Journal of neuroscience : the official journal of the Society for Neuroscience* 26.23, pp. 6213–6229.

Womelsdorf, T., Johnston, K., Vinck, M., and Everling, S. (2010). "Theta-activity in anterior cingulate cortex predicts task rules and their adjustments following errors." In: *Proceedings of the National Academy of Sciences* 107.11, pp. 5248–5253.

Womelsdorf, T., Fries, P., Mitra, P. P., and Desimone, R. (2006). "Gamma-band synchronization in visual cortex predicts speed of change detection." In: *Nature* 439.7077, pp. 733–736.

Womelsdorf, T., Schoffelen, J. M., Oostenveld, R., Singer, W., Desimone, R., Engel, A. K., and Fries, P. (2007). "Modulation of neuronal interactions through neuronal synchronization." In: *Science* 316.5831, pp. 1609–1612.

Wulff, K., Gatti, S., Wettstein, J. G., and Foster, R. G. (2010). "Sleep and circadian rhythm disruption in psychiatric and neurodegenerative disease." In: *Nature Reviews Neuroscience* 11.8, pp. 589–599.

Wurts, S. W. and Edgar, D. M. (2000). "Circadian and Homeostatic Control of Rapid Eye Movement (REM) Sleep: Promotion of REM Tendency by the Suprachiasmatic Nucleus." In: *Journal of Neuroscience* 20.11, pp. 4300–4310.

Xu, W., Morishita, W., Buckmaster, P. S., Pang, Z. P., Malenka, R. C., and Südhof, T. C. (2012). "Distinct neuronal coding schemes in memory revealed by selective erasure of fast synchronous synaptic transmission." In: *Neuron* 73.5, pp. 990–1001.

Yackle, K., Schwarz, L. A., Kam, K., Sorokin, J. M., Huguenard, J. R., Feldman, J. L., Luo, L., and Krasnow, M. A. (2017). "Breathing control center neurons that promote arousal in mice." In: *Science* 355.6332, pp. 1411–1415.

Yajima, Y and Hayashi, Y (1983). "Ambiguous motoneurons discharging synchronously with ultrasonic vocalization in rats." In: *Experimental Brain Research* 50-50.2-3.

Yang, C. F. and Feldman, J. L. (2018). "Efferent projections of excitatory and inhibitory preBötzinger complex neurons." In: *Journal of Comparative Neurology* 526.8, pp. 1389–1402.

Yang, Y., Liu, D.-q., Huang, W., Deng, J., Sun, Y., Zuo, Y., and Poo, M.-m. (2016). "Selective synaptic remodeling of amygdalocortical connections associated with fear memory." In: *Nature neuroscience* 19.10, pp. 1348–1355.

Yanovsky, Y., Ciatipis, M., Draguhn, A., Tort, A. B. L., and Brankack, J. (2014). "Slow oscillations in the mouse hippocampus entrained by nasal respiration." In: *Journal of Neuroscience* 34.17, pp. 5949–5964.

Yassa, M. A. and Stark, C. E. L. (2011). "Pattern separation in the hippocampus." In: *Trends in Neurosciences* 34.10, pp. 515–525.

Ye, L., Allen, W. E., Thompson, K. R., Tian, Q., Hsueh, B., Ramakrishnan, C., Wang, A. C., Jennings, J. H., Adhikari, A., Halpern, C. H., Witten, I. B., Barth, A. L., Luo, L., McNab, J. A., and Deisseroth, K. (2016). "Wiring and Molecular Features of Prefrontal Ensembles Representing Distinct Experiences." In: *Cell* 165.7, pp. 1776–1788.

Yiu, A. P., Mercaldo, V., Yan, C., Richards, B., Rashid, A. J., Hsiang, H. L. L., Pressey, J., Mahadevan, V., Tran, M. M., Kushner, S. A., Woodin, M. A., Frankland, P. W., and Josselyn, S. A. (2014). "Neurons Are Recruited to a Memory Trace Based on Relative Neuronal Excitability Immediately before Training." In: *Neuron* 83.3, pp. 722–735.

Ylinen, A., Soltész, I., Bragin, A., Penttonen, M., Sik, A., and Buzsaki, G. (1995). "Intracellular correlates of hippocampal theta rhythm in identified pyramidal cells, granule cells, and basket cells." In: *Hippocampus* 5.1, pp. 78–90.

Yuan, H., Zotev, V., Phillips, R., and Bodurka, J. (2013a). "Correlated slow fluctuations in respiration, EEG, and BOLD fMRI." In: *NeuroImage* 79, pp. 81–93.

Yuan, P., Gao, X., Allison, B., Wang, Y., Bin, G., and Gao, S. (2013b). "A study of the existing problems of estimating the information transfer rate in online brain-computer interfaces." In: *Journal of Neural Engineering* 10.2, p. 026014.

Zagha, E., Casale, A. E., Sachdev, R. N. S., McGinley, M. J., and McCormick, D. A. (2013). "Motor cortex feedback influences sensory processing by modulating network state." In: *Neuron* 79.3, pp. 567–578.

Zagha, E., Ge, X., and McCormick, D. A. (2015). "Competing Neural Ensembles in Motor Cortex Gate Goal-Directed Motor Output." In: *Neuron* 88.3, pp. 565–577.

Zeidan, F. and Vago, D. R. (2016). "Mindfulness meditation-based pain relief: a mechanistic account." In: *Annals of the New York Academy of Sciences* 1373.1. Ed. by S. Sequeira, pp. 114–127.

Zelano, C., Jiang, H., Zhou, G., Arora, N., Schuele, S., Rosenow, J., and Gottfried, J. A. (2016). "Nasal respiration entrains human limbic oscillations and modulates cognitive function." In: *Journal of Neuroscience* 36.49, pp. 12448–12467.

Zhang, J. X., Harper, R. M., and Frysinger, R. C. (1986). "Respiratory modulation of neuronal discharge in the central nucleus of the amygdala during sleep and waking states." In: *Experimental Neurology* 91.1, pp. 193–207.

Zhang, S. P., Davis, P. J., and Bandler, R (1994). "Brain stem integration of vocalization: role of the midbrain periaqueductal gray." In: *The Midbrain Periaqueductal Gray Matter* Chapter 5, pp. 57–66.

Zhao, W.-J., Kremkow, J., and Poulet, J. F. A. (2016). "Translaminar Cortical Membrane Potential Synchrony in Behaving Mice." In: *Cell Reports* 15.11, pp. 2387–2399.

Zhong, W., Ciatipis, M., Wolfenstetter, T., Jessberger, J., Müller, C., Ponsel, S., Yanovsky, Y., Brankačk, J., Tort, A. B. L., and Draguhn, A. (2017). "Selective entrainment of gamma subbands by different slow network oscillations." In: *Proceedings of the National Academy of Sciences* 114.17, pp. 4519–4524.

Zhou, M., Liang, F., Xiong, X. R., Li, L., Li, H., Xiao, Z., Tao, H. W., and Zhang, L. I. (2014). "Scaling down of balanced excitation and inhibition by active behavioral states in auditory cortex." In: *Nature Neuroscience* 17.6, pp. 841–850.

Zhou, Y., Won, J., Karlsson, M. G., Zhou, M., Rogerson, T., Balaji, J., Neve, R., Poirazi, P., and Silva, A. J. (2009). "CREB regulates excitability and the allocation of memory to subsets of neurons in the amygdala." In: *Nature neuroscience* 12.11, pp. 1438–1443.

Zumer, J. M., Scheeringa, R., Schoffelen, J.-M., Norris, D. G., and Jensen, O. (2014). "Occipital Alpha Activity during Stimulus Processing Gates the Information Flow to Object-Selective Cortex." In: *PLoS Biology* 12.10. Ed. by E. Vogel, e1001965.

LMU LUDWIG-MAXIMILIANS-UNIVERSITÄT MÜNCHEN

Dean's Office
Medical Faculty

Affidavit

Nikolaos Karalis

Surname, first name

Street

Zip code, town

Country

I hereby declare, that the submitted thesis entitled

Oscillatory architecture of memory circuits

is my own work. I have only used the sources indicated and have not made unauthorised use of services of a third party. Where the work of others has been quoted or reproduced, the source is always given.

I further declare that the submitted thesis or parts thereof have not been presented as part of an examination degree to any other university.

Munich, 27 February 2018

Place, date

Nikolaos Karalis

Signature doctoral candidate